The determination of respiratory impedance by the oscillatory airflow technique

Scott, Richard Stephen

Award date:
1993

Awarding institution:
University of Bath

The Determination of Respiratory Impedance by the Oscillatory Airflow Technique

Submitted by Richard Stephen Scott

for the degree of PhD
of the University of Bath

1993

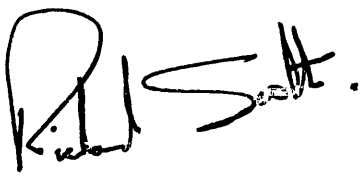

ProQuest LLC
789 East Eisenhower Parkway
P.O. Box 1346
Ann Arbor, MI 48106-1346

Abstract

The assessment of respiratory mechanics is important when evaluating lung disease and monitoring the efficacy of drug therapy. The measurement of respiratory impedance by the oscillatory airflow method is a sensitive test requiring minimal subject cooperation. It is therefore less distressing for patients than routine lung function tests which require a forced maximal expiration. The method has potential as a sensitive test of lung function as it provides information on peripheral airway resistance and it is in these small airways that the first signs of lung disease are apparent.

A prototype system is described and evaluated in terms of errors associated with impedance estimates. This led to an improved system, with changes to the airflow structure and the use of digital bandpass filtering techniques contributing to more reliable impedance estimates. Data is shown predominantly in normal subjects, although a few asthmatic results are included, with the second stage of the work focusing on the increased variability of low frequency impedance data. Physiological sources of interference were considered and it became apparent that cardiac activity was influencing data quality. The impact of interference on the coherence function, used as an index of data reliability, was investigated and it was concluded that information regarding the frequency distribution of the interfering noise was necessary to have confidence in coherence values. Finally, the impedance calculation was reconsidered in terms of multiple input systems theory, considering the cardiac signal as a second system input to consider the effects further.

Contents

Acknowledgements

The work in this thesis was undertaken on a part-time basis in conjunction with my role, as a medical physicist/electronics engineer, in the Regional Medical Physics Service, Royal United Hospital, Bath. I therefore had two supervisors, Dick Lipczynski, Bath University, and Lindsay Grant, Medical Physics Service, both of whom I would like to thank for their guidance during the project. My thanks also go to Professor Lillicrap, Head of the Medical Physics Service, for helping to fund my registration and the Wessex Regional Research Committee for providing a grant to purchase equipment.

I must also thank Chris Jordan, Clinical Research Centre, Harrow for his advice and many thought provoking discussions. Dr Tanser, Consultant Physician, and his staff have provided continuing advice and assistance with the clinical evaluation of the work, for which I am most grateful.

I am appreciative of the support offered by my colleagues throughout the Medical Physics Service. Finally, my grateful thanks go to my wife, Anne, for her support throughout my studies.

Chapter 1 Background

1.1 Introduction

The role of the human respiratory system is to deliver oxygen to the blood and to expel carbon dioxide, a by-product of metabolism. To ensure the optimum performance of the respiratory system a timely and adequate supply of oxygen is necessary, deep within the lung, at the site of gas exchange. The physical properties of the system, together with any pathological changes govern the relationship between gas pressures and flows throughout the lung, thereby influencing the transport of gas. The theme of this thesis is the quantitative assessment of the mechanical properties of the respiratory system.

Such information is necessary for the clinical evaluation of lung disease and to monitor the efficacy of drug therapy. Mechanical indices are often used in epidemiological studies, as well as in the characterisation of occupational lung injury. There now exists a standard set of equipment routinely encountered in pulmonary physiology laboratories to assess mechanical status, lung volumes and gas transfer efficiency.

Focusing on the mechanical assessment, the device most commonly used is a recording spirometer, which graphically shows the change in lung volume with time as the subject forcefully exhales into the instrument. Numerical values, including the commonly quoted, forced expiratory volume in one second, $FEV_{1.0}$, are measured and used to quantify lung function. Spirometers will always have a place in pulmonary laboratories due to their ease of use reproducibility of results and low cost. The results, however, are not as sensitive as

those available from more sophisticated methods, (Cotes, 1979:108). Such methods, including airway resistance determination by body plethysmography, dynamic compliance measurements and closing volume assessments, tend to be restricted to larger research laboratories due to their increased complexity and cost. An additional major limitation of all such techniques is that they require considerable subject cooperation, the implication being that they are restricted to application in cooperative subject groups.

There is a role for a method that is a sensitive indicator of lung function, requiring minimal subject cooperation while being easy to use. A suitable test is the calculation of respiratory impedance by the oscillatory airflow method. Impedance, defined as the ratio of pressure to flow, is a complex, frequency dependant parameter which characterises system mechanics. Impedance determination involves the application of a low amplitude sinusoidal airflow to the lung, often via the mouth and the analysis of the resultant pressure and flow signals. The technique was developed by Dubois *et al*, (1956), with single frequency oscillations being employed. During the seventies the method was extended, (Michaelson *et al*, (1975) and Landser *et al*, (1976)), to make simultaneous multiple frequency impedance measurements. During the measurement the subject continues to breathe normally, as the applied airflow is simply superimposed onto the spontaneous respiration. The technique therefore may be applied in a wide range of patient groups, from neonates to adults and even in unconscious patients.

The approach, discussed in detail later, offers a number of advantages over established lung function tests. As no forced expiratory manoeuvres are required the volume history of the lung is

unaffected between consecutive measurements and the procedure is less distressing for patients. Consequently the method is particularly well suited to monitoring bronchial challenge responses. Furthermore it has been suggested that analysis of the frequency dependence of impedance may be used to identify changes in peripheral airways resistance (Grimby *et al*, 1968, Pimmel *et al*, 1978). These airways are thought to be the site of the early manifestation of lung disease, (Mead *et al*, 1967, Macklem and Mead, 1967 and Hogg *et al*, 1968), yet despite considerable changes in the small airways routine tests will not identify this (Macklem, 1972). The reason being that despite their prodigious number peripheral airways act in parallel and in fact only contribute around 20% of the total resistance measured at the mouth. In summary the approach is appealing due to its versatility; it may be applied in a range of patient groups, and the data may be used for routine or research work.

The technique has not yet achieved widespread clinical use. There are a variety of reasons for this, including the complexity of the instrumentation and signal processing. Other problems include the differences in reported data between groups, accounted for in part by equipment related artifacts. Also, as the subject breathes during the test the fact that lung volume is not known has been a source of concern to clinicians as resistance is volume dependent. Reliable low frequency results have been difficult to obtain due to low signal levels at these frequencies. The affected frequencies are where the compliance impedance dominates, increasing the reactive component and thereby reducing flow. The problem is compounded by sources of physiological interference, such as respiration and cardiac activity which may introduce errors to the impedance estimate. The applied

oscillatory signal cannot be arbitrarily increased as this may lead to non linear system behaviour which is undesirable.

From a clinical viewpoint, a robust impedance measurement system capable of differentiating between central and peripheral airways resistance, that is easy to use, portable and applicable in a wide range of patient groups would be a valuable tool. With these criteria in mind instrumentation has been developed and evaluated, in an attempt to realise the full potential of respiratory impedance measurements. Additionally, particular attention has been given to the reliability of low frequency data as this data is of fundamental importance.

1.2 Focus of the Work

The thesis is written from an engineering perspective, a major component of the work has been the application of digital signal processing techniques to obtain an optimum impedance frequency response function. In terms of hardware, the aim was to develop instrumentation which could be used on a routine basis in a general hospital pulmonary physiology department. The frequency range considered was 2Hz to 40Hz, with measurements being made in conscious groups of adult volunteers and patients.

Robust respiratory impedance results were a pre-requisite to both the routine use of the system and its application in modelling. The main focus of the work has been to achieve reliable impedance estimates, particularly at frequencies of 10Hz and less. Specifically, there was a need to identify and minimise the effects of physiological sources of interference. In summary, the emphasis of the work has been considering the integrity of the data, so most results presented are in normal volunteers. A small number of asthmatic subject results

have been included, to show the ability of the technique to differentiate them from normals and to illustrate changes following medication.

In terms of the thesis structure, chapters one, two and three serve as an introduction to the subject, providing background material, reviewing the literature and discussing the theory involved in the analysis. All subsequent chapters detail research undertaken at the Royal United Hospital, Bath. A prototype instrument was developed, which enabled an initial assessment of the technique, its acceptability to patients and operators and the development of a local results database. Preliminary results, on a group of volunteers highlighted some problems with the prototype, the most serious was the poor quality of low frequency data. Investigations into the choice of oscillatory waveform and the use of filtering techniques prior to analysis, led to a dramatic improvement in data quality. The modified prototype was then evaluated in the Pulmonary Physiology department. Attention then turned to a detailed consideration of the effects of physiological interference. Respiration as a source of interference had been widely discussed in the literature (Landser *et al*, 1976, Franken *et al*, 1983), however, cardiogenic activity had not. The effect of cardiac activity on impedance estimates was investigated and a new approach to the assessment of respiratory impedance proposed.

1.3 Respiratory Impedance Principle

As previously outlined, respiratory impedance is determined by the application of a sinusoidal airflow to the lung and then analysing the resulting pressure and flow signals. Figure 1.1 shows a block diagram of the equipment components. If the airflow is applied at the

mouth, with pressure and flow also measured there then the result is referred to as the input impedance of the system. Alternatively if one parameter is measured at the chest then the transfer impedance is obtained. The thesis concentrates on input impedance measurements.

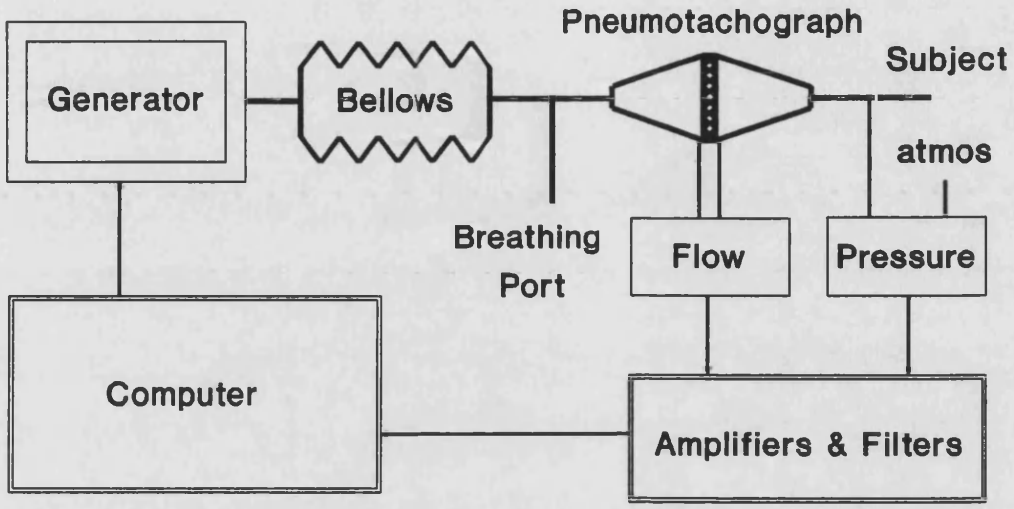

Figure 1.1 Respiratory Impedance Apparatus - Block Diagram

An airflow is designed, generated and applied to the subject with a port to atmosphere through which the subject breathes. Flow is usually measured with a pneumotachograph and pressure transducer which determines the pressure drop across a resistive element. Mouth pressure is measured with respect to atmosphere so the resulting resistive component is total respiratory resistance, including lung tissue and chest wall components, rather than purely airways resistance. Pressure and flow are divided to yield the impedance at the frequency of the applied airflow. Mathematically a complex quantity, impedance comprises a real and imaginary part and may be presented in either polar or cartesian coordinates. In physical terms the real part represents the resistive contribution to the impedance, with the imaginary term reflecting the reactance which combines components associated with the elastic and inertial properties of the

system. This means that the results differentiate between changes in airway resistance and lung elasticity, whereas a change in $FEV_{1.0}$ might be caused by either of these. At breathing frequencies, typically 0.2Hz to 0.4Hz, the inertial component, due to the acceleration of gas and tissue, is trivial.

A sinusoidal signal is used as the basic excitatory signal as it lends itself well to mathematical analysis. Resultant flows, volumes and accelerations are delayed with respect to each other but otherwise similar. The derivative of volume is flow and the derivative of flow is acceleration, each waveform being delayed by 90°. By varying the frequency of the applied oscillation the frequency response of the respiratory system may be developed. Alternatively by applying many frequencies simultaneously this may be achieved more efficiently, with the use of Fourier analysis to resolve the signals into their individual frequency components.

The amplitude of the oscillations are kept small to ensure the response of the respiratory system is linear. Being small compared to the tidal volume the signal does not replace the air column in the tracheo-bronchial tree, it simply advances and returns it throughout the oscillatory cycle. The applied frequencies traditionally have been higher than the breathing frequency in an attempt to enable separation of results from the respiration. Frequencies are chosen to be as low as practically possible as they will be of direct clinical significance. Also, at low frequencies compliance dominates the reactive component so this data is important in deriving capacitive elements in electrical analogue models. Most groups, unless specifically interested in say high frequency ventilation, do not obtain results above 40Hz as they have little apparent clinical

applicability. Additionally at these higher frequencies inertia becomes the dominant reactive component associated with the inertia of gas and lung tissues.

1.4 Basic Respiratory Physiology

It is the function of the respiratory system to transport oxygen into and carbon dioxide from the body, exchanging these gases between blood and air. The lung is the organ of gas exchange and is remarkable both in structure and function. The anatomy comprises a series of branching airways becoming progressively shorter, narrower and more numerous, until, deep within the lung they terminate in small air sacs. The airways enable gas transport, with the readily expandable sacs, or alveoli, being the site of gas exchange. The mechanism of gas exchange is simple. Air is delivered close to the blood separated by a thin layer of tissue across which oxygen and carbon dioxide diffuse. By wrapping numerous blood vessels around the three hundred million alveoli the effective surface area for gas exchange, in the adult human, is around eighty square metres, yet the lungs occupy a volume of only four litres. The huge area contributes to the efficiency of gas exchange, with equilibrium being reached in the second or so it takes a blood cell to traverse two or three alveoli. Another feature which ensures rapid equilibration is the one to one volume correspondence between air and blood. During a minutes respiration, for example, around five litres of air are brought to the gas exchange site which equals the volume of blood flowing through the pulmonary vasculature over the same period. The actual gas concentrations in the blood depend not only on the performance of the exchange mechanism but also the supply of oxygen to the exchange site. The transport of gas is

influenced by the relationship between gas pressures and flows throughout the lung. The purpose of this section is to introduce some basic respiratory physiology and terminology, with specific reference to lung mechanics. The following figures and table have been reproduced from data in either West's excellent introductory text, "Respiratory Physiology - the essentials", (1985), or from Cotes' definitive text "Lung Function", (1979).

1.4.1 The Respiratory Process

Air is drawn into the nose, warmed and humidified then passed through the pharynx, larynx and into the trachea. The trachea divides into the two bronchi, with each subsequent generation of airways dividing into shorter and narrower ones. This process continues down to the terminal bronchioles which are the smallest airways without alveoli. All airways to this point are termed the conducting airways as they play no part in gas exchange. The airway generations are numbered, with the trachea as zero through to the alveolar sacs as generation 23, with figure 1.2 showing the extremely rapid increase in total cross-sectional area of the airways in the respiratory zone where gas exchange occurs by a process of diffusion. Airway generations up to 16 represent the conducting airways with further generations being termed the respiratory zone.

During inspiration the diaphragm lowers, increasing the volume of the thoracic cavity. The resulting negative, sub-atmospheric, pressure within the lungs causes air to enter. Expiration is passive, with the lung returning to its pre-inspiratory volume due to its own inherent elasticity. The lung requires small pressures to distend it. West, (1985), illustrates this by noting that a normal breath of 500ml needs

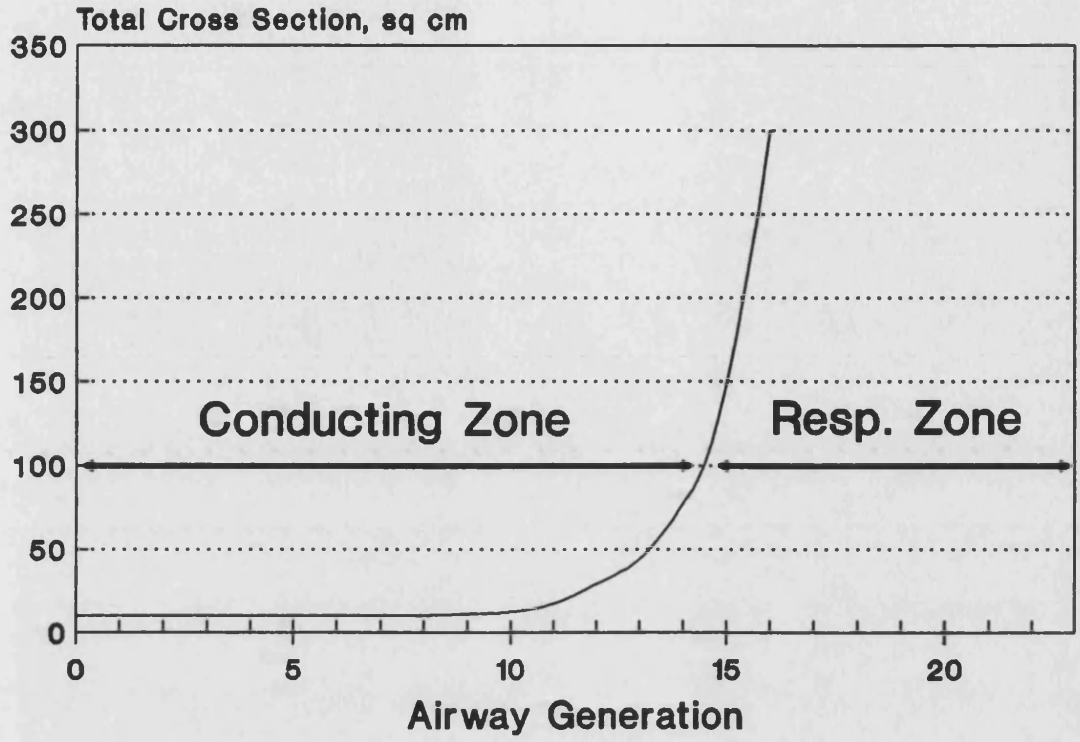

Figure 1.2 Lung Cross Sectional Area versus Airway Generation

a distending pressure less than 3hPa, while a child's balloon may need some 300hPa for the same volume change. Table 1.1 quantifies typical volumes and flows in the normal adult lung, it is remarkable that the alveolar ventilation is virtually the same as the pulmonary blood flow. Tidal breathing refers to the volume changes associated with normal breathing, with anatomic deadspace describing the volume of air not involved in the gas exchange process. It is useful to define a number of static lung volumes often referred to and this is done in figure 1.3. The lung is a passive organ, that is to say external forces need to be applied to expand the structure. These forces are exerted by the muscles associated with respiration. The lungs are situated within the thoracic cage, which also exhibits elasticity and it is this that opposes the lungs natural tendency to collapse, thereby keeping the system in equilibrium. This results in a sub-atmospheric pressure existing in the pleural space between lung and chest wall.

Volumes - millilitres	Flows - millilitres/minute
Tidal Volume 500	Total Ventilation 7,500
Anatomic Deadspace 150	Breathing Rate 15 breathes/minute
Alveolar Gas 3,000	Alveolar Ventilation 5,250
Pulmonary Capillary Blood, 70	Pulmonary Blood Flow 5,000

Table 1.1 Typical Volumes and Flows in the Healthy Lung

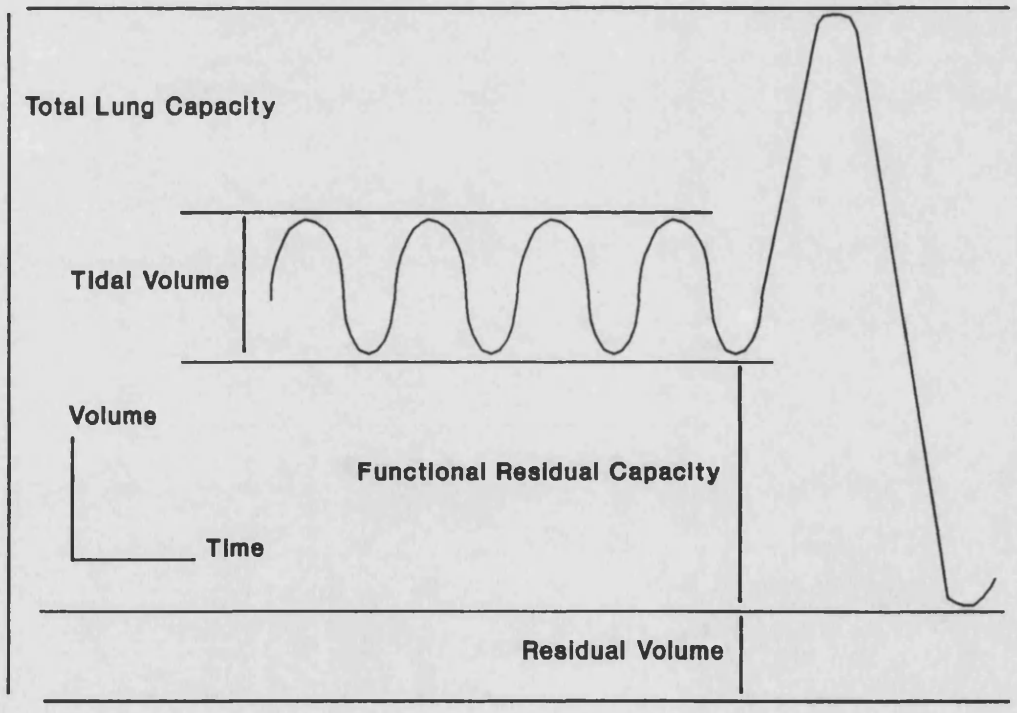

Figure 1.3 Lung Volume Definitions

1.4.2 Mechanical Definitions

During breathing work has to be done to overcome the elastic forces resisting expansion and the resistance offered by the airways. The elasticity of the lung is characterised by its compliance, which is defined as the volume change per unit pressure. Resistance is calculated as the ratio of pressure to flow. Inertial effects of gas and lung tissues are not of significance at low respiratory frequencies, so this is a parameter not normally discussed in respiratory physiology text books. The reactive component of high frequency impedance measurements using the oscillatory airflow technique will, however, be influenced by inertial effects.

If laminar flow exists then the resistance of straight circular tubes may be computed from Poiseuille's equation, (Equation 1.1).

$$R = \frac{8\eta l}{\pi r^4} \qquad 1.1$$

Where R represents resistance, l tube length, r tube radius and η viscosity. Note the critical influence of tube radius. This formula may be used to obtain an estimate of resistance with laminar flow, however, if flow is turbulent this does not apply. With turbulent flow gas density becomes more important and viscosity less so, also the pressure becomes proportional to the square of the flow. Turbulence may be predicted from Reynold's number values, which show it to be most likely for high flow rates and large tube diameters. Considering the bronchial tree it is difficult to apply the above relationships due to the complexity of the structure. It is thought that the flow is largely turbulent in the upper, large airways only becoming laminar in the terminal bronchioles.

Airway resistance is defined as the pressure drop between the

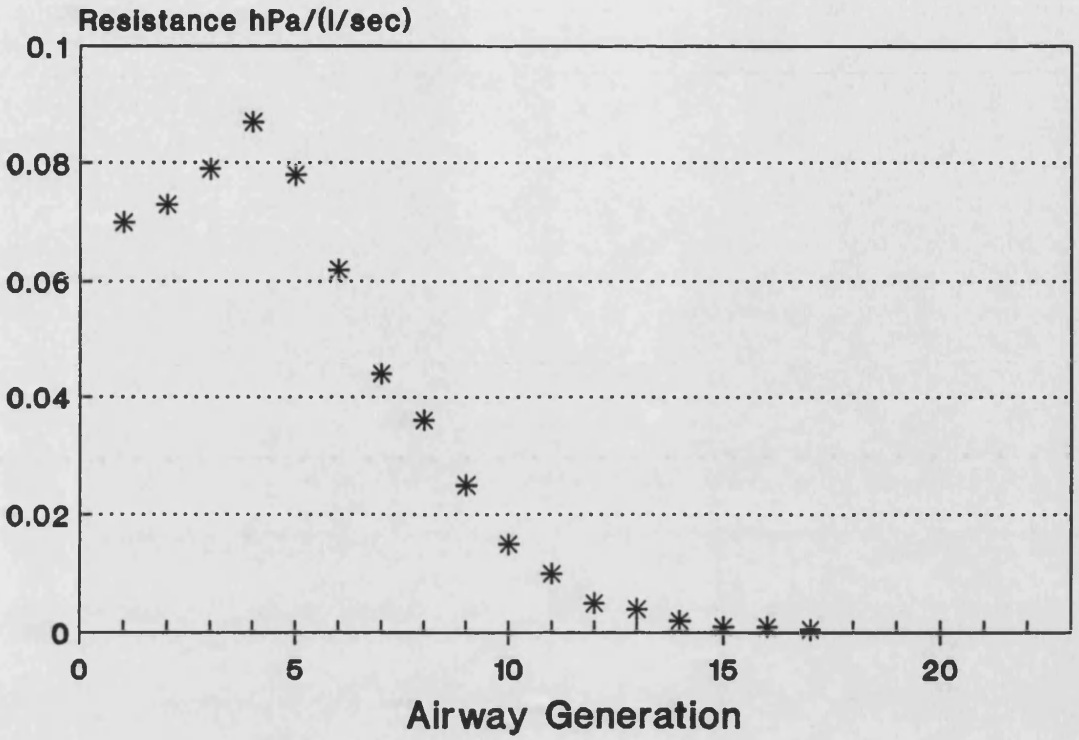

Figure 1.4 Resistance of Airway Generations

mouth and alveoli, with alveolar measurements being deduced from body plethysmograph measurements. It is of interest to note the distribution of resistance throughout the airway tree. It has been shown that less than 20% of the total resistance is from airways of 2mm diameter and less (Macklem and Mead, 1967). The remainder arises from the medium size bronchi. Although the peripheral airways are narrower their small contribution is due to their prodigious number acting in parallel, illustrated graphically in figure 1.4. Resistance is a function of lung volume increasing hyperbolically as volume falls. At very low lung volumes small airways close completely trapping gas in the lung. The compliance of the lung is reduced at large lung volumes due to the increased recoil pressures. In addition to airway resistance there are resistive contributions from the lung and chest wall tissues. Resistance values including these components are generally referred to as total respiratory resistance, with table 1.2

Contribution	Resistance	Method
Mouth	0.5	
Larnyx	0.5	
2-3mm Airways	0.2	
Alveoli	0.2	Plethysmography
Lung Tissue	1.2	Interrupter Method Oesophageal Balloon
Chest Wall		Oscillatory Method
Total hPa/(l/sec)	2.6	

Table 1.2 Breakdown of Total Respiratory Resistance Components

illustrating the contributions to the total from different components, in normal males. Additionally the table shows which components are determined by a number of techniques. It is important when comparing techniques to be aware they are actually measuring different components. Oscillatory resistance values will therefore always be highest as they contain the chest wall component. Nevertheless the measurements are useful in monitoring airway calibre as chest wall resistance is relatively unaffected by diseases of the lung, (Cotes, 1979:124). The oesphogeal balloon method is invasive with a pressure transducer being introduced into the lung. Interrupter techniques involve occluding the mouth and assuming measured pressure at the mouth will be representative of alveolar pressure. Plethysmographic methods require subjects to sit in a body box and breathe at certain frequencies during which pressure and flow are measured and lung volume may be determined. The latter method is probably the most widely used approach for measuring airway resistance.

Alternative techniques for measuring small airway function will

not be discussed as they are clearly documented and reviewed in the literature (McFadden *et al*, 1974). Figure 1.5 is taken directly from Cotes' text and shows the relative magnitude of changes in a number of measurements following provocation tests. This is included to illustrate that the spirometric indices are the least sensitive. Compliance and conductance, (the reciprocal of resistance), measurements exhibit a greater change. Respiratory impedance data may be used to distinguish between compliance and resistance changes by considering the real and imaginary components separately.

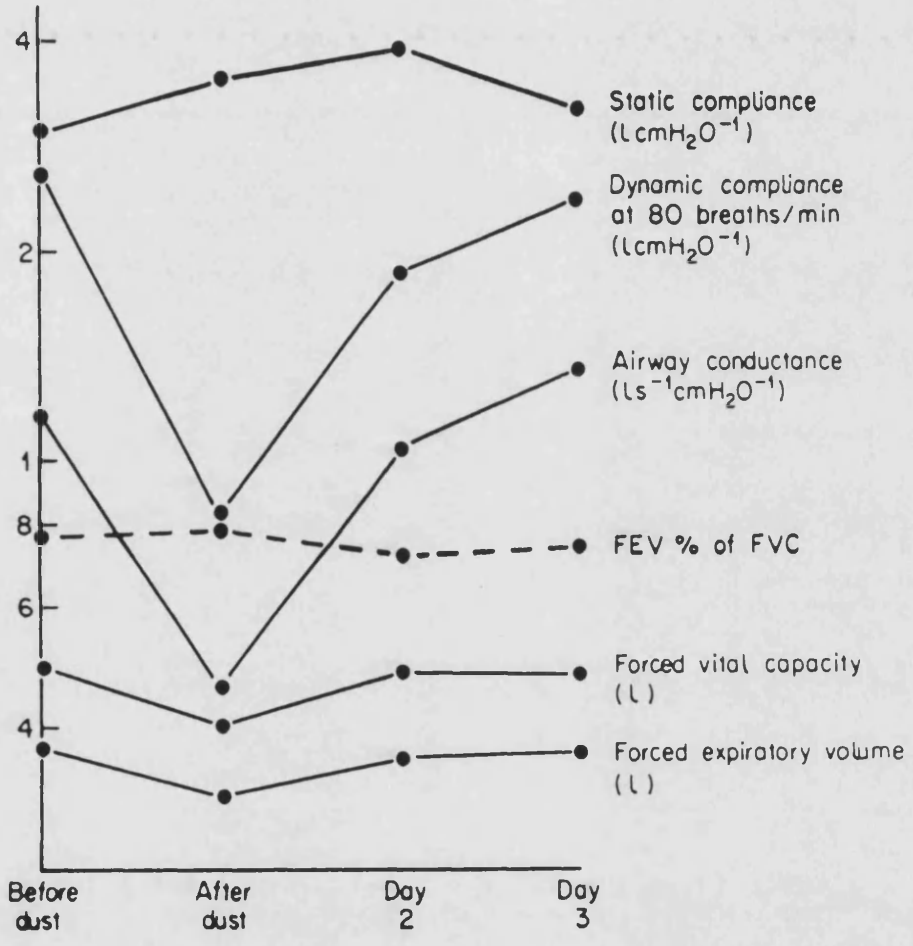

Figure 1.5 Magnitude of Change Following Provocation Test

Chapter 2 The Literature Reviewed

2.1 Introduction

The literature section reviews publications associated with the oscillatory airflow method. The review is composed of a number of sub-sections, enabling individual discussion of specific aspects. Initially the pioneering work is described, illustrating the original instrumentation and processing. The technique was developed and applied by more groups and gradually the range of results and reproducibility of the test were quantified. Enhancements to the processing were made enabling the automation of impedance calculation, which was originally achieved manually. A common feature of the first sub-section is that all measurements were single frequency, the second sub-section describes multiple frequency determinations and the extra processing involved. Subsequently the use of results to model the respiratory system are discussed.

The section describes the literature as it was in early 1988, the commencement of this project. During the research additional papers were published which influenced the direction of the research. A major development during 1990 was the discovery of a group, originated as part of the European Economic Community Concerted Action Strategy, addressing technical issues associated with the determination of respiratory impedance. The group of engineers, scientists and clinicians considered improvements to instrumentation and processing to ensure high quality data, leading to standardisation of equipment and results. The Medical Physics Department at the Royal United Hospital, Bath subsequently became contributing members of the group. To reflect the importance of these developments information emerging from the

group and other published work will be introduced as necessary. This ensures the chronological order of events is accurate and illustrates how the latest published research influenced the work in our laboratory.

The technique is often described in the literature as the forced oscillation technique. It is unfortunate that the word forced was used to describe the method as it conveys a misleading impression. Among respiratory clinicians it is generally associated with a maximal subject effort, as in forced expiration for example. While it is true that a small forcing function is applied to the respiratory system the subject cooperation is minimal, and clearly sub-maximal Therefore throughout the thesis the technique is deliberately referred to as the oscillatory airflow method.

A criticism of much of the literature is the manner in which the normal data is presented. Often the groups are small, of mixed sex and include smokers. When validating a technique, particularly if it is claimed to be sensitive, it would seem sensible to keep the normal group as pure as possible. Smokers therefore would be more suited to a group of their own. Male and female results should be differentiated between, as on average women have a higher respiratory resistance then men. This is probably due to the slighter smaller geometry of the large airways. Figures taken from Reference Man, (ICRP Publication No. 23), give the diameter of the right bronchi as 17mm in males and 15mm in females, the lengths being 23mm and 21mm respectively. Using Poiseuille's formula, equation 1.1, to estimate the resistance of this airway alone gives the female value some 50% greater than the male, reflecting the importance of the fourth power of the radius in the denominator of the calculation. Although the flow is not laminar in

these airways and hence the resistance values not accurate, nevertheless the estimate serves to illustrate that female resistances will be higher. The effect of grouping male and female results will be to broaden the range of results.

Whenever possible results will be extracted from the literature, although sometimes this is difficult if results are only presented graphically. The group size and composition will be given to aid comparison. It is important to the acceptability of the technique that comparable results are obtained between groups. Originally much of the data was quoted using pressure units of centimetres of water, in order to standardise, using SI units, all pressures have been converted to Pascals.

2.2 The Single Frequency Work

The origins of the oscillatory airflow method to asses lung mechanics dates back to the mid 1950's when DuBois *et al* (1956) published their classic paper on the oscillation mechanics of lungs and chest in man. The idea was, and still remains, an elegant technique for non-invasively characterising the pressure-flow response of the respiratory system. A common feature of work reported in this section is that measurements are made at one frequency at a time. To build up a frequency response profile therefore requires a series of measurements at different frequencies.

DuBois *et al* used a fixed stroke volume, variable frequency mechanical pump to apply a sinusoidal oscillation at the mouth. Volunteers were asked to relax, not to breathe, with pressure and flow measured at the mouth. Peak to peak pressures and flows were divided to yield the magnitude of the impedance, with the phase angles between

the waveforms giving the argument. Successive measurements were made to build up a frequency range of 2 to 15Hz, with subjects lying on their backs. This enabled horizontal, head to foot and vertical chest and abdomen motion to be recorded as the oscillations will cause movement external to the lung.

Impedance results in the paper were presented graphically for the seven volunteers. The results were variable and the group small, nevertheless the paper demonstrates the feasibility of the method, albeit technically demanding as results were computed by hand. It is difficult to summarise the results accurately, however, the magnitude of the impedance at 5Hz was around $4hPal^{-1}s$, with a phase angle of -10°. By 10Hz the magnitude had risen slightly, the phase angle had become positive.

The work of DuBois *et al* inspired a number of other groups who saw the potential of the technique. The first major development was to allow patients to breathe during the test by adding a side tube, of low resistance, between the generator and flow transducer. This advance is generally attributed to Mead, whose clinical system was described at a meeting in 1965 by Schwaber *et al*. In terms of processing it was possible to distinguish between spontaneous respiration and the applied signal due to its much higher frequency, typically a thirty fold difference. By 1968 most groups were attempting to make measurements at the resonant frequency where the impedance is purely resistive. The work of Fisher *et al*, 1968, reports respiratory resistance in a group of 42 normal subjects, using a mechanical pump and varying the frequency until resonance is achieved. Sobol *et al*, 1968, also reports normal values for 35 subjects, however they are unable to achieve resonance in some subjects in the 3 to 9Hz frequency range. Therefore

they artificially achieved resonance by correcting the pressure signal electrically until pressure and flow were in phase. Knowing the correction factor enabled an estimate of the phase angle at which the 6Hz measurement was made. They choose to quote impedance magnitude and the phase angle at this set frequency. Table 2.1 summarises the impedance data from both papers, with airway resistance determined by body plethysmography and the final three columns detailing the impedance measurements. The group of results from Fisher *et al* comprised 25 men and 17 women, including 13 smokers. Sobol *et al* do not describe the composition of their group and chose the frequency of 6Hz based on the resonant frequency quoted by other workers. This was fortunate as it makes the results comparable, both groups measured airway resistance by body plethysmography with Sobol's results a little lower. The data is useful as it begins to illustrate the normal range of respiratory resistance and the statistical spread of the results. The airway resistance values are lower as they do not include a tissue and chest wall component. The impedance values are considerably lower than quoted by Dubois *et al* as their measurements were made with supine subjects whereas the later measurements were in seated subjects. By comparison to Fisher *et al* it seems surprising that Sobol *et al* observed such a wide range of phase angles in the normal group. The data of Fisher *et al* comprises both male and female results, the paper reports that women, on average, have a higher respiratory resistance by around $0.4 hPa l^{-1} s$. Patient results will not be discussed yet as it would confuse the issue, as the equipment used by all groups was yet to yield comparable results in the normal groups. Fisher *et al* quotes resonant frequencies for patients lower than normals, whereas Sobol *et al* quotes them being higher. Grimby *et al* (1968), concurs with Sobol

et al stating that while resonance in normals is to be found in the range 5 to 7Hz, patients with lung disease had no demonstrable resonant frequency below 10Hz. Grimby *et al*, who used a loudspeaker to generate the airflow, also applied an electrical correction to simulate resonance. Data was given for the frequency dependence of resistance in patients by making measurements at 3, 5, 7 and 9Hz. This showed a marked rise in resistance as frequency falls, which is interesting as it remains broadly constant in normals, which is substantiated by including, on the graph, a colleagues unpublished results. This is the first sign of the potential sensitivity of the technique.

Group	Size	Ages	Airway Resistance $hPa^{-1}s$	Respiratory Impedance $hPa1^{-1}s$	Frequency Hz	Phase °
Fisher	42	18-79	1.3±0.3 0.8-2.4	2.3±0.5 1.3-3.3	6.6±0.7 5.2-7.9	0
Sobol	34	19-58	0.92±0.32 0.52-1.78	2.2±0.58 1.2-3.9	6 fixed	7.6±6.7 0-22

Table 2.1 Comparison of Impedance and Body Plethysmography Results, results are means±standard deviations and data ranges.

In 1970 the technique took a step forward when the processing was automated. Goldman *et al*, 1970, noted that by analyzing specific points on the pressure and flow waveforms eliminated the need to

achieve resonance at all. They argued that if consecutive points of peak flow were sampled, and the corresponding pressure values at these points determined, then resistance was obtained by dividing the pressure difference by the peak to peak flow value. Points of peak flow correspond to points of zero acceleration so there can be no reactive inertial component. Also these points occur at equal volumes so the pressure relating to elastic components must be the same, hence the difference must be wholly attributable to the resistance of the system. Instrumentation was built to achieve this measurement, with a loudspeaker used to generate a fixed frequency airflow of 6Hz. The paper reported the processing, although did not present any significant body of data. A few months later, Hyatt *et al*, 1970, described a similar instrument which used the same philosophy but produced a direct write out of resistance to a chart recorder.

The early pioneering work established the technique as a means of non-invasively assessing respiratory resistance in a manner requiring minimal subject cooperation. The initial instrumentation was complex, although automated analysis of pressure and flow were beginning to emerge. The airflow began to be generated by loudspeakers rather than mechanical pumps. Using a readily available component seemed a logical move, additionally the loudspeaker could follow any applied voltage whereas pumps were limited by their mechanical complexity. Normal ranges for respiratory resistance began to emerge, which were compared with airway resistance values from existing methods, predominantly body plethysmography. Little attention at this stage had been given to measurements above 10Hz, or the reactive component of the impedance. Normal resistance appeared roughly constant over the frequency ranges considered, yet patients appeared to exhibit a marked frequency

dependence of resistance.

2.3 Multiple Frequency Impedance Measurements

The benefits of determining the respiratory impedance frequency response having been identified, more groups began to publish such data. The build up of these results by successive single frequency measurements is time consuming, especially if an extensive frequency range is considered. Indeed, Pimmel *et al*, 1980, quoted a measurement time of fifteen minutes to obtain results at all frequencies. The question which then arises is how comparable are the results, particularly if they are taken after drug administration. It became clear that for meaningful impedance versus frequency data it was necessary to make simultaneous multiple frequency measurements. It also became apparent that mechanical pumps were unable to produce adequate sinusoidal airflows due to their limited mechanical response time. The result was that the loudspeaker became the generator of choice for most groups, which began to offer greater flexibility in the choice of airflow. With pumps the design of the airflow was incorporated into the mechanics of the drive mechanism, to generate more sophisticated signals meant prohibitively complex mechanics. The loudspeaker, however, would follow any driving signal. The signal may be designed electronically and used to excite the speaker. This enabled multiple frequency airflows to be produced. Michaelson *et al* in 1975 used a random noise signal containing all frequencies up to 40Hz. This required more sophisticated processing techniques using Fourier analysis to resolve the composite pressure and flow signals into their individual frequency components from which impedance was calculated at each frequency. Equipment was now available which

achieved the spectral analysis and gave results at the time of the measurement, spectra were subsequently stored and plotted off-line. Their work was very thorough and the method was described in detail, indeed the analysis formed the basis of the work in our laboratory. Effectively the procedure uses the band-width limited noise signal to probe the respiratory system, in a similar fashion to using a random voltage signal to characterise an electrical network.

As the approach is based on statistical techniques the impedance was no longer calculated by the direct division of pressure and flow values. The processing builds up an average impedance estimate. A summary of the analysis is presented in table 2.2, the underlying theory will be discussed later. Having transformed the pressure and flow into the frequency domain, power and cross power spectra were determined, with the latter preserving the phase information between pressure and flow. Impedance was then calculated in polar form as shown in the table. By substituting the constituent elements of the cross power spectra into the expression for the modulus it becomes clear that it effectively reduces to pressure over flow. By computing impedance in this manner it is then possible to obtain the coherence function, an index of data integrity, which is analogous to correlation in the time domain. Varying between zero and one, low coherence values suggest poor signal to noise ratio, system non-linearities or the presence of extraneous noise. To obtain smooth spectral estimates the collected data is split into smaller sections and averaged in the frequency domain.

Results were presented for groups of normals, smokers and patients with obstructive lung disease. The data was presented graphically over the range 5 to 40Hz, with the measurements being made

Description	Formula and Symbols	Spectral Result
Pressure Fourier Transform	S_x	Complex
Flow Fourier Transform	S_y	Complex
Pressure Power Spectra	$G_{xx} = S_x \cdot S_x^*$	Real
Flow Power Spectra	$G_{yy} = S_y \cdot S_y^*$	Real
Cross Power Spectrum	$G_{yx} = S_y \cdot S_x^*$	Complex
Impedance Modulus, Z	$\frac{G_{xx}}{\sqrt{Re(G_{yx})^2 + Im(G_{yx})^2}}$	Real
Phase Angle, θ	$-\arctan\left[\frac{Im(G_{yx})}{Re(G_{yx})}\right]$	Real
Coherence Function, γ^2 $0 \leq \gamma^2 \leq 1$	$\frac{Re(G_{yx})^2 + Im(G_{yx})^2}{G_{xx} \cdot G_{yy}}$	Real

Table 2.2: Respiratory Impedance Formulae

in seated subjects, breathing continuously while wearing a nose clip. The measurement duration was 16 seconds. The results are interesting for a variety of reasons. They show, as earlier work suggested, patients have a different impedance frequency response compared to normals and that the groups are clearly distinguishable. It is also of interest to note the ability of the technique to discriminate between smokers and non-smokers. Data was now available in a form whereby it could be used for modelling the respiratory system. They discussed the normal results in terms of a second order system and modelled them using a three component series network, comprising resistive, R, inductive, L, capacitive, C, elements. This will be discussed in more detail later, briefly, it appeared the normal system exhibited a resonant frequency around 8hz below which the phase was negative and impedance rose due to the compliance effects, with phase becoming positive above resonance again with a rise in impedance associated with inertial effects. The work presented was extensive, illustrating the effects of different lung volumes on impedance as well as the ability of the system to follow changes due to bronchodilator administration.

At first sight the data seems remarkably smooth having been obtained from such a complicated network as the lung. This is due, in part, to the processing approach. The sixteen seconds of data were split into one second epochs, each of which was averaged in the frequency domain, from which the smoothed impedance estimate was calculated. The flow amplitude was adjusted to be the same for all subjects, additionally the power spectrum was checked to ensure it was constant with frequency. As resistance is flow dependent the latter point ensures comparable resistance values at all frequencies. As mouth pressure is measured the impedance also includes contributions

from the mouth, cheeks and extra-thoracic airways. In an attempt to eliminate the effect of these structures Michaelson *et al*, (1975), estimated mouth impedance by making a measurement while subjects maintained a closed glottis. This data was used to correct the resultant impedance. The system used a 30cm diameter loud speaker, producing peak to peak pressures of 2hPa and flows of $1ls^{-1}$.

The mean value of normal resistance, for ten male volunteers breathing continuously, of $2.08hPal^{-1}s$ quoted at the resonant frequency of 8.04Hz, which compared well with the results from the single frequency work. Numeric data values are summarised in table 2.3, for normals, smokers and patients with chronic obstructive pulmonary disease, (COPD). The coherence function was used to reject data, with a threshold of 0.85 used as a lower limit for acceptable data. Values below 5Hz appeared to fall below this and therefore the data was rejected, although the oscillatory airflow appeared to contain frequencies down to 1Hz. The use of a coherence function threshold as a criteria for data rejection will be discussed separately. Extending measurements up to 40Hz meant that transducers had to be checked to ensure they were matched for amplitude and phase and hence did not introduce any artefacts.

The following year Landser *et al*, (1976), published a paper making impedance measurements between 2 and 30Hz. The driving signal in this case was an impulse containing all harmonics of 2Hz up to the maximum frequency of 30Hz, hence impedance is available at 2Hz increments.

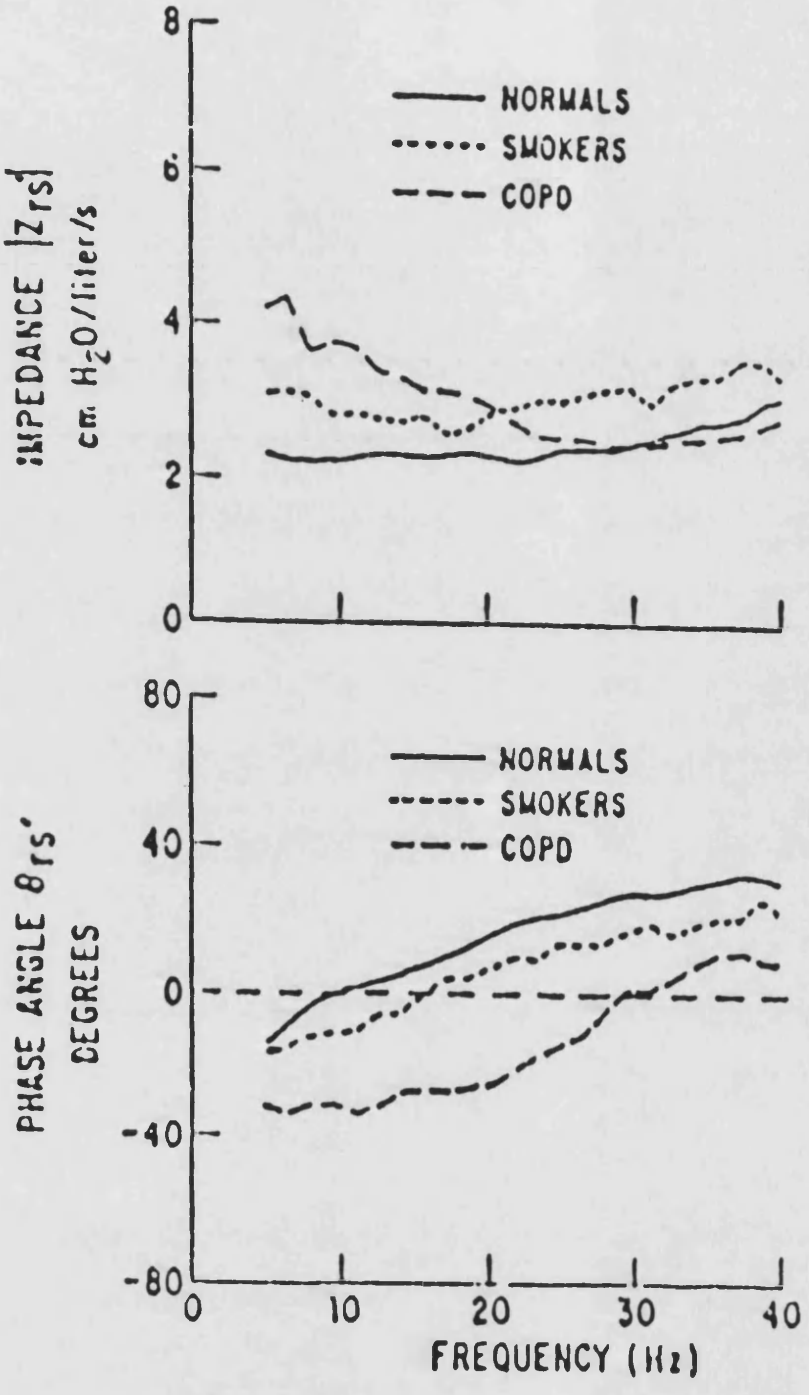

Figure 2.1 Michaelson *et al*, (1975), Mean Impedance Curves

Group	Resonant Frequency, f_n Hz	Impedance Modulus @ f_n $hPal^{-1}s$	Impedance Modulus @ 40Hz $hPal^{-1}s$	Phase Angle @ 40Hz degrees
Normals:mean±sd (10 subjects)	8.04±0.96	2.08±0.41	4.12±0.88	64.9±9.5
Smokers:mean±sd (5 subjects)	7.96±1.24	2.65±0.37	5.24±1.75	56.8±5.67
COPD:mean±sd (5 subjects)	19.12±6.35	3.90±0.96	5.43±1.57	37.4±12.9

Table 2.3 Michaelson *et al* (1975), data summary.

Otherwise the analysis was as described by Michaelson *et al*, (1976), with an identical Fourier analyser being used. Landser *et al*, (1975), concentrate on the technique rather than its application, although data is presented for ten normal, non-smokers appearing to be similar to the results above. A coherence function value of 0.95 was proposed as a threshold for data rejection on the basis that this gave an error in the measurement of under 10%. This gave coefficients of variation of 12% and 20 to 30% for the resistance and reactance respectively. In healthy subjects Landser *et al*, (1976), observed a small progressive increase of resistance with rising frequency above 12Hz whereas Michaelson *et al*, (1975), did not. Another difference between the data was that Landser's group did not apply the correction factor for the

upper airway artefact.

Both these papers described a practical implementation of the oscillatory airflow method. Most current systems are based on these earlier works, as the instrumentation in this form was clinically applicable. The execution of the test was now rapid, as the need for successive single frequency determinations had been eliminated. The advent of dedicated spectral analysers and improvements in technology in general having made the analysis achievable on-line. In particular the development of the fast Fourier transform by Cooley and Tukey, (1965), a numerically efficient implementation of the discrete Fourier transform, has made a considerable impact on processing times. Michaelson *et al* described their technique as the forced random noise technique, with Landser *et al* adding the adjective pseudo to illustrate the latter work used a non-continuous frequency spectrum. The results both groups obtained were in a form suitable to develop respiratory system models, comprising electrical component analogues.

2.4 Modelling the Healthy Respiratory System

The impedance versus frequency data may be used to model the respiratory system by fitting curves to the data representing the impedance of electrical networks. Electrical components are used due to the similarity between voltage and current and pressure and flow. Resistors, inductors and capacitors are used to model the resistive, inertial and compliant properties of the lung and chest wall.

The motivation for modelling arises from the observation that respiratory resistance exhibits frequency dependence in the presence of obstructive lung disease. this was shown by the early work of Grimby *et al* 1968. Yet in normals the resistance is more constant with

frequency. The marked frequency dependence implies that an electrical model would need to include more than one resistor to mimic this behaviour. If physiological significance could be attached to these resistors it means that the mechanics of the lung could be divided into regions of contribution. This is particularly exciting if model elements can be attributed to peripheral airway resistance as this is thought to be the site of the onset of lung disease (Mead *et al*, 1967, Macklem and Mead, 1967 and Hogg *et al*, 1968). Bearing in mind the peripheral airways contribute less than 20% to the total resistance they may be considerably occluded yet not increase the total value to fall outside normal limits, as assessed by conventional indicators of lung mechanics. If the impedance method can be shown to identify increased peripheral resistance it would have potential as a screening test.

The use of models is also appealing as normal results seem to be described by a simple, second order model comprising a series connection of a resistor, inductor and capacitor, figure 2.2. This model gives a constant resistance versus frequency, with the capacitive and inductive element being selected according the reactive nature of the data. More complicated, higher order, models have been suggested but over the frequency range 1 to 40Hz this simple model seems acceptable. It also has the advantage that the model elements can be uniquely determined using linear calculations. Further complicating the normal model would also complicate a more sophisticated patient model leading to difficulty in uniquely determining components within the model. Bearing in mind this limitation the simple three component model was a logical starting point, plus the addition of an additional resistive, capacitive element in an attempt to model the patient data.

If such an approach yields information distinguishing central and peripheral airway components this may well be all that is required clinically.

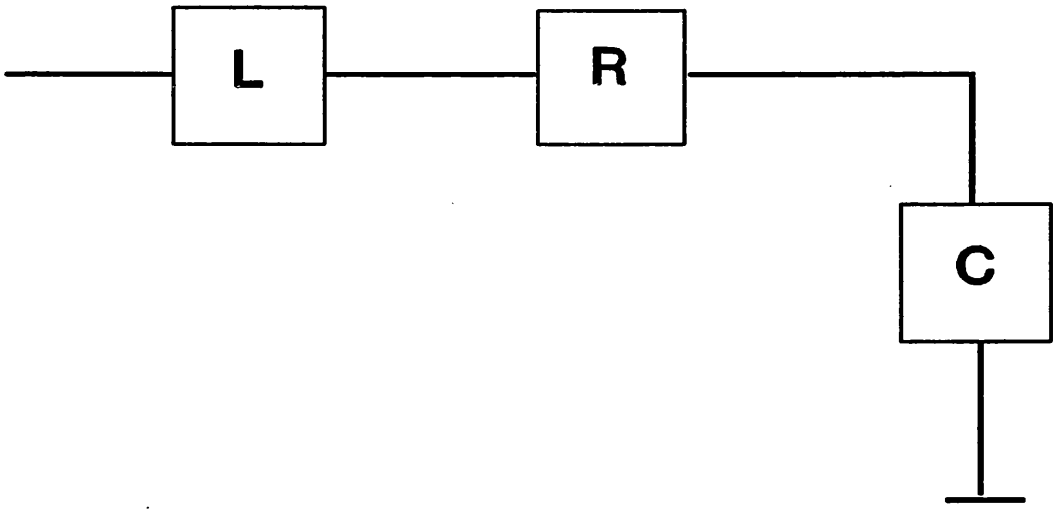

Figure 2.2 Series RLC Component Model - Healthy Lung

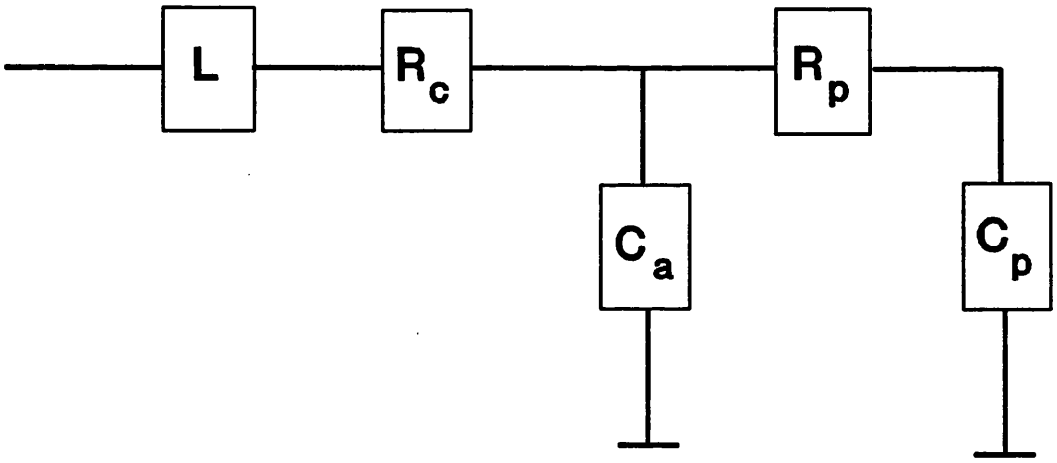

Figure 2.3 Extended Model - Diseased Lung

Mead, (1969), described a five compartment model to explain the rise of resistance with falling frequency. The model comprises the three compartment RLC model, with an additional RC element, as shown in figure 2.3. The inductor represents the inertia of air in the lungs, R_c represents central airways resistance, with C_a representing the

compliance of the airways. R_p and C_p refer to the resistance of the peripheral airways and the compliance of the alveoli respectively. In the healthy lung the alveoli are considerably more compliant than the airways. If peripheral resistance increases the point could be reached where, considering the time constant units of the model, R_cC_a is very much greater than R_pC_p. At low frequencies the total resistance would be the sum of R_c and R_p, as both units could respond. As the frequency increased the longer time constant unit comprising the peripheral resistance and alveolar compliance would be unable to fill and empty. The total effective resistance would become purely the central component, R_c. Hence at low frequencies a higher resistance would be observed, which fell with increasing frequency towards the central value. This appears to fit with the observed data, in the case of normal data the second resistor capacitor combination does not play a significant part and may be ignored.

Michaelson *et al* used Mead's model to explain their data and later Pimmel *et al* (1978) described a method for estimating central and peripheral resistance from resistance versus frequency data. The work was done in dogs and based on the work of Mead as his model suggests a method whereby the slope of the resistance versus frequency curve, plotted on a log-log scale can be used to fractionate total resistance into central and peripheral components. They tested the method by adding an external resistor which should, in theory, only increase the central resistance. The increase of the added resistance represented 85% of the value of the added component. Pimmel's work assumed that the 1Hz experimental resistance value obtained was representative of the steady state flow resistance. Slutsky and Drazen, (1978), reanalysed Pimmel's work based on an alternative fractionation

algorithm by using linear regression to fit the resistances to the exact equation of the model network. With the added resistor they estimated central and peripheral resistances as 2.71 and 1.84hPal^{-1}s respectively, while Pimmel *et al* found values of 3.13 and 1.63hPal^{-1}s.

Williams *et al* (1979) reported the respiratory impedance in sixteen children, aged 3 to 5 years old, This is an interesting paper as it shows the applicability of the technique in those who are unable to cooperate fully, thereby rendering conventional tests useless. Also it gives an insight into impedance values and their reproducibility in children. Measurements were made over a 15 to 35Hz frequency range and the results were fitted to the standard RLC model. Values were a resistance of 5.61hPal^{-1}s, an inductance of 0.012hPal^{-1}s^{2} and a capacitance of 4.03mlhPa^{-1}, with coefficients of variation of 15% for the resistance and 25% for the inductance and capacitance. As expected the resistance would be higher than the normal adult group due to the smaller airway dimensions, yet the reproducibility is similar. The resistance results seemed to exhibit a slight fall with increasing frequency.

Eyles and Pimmel, (1981), went on to evaluate a variety of parameter · estimation routines in three parallel models of the respiratory system. They concluded that the five parameter model of figure 2.3 was better than two variant six parameter models. They used data from their laboratory to evaluate the models with a two stage Simplex algorithm giving the best estimates.

Tsai and Pimmel in 1979 presented equations for obtaining resistance, R, inductance, L and capacitive, C, estimates from impedance data. These equations have been used in our laboratory to fit normal data to the three component model, and are presented as

equations 2.1, 2.2 and 2.3, with coefficients used in the equations defined in equation 2.4. The equations are based on the minimisation of the sum squared difference between the experimental data and the models response. For more complex models, such as figure 2.3, where both series and parallel paths exist simple equations cannot be stated. In this case iterative gradient descent algorithms provide an approach for obtaining parameter estimates.

$$R = \frac{1}{N} \sum_{i=1}^{N} Re[Z(f_i)] \qquad 2.1$$

$$L = \frac{N}{C} \sum_{i=1}^{N} \frac{Im[Z(f_i)]}{2\pi f_i} - \frac{a}{C} \sum_{i=1}^{N} 2\pi f_i Im[Z(f_i)] \qquad 2.2$$

$$E = \frac{b}{C} \sum_{i=1}^{N} \frac{Im[Z(f_i)]}{2\pi f_i} - \frac{N}{C} \sum_{i=1}^{N} 2\pi f_i Im[Z(f_i)] \qquad 2.3$$

$$a = \sum_{i=1}^{N} \frac{1}{(2\pi f_i)^2} \quad b = \sum_{i=1}^{N} (2\pi f_i)^2 \quad c = N^2 - ab \qquad 2.4$$

Where Z(f) = impedance versus frequency data

N = Number of frequency points

f_i = ith frequency point

Im = imaginary component

Re = real component

E = Elastance, the reciprocal of compliance

It is worth commenting that even in normals the resistance is not entirely flat at all frequencies. A consensus appeared to be emerging that in normals, resistance has a slight positive slope with frequency. Nevertheless this does not render the RLC model inapplicable as an

approximation to the normal respiratory system.

In addition to fitting models to the data a variety of alternative numerical estimates can be extracted from the results. As in the early work, single frequency resistance or impedance values may be quoted. The resonant frequency clearly differentiates between normals and patient groups. Pimmel has quoted average values of resistance over the frequency range 5 to 9Hz and 20 to 24Hz. The ratio of these resistances have been used to give an index of frequency dependence of resistance. Increase in low frequency resistance measurements had been found between normals and asymptomatic cigarette smokers (Kjeldgaard, 1976). He reported 3Hz resistance values of $2.2\pm0.4 hPal^{-1}s$ in 10 non smoking normals and $4.0\pm1.7 hPa^{-1}s$ in 14 asymptomatic smokers.

To conclude this section, values for RLC in normal subjects is compared between groups. The results shown in table 2.4 are extracted from Peslin's 1986 review paper. The definition of the resistance varied between groups, either being the resistance at 4Hz, 5Hz or the resistance at resonance. The resistances agree reasonably well, with the female group of Peslin having the highest mean resistance. Estimates of inductance and capacitance varied quite dramatically between groups. Peslin does not quote the frequency range over which the data is obtained. The capacitance estimate will be influenced by low frequency data, which is often poor and rejected due to low coherence values. The inertial estimate is influenced by high frequency data which may suffer from artefacts associated with the flow transducer. Even with the normal data results vary, there is little point trying to quote patient model data as the values depend on the severity of the condition and not enough published data exists to

warrant comparison of results between these small, illustrative, groups.

Group	No	Sex	R $hPal^{-1}s$	L $Pal^{-1}s^2$	C $lhPa^{-1}$
Michaelson	10	male	2.08±0.41	1.46±1.07	.029±0.17
Hayes	12	mixed	2.09±0.44	0.74±0.24	.053±0.31
Nagels	15	mixed	2.47±0.19	1.00±0.10	.054±0.17
Peslin	28	male	2.36±0.83	1.01±0.27	.030±0.08
Peslin	19	female	3.24±0.79	1.19±0.37	.021±0.05
Eyles	5	mixed	2.66±0.65	0.68±0.26	.057±0.14

Table 2.4 Peslin's survey of available impedance results

2.5 Summary

By the mid 1980's, some twenty years after the impedance technique was first described, considerable advances had been made in the sophistication and application of the method. Many groups having identified the benefits of the technique invested considerable effort in improving the processing and developing modelling algorithms. The data showed the frequency dependence of respiratory resistance in disease and work was undertaken to divide resistance into central and peripheral components. The equipment had become easier to use, due to the advent of micro computers the processing times were being reduced. The technique had been validated by comparison with airway resistance measurements, obtained by body plethysmography. The correlation

between low frequency impedance results and airway resistance was high (Pimmel *et al* 1981), with higher frequency results not being directly comparable. Most papers cited have been published by engineers who have developed their own instrumentation. The technique at this stage was not in widespread clinical use, partially due to the complexity of the instrumentation and lack of commercial products. Other factors affecting its use were the lack of large groups of reference values.

The upper, extra-thoracic airways act as an impedance in series with the lower airways and a shunt impedance for the applied flow. The lower airways within the thorax are all that are of interest, the upper airways act as an artefact. Many groups have instructed subjects to support their cheeks with their hands during the measurements. This increases the upper airway impedance, stiffens the cheeks so less signal is lost moving them. Alternatively other groups have corrected for this by making measurements with the subject closing their glottis. The result is used to correct subsequent impedance measurements. There are two problems with this approach, firstly it requires subject training and cooperation which defeats one of the main advantages of the technique. More fundamentally, however, it has been questioned how valid the correction is, as the muscle activity to close the glottis changes the upper airway characteristics as compared to during normal breathing. The resistance of the upper airway is high compared to the normal respiratory system so does not affect the measurement. In patients whose respiratory resistance is higher and perhaps comparable with the upper airway show underestimates of impedance due to the effect of the now important shunt, (Cauberghs and van de Woestijne, 1983). At this stage there was no consensus on how to deal with the problem. Peslin, 1985, suggested applying the oscillations around the

entire head, so pressures inside the mouth and externally at the cheek surface would be the same.

Poor low frequency data has resulted in few groups publishing data below 5Hz. The reason for this poor data quality is often attributed to spontaneous respiration acting as an interfering signal and introducing extraneous noise. This results in decreased coherence values and spurious data estimates. Landser, 1976, therefore suggested that data with coherence values below 0.95 should be rejected, commenting that this meant there were errors of less than 10% in the data. Franken, 1983, concurs with this and goes on to say that a coherence value may be used to compute the standard error of the measured impedance. He concludes that reliable results can only be obtained at low breathing power.

Chapter 3 Spectral Analysis Considerations

3.1 Introduction

One of the main aims of this work was to apply digital signal processing techniques in the calculation of respiratory input impedance. It is important to ensure that errors associated with the impedance estimate are acceptable and that influences due to sources of interference are minimised. In this chapter the fundamental techniques employed in the analysis are presented, together with a discussion of associated errors. The coherence function, as an indicator of data reliability, is defined and its application reviewed.

The results are used to characterise impedance variations with frequency, therefore all work has been done in the frequency domain. The major steps involved in the analysis are briefly outlined. Having collected time varying pressure and flow waveforms they are transformed to the frequency domain using Fourier analysis. The resulting frequency spectra are then used to compute power spectra from which impedance, defined as the ratio of pressure to flow, may be estimated. The coherence function is also calculated from the power spectra.

3.2 The Fast Fourier Transform

The first stage in the impedance calculation is to use Fourier analysis to resolve the time varying signals into their constituent frequencies. As only finite blocks of digitised data are available the discrete Fourier transform, DFT, as defined in equation 3.1, is used, with N representing the number of points transformed.

The direct implementation of this equation is computationally intensive. If x(n) is a complex sequence N^2 complex multiplications and

$$X(k) = \sum_{n=0}^{(N-1)} x(n)\,\omega_N^{kn} \qquad 3.1$$

$$\omega_N = e^{-j\left[\frac{2*\pi}{N}\right]}$$

N(N-1) complex additions will be required. Thus execution time is proportional to the square of the number of points transformed, which for large N rises rapidly. Efforts have been made therefore to develop computationally efficient algorithms to compute the DFT. Such algorithms exploit the symmetry and periodicity of ω_N, defined above, to achieve reductions in the number of arithmetic operations necessary. This has led to the development of a class of algorithms known as fast Fourier transforms, (FFT). Cooley and Tukey, 1965, developed algorithms enabling dramatic reductions in the number of computations necessary. Bergland 1969 wrote an informative overview of the use of FFT algorithms. Their work was based upon ensuring the number of points to be transformed was a composite number. The fundamental principle involved was to divide the original N point DFT into successively smaller N/2 point transforms, until the whole process was reduced to number of 2 point transforms. Each two point transform being determined by one complex multiplication, a complex conjugation and two additions. The complete transform now requires a number of calculations proportional to $N\log_2 N$, considerably less than the direct implementation. These algorithms are now widely used and have enhanced the use of Fourier analysis in practical engineering problems.

When considering transforming data there are a number of practical considerations. Firstly the data must be correctly sampled to ensure the Nyquist criterion is met, namely that the sampling rate is at least twice the highest frequency present in the signal being digitised. Violation of this theorem leads to frequencies above the

Nyquist frequency incorrectly appearing as lower frequencies. Additionally, due to the finite nature of the transform, data blocks may begin and end abruptly, producing a phenomenon known as leakage, causing the power at a particular frequency to spill over into adjacent frequency elements. This effect may be minimised by multiplying the time domain data with a window function of the same length as the data block, which tapers to zero at each end thus eliminating any abrupt changes. The required frequency resolution will dictate the choice of transform length, with longer transforms having greater resolution. The result of an FFT is complex and is a two sided frequency spectra, theoretically representing both positive and negative frequencies. When using results practically these spectra are generally converted to be one sided and hence represent only positive frequencies. So, considering an N point FFT applied to data sampled at a frequency f. The highest allowable frequency is 0.5f and the one sided spectrum will be of length 0.5N, with a frequency resolution of f divided by N.

3.3 Spectral Estimates and Frequency Response Functions

Considering a system with input x(k) and output y(k), which are the digitised versions of the analogue waveforms, where k is an integer from zero to N, the number of points in the sequence. Let $S_x(f)$ and $S_y(f)$ represent the Fourier transforms of the input and output respectively. Three one-sided spectra are of interest, namely the input and output auto spectra and the cross spectrum, as defined in equations 3.2, 3.3 and 3.4 respectively, with the star symbol denoting complex conjugation.

$$G_{xx}(f) = S_x(f) . S_x(f)^* \qquad 3.2$$

$$G_{yy}(f) = S_y(f)\,S_y(f)^* \qquad 3.3$$

$$G_{xy}(f) = S_x(f)^*S_y(f) \qquad 3.4$$

The defined spectra are commonly referred to as power spectra and are all functions of frequency. Auto spectra, which are real, give information regarding the spectral density of the frequencies present in the time varying signals. The cross spectrum is a complex result describing joint properties of the two data sequences, specifically it preserves the phase relationship between x(k) and y(k). An important relationship between the spectra exist as shown in equation 3.5.

$$G_{xy}(f) = H(f)\,G_{xx}(f) \qquad 3.5$$

Where H(f) is the system frequency response function. Describing H(f) using this terminology rather than as a transfer function is deliberate, as it more aptly fits the impedance estimates. Classically, transfer functions are thought of as relating input and output signals, which, in the case of the respiratory system is inappropriate, as signals are often measured at a common point. Furthermore, strictly speaking, transfer functions are derived from Laplace rather than Fourier transforms.

Cross spectrum measurements enable the complete frequency response function of linear systems to be evaluated. By rearranging equation 3.5 yields H(f), (equation 3.6).

$$H(f) = \frac{G_{xy}(f)}{G_{xx}(f)} \qquad 3.6$$

The result of equation 3.6 is complex and is commonly expressed in polar coordinates, the modulus giving information regarding the system gain and the argument characterising the phase response. The

system gain is obtained by taking the modulus of equation 3.6, with the argument being extracted from the cross spectrum, (equation 3.7).

$$\theta(f) = \arctan\left[\frac{Im(G_{xy}(f))}{Re(G_{xy}(f))}\right] \qquad 3.7$$

The discussion so far has resulted in expressions for system gain and phase response, the question which now arises is how to use these techniques to obtain impedance estimates. Classically, the system response, H(f), is defined as the output, y(k), divided by the input, x(k). If, however, x(k) now represents the pressure signal applied to the respiratory system and y(k) is the resulting flow, then impedance, by definition, is x(k) over y(k). Thus the above techniques may be used to estimate impedance, which is simply the reciprocal of H(f) as defined in equation 3.6. For clarity, equations 3.8 and 3.9 express the modulus, Z(f), and phase angle, θ(f), of the impedance.

$$Z(f) = \left|\frac{G_{xx}(f)}{G_{xy}(f)}\right| \qquad 3.8$$

$$\theta(f) = -\arctan\left[\frac{Im(G_{xy}(f))}{Re(G_{xy}(f))}\right] \qquad 3.9$$

The cross spectrum technique for determining respiratory impedance, as outlined in summary form in the literature review, was first used by Michaelson *et al*, (1975), and has since been widely adopted by others, including our own laboratory. The specific merits of this approach will be discussed more fully in the section considering errors associated with the analysis.

3.4 The Coherence Function Defined

A further relationship, stated in equation 3.10, exists between

the auto spectra and the cross spectrum.

$$|G_{xy}(f)|^2 \leq G_{xx}(f)\,G_{yy}(f) \qquad 3.10$$

This relationship may be used to compute a real valued parameter, known as the coherence function, $\gamma_{xy}^2(f)$, defined in equation 3.11.

$$\gamma_{xy}^2(f) = \frac{|G_{xy}(f)|^2}{G_{xx}(f)\,G_{yy}(f)} \qquad 3.11$$

Varying between zero and unity, coherence, analogous to a correlation function, provides valuable information regarding the relationship between the two series, x(k) and y(k). With unity signifying total coherence, lower values may be used to act as an indicator of data reliability. The coherence estimates may be used to calculate frequency dependent random errors, which in turn may be used to compute confidence intervals.

3.5 Analysis Related Errors

As the impedance calculation is achieved using a finite sample of data it is important to be aware of bias and random errors in the estimates. The design of the analysis can help in reducing errors and statistical indices of reliability, such as confidence intervals, are instructive when interpreting results. Additionally when considering biological signal processing the experimental conditions are often far from ideal. In determining respiratory impedance, for example, measurement duration will be limited by patient tolerance and it is impossible to remove sources of interference such as breathing or cardiac activity. The impact of physiological interference on the data is discussed later, this section addresses errors associated with the analysis and strategies for their minimisation.

The following discussion draws on the extensive material published by Bendat and Piersol, (1971 and 1980). In terms of nomenclature, a caret above a variable identifies it as an estimate of the true parameter value. The total analysis error comprises two components; a bias error and a random error. It is useful to normalise errors by defining them as the error divided by the parameter value, the dimensionless result is then quoted as a percentage. Table 3.1 is adapted from Bendat and Piersol, 1981, describing expressions approximating errors arising from power spectra estimates using Fourier analysis.

Parameter	Bias Error	Random Error
$\hat{G}_{xx}(f)$, $\hat{G}_{yy}(f)$	$-\frac{1}{3}\left[\frac{B_e}{B_r}\right]^2$	$\frac{1}{\sqrt{n_d}}$
$\hat{G}_{xy}(f)$	$-\frac{1}{3}\left[\frac{B_e}{B_r}\right]^2$	$\frac{1}{\lvert\hat{\gamma}_{xy}(f)\rvert\sqrt{n_d}}$
$\hat{\gamma}^2_{xy}(f)$	Undefined	$\frac{\sqrt{2}\,[1-\hat{\gamma}^2_{xy}(f)]}{\lvert\hat{\gamma}_{xy}(f)\rvert\sqrt{n_d}}$

Table 3.1 Approximations for Bias and Random Errors

A full derivation of these expressions is presented by Bendat and Piersol, (1971, and 1980), they are particularly useful as they allow an evaluation of errors using estimated values of coherence and other factors which are fixed prior to the analysis. A number of interesting points arise from table 3.1, an immediate observation that may be made is that certain errors are functions of frequency, while others are not. Furthermore, if only one Fourier transform result is used to compute auto spectra, then the random error equals one. This is unacceptable as it means the standard deviation is as large as the parameter being measured. To reduce the error the spectra must be computed from smoothed data, obtained by either ensemble averaging or, less commonly in respiratory impedance estimation, frequency averaging. Ensemble averaging is the process by which data is split into numerous blocks, with each Fourier transformed block contributing to the final spectral estimate. The larger the number of blocks in the final analysis the less the random error, however due to the square root effect in the random error denominator term, to halve the error the number of blocks must be increased fourfold. Unlike the auto spectra random errors associated with the cross spectrum depend not only on the number of blocks but also the coherence function. If the coherence values are unity then cross spectrum random errors are the same as for auto spectra. Such expressions begin to illustrate the value of using coherence function values directly to assess the integrity of impedance estimates. Coherence estimates themselves have associated errors and the expression in table 3.1 shows that for perfect coherence the random error falls to zero.

Considering the bias errors, which are equivalent for all power spectra, they are not influenced by the number of data blocks. Rather,

they depend on two frequency related parameters, B_e and B_r, the former being a function of the analysis, while the latter is an attribute of the system under test. To clarify this further, B_e, is the resolution bandwidth of the Fourier transform, broadly speaking the more points transformed the greater the frequency resolution and the smaller B_e. Clearly this is desirable, for as B_e reduces so does the bias error. Many systems under investigation exhibit a peak in their system gain, or indeed impedance, frequency response. Bendat and Piersol, (1981), define the effective bandwidth of such peaks as B_r, the difference between the upper and lower half power points of the peak. So, as the peak becomes more pronounced B_r reduces and the bias error rises. It is clear that the ratio of B_e to B_r will influence the bias error if the limiting case is considered. If the system under test exhibits a peak in the response which is narrower than the analysis is able to resolve then potentially it may be missed, clearly such a result would be biased.

The subject of bias error analysis is complex, the above discussion has focused on biases in the spectra used to compute impedance. Other factors which lead to bias errors include non linearities in the system under test and propagation time delays in measuring waveforms used in the analysis. Noise correlated with inputs will lead to bias, however uncorrelated noise will not, although the latter will increase random errors at the output. Ideally both bias and random errors would be as small as possible, unfortunately compromises are necessary in the choice of analysis parameters as conflicts begin to arise. For example, for a fixed data length the random errors are smallest if the available points are split into many small blocks. The resulting, shorter, Fourier transforms will,

however, have less frequency resolution thereby increasing bias errors.

3.6 Errors in the Impedance Estimate

It is necessary to consider the errors associated with the final impedance estimate. The preceding discussion stated errors in the spectral estimates developed from Fourier transform results, which are used to compute impedance. Additionally it is important to consider any errors in the actual estimation algorithm. The impedance magnitude is calculated by considering the ratio of the cross spectrum and the pressure auto spectrum. An alternative would be to simply take the ratio of the pressure and flow auto spectra. This is not done, however, as there are greater errors implicit in such an approach. A bias error, which is not present in the cross spectra method, occurs giving increasing positive bias with decreasing coherence function values. The auto spectra estimates of the modulus would exhibit errors of around 20%, for coherence estimates of 0.7. Furthermore, the random errors arising from the cross spectrum related measurements are less by a factor of one over the modulus of the square root of the coherence function. An obvious practical implication of this is that the cross spectra method will achieve lower impedance modulus random errors with fewer blocks of data. Therefore the cross spectrum method is considered to be the optimum frequency response function estimator.

Having chosen the estimation expression the next step is to consider the implications of bias errors in the spectra used to compute impedance. Here it is possible to use the respiratory impedance frequency response data already published and to note that it exhibits no sharp peaks. The impedance modulus minimum value, occurring at about 8Hz, is not remarkably pronounced with a relatively gradual rise

either side of the resonant frequency, which accompanies the minima. Therefore, the peak bandwidth in terms of -3dB frequencies, if the reciprocal of the impedance is considered as the system gain, may well exceed the 2 to 40Hz observation range envisaged. Using the formula presented in table 3.1, considering a spectral resolution of say 1Hz and conservatively picking 40Hz as the spectral bandwidth, (b_r in table 3.1), then the bias error would be less than one percent. It is therefore reasonable to assume that random errors are more likely to dominate the total error. The random errors for spectra presented in table 3.1 enabled a discussion of factors influencing the errors, the same parameters have a bearing on the final impedance estimate. Bendat and Piersol, 1980, give an approximation to the random errors of the frequency response function modulus, ε_r, when derived via the cross spectrum method as shown in equation 3.20.

$$\epsilon_r = \frac{\sqrt{1-\hat{\gamma}^2_{xy}(f)}}{|\hat{\gamma}_{xy}(f)|\sqrt{2n_d}} \qquad 3.20$$

The error analysis presented by Bendat and Piersol is particularly useful if, as is the case currently, the bias error is negligible and random errors are constrained to values of, say, 20% or less. The reason being that under these conditions the sampling distribution will be approximately normal, as opposed to a more complex chi-square or F distribution. Thus 95% confidence limits are simply computed from equation 3.21.

$$\hat{Z}(1-2\epsilon_r) \leq Z \leq \hat{Z}(1+2\epsilon_r) \qquad 3.21$$

Where Z is the true value, Z with caret the estimate and ε_r the random error computed from equation 3.20. Their analysis also enables a statement regarding the accuracy of the phase factor. Namely that it

approximates the modulus random error if that error is small. The modulus error approximation, using the number of spectra, n_d, and coherence estimate is therefore equally applicable to the phase estimates, requiring a simple conversion to degrees.

3.7 The Coherence Function Discussed

The coherence function has been a key parameter in assessing the reliability of impedance estimates. Throughout the research period in our laboratory it has been employed as a means to reject data and to quantitatively assess improvements in processing regimes.

Although a powerful tool for use in conjunction with frequency response estimates, care must be taken when computing the function, as the errors associated with the function itself must not be overlooked. In particular it must be computed from smoothed frequency spectra, if not then the estimate will be unity at all frequencies irrespective of the true coherence values. To clarify this point, it is known that two degrees of freedom are inherent in the first estimate of power spectra direct from the Fourier transform. The unity coherence result is analogous to drawing a line, without error, between two points; always possible irrespective of the true relationship between the coordinates. The coherence estimate therefore is biased, however the bias reduces as the number degrees of freedom, proportional to the number of spectra averaged, increase. Table 3.1 once more assists in the determination of random errors with the coherence function exhibiting a decreasing random error, which vanishes at total coherence. If coherence values are high, around 0.9 for instance then the associated error, assuming 30 spectra contribute to the average, equals approximately 3%. Even if the coherence falls to 0.5 the error is still respectable, below 20%.

The sample distribution therefore is also approximated by a normal distribution and equation 3.21 may be applied to yield 95% confidence limits. A check on the errors associated with coherence is important as the values themselves are used to compute impedance related errors. Therefore if coherence errors are high data should be rejected. When considering an error evaluation strategy it may seem computationally efficient to use coherence errors as indicative of impedance errors. Considering the random error formulae, however, suggests that, for certain values of coherence, the impedance modulus random errors will always be greater. Thus it is necessary to assess the coherence function and additionally to use it, if acceptable, to compute the impedance error. The coherence function is particularly sensitive, changes to the analysis regime can dramatically alter the value with little change to the frequency response function estimates. In particular, coherence estimates are prone to fall in value at sharp peaks in the system frequency response, possibly due to the inability of the analysis to resolve the spectral peaks. If this problem is suspected the frequency resolution should, temporarily, be improved to assess any improvement in coherence values. Otherwise other explanations must be sought to explain the reduced coherence. Factors to consider include system non-linearities, signal to noise ratio problems, including the presence of extraneous noise at the system input. It is important to note that correlated noise in the input and output will not reduce the coherence values.

3.8 Analysis Overview

The chapter has presented the fundamental signal processing techniques employed in the estimation of respiratory impedance. The

fast Fourier transform has been discussed and is the tool used to transform the data to the frequency domain. The cross spectrum method of obtaining the impedance frequency response function will be used as it is a more robust impedance estimator. Errors have been discussed and their relative importance identified, together with expressions to approximate them using the coherence estimate and the number of data blocks processed. The analysis was subsequently designed to ensure bias errors were negligible and random errors constrained, to below 20%, to enable normal distribution confidence limits to be calculated. The information presented enables an informed choice of the analysis parameters, including spectral resolution and the number of data blocks necessary. The use of the coherence function as an indicator of data integrity will be discussed later.

The discussion so far has considered the respiratory system to be linear in response and implicit in the analysis is the assumption that it is a single input and output system. This assumption was considered in more detail after the initial prototype was built and experience gained in obtaining impedance estimates and errors. A particular concern was that cardiac and breathing activity may introduce further errors requiring the analysis regime to be reconsidered and these ideas are also discussed later in the thesis.

Chapter 4 Respiratory Impedance Prototype

4.1 Respiratory Impedance Prototype

Chapter four describes the prototype respiratory impedance system built at the Royal United Hospital, Bath. It is based largely on the work of Michaelson *et al*, (1975), as their technical descriptions of the hardware and processing were detailed enough to act as a foundation for the system. The prototype work proved valuable in evaluating the technique locally, confirming its merits and enabling the deficiencies to be identified. The preliminary stage of the research highlighted those aspects of the system which required more investigation. The chapter describes the airflow generator, the system hardware, and the processing regime.

It was decided, in discussion with clinical colleagues, that no attempt would be made to initially correct for upper airways artefacts. The procedure would require training, increase the procedure time and the validity of the Valsalva manoeuvre for this purpose was questioned by our clinical colleagues. The manoeuvre involves voluntary closure of the glottis, however, the muscular activity involved will change the mechanics of the upper airways for the duration of the closure, thereby giving values of upper airway impedance unrepresentative of those during quiet breathing. Subjects were requested to support their cheeks to minimise the effect of this component. Also no attempt was made to equate the results to specific absolute lung volumes, as it would render the equipment dependent on other instrumentation. The impedance measurement therefore represents the average throughout the respiratory cycle. Effectively this measurement is different to quoting airway resistance at a set lung volume, however it was felt to

be a useful measurement in its own right. Initially one of the test's main uses was the evaluation of broncho-dilators. In this case the absolute parameter values are of secondary importance to the change between results before and after administration.

The raw pressure and flow results were saved to enable reanalysis with no high pass filtering, therefore they included the respiratory component. This meant alternative processing regimes could be evaluated and, if necessary, the results could be linked to a specific instant of the respiratory cycle. The instrumentation was designed for use in conscious, spontaneously breathing adults with measurements made in the seated position up to frequencies of 40Hz.

4.2 The Airflow Generation

The goal was to generate an oscillatory airflow containing frequencies in the range 2 to 40Hz. This involved two steps, first the generation of an electrical signal with the desired characteristics, then the translation of this into an airflow. It is the role of the generator to faithfully reproduce the required signal and to maintain the signal when loaded with the impedance of the human lung.

Traditionally loudspeakers have been used to produce the airflow, as the cone movement will follow the driving signal. It was felt that loudspeakers were not ideal as they are not designed to work against a load and respiratory efforts will create pressures that will force the cone to distort and displace. Large diameter (30cm) devices are used to achieve the necessary airflow, thus exacerbating the problem as the pressure acts over a greater area thereby applying a greater force. Due to the limited travel of loudspeakers such forces can cause the cone to reach its end stops and thereby no longer produce the correct

flow profile. The effects will be more pronounced in patients whose load is greater and respiratory efforts more. Additionally the frequency response is often not specified below 20Hz, as this is the limit of the audio range. It is interesting to note that there has been little discussion of the characteristics of loudspeakers and the resultant flow waveforms in the literature.

It was therefore decided to develop an alternative airflow generator, capable of developing a constant flow power spectrum versus frequency and being more tolerant to loads and respiratory efforts. It soon became apparent that bespoke systems would be economically unfeasible and that many mechanical solutions were impractical. The mechanical pumps, such as piston devices, cannot produce distortion free high frequency sinusoidal airflows due to their limited response when changing stroke direction. Additionally the mechanical linkages necessary to describe a multiple frequency flow are prohibitively complex. Such a solution would be inflexible as it would not be easy to change the waveform, which would effectively be an integral part of the generator.

The final solution represented a compromise. An electro-dynamic vibration generator was used to drive a set of metallic bellows. An electrical signal, applied via a power amplifier (Ling Dynamic Systems, PA100E), excited the generator platform which drove the bellows. The device (Ling Dynamic Systems, 406 generator) is designed for the vibration testing of loads applied to the platform. The advantage of this combination was a dramatically increased suspension stiffness of 16kgcm^{-1}, considerably in excess of a loudspeaker and having an available travel of ±8.8mm. The solution proved effective as the assembly was capable of producing distortion free airflows even in the

presence of sizeable static loads. This was assessed by generating single frequency airflows and comparing the resultant flow with the driving signal. The system is capable of producing either single frequency or composite airflows. An additional benefit of this combination is that the bellows' dimensions are reduced compared to a loudspeaker. This reduces the force produced associated with respiration and also reduces the inherent deadspace of the system. Thinking ahead to future applications, in say neonates, it would be possible to change the bellows for one of a smaller size. No special treatments are necessary to make the bellows airtight, often loudspeaker cones need to be coated. Preliminary investigations suggested that the generator would be capable of making measurements during anaesthesia where static ventilator pressure would render loudspeakers inoperable.

The system is, however, still limited in its low frequency response. It is effectively a more mechanically robust loudspeaker, yet the vibration generator is not designed to operate at frequencies below 20Hz. It is considerably more expensive and bulky than a loudspeaker yet the benefits were deemed sufficient to warrant the additional cost. To assess the performance of the system the frequency response of the assembly was obtained by applying constant amplitude sinewaves at 1Hz intervals in the range 1 to 40Hz, the resultant airflow being measured using a screen pnuemotachograph, (Mercury F3001) and plotted in figure 4.1. The response of the system acts like a differentiator, the output increasing with frequency. The inverse of this response was used to obtain a flat frequency response in the range 2 to 40Hz. The system was incapable of generating an adequate power level at 1Hz. This was partly due to the poor response of the

generator and the low frequency cut off of the commercial power amplifier. Nevertheless if reliable measurements are obtainable down to 2Hz this would represent a considerable improvement over the existing published literature. At this point is was decided that no further effort were made to achieve a 1Hz frequency component in the signal.

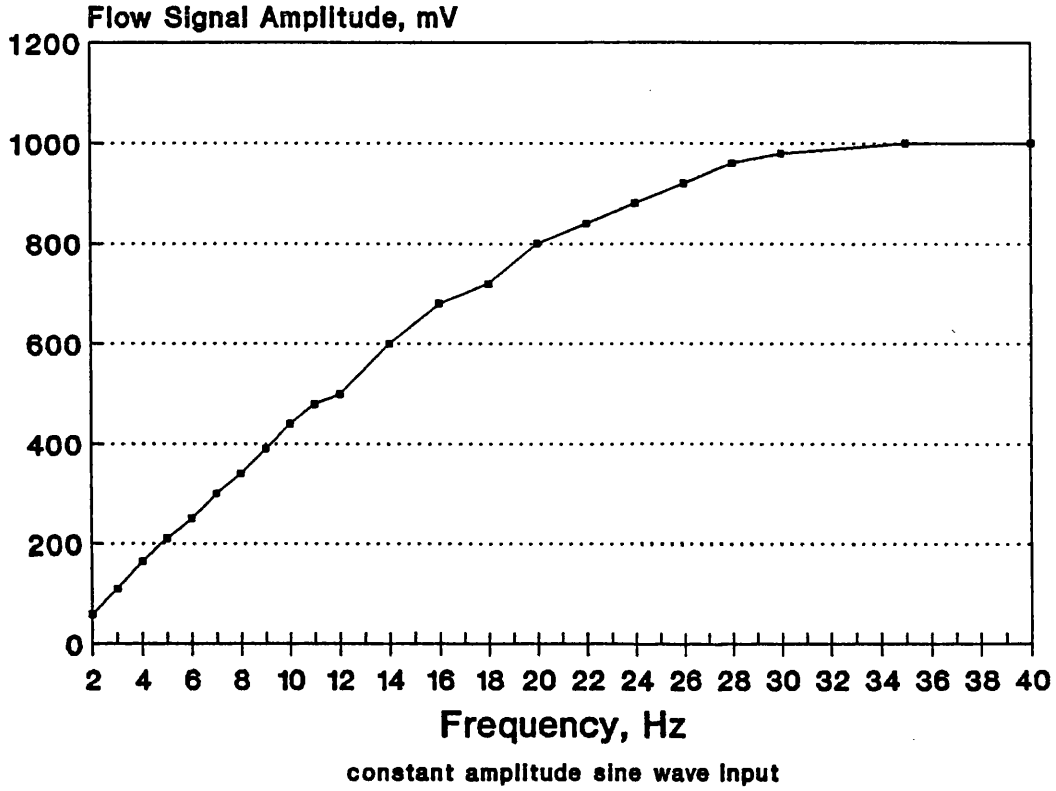

Figure 4.1 Generator-Bellows Frequency Response

An electrical random noise signal was derived from a purpose built random noise generator. The logic circuit comprised an 18 stage shift register with tapped feedback through an exclusive OR gate network, clocked at 500Hz. The result was a pseudo random binary sequence, with a flat frequency spectrum, which was low pass filtered at 50Hz. The result was a signal containing all frequencies in the range 1 to 50Hz in equal measure. A correction network comprising a network of integrators and differentiators was used to condition the

noise signal and inverse model the generator response. The resultant electrical noise spectrum, obtained using a spectrum analyser, (Hewlett Packard, 35660A), is shown in figure 4.2. The repeat sequence of the sequence was considerably in excess of the measurement period. The motivation for obtaining a flat flow power spectrum is to ensure resistances are comparable at all frequencies, as resistance is flow dependent. The ability of the system to tolerate static loads was investigated, with figure 4.3 illustrating the frequency response of the equalisation circuit and the resultant airflows in the presence of loads.

4.3 System Hardware

The generator was horizontally supported on a commercially available trunnion (Ling Dynamic Systems), with the bellows and transducers on a simple, purpose built framework. The assembly is shown in figure 4.4. All components were located as closely as possible to minimise the system deadspace and the mechanical effect of connecting tubing. The breathing port was between the bellows' outlet and the pneumotachograph, which was followed by the pressure measuring point and then the mouthpiece assembly. A screen type pnuemotachograph, (Mercury Electronics, F3001), was used to record flow, selected in preference to a Fleisch type due to its superior high frequency response associated with the smaller deadspace. The pressure drop across the screen was determined using a Validyne transducer (MP45-16). Mouth pressure is measured with respect to atmosphere using a similar device (Validyne MP45-32). The mouth pressure transducer has a range of ±140hPa, while the flow transducer gauge has a range of ±3hPa. The transducers operate on the principle of magnetic

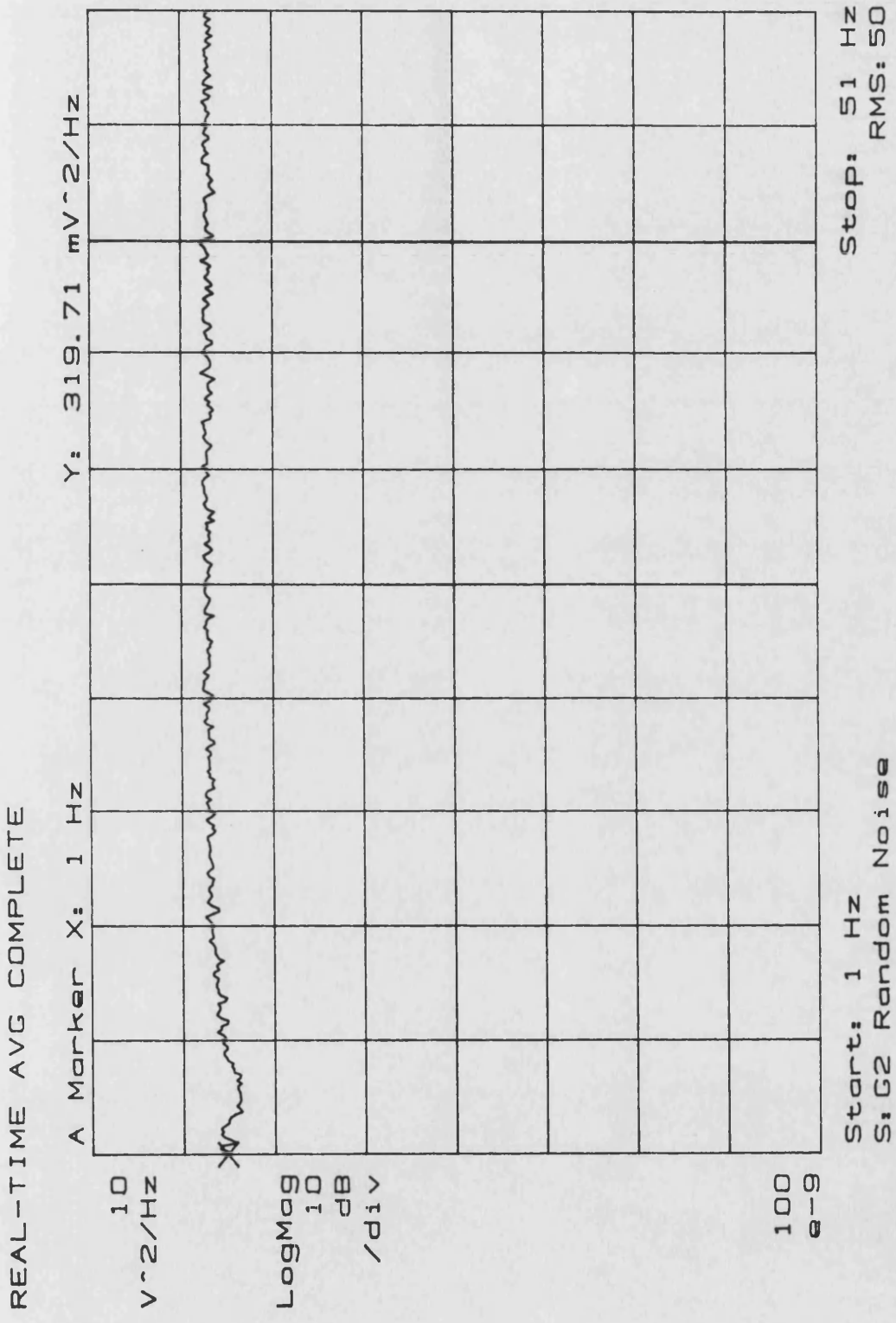

Figure 4.2 Random Noise Frequency Spectrum

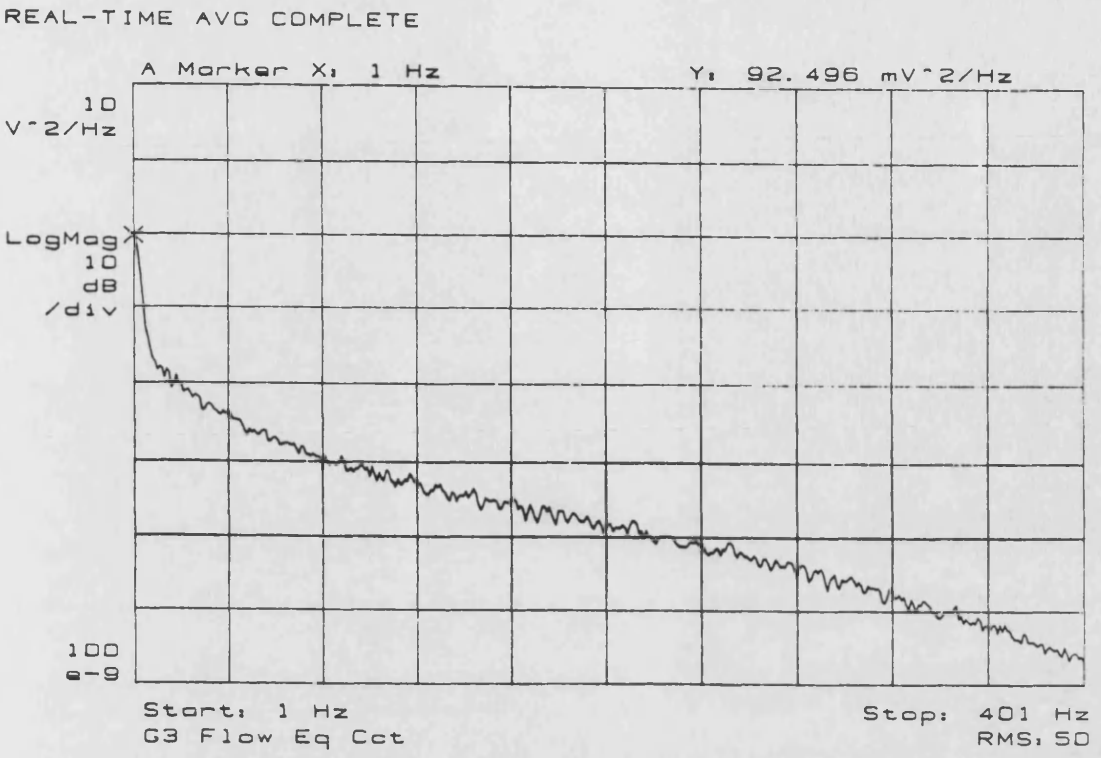

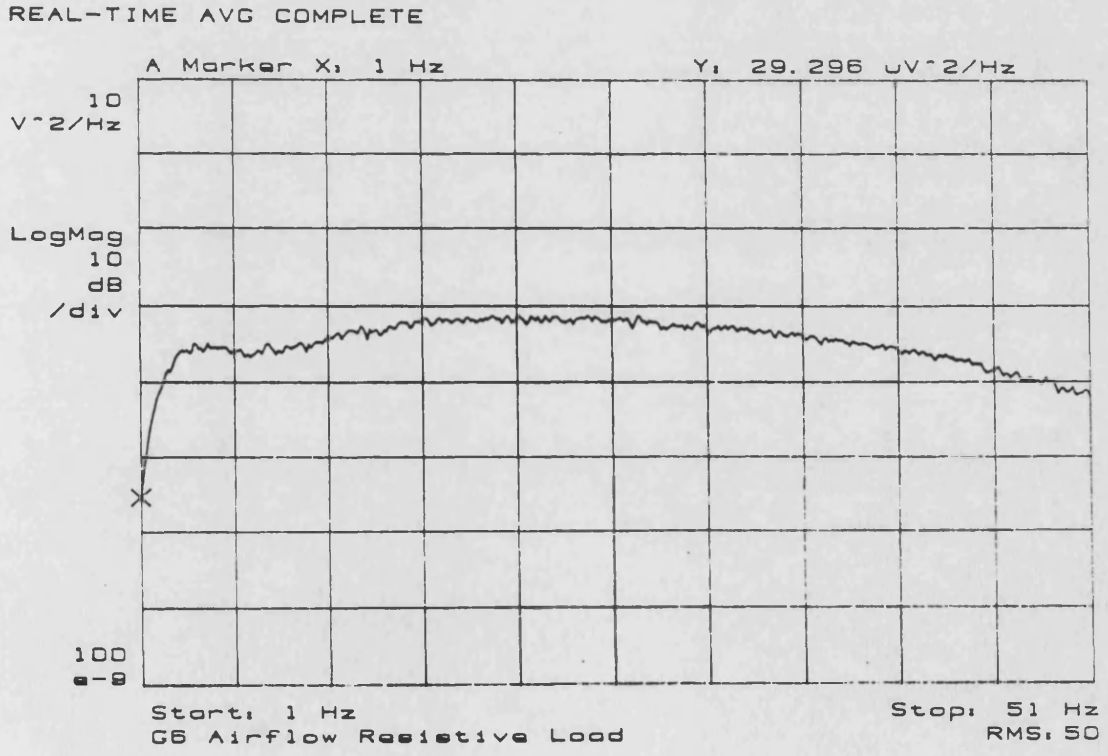

Figure 4.3 Flow Power Spectra - Equalisation Circuit (top)
& Final Corrected Spectra With Resistive Load (lower)

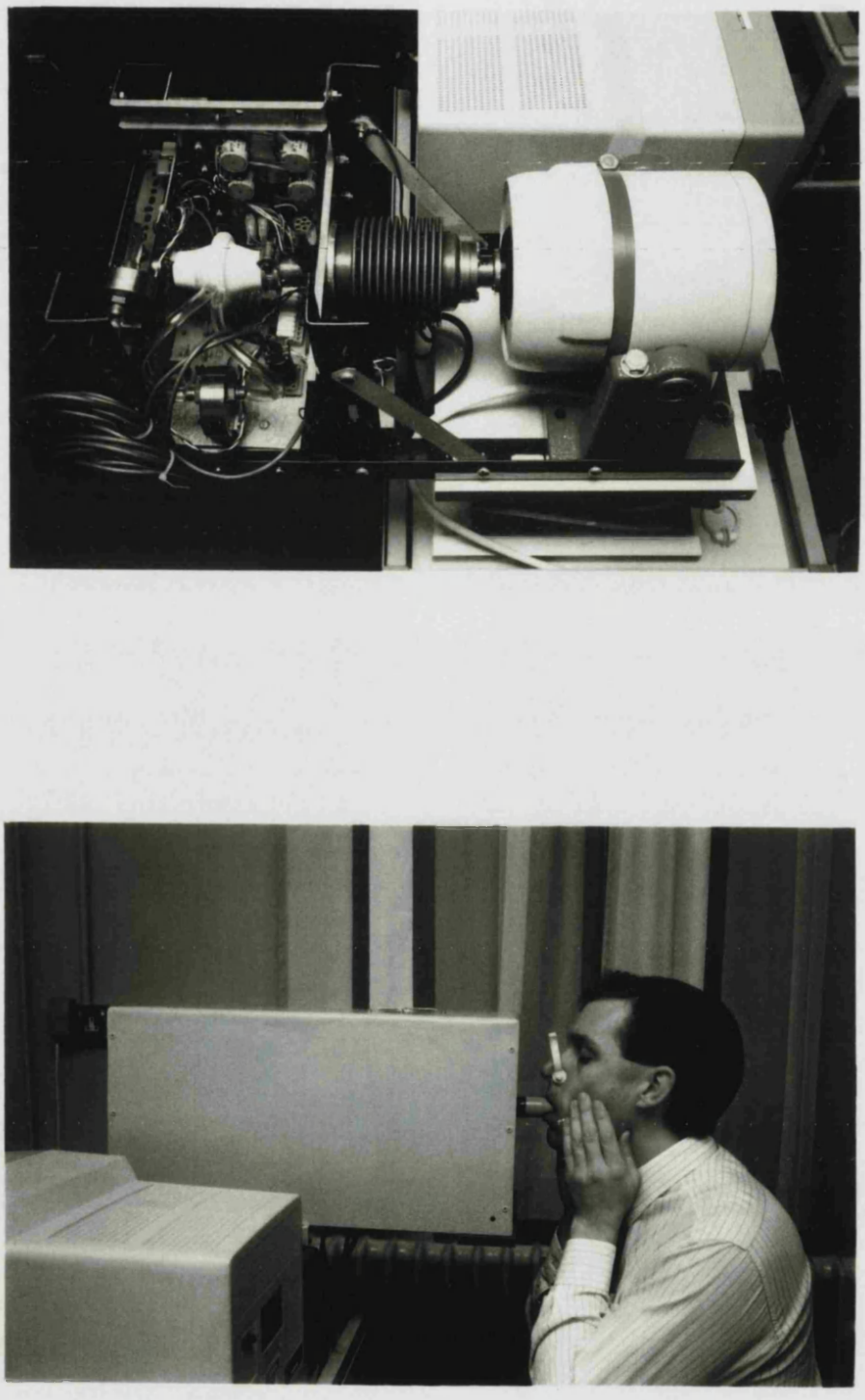

Figure 4.4 Photograph of Instrumentation

reluctance and were selected for their excellent dynamic response characteristics. This is due to their high natural frequency, low volumetric displacement and small internal volume. A carrier signal is used to excite a bridge circuit whose output varies proportionally with applied differential pressure. Of particular importance, especially in the case of the flow signal where the pressure difference is small, is the physical symmetry of these devices either side of the pressure sensing diaphragm. Stiff, clear plastic tubing of 12mm internal diameter was used to connect to the transducer ports, with all tubing being of equal length, (150mm), in order to maintain symmetry.

The breathing port is a route to atmosphere, via a load, to allow respiration. Traditionally, long, wide bore tubes (200cm, 25mm internal diameter) have been used as they act as inductors. At breathing frequencies the impedance is low, while at higher frequencies the reactive component increases due to the inertial properties of gas in the tube. The aim is to minimise the proportion of the applied signal lost through the port, though offering a low resistance route to respiration. The one litre volume of such tubes adds to the deadspace of the system and traditionally flows of fresh air have been introduced to eliminate the build up of carbon dioxide. The tube we used initially was 190cm long with an internal diameter of 11mm. This is narrower than used by most groups, yet it seemed to pose no problem for the normal volunteers and was used in the early system trials. The tube had a smaller volume than traditionally used ones, this coupled with the smaller deadspace of the system reduced the need for a bias flow. During the development phase a number of subjects tolerated periods of in excess of one minute on the system with no problems. So, no bias flow was used in the prototype to reduce the complexity of the

instrumentation, however, the system was purged between measurements by passing air through the assembly using a fan connected to the mouthpiece adapter. The tube is not shown in the photograph, as it was subsequently replaced by a resistive load comprising of a small bundle of short tubes, this will be discussed in chapter 5.

Pressure and flow signals were low pass filtered prior to digitisation to avoid aliasing. The filters had 4th order Butterworth responses, with a 50Hz -3dB frequency and were empirically matched for amplitude and phase responses, so both signals were processed in a similar manner.

4.4 Signal Processing

The impedance application code was written in-house using Borland Turbo Pascal and runs on an Opus PC V micro computer, (12Mhz 80286 processor). The code was structured to run under menu control and the general outline of the main application program is summarised in figure 4.5. The figure shows the key loops of the main program, with code indentation to the right indicating menu levels beneath the main menu. The program is characterised by four code levels, indicated by the dotted lines shown in figure 4.5. The single dotted lines illustrate global program activities, such as initialisation of memory and graphics and menu management. The double lines illustrate the main functional elements of the program, namely data acquisition, signal processing and data storage. The code was constructed in a modular fashion using a number of pre compiled units, each devoted to a particular group of program functions, the detail of which is presented in the next chapter showing the final impedance program structure.

A commercially available library of signal processing routines,

```
BEGIN (* Main Code Commences *)
  (* Program Initialisation *)
  REPEAT
    (* Menu Control *)
    CASE MENU_CHOICE OF
      1:(* Collect Data *)
        REPEAT
          CASE MENU_CHOICE OF
            1: (* Enter Patient Details                      *)
            2: (* Clear Display Area                         *)
            3: (* Collect & Analyse Data                     *)
               (* Increment Run Number & Get Comment         *)
               (* Data Collection Interrupt Service Routine *)
               (* Impedance Analysis & Display              *)
            10:(* Quit                                       *)
          END
        UNTIL QUIT_THIS_LEVEL
      2:(* Edit & Save Data *)
        REPEAT
          IF DATA_AVAILABLE THEN
          CASE MENU_CHOICE OF
            1: (* Edit Data *)
            2: (* Save Data *)
            10:(* Quit     *)
          END
        UNTIL QUIT_THIS_LEVEL
      3:(* Recall & Re-process Data *)
        REPEAT
          CASE MENU_CHOICE OF
            1: (* Recall Data     *)
            2: (* Re-analyse Data *)
            10:(* Quit            *)
          END
        UNTIL QUIT_THIS_LEVEL
      4:(* Quit Program *)
    END
  UNTIL QUIT_PROG
  (* Program Termination Sequence *)
END  (* Main Code Complete *)
```

Figure 4.5 Generalised Impedance Program Structure

(Cambridge Electronic Design, Spectrum Arithmetic Library), was used to implement the Fourier transforms and subsequent spectral computations. The computer controlled a 16 channel, 12bit analogue to digital converter, (Data Translation, DT2814) with on board timer. Two of the channels were used to digitise the pressure and flow signals, with the timer setting a sampling rate of 120Hz. As the highest frequency present was 40Hz this rate satisfied the Nyquist sampling criteria. Data was sampled for 16 seconds, which was an easily tolerable measurement period that provided sufficient data to calculate smooth impedance estimates. The data collection routine was programmed as an interrupt service routine, with the background program calculating impedance.

To achieve smooth spectral estimates the pressure and flow points were divided into one second epochs and averaged in the frequency domain. The spectrum library, which was integrated with the impedance programme, was used to compute the fast Fourier transform, which, as discussed in chapter 3, is a computationally efficient implementation of the discrete Fourier transform. A transform length of 128 points, coupled with the sampling rate of 120Hz gave a frequency resolution of 0.9Hz. Each data block was windowed prior to transformation to minimise leakage, with the blocks being overlapped by 50% to reduce loss of data due to the windowing process. A super Gaussian window was used. The overlap meant that thirty sets of pressure and flow spectra were available from the 16 second data set. The frequency domain spectra were used to compute impedance using the cross spectrum approach of Michaelson *et al*, 1975. Each data set was used to compute pressure, flow and cross power spectra which were accumulated set by set. Impedance and coherence were computed from the averaged results,

as shown diagrammatically in figure 4.6. The averaged flow power spectrum was retained and displayed to show the applied flow. The Spectrum library enabled rapid determination of the fourier transform, achieved using integer arithmetic and scaling to maintain precision. The impressive performance of the library enabled impedance to be calculated either in real time or off line for reanalysis. To do a complete retrospective analysis on the 16 second data set took less than a second. In practice, during data collection the results were updated on a second by second basis during the measurement. The quality of data could then be assessed and if a patient was unable to tolerate the 16 second measurement period results, although somewhat noisy, would be available after a minimum of a seconds data collection. When a complete data set has been collected the raw data is stored to disk, which enables subsequent reprocessing and examination of the data. The analysis and display of a full 16 second data set off line has been timed and takes less than one second. The display, figure 4.7, comprises four data versus frequency windows and being in colour enables multiple graphs to be displayed in a single window. The panel at the top of the screen displays the subjects name and the date and time of runs. The lower panel displays menu options, prompts and messages during program execution, as well as the impedance data or derived indices. The complete numeric impedance data set is available to browse through under cursor control or in tabular format. The graph display format, showing impedance in polar form in the lower two windows, was selected as it presents results in a form directly comparable with Michaelson *et al.* The real, resistive, component was extracted and displayed as this is a familiar lung function measurement. The coherence function and flow power spectrum were

included mainly for technical reasons to enable assessment of the technique during the development phase. Alternatively, the two upper data windows may be used to view the time varying pressure and flow signals, often this is useful to assess whether the transducers have saturated or if the signals are contaminated by glottis closure, two examples showing eight second data blocks are shown in figures 4.8 and 4.9. The code is easily adapted to display different parameters, collect data at a different rate, or change the frequency domain resolution by altering constants in a global control unit.

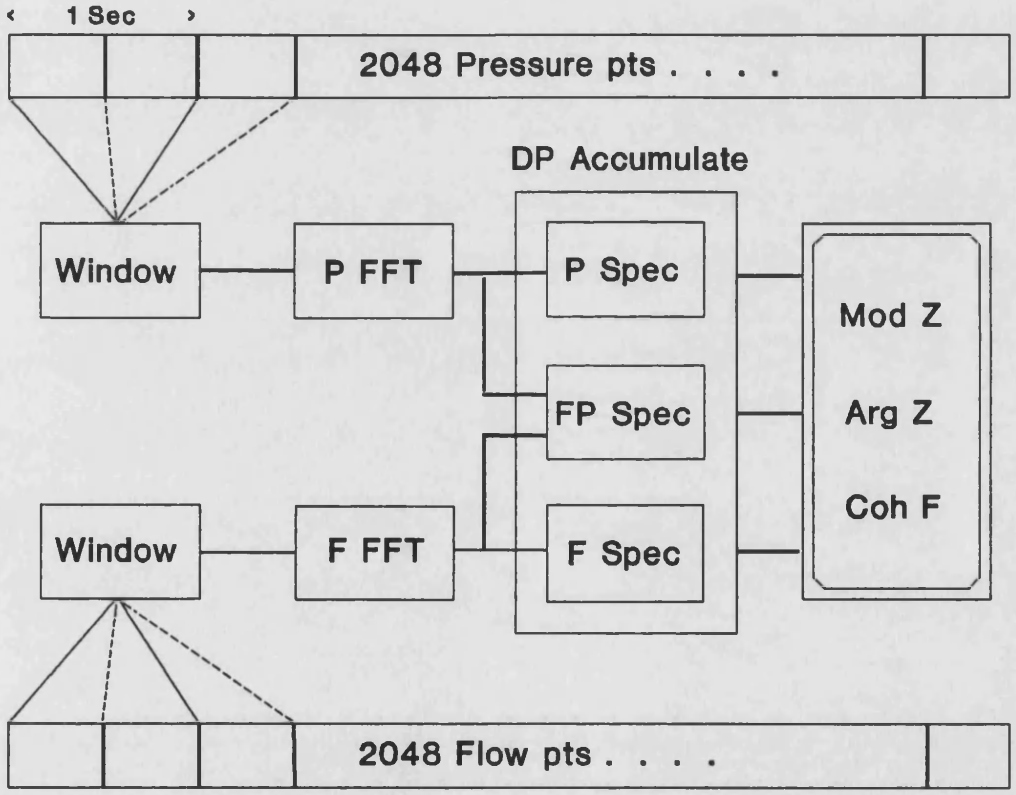

Figure 4.6 Impedance Analysis Schematic Summary

4.5 System Verification

The processing regime was validated by applying the output of the random noise circuit across a number of resistor and capacitor networks. Voltage and current were digitised and processed in place of

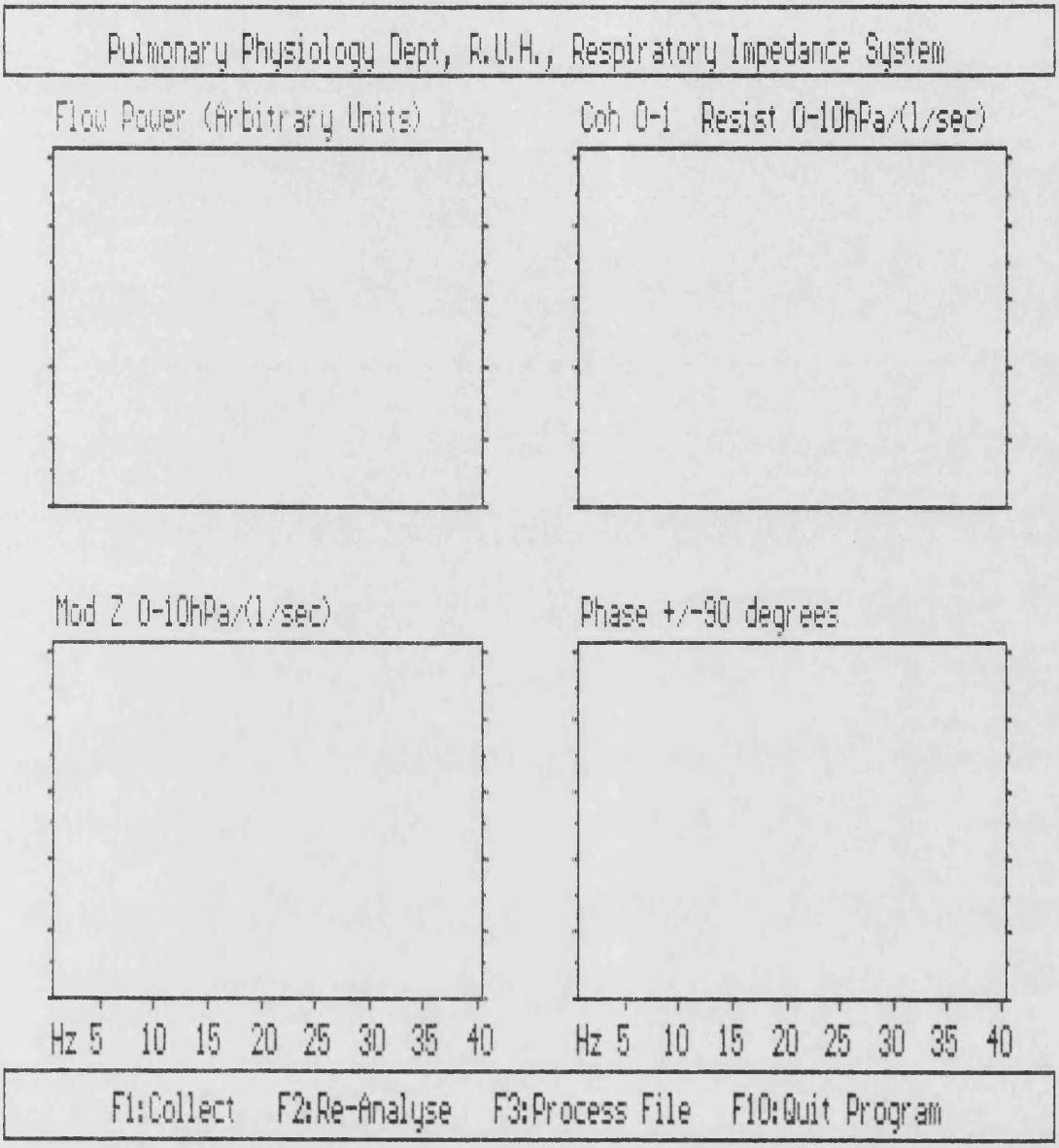

Figure 4.7 Screen Layout Example

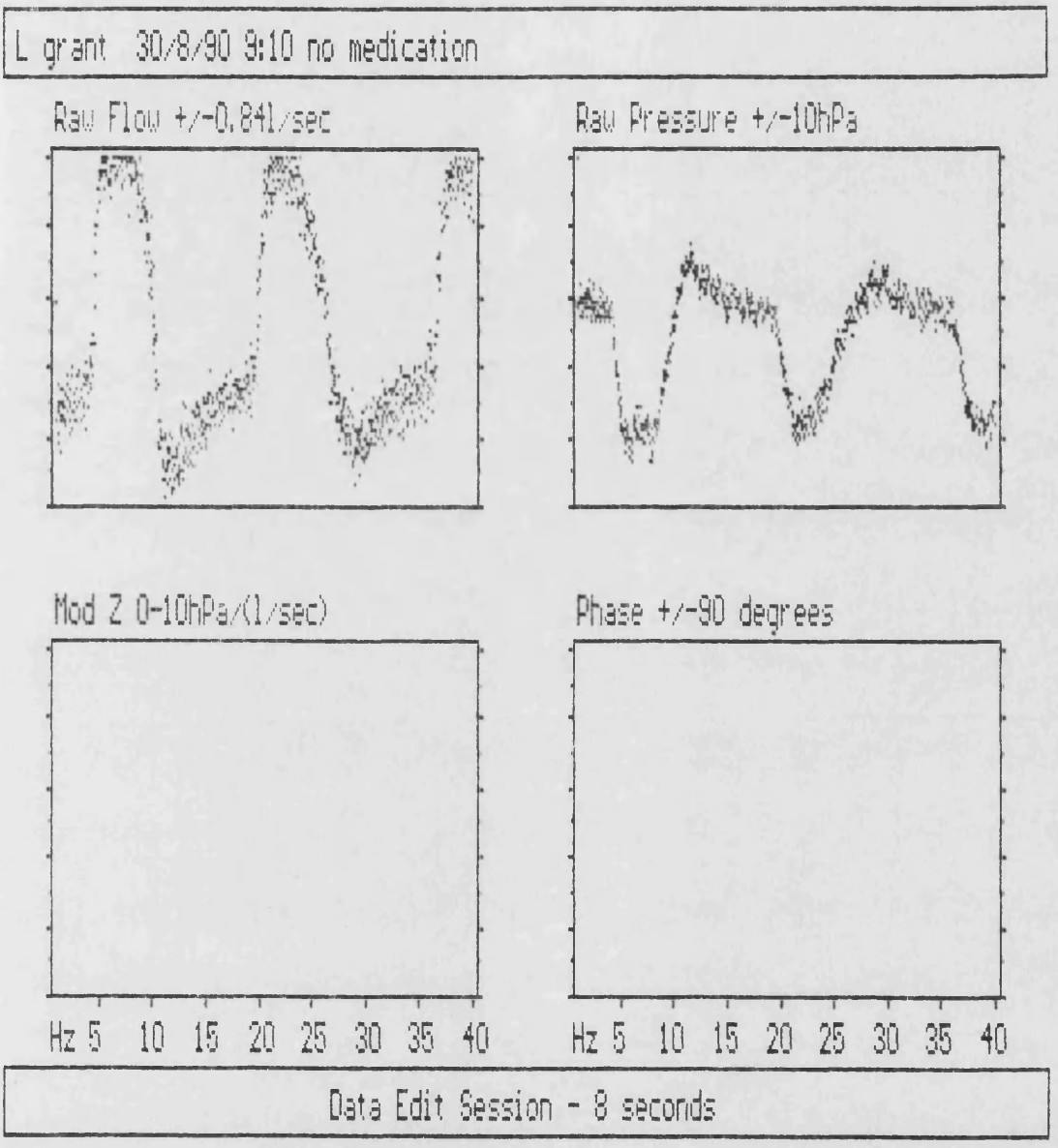

Figure 4.8 Screen Showing Pressure and Flow Signals - example 1

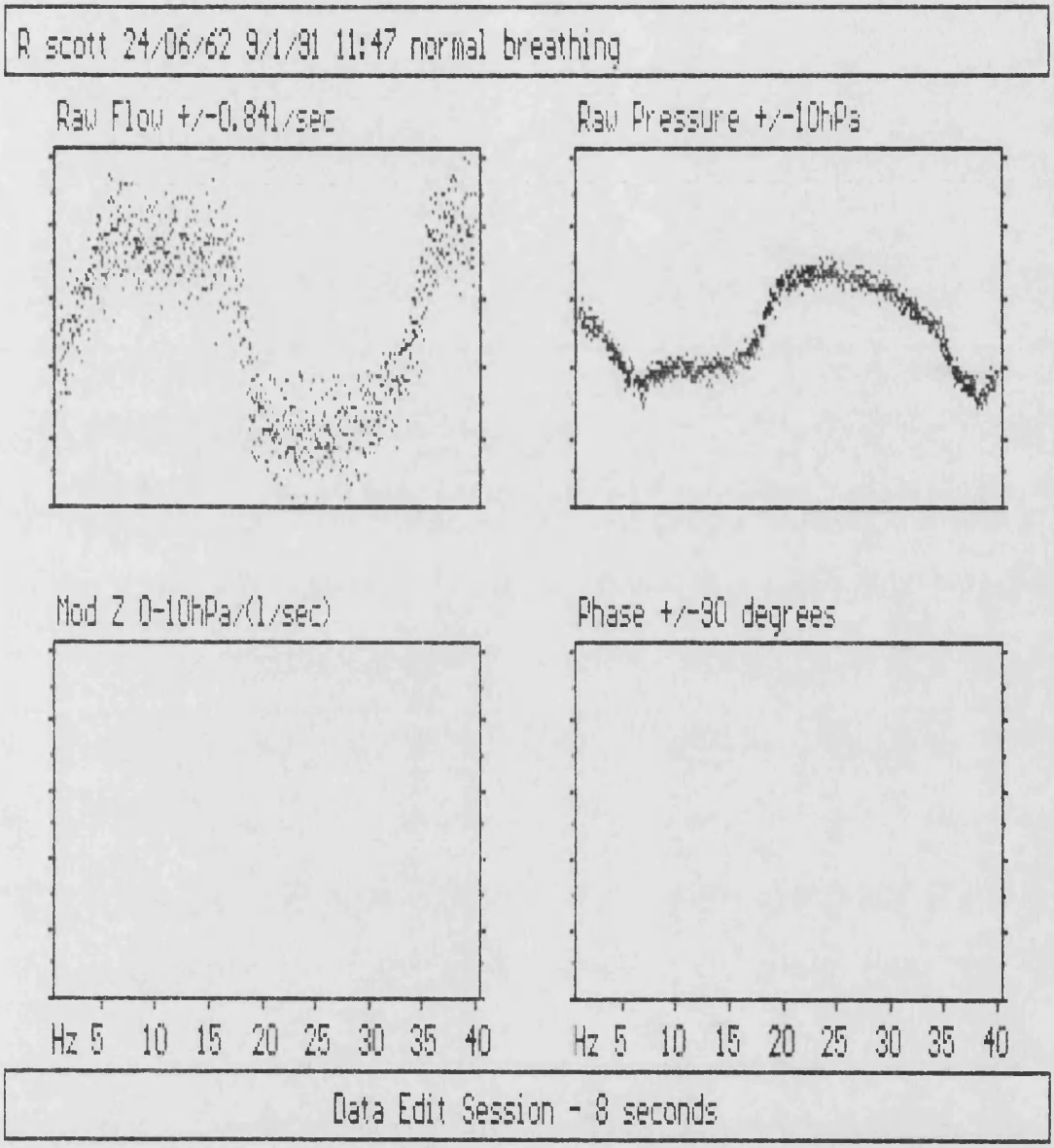

Figure 4.9 Screen Showing Pressure and Flow Signals - example 2

pressure and flow and the impedance results were compared with the theoretical values for the circuits and were within the ranges set by the component tolerances.

The pressure transducer was calibrated against an inclined manometer. Having calibrated the pressure channel at ±10hPa, (±2.5V input to the converter), a known resistance was used to calibrate the flow channel. A Fleisch pnuemotachograph was used as these devices are supplied with figures for the flow produced by a known pressure drop across the resistive element. The device, a Fleisch number 2, (serial no 1466), had a flow of $0.388ls^{-1}$ for a pressure drop of 1hPa, giving a resistance of $0.296hPal^{-1}s$. A sine wave of 3Hz was used to create the pressure drop of 1hPa by generating a sinewave of peak amplitude 1.4hPa. The resulting output from the flow transducer equated to a flow of $0.338ls^{-1}$. The gain of the flow transducer amplifier was increased virtually to its maximum value and gave a flow measurement range of $\pm 0.84l^{-1}s$, represented by a voltage range of ±2.5V. The load resistance was determined as $0.29hPal^{-1}s$ at 3Hz, with the pressure drop during the measurement being the difference across the pneumotachograph screen, rather than with one port referenced to atmosphere and the breathing port was occluded for this measurement. The measured resistance agreed well with the theoretical value, exhibiting a difference of less than 2%. Although the Fleisch values are for static pressures and constant flows it was argued that there would be little difference between this and a 3Hz measurement. This assumption was substantiated by examining the 3Hz pressure and flow waveforms on an oscilloscope and observing no measurable phase difference. While acknowledging this calibration resistance is small compared to that of a patient it is accurate and the transducers and electronics known to

be linear. Subsequently, however, the system was checked with more representative resistive loads, an example of which is shown in figure 4.10. The resistor was a sintered bronze device, actually designed for use as a filter element in a compressor unit, with little associated deadspace. The resistance of this device was measured as 6.6hPal^{-1}s using a steady flow generated by a small fan, the resistance at 2Hz is seen from the figure to be 6.55hPal^{-1}s with a pressure to flow phase shift of 1.1°. The higher frequency drop in resistance and slight increase in phase is probably due to inertia of air and possibly the frequency response of the pneumotachograph.

In addition to static calibration it is important to ensure that the pnuemotachograph does not introduce errors at higher frequencies. Pelle *et al*, 1984, have considered this subject and modelled the pnuemotachograph using a second order transfer function, as equation 4.1.

$$H = \frac{C}{1 + 2j\zeta\frac{f}{f_n} - \frac{f^2}{f_n^2}} \qquad 4.1$$

Where C is the gain, ζ the damping ratio and f_n the undamped natural frequency. Using the parameter values determined by Pelle *et al* for the frequency range 0 to 70Hz the transfer function may be calculated. The response is plotted over the 0 to 40Hz range in polar form in figure 4.11. This response was determined using a load whose properties were known theoretically. The difference between the experimental results and the predicted values being the response of the pneumotachograph system. This approach is appealing as not only does it allow for correction of the data it also ensures the system is calibrated. The response shown is for a screen type device but of

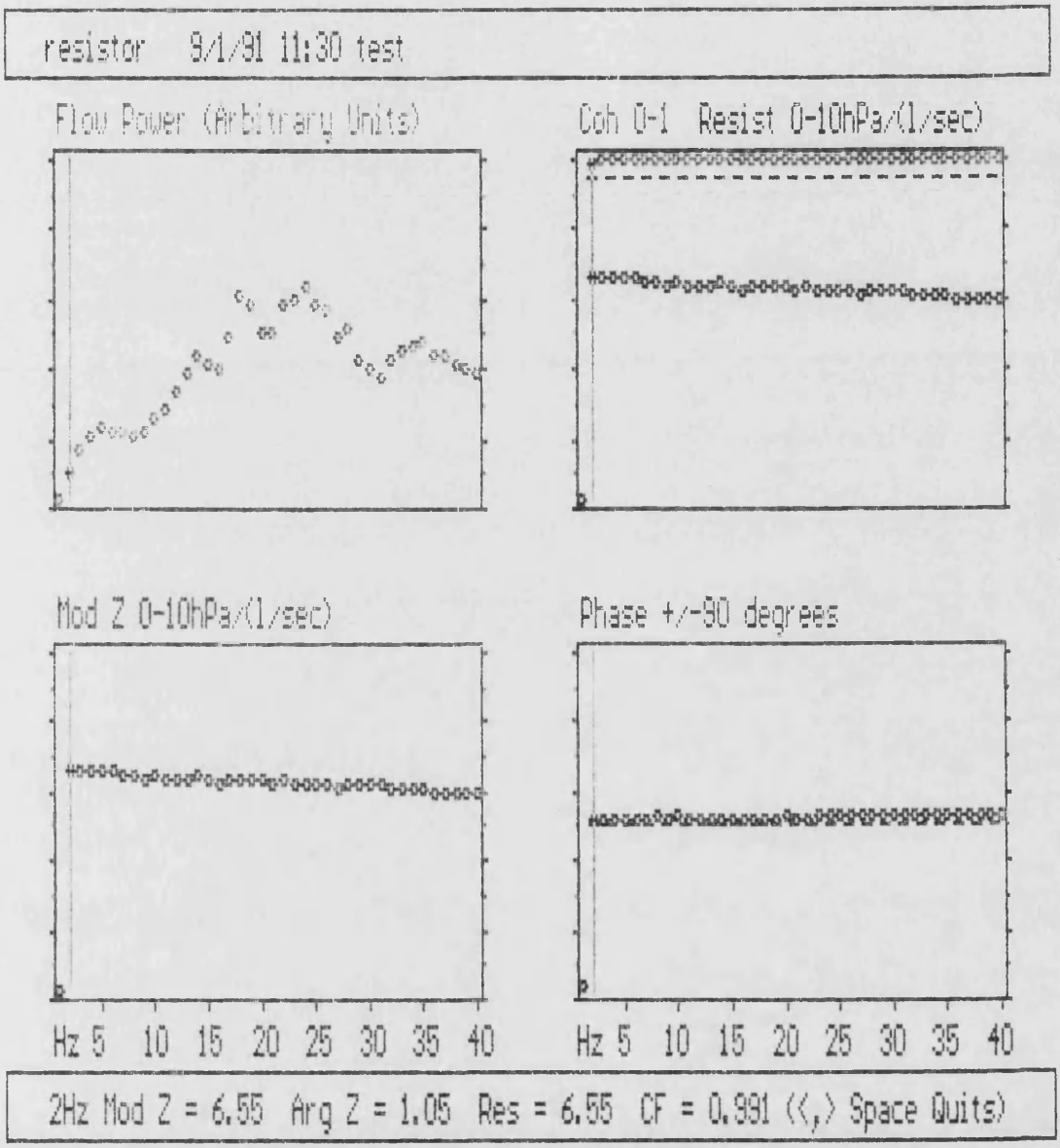

Figure 4.10 Impedance Calculation with Resistive Load

different manufacture to the Mercury device used in the prototype, nevertheless the results are likely to be similar. It is clear to see that errors in the phase will effect the variation of resistance with frequency. Resistance, calculated as the modulus multiplied by the cosine of the phase, will be overestimated by phase estimates that are too negative with the cosine result being more positive, ie closer to unity. Similarly an overestimation of the impedance modulus would artificially increase the resistance. This may well account, in part, for some of the variation of impedance with frequency which has varied between groups.

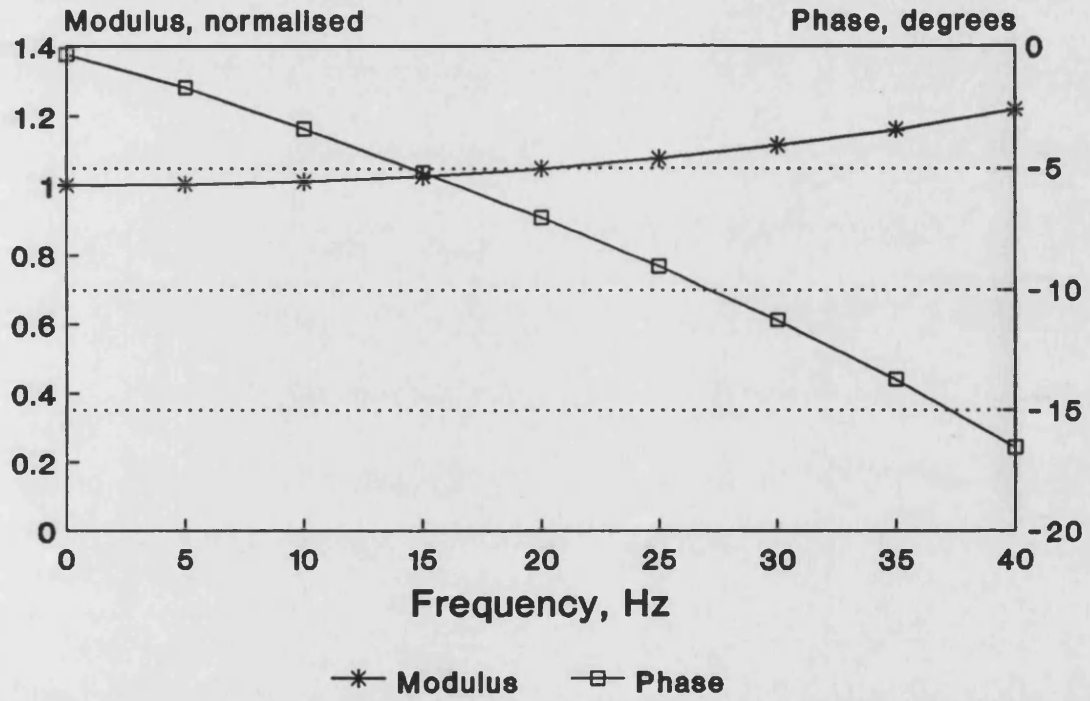

Figure 4.11 Second Order Model of Pneumotachograph Response

It would be inappropriate to have used Pelle's correction directly as the exact geometry of the pnuemotachograph which it applies to is unknown. The philosophy, however, seems wholly appropriate with the only remaining question being what to use as a test load. Using a purely compliant load relies on the assumption that pressure changes

result in adiabatic compression of the gas. As the load has to physically couple to the system the bore of the load must be reduced to the dimensions of the mouthpiece adapter. It is then difficult, when measuring pressure externally to be sure this accurately reflects the mean pressure within the load. This concern was expressed by Delevault *et al*, 1980, who proposed a load with both resistive, R and inertial properties, L. The resistive component must be greater than the resistance of the cylinder of known inertial properties for the approximations they develop to hold. In fact the inductance of the tube, L, is calculated from the simple formula $\rho l/a$, where ρ is density of air, l length and a the tube surface area. The impedance of the tube is then described by Equation 4.2

$$\begin{aligned} Z_{tube} &= R + j\omega L \\ j &= \sqrt{-1} \\ \omega &= 2\pi f \end{aligned} \qquad 4.2$$

This general approach was followed and a load was created, for use with the prototype system, using a filter of 30μm polypropylene mesh sandwiched between two tubes. Considering the two tubes as one, their dimensions were, length 20.15cm, diameter 26.75mm, area 5.62cm^2 with ρ taken as 0.001293gcm^{-3}, giving an inductance of 4.63gcm^{-4}. The resistance measured at a steady flow and was found to be 1.0hPal^{-1}s. The theoretical impedance was calculated and the experimental results obtained with the load connected to the system. The theoretical and results for five consecutive impedance determinations are presented in figures 4.12 and 4.13, illustrating impedance modulus and phase respectively. The experimental results are plotted as points. A correction was then introduced based on the difference between the measured and calculated values. The correction was subsequently used

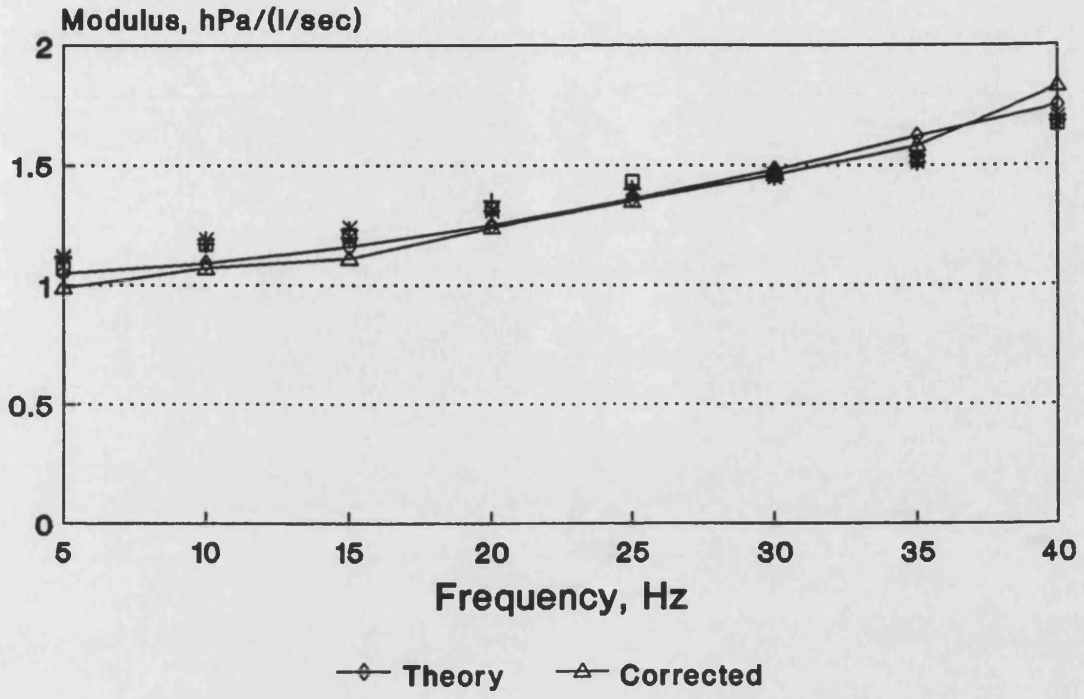

Figure 4.12 RL Test Load - Impedance Modulus

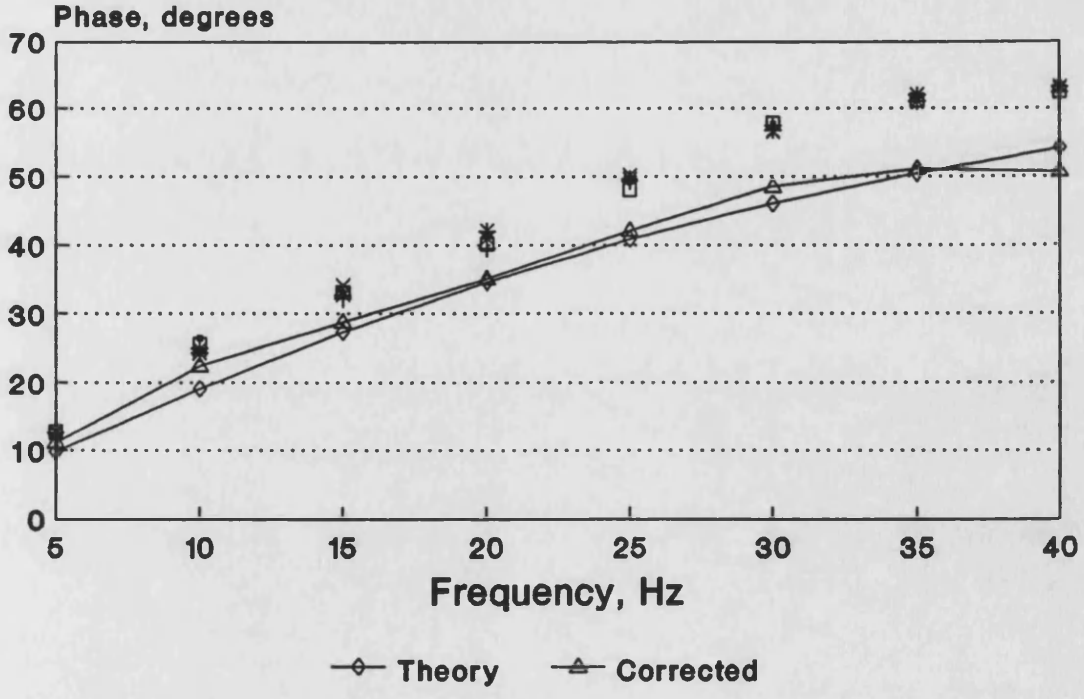

Figure 4.13 RL Test Load - Phase

to correct impedance data for the effects of the pneumotachograph, the corrected results with the load attached are also shown on the figures.

A further cause for concern was that at high frequencies the flow transducer assembly may have poor common mode rejection, (Peslin *et al*, 1984 and Farrē *et al* 1989). The problem is more pronounced with asymmetrical pressure transducers which is why the validyne gauges were used. The flow transducer comprises a resistive element across which there is a small pressure drop proportional to flow, however, the pressure common to both sides is not zero. The consequence being that errors may arise if the mechanical properties either side of the measuring element differ. To assess this, a constant amplitude sinewave was applied while the breathing port and mouthpiece element were occluded and pressure and flow measured at a number of sinusoidal frequencies. An effective common mode rejection may then be computed by computing $20\log_{10}$ of the pressure to flow ratio. At 3Hz the value is 70dB which gradually falls to 50dB at 40Hz. Peslin *et al*, (1984), suggest values of 60dB at 40Hz. The measurement described although 10dB less, was felt to be adequate as pressure and flow were measured at different sites, as they were in the instrumentation. The properties of the gas between the sites accounting for the lower high frequency values. In practice this difference in measurement sites is accounted for by the RL load correction described above.

4.6 Summary

A prototype system has been developed to determine respiratory impedance over the 2Hz to 40Hz frequency range. A mechanical vibration generator driving a set of bellows produced a random noise oscillatory airflow. Pressure and flow signals were measured close to the mouth

and digitised at a rate of 120Hz, with the impedance program collecting 16 seconds of data. The Fourier analysis splits the data into one second blocks, giving a frequency resolution of 0.91Hz. The impedance application program has been written with flexibility in mind and is easily configurable to allow alternative sampling rates, analysis resolution and display formats. The software has been designed to be simple to use as it was envisaged that it may be used by a variety of users. The coherence function is available as an index of data integrity for each measurement frequency, from which standard errors and confidence limits could be computed.

The system has been calibrated and the high frequency performance of the pneumotachograph investigated and corrected for. Additionally the frequency response of the vibration generator was characterised and corrected to ensure a flat flow power spectrum. In summary, the system was ready to make respiratory impedance measurements.

Chapter 5 Preliminary Impedance Results

5.1 Introduction

The prototype was used to develop a normal group of impedance results by recruiting volunteers from around the hospital. At least three impedance measurements were made in each subject, they continued to breathe during the test, a nose clip was worn and measurements were made with subjects seated. A group of around 100 volunteers were studied in order to evaluate the equipment, both in terms of the impedance results and acceptability of the manoeuvre.

5.2 Impedance Results in Healthy Subjects

Figures 5.1 through 5.6 show typical impedance results for three female and three male subjects. The results illustrate the variation of impedance with frequency, with three numeric indices being quoted in the information box at the bottom of the display. The figures give the average resistance between 5Hz and 8Hz, as well as the average over 27Hz to 30Hz and the resonant frequency. The resistance values have units of $hPal^{-1}s$. If the coherence values fall below 0.6 then the associated data is not displayed, with the affected data points defaulting to the lower screen boundary. The dotted line in the coherence/resistance window is set at 0.95 which was the proposed target coherence threshold value. It became clear from these preliminary results that using 0.95 as the data rejection threshold meant that for the results shown the majority of data below 10Hz had to be rejected and this point is discussed. The overall form of the results were in broad agreement with the published literature, with women exhibiting slightly higher resistance values compared to men.

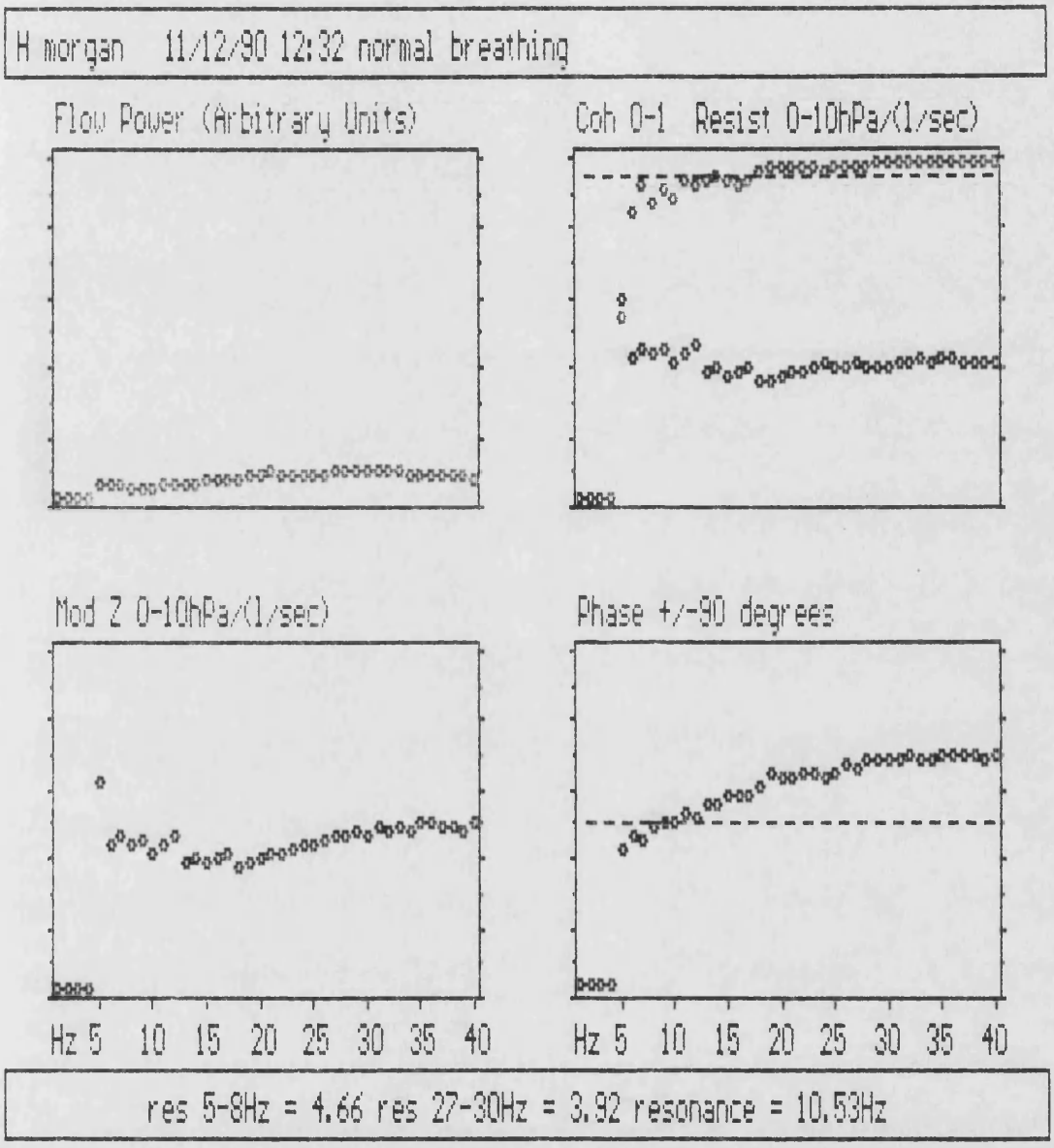

Figure 5.1 Impedance Results - Female Volunteer 1

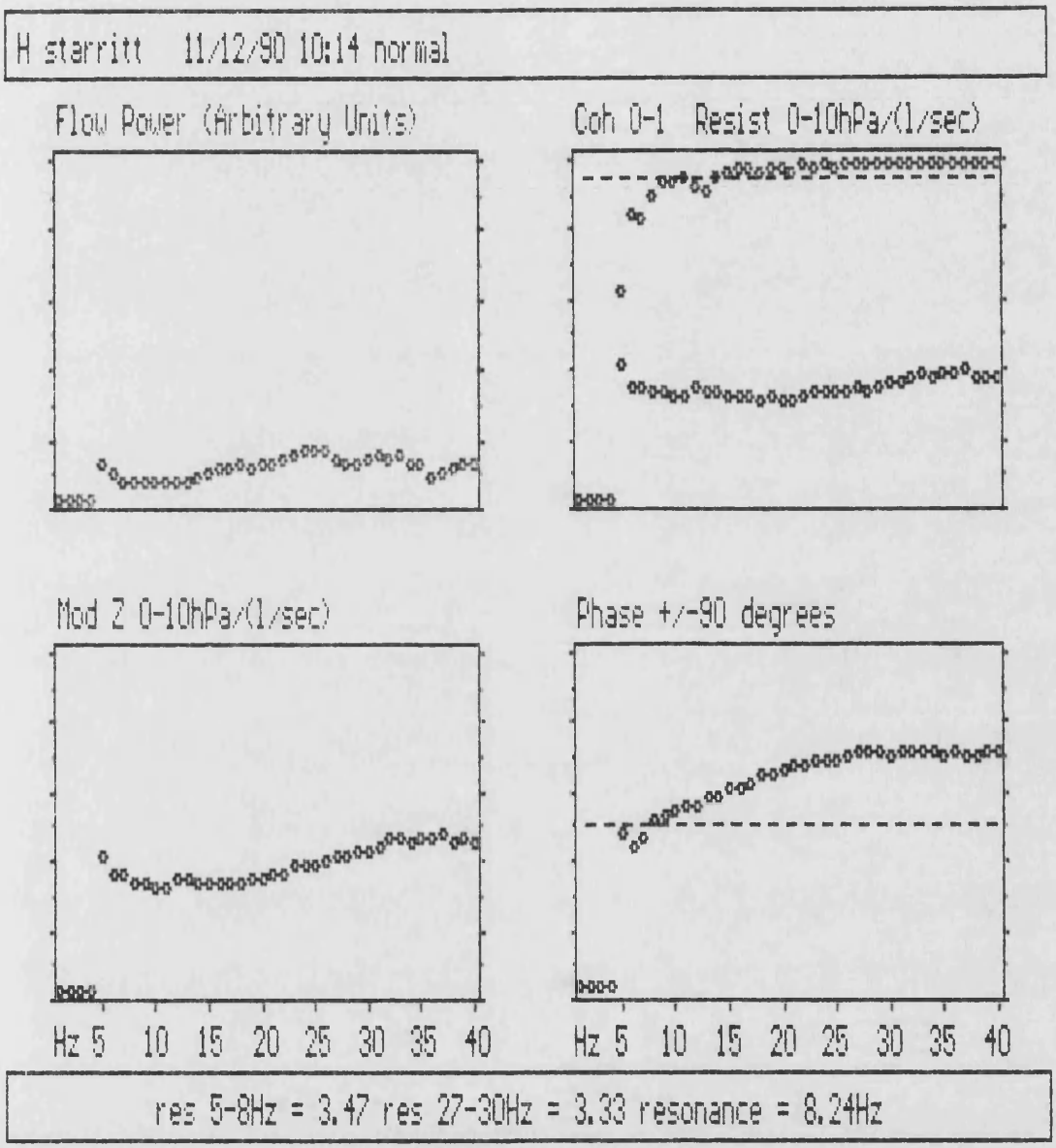

Figure 5.2 Impedance Results - Female Volunteer 2

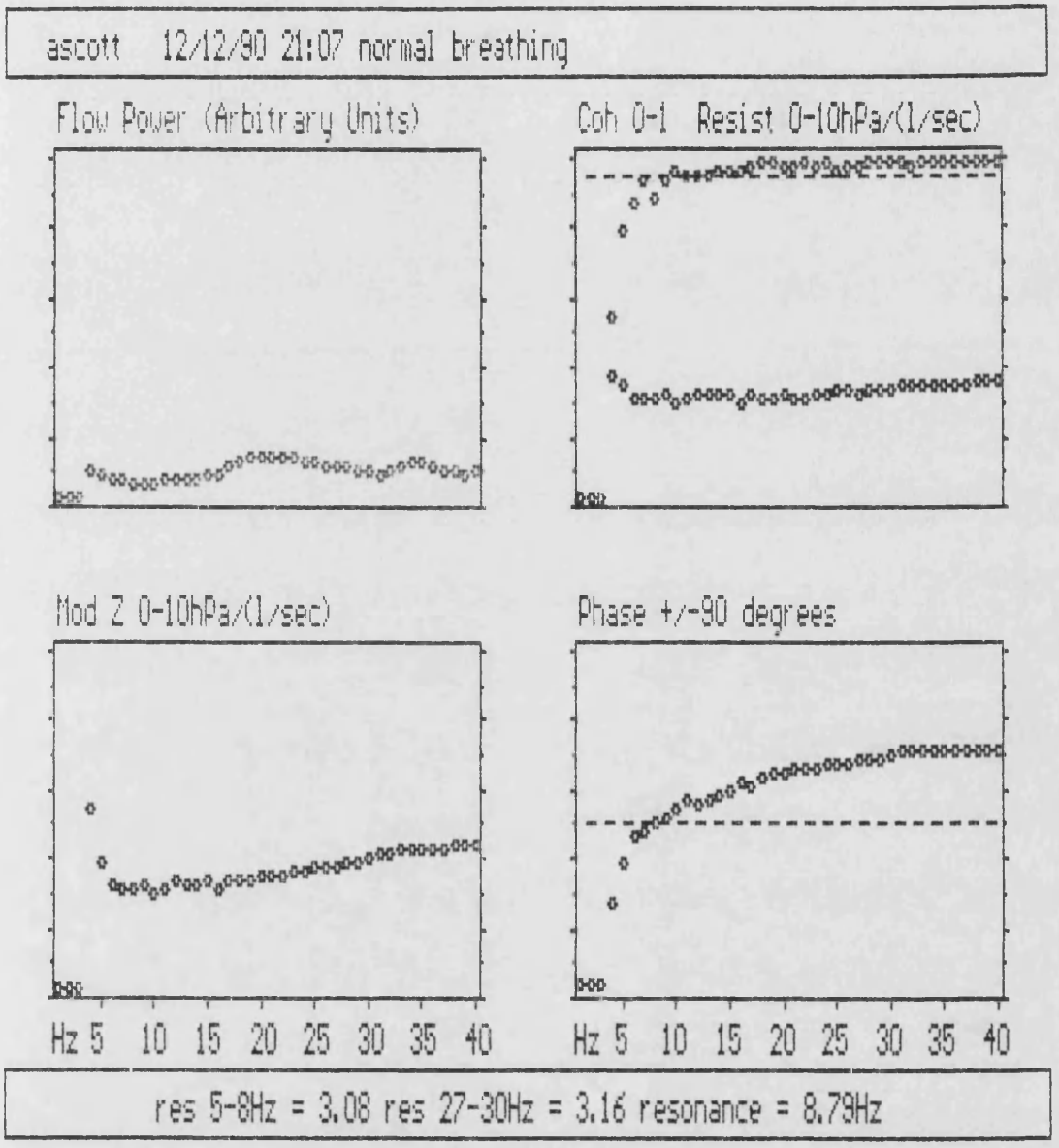

Figure 5.3 Impedance Results - Female Volunteer 3

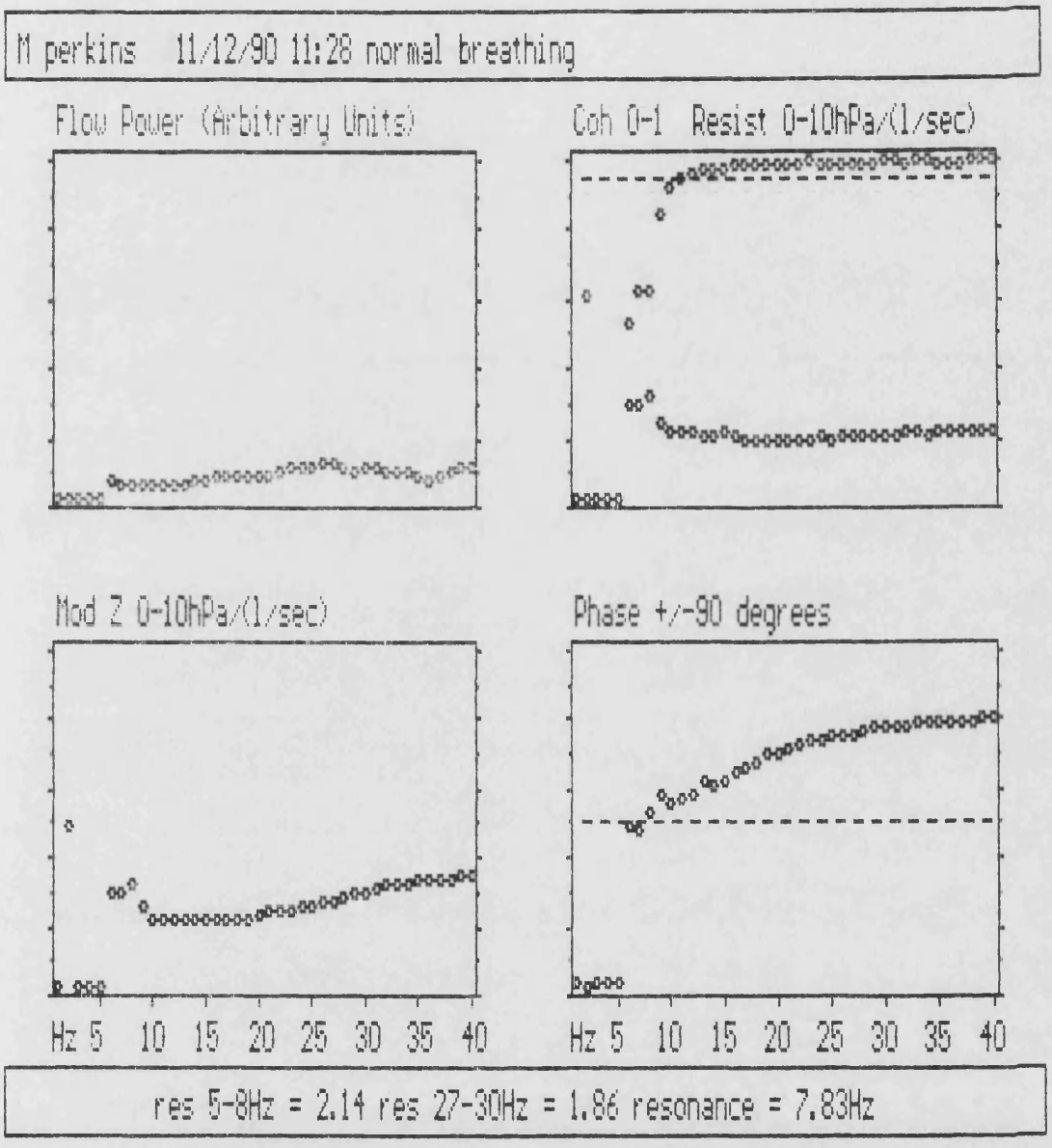

Figure 5.4 Impedance Results - Male Volunteer 1

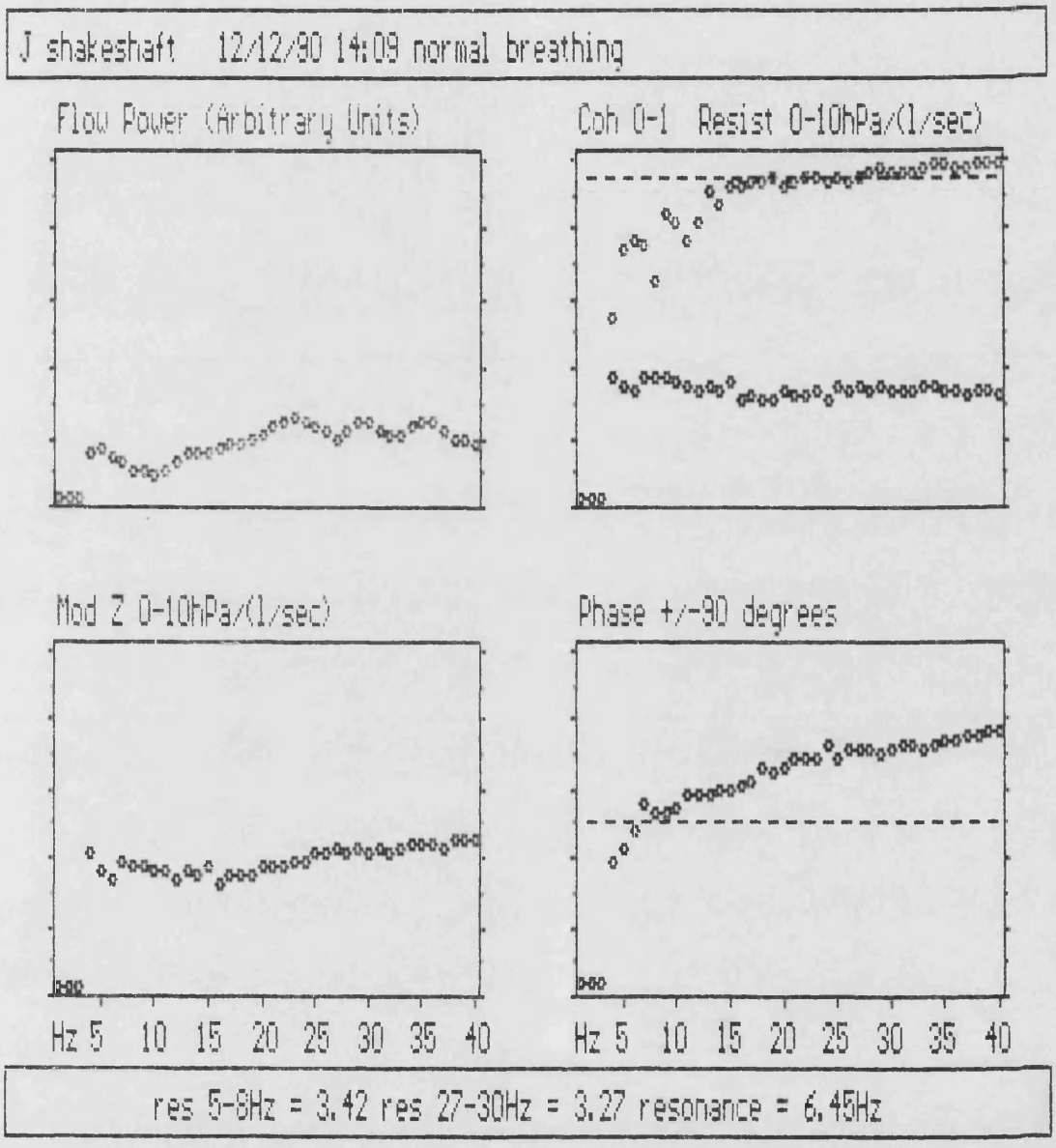

Figure 5.5 Impedance Results - Male Volunteer 2

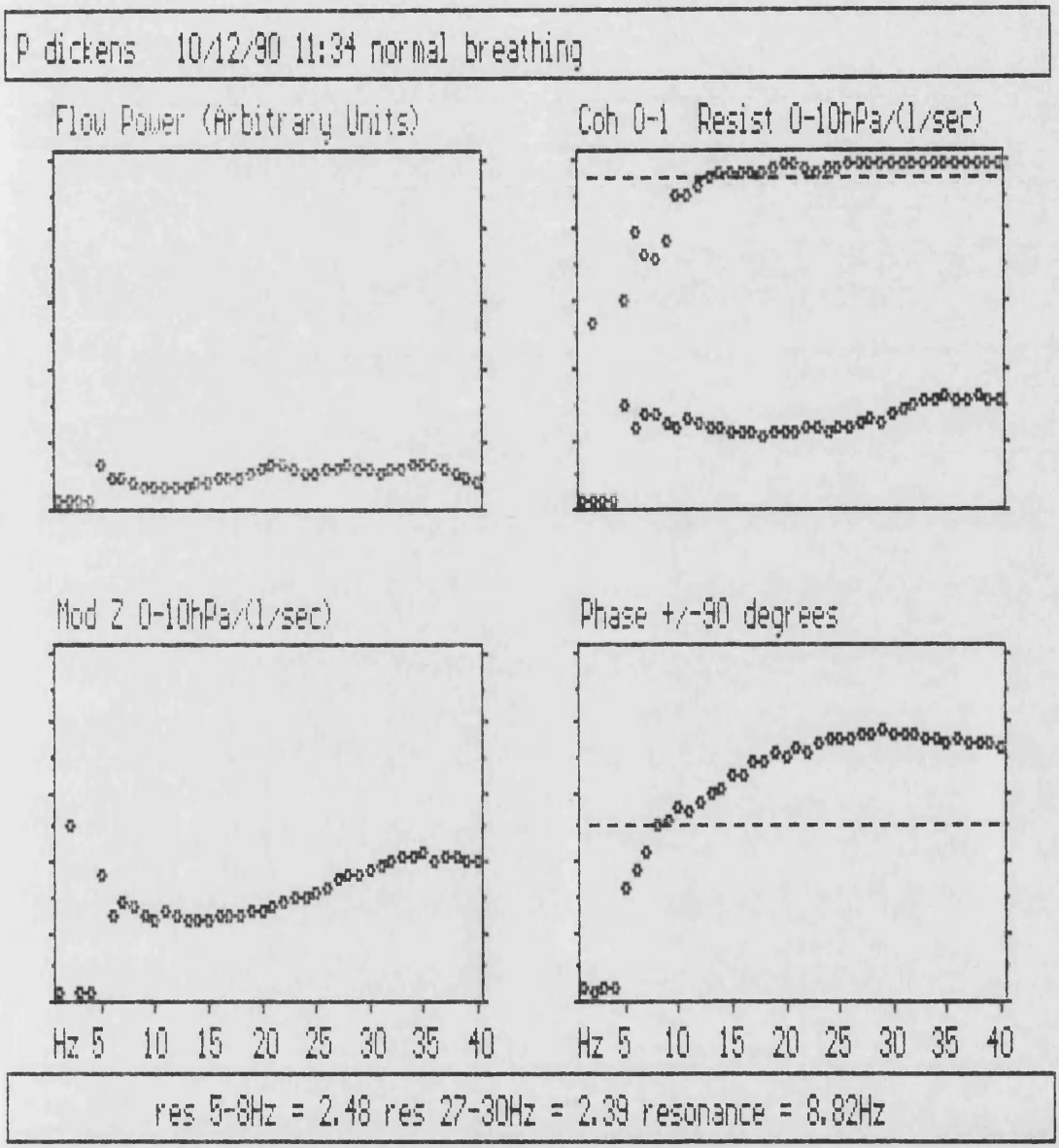

Figure 5.6 Impedance Results - Male Volunteer 3

The resonant frequencies are around 8Hz to 10Hz in all examples.

Figure 5.7 shows graphically the spread of results within a subject, with ten consecutive measurements overlaid. In numeric terms table 5.1 shows the spread of results for the same subject, quoting ten measurements of resonant frequency and the resistance at resonance obtained over a four hour period. The resonant frequency is f_n, with units of Hz, $R(f_n)$ represents the resistance at resonance, having units of $hPal^{-1}s$ and the $FEV_{1.0}/VC$ term is the ratio of the forced expiratory volume in one second to the vital capacity, expressed as a percentage.

Descriptive Index	Resonant Frequency, f_n Hz	Resistance @ Resonance, $R(f_n)$ $hPal^{-1}s$
Range	5.2 - 7.8	1.5 - 2.2
Mean	6.4	2.0
Coefficient of Variation, %	12.0	10.0

Table 5.1 Range of Results - Normal Male Subject.

The resonant frequency and resistance at resonance were chosen to illustrate the typical spread of data of the normal non smokers, there is little point in quoting the complete impedance data set until the problem of coherence values at low frequencies had been improved. Additionally a spirometric ratio is included for comparison. As the group is small the data is shown for each subject in table 5.2 and split into male and female results, with the average of three consecutive impedance measurements being quoted.

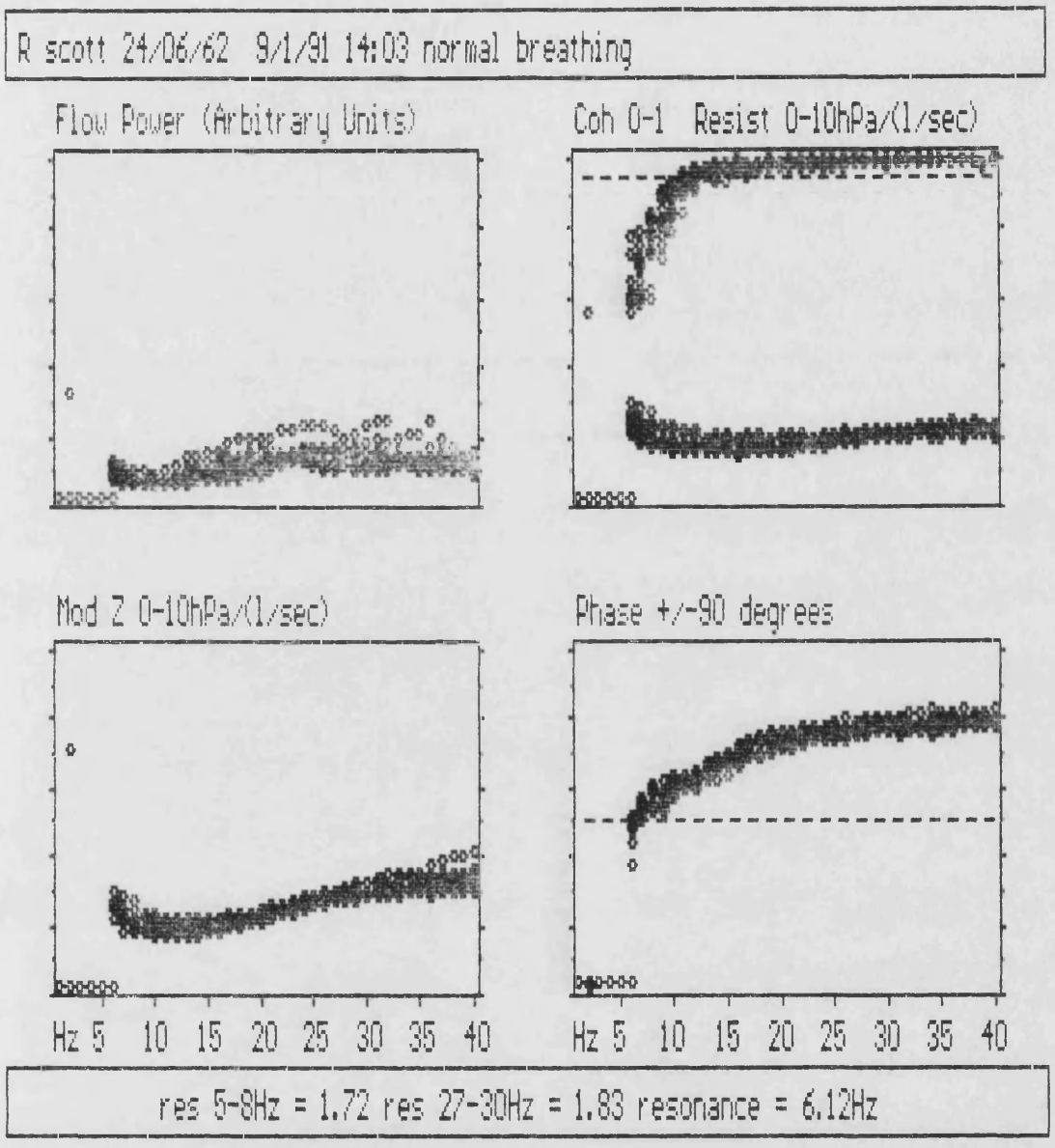

Figure 5.7 Impedance Results - Male Volunteer 10 Consecutive Runs

	Male Volunteers			Female Volunteers		
	$FEV_{1.0}$ /VC	f_n	$R(f_n)$	$FEV_{1.0}$ /VC	f_n	$R(f_n)$
mean	88.0	7.6	2.9	90.13	8.6	3.6
sd	7.47	1.2	0.8	7.11	1.4	0.9
coefficient of variation, %	8.5	16	27	7.9	16	25

Table 5.2 Male and Female Non Smokers

5.3 Impedance Examples in Smoking and Asthma

A small number of the normal group were smokers and the results are shown for each subject in table 5.3. It is interesting to note that the smoking groups both had higher resistances and resonant frequencies than the non smoking equivalents. The group, however, was too small to draw any significant conclusions from, in particular the male group had a number of subjects very close to the normal mean. Yet the spirometric indices showed no distinction between the groups. Figures 5.8, 5.9 and 5.10 show the ability of the system to follow changes in lung mechanics before and after medication in one asthmatic volunteer. The subject deliberately suspended his medication and became severely wheezy in order to show a gross change from the normal group. Following medication the impedance of the system falls, with the resonant frequency and resistance reducing towards normal levels. It is also apparent that the shape of the impedance versus frequency curves are different to the normal examples of figures 5.4 through 5.6.

The three graphs enable the time course of the response to treatment to be assessed, with the resonant frequency, 6Hz and 30Hz resistance values given in table 5.4. As the resistance in the subject exhibits considerable variation with frequency it is inappropriate to average consecutive values as done in the normal group. The screen information window was therefore left in cursor display mode, with the cursor indicating the resonant frequency, which following medication moves to lower frequencies. By quoting resistance at 6Hz and 30Hz, for

Male Volunteers				Female Volunteers			
Age	$FEV_{1.0}$/ VC	f_n	$R(f_n)$	Age	$FEV_{1.0}$/ VC	f_n	$R(f_n)$
27	90.1	7.7	2.6	37	96.3	9.0	3.3
30	85.1	8.0	2.7	37	91.4	10.5	4.6
31	91.7	6.6	2.9	28	86.3	11.5	4.3
33	90.1	8.0	4.2	46	80.8	16.2	5.1
35	79.5	8.7	2.7	32	84.1	9.9	3.8
53	78.4	11.4	3.7	30	---	6.1	2.5
27	91.9	7.3	2.9	51	90.9	11.8	6.0
mean	86.7	8.3	3.1	mean	88.3	10.7	4.2
sd	5.75	1.5	0.6	sd	5.63	3.1	1.6

Table 5.3 Male and Female Smokers

example, it is possible to quantify the change in the shape of the resistance curve by considering the ratio of these two values, as shown in the table.

Comment	Resonant Frequency Hz	6Hz Resistance $hPal^{-1}s$	30Hz Resistance $hPal^{-1}s$	30/6Hz Resistance Ratio %
Pre Med	36	8.82	4.66	53
5 minutes after	21	7.12	3.64	51
40 minutes after	10	4.34	3.43	79

Table 5.4 Numeric Indices in Asthmatic Volunteer pre and post medication

5.4 Consideration of Errors

The collection of impedance data using the prototype allowed a detailed error analysis of the data. This is not easily obtainable from published literature as full impedance versus frequency results are not commonly quoted. Initially the coherence function was used to develop random errors for the impedance modulus using equation 3.20, which, for convenience, is repeated as equation 5.1. The random error terms are then used to determine the 95% confidence limits for the modulus using equation 5.2, (previously 3.21), with Z representing the true impedance modulus and Z with caret being the calculated impedance

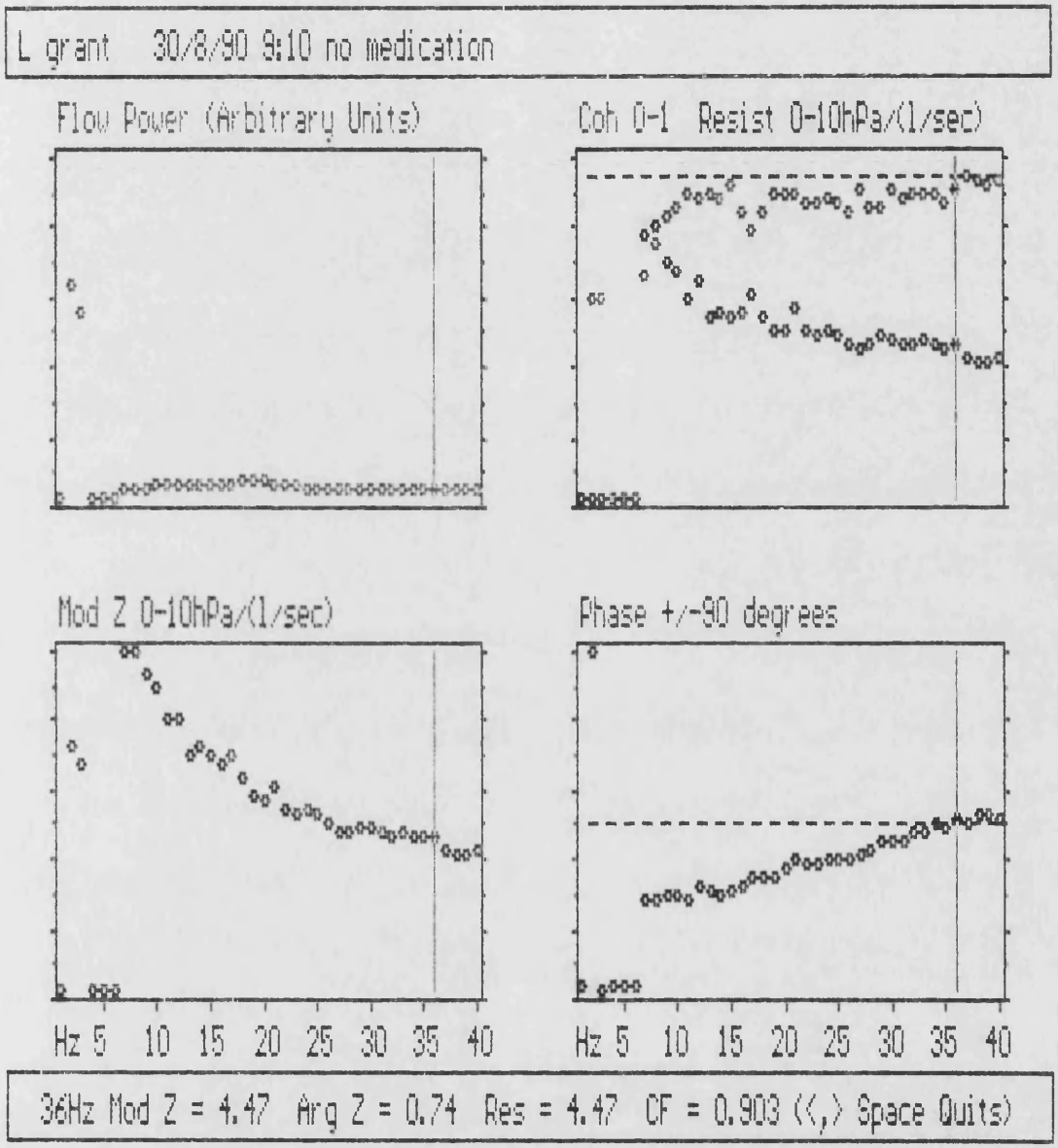

Figure 5.8 Impedance Results - Male Asthmatic Pre-medication

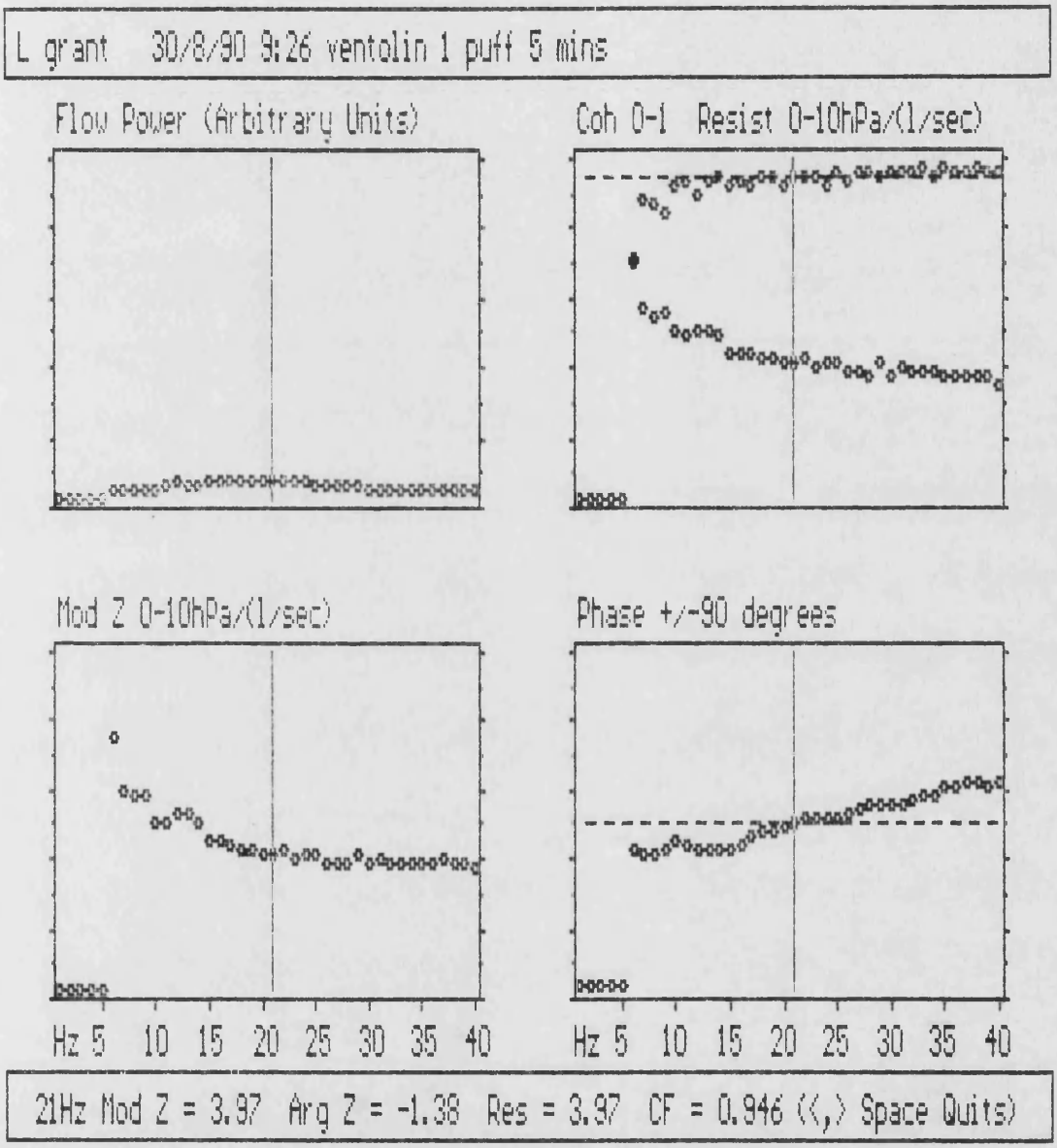

Figure 5.9 Impedance Results - Male Asthmatic Post Medication

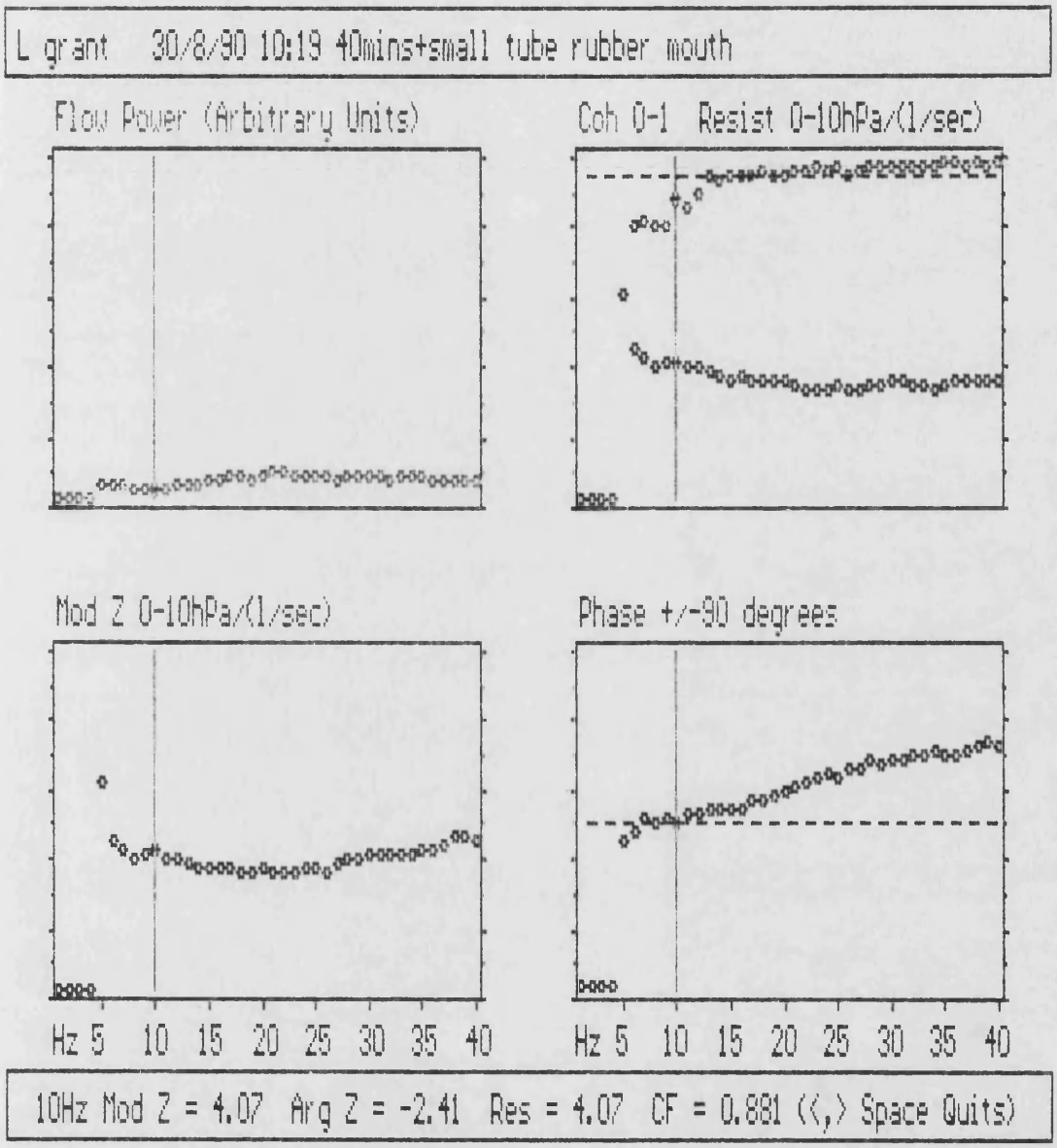

Figure 5.10 Impedance Results - Male Asthmatic Post Medication

estimate. The errors are functions of frequency and are computed using the coherence values and the number of data blocks averaged in the frequency domain, n_d, which in the prototype was 30. Referring to chapter 3 the assumption that the sampling distribution is normal and the confidence intervals in 5.1 hold, is only true if the random errors are constrained to around 20%. For n_d=30 equation 5.1 will exceed 20% when coherence values fall below 0.30, therefore no errors will be calculated for coherence values less than 0.5, ensuring that the maximum random error will be around 13% and the confidence limits may be computed.

$$\epsilon_r = \frac{\sqrt{1-\hat{\gamma}^2_{xy}(f)}}{|\hat{\gamma}_{xy}(f)|\sqrt{2n_d}} \qquad 5.1$$

$$\hat{Z}(1-2\epsilon_r) \leq Z \leq \hat{Z}(1+2\epsilon_r) \qquad 5.2$$

It is informative to show the variation of coherence with frequency obtained from the normal group. Figure 5.11 shows coherence values in the 3Hz to 20Hz range for 8 males, although the variation in coherence is the same for females. Eight curves are shown as this is the limit of the plotting package used, however, they were representative of the group as a whole. Frequencies below 6Hz were not included as the coherence values dipped below 0.5, although they did rise again at 2Hz, however, the reason for that will be discussed in subsequent chapters. Above 20Hz there is no significant change in the coherence levels, they remained similar having reached a plateau above about 15Hz. The values are taken from one impedance data set per subject. Using the coherence values, random error values may be computed using equation 5.1, the results are illustrated in figure 5.12. As dictated by equation 5.1 the random errors reduce as the

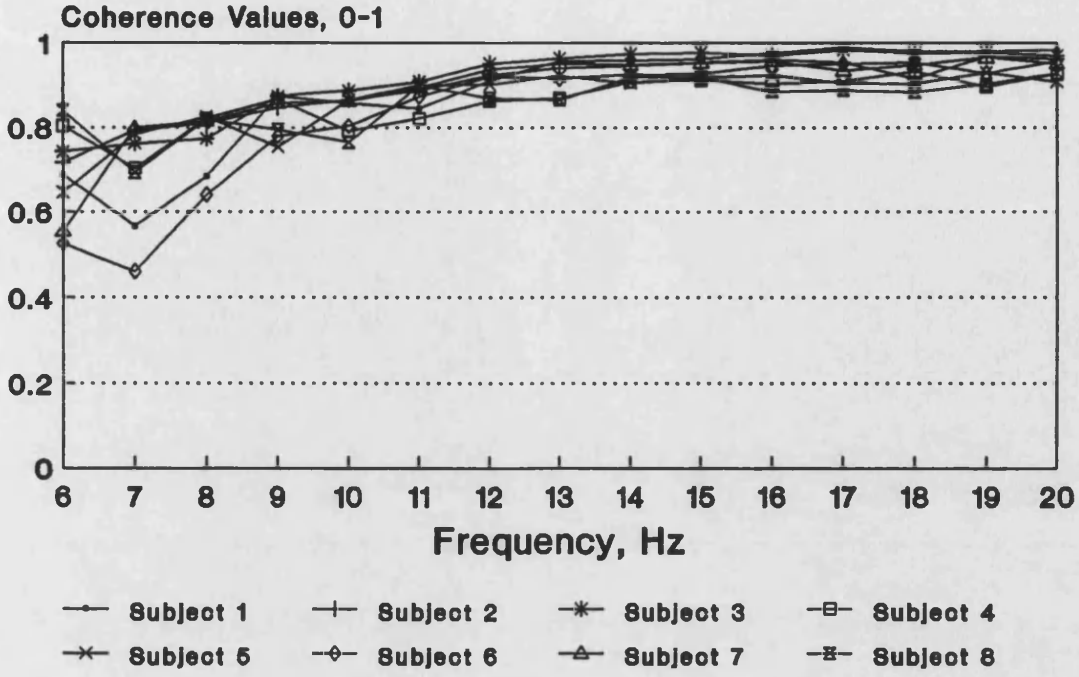

Figure 5.11 Normal Subjects - Variation of Coherence with Frequency

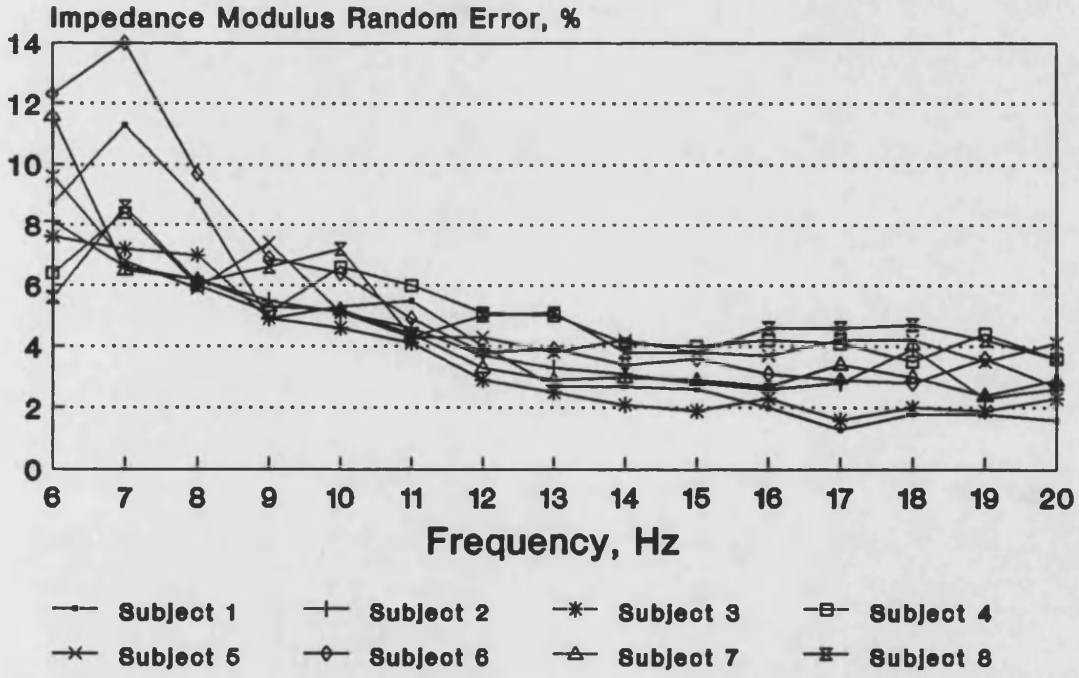

Figure 5.12 Errors Computed from Coherence Values.

coherence values increase, at frequencies above 15Hz the errors do not exceed 5%, however, as frequency falls the errors rise, lying between 5% and 14% in the 6Hz to 10Hz range.

The errors were then used to compute 95% confidence limits which were applied to the impedance data and shown for four subjects in figure 5.13. Errors associated with the modulus have been concentrated upon as they are representative of the errors associated with the phase (Bendat and Piersol, 1981).

5.5 Summary

The instrumentation proved easy to use and the measurements in volunteers enabled local experience to be gained in the application of the technique. The results obtained agree broadly with other published data, however, the quality of the data at low frequencies is unacceptable. Even considering data between 6Hz and 10Hz the errors are poor. The spectral resolution was increased to see if the falls in coherence were associated with resolution bias errors, however, no improvement in coherence was seen. Increasing the resolution gave less smooth estimates as fewer blocks were available to average.

On a more positive note the instrument did distinguish an asthmatic subject from the normal group and changes following medication were observed. The resistance in this subject also exhibited marked frequency dependence which changed after medication.

No attempt was made to fit a 3 element RLC model to the data as the errors associated with the modulus would be carried through to the parameter estimates. In particular the compliance estimates would be affected by the lack of reliable low frequency data. If the technique is to prove useful as a sensitive indicator of lung function the errors must be reduced. Low frequency data is also of importance, as a rise in low frequency resistance is indicative of increased peripheral resistance. Unlike the asthmatic results shown, the early stages of

any disease in the periphery of the lung will produce a much smaller change in the frequency dependence of resistance.

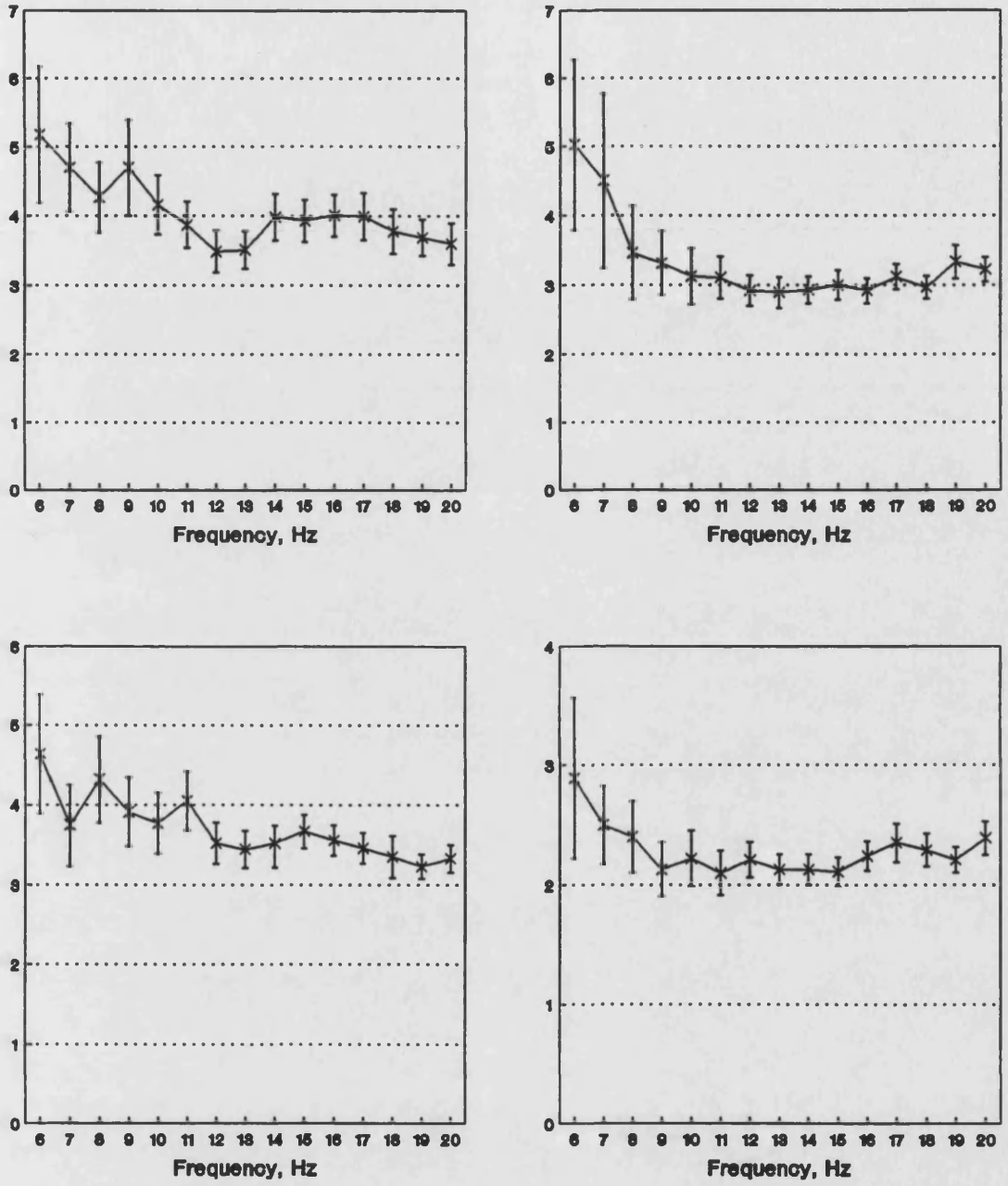

Figure 5.13 Impedance Modulus ($hPal^{-1}s$) with 95% Confidence Limits - 4 Subjects

Chapter 6 Respiratory Impedance Instrumentation: Phase 2

6.1 Review of Phase One

The previous chapters described the prototype instrumentation and preliminary results. The system has enabled the technique to be evaluated locally, with experience being gained in the application of the equipment in the clinical environment.

One of the advantages of the technique is the minimal subject cooperation required. Having made measurements in around one hundred subjects it is apparent that the procedure is well tolerated, with all subjects completing at least three consecutive impedance determinations. To further emphasise this point, measurements have also been made in two patients whose conditions were so severe they could not undertake any conventional lung function tests available at the hospital. Furthermore the equipment has proven to be reliable and easy to use, with the lung function technicians finding no major criticisms of the system. The style of the equipment therefore seems to be acceptable and as it is contained on a trolley it enables measurements both at the bedside and in the laboratory. In terms of the sensitivity of the technique this has yet to be fully explored. The preliminary work also confirmed that the results are in broad agreement with published impedance data.

As the normal reference group grew in size it became apparent that low frequency data exhibited poor coherence values. The implication of this was that impedance data had large errors associated with it and therefore had to be rejected. Considering the group as a whole, on average, data was only acceptable from around 10Hz upwards, which in many subjects was above the resonant frequency. Low frequency

data is important for a variety of reasons. Firstly the low frequencies, 2-3Hz, are closest to the natural respiration rate, around 0.2 to 0.3Hz, and although higher, will reflect the impedance most representative of the physiological condition. Secondly low frequency resistance rises have been suggested as indicative of increased peripheral resistance which is associated with the early stages of lung disease. To exploit the claimed sensitivity therefore requires good quality data at all frequencies. Modelling the data also requires acceptable data, the effect of not using the low frequency data would result in unreliable model compliance components. These components dominate the low frequency impedance and their contribution to the impedance falls with increasing frequency. It remains a priority to strive to improve the low frequency data, the boosting of the power of the applied airflow at these frequencies has not solved the problem.

Clearly the system at this stage was not yet suitable for clinical use, the above deficiencies needed to be addressed, the aim being to make the system more flexible to allow the evaluation of more sophisticated processing techniques. In particular it would be useful if the airflow signal was more adaptable. Minor alterations to the hardware following feedback from volunteers are also discussed. When the apparent deficiencies are overcome the system can enter routine clinical use and the data can be used to explore the full sensitivity of the method.

6.2 Improving the Low Frequency Data Quality

Achieving reliable low frequency impedance data has proved difficult for all workers in the field, with 6Hz often being the lowest frequency at which results are quoted. The main obstacle is the low

amplitude signals due to the increase in the reactance due to compliant effects. Additionally spontaneous respiration acts as a source of interference which compounds the problem.

The fundamental problem was how to improve the reliability of data in the range 2 to 10Hz. The coherence function is the indicator of data quality and was used to quantify improvements. In review, the factors which lead to reduced coherence include, system non linearities, poor signal to noise ratio and signal corruption by extraneous noise. The respiratory system appeared to be behaving linearly as if the power in the airflow was increased, within limits, the impedance data where reliable was the same at several powers. This seemed to suggest the problems of poor data were associated with signal to noise ratio and sources of interference. Two main areas were considered, firstly the characteristics of the applied airflow and secondly the processing of the data.

6.3 A New Oscillatory Airflow

The airflow used in the prototype was generated by a digital circuit creating a pseudo random binary sequence. The output was low pass filtered and followed by an analogue circuit to compensate for the frequency response of the generator. This approach created a signal which contained all frequencies in the range 1 to 40Hz.

The content of the airflow signal was reconsidered as it was realised this may have a bearing on the signal to noise ratio. The random sequence had a repeat period considerably in excess of the measurement duration, which upon reflection gave cause for concern as it meant that each one second block analysed had a different frequency content. Examining the block by block flow power spectra showed that

some blocks had little low frequency content.

When considering improvements to the airflow signal it became apparent that the hardware generation of an electrical signal was limited; new signals required new circuits. It was therefore decided that to offer maximum flexibility, especially during the system development phase, the computer would be used to design the airflow profile. This would enable rapid evaluation of modification to the airflow, which was then produced using a digital to analogue, (D/A), converter. A 12 bit D/A, (Bede Technology, PC4DAH), was installed in the computer and controlled by the main impedance application code. the existing interrupt service routine, (ISR), which gathers pressure and flow data, was extended to incorporate the output of the next airflow signal component to the power amplifier. The ISR was triggered by a timer on the D/A board set to run at a rate of 128Hz, previously the timer on the analogue input board had been used offering a slightly less convenient sampling rate of 120Hz. Signals were created by developing a frequency spectrum and using the inverse Fourier transform to produce a time domain signal. This enabled the exact frequency content of the airflow to be controlled.

Having modified the system generating the airflow signal in software it was then necessary to consider the changes to the airflow content. It was observed that the analysis had been designed to produce results with 1Hz resolution; greater resolution gave less smooth estimates as fewer blocks available to average, yet no additional information was observed. There then seemed little point having frequencies present which would effectively be eliminated at the display stage. Thus it was decided to create a frequency spectrum with power concentrated at integer values between 2 and 40Hz, in 1Hz

increments. Indeed other groups, notably Landser *et al*, (1976), have used this approach, using a fundamental frequency and subsequent harmonics. To ensure a known frequency content in the one second flow spectra the length of the generated airflow sequence was set equal to the length of the analysis transform. A 64 point complex frequency spectrum was established, resulting in a 128 point time varying sequence. So after each second of data was collected the sequence was repeated. Hence for each of the 16 one second blocks collected the same signal is used as a stimulus. It was reasoned that this would improve the signal to noise problem, by ensuring a known signal was present in each block analysed.

By assigning larger amplitudes to the lower frequency array elements it was possible to compensate for the frequency characteristics of the generator assembly. The same scheme also enabled the low frequency airflow content to be increased in an attempt to improve the data reliability. It was established that increasing the airflow amplitude did improve the coherence values and that the increase did not produce any non linear effects. It seemed unnecessary to increase the power at frequencies where the coherence was already acceptable. In common with Rotger *et al*, (1991), it was concluded that there was no harm in this strategy. The increase observed, however, still left the coherence values beneath the acceptance threshold. The amount by which the power could be increased was ultimately limited by the upper limit of the D/A. In any case a limit would be reached where the signal amplitude would cause discomfort for the individual. In retrospect the correction for the frequency response of the vibration generator could have been done in hardware as this will remain constant, thus offering a greater dynamic range of the D/A for the

delivered airflow.

The next question which arose was how to allocate the phase angles in the signal. Filling only the real array elements with values prior to the inverse transform leads to constructive interference between frequencies, with amplitudes overflowing array limits. A solution to this was the random allocation of phase angles by multiplying amplitude by the cosine or sine of the random phase to realise real and imaginary components respectively. Obviously each time the algorithm was executed a different signal was realised, some of which exhibited large peaks in the time varying signal. It was necessary to define criteria for selecting a waveform and then to use that waveform for all measurements, thus ensuring compatibility between subjects. The strategy adopted was based on a similar idea to crest factor measurements. It was argued that a factor could be calculated relating the average power in the signal to the peak value present. If the peak exceeded a given threshold than a large factor was obtained and the signal rejected. The factor threshold was set at a value of 1.4. This value was based on the fact that it is known doubling the amplitude at certain frequencies is acceptable, indeed this is the approach used to boost the low frequency data. Additionally, on an empirical note, signals which exceed this limit subjectively felt uncomfortable when applied to the lung. Often accompanied by drops in coherence values at high frequencies. Rejected waveforms had large peaks and it is possible that these large peaks act like an impulse which may be promoting non linear system behaviour. This method still yielded a number of acceptable waveforms having run the algorithm around fifty times, all of which appeared to give similar results.

At the time of this section of the research it was discovered

that Darcozy and Hantos, (1991), had considered the problem more formally. The result of their work showed that the optimum signal to use was one whose amplitude distribution is not maximally centred around the signal mean. Although our approach was less formal the merits of minimising the crest factor are confirmed by Darcozy and Hantos. The shape of the flow power spectrum of the signal used is shown in figure 6.1, together with an example flow spectrum when a subject is connected as a load. The graphs have been overlaid to illustrate that the shape of the spectra are the same.

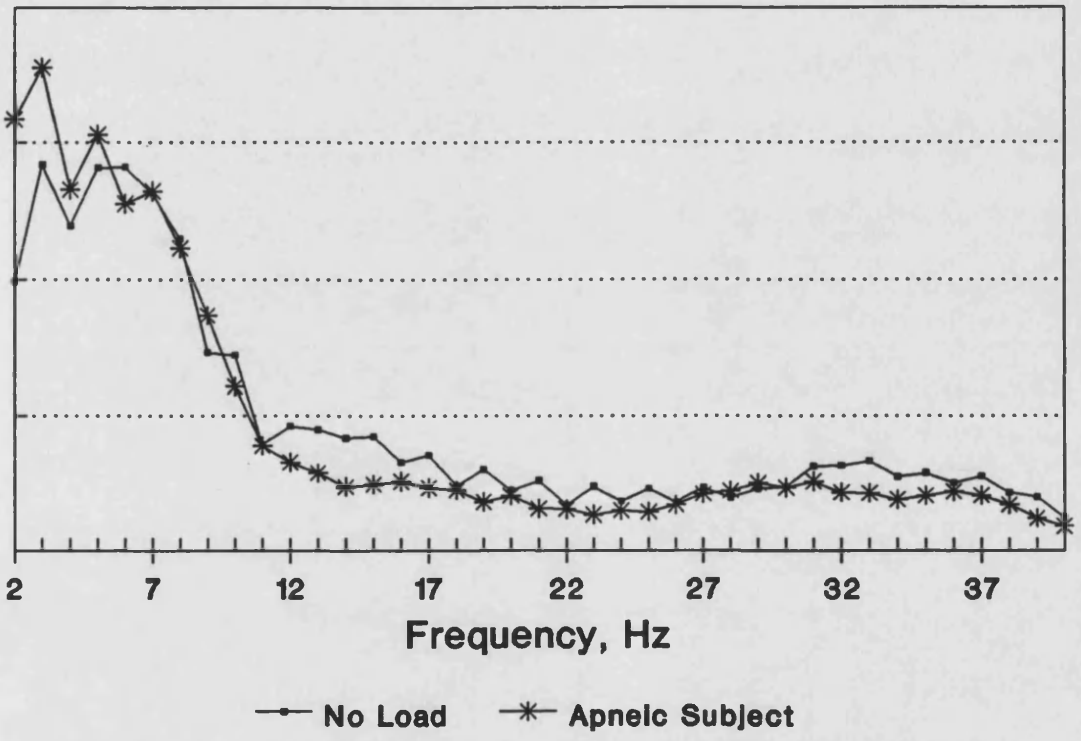

Figure 6.1 Flow Power Spectra of New Signal

The new oscillatory signal was used to make measurements in a small group of volunteers to assess whether any improvement had been achieved. Figure 6.2 shows the average coherence values for a group of 5 male volunteers and the average values of for five volunteers using the initial random noise signal. An improvement in coherence is apparent though not as significant an improvement as had been hoped

for. The rejection threshold of 0.95 would still mean that data is only acceptable from 8Hz upwards and little data acceptable below the resonant frequency.

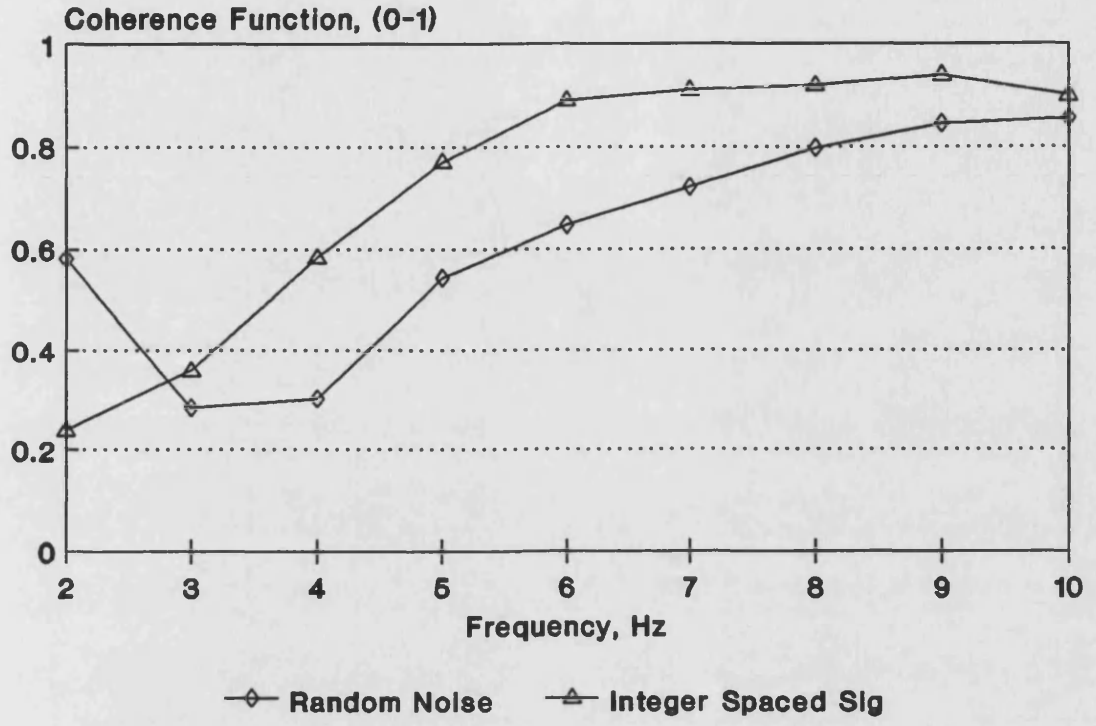

Figure 6.2 Coherence Comparison - Different Oscillatory Signals

6.4 Improving the Signal Processing

Having realised an improvement in coherence values by modifying the oscillatory airflow, the next step was to reconsider the analysis regime. The problem centres around data in the range 2 to 10Hz, above which data appears to be more reliable. The poorer quality data at low frequencies is thought to be associated with respiration acting as a source of interference. Although filtering out the breathing signal or varying the Fourier transform length, to include more low frequency power, has not resolved the problem. It was felt that better quality data, with lower errors, could be achieved, as after all many groups have made single frequency measurements at these low frequencies with

no apparent problems.

The oscillatory airflow now only comprises integer frequency multiples, therefore any signals at non integer frequencies must be associated with interference sources. These frequencies could be filtered out using a comb filter to pass signals only at integer frequency values. By creating a series of band pass filters centred around the airflow frequencies pressure and flow signals could be pre-processed in the time domain prior to Fourier transformation. To achieve this it was decided to implement the filters digitally, thus ensuring each filter had an identical response. The comb filter had 39 bandpass elements at 1Hz intervals in the range 2 to 40Hz, the pressure and flow data were applied to each element connected in parallel, hence the algorithm was executed 78 times. It would have been prohibitively complex to achieve this with analogue components as it is necessary to ensure comparable pressure and flow frequency components retain their phase relationship. Additionally the digital filter can be configured to have a remarkably narrow bandwidth, again this is not feasible with analogue components. The building block for the filter was a second order band pass filter based on an analogue transfer function. This was used to create a digital filter difference equation, using the bilinear transformation, which is given in equation 6.1. (Hirano *et al* 1974, Oppenheim and Schafer, 1975).

The filter bandwidth, β, was set to 0.05Hz and the filter centre frequencies, f_i, set to coincide with the applied signals. The filtering regime was validated by creating sinewaves in software and applying them to the filter, with figure 6.4 showing the frequency response. As this section of work was being completed it came to light that another group had published a paper outlining an identical pre-

$$y(k) = a_1 y(k-1) - a_2 y(k-2) + \frac{(1-a_2)}{2} x(k) + \frac{(a_2-1)}{2} x(k-2)$$

$$a_1 = \frac{2\cos(2\pi f_i \tau)}{1+\tan(\pi\tau B)} \qquad 6.1$$

$$a_2 = \frac{1-\tan(\pi\tau\beta)}{1+\tan(\pi\tau\beta}$$

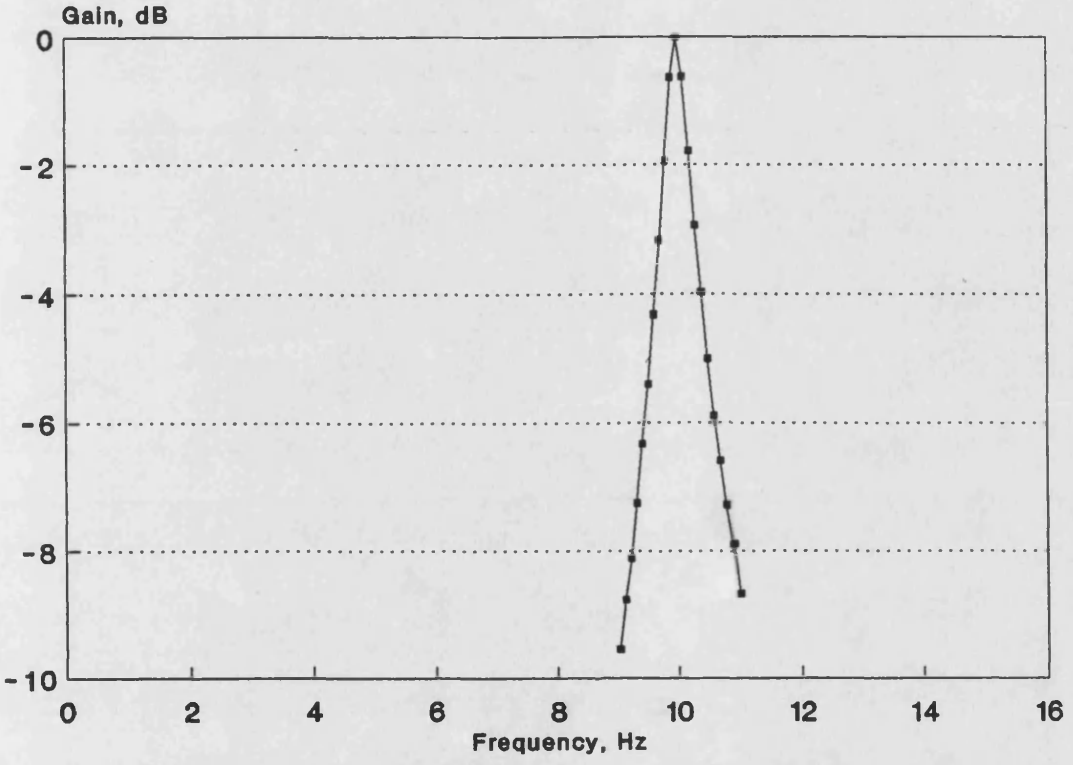

Figure 6.3 Bandpass Filter Response - 10Hz Centre, 0.5Hz Bandwidth

processing approach, (Farré *et al*, 1990). It was encouraging to see that their paper also showed considerable improvements in coherence function data using the filters. The paper proposed filtering the data in the forward and reverse directions to minimise the loss of data due to the settling time of the filters. This seemed very sensible and therefore this approach was adopted in our laboratory as well.

The new oscillatory signal and filtering regime were tested on the same small group of volunteers to assess improvements to the data

quality. Figure 6.4 illustrates coherence function values in eight subjects after the results have been filtered, with figure 6.5 showing the random errors associated with the impedance modulus estimate. There is a significant improvement in data quality following the modifications introduced, with the impedance modulus and 95% confidence limits being shown for 4 of the subjects in figure 6.6. The forward and reverse application of the filters took 120 seconds, (using the 12MHz Opus Turbo V computer), to execute and was achieved off line.

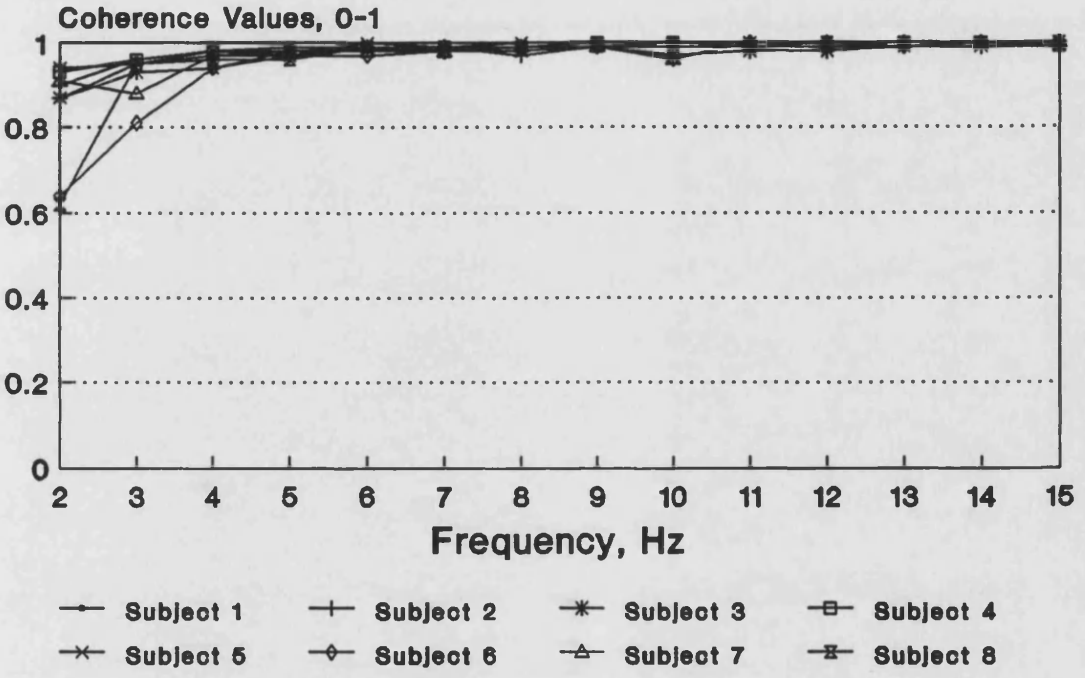

Figure 6.4 Coherence Values Post Filtering - 8 Male Subjects

6.5 Program Structure

The impedance application program used in the prototype has been extended to produce the oscillatory airflow and to digitally filter the pressure and flow data. The Pascal code is easy to modify due to the unit based structure, with the main program retaining the structure outlined in chapter 4, calling procedures from the units as required. In addition to using internal Pascal units supplied with the compiler

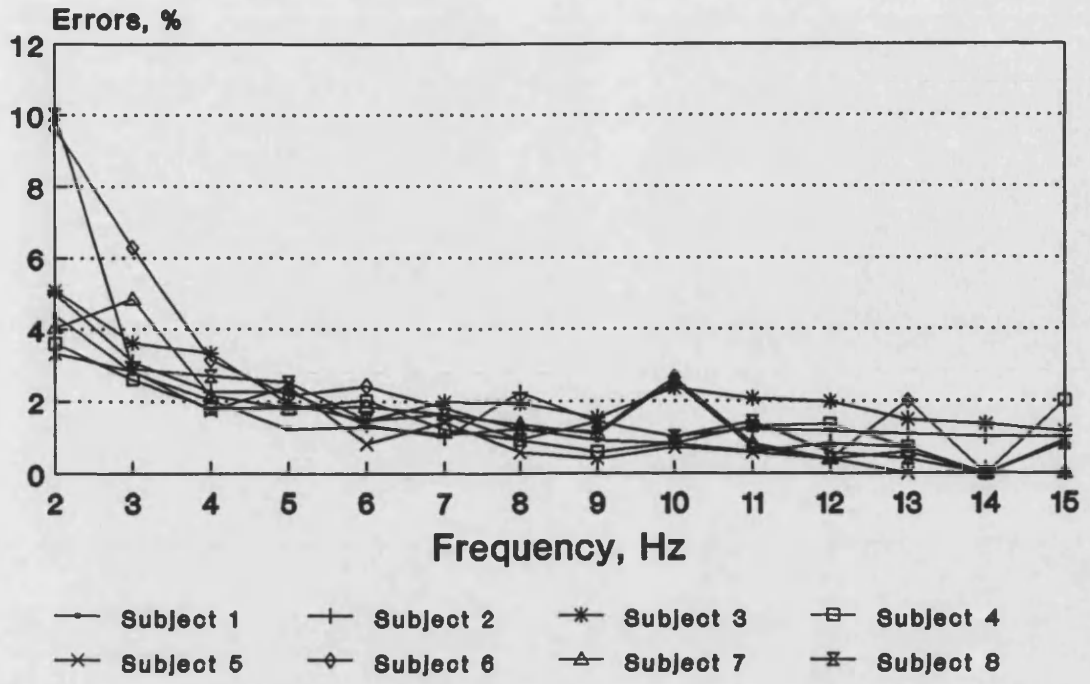

Figure 6.5 Impedance Modulus Errors - 8 Male Subjects

the impedance program uses six units developed specifically for this work. The Spectrum Array Arithmetic library, purchased from Cambridge Electronic Design and used to achieve the Fourier analysis is also a separate unit. The units and the public functions or procedures they offer are summarised in table 6.1, showing the number of code lines per unit and the disk file size of the compiled unit. The main impedance program has 286 lines and compiles to a disk file of 76.24kiloBytes, (kB). An instruction manual describing the operation of the system was written, (appendix A), to assist new users in becoming familiar with the system.

6.6 Changes to the Instrumentation.

One problem which became apparent during the early impedance measurement was the lack of adjustment of the height of the mouthpiece. This was overcome by mounting the airflow assembly on an adjustable

Unit Name	Content	No of Lines
Global	Constant Declarations Type and Variable Declarations	122 4.00kB
General	Initialisation and Program Termination Menu Management User Input Interface Data Storage and Retrieval Routines Data Display: Cursor, Tabulated & Summary Batch File Processing Background Code	1087 38.48kB
Interrupt	Interrupt Service Routine A/D and D/A Control Oscillatory Signal Design	486 14.45kB
Analyse	Frequency Domain Processing Data Windowing Impedance Calculation	299 10.18kB
Display	Graphics Control Routines Data Display Management	365 11.57kB
Filtering	Comb Filtering	144 5.14kB
Spectrum	Commercial Signal Processing Package	----

Table 6.1 Pre Compiled Units Accessed by the Main Impedance Program.

height laboratory jack. The only other change to the hardware was the removal of the long length of tubing through which the subject breathed. The diameter of this tube (11mm), was felt to be too narrow creating a high resistance pathway in excess of $1hPal^{-1}s$ at respiratory frequencies. While this had little significance for normal subjects it may have proved too much for many patients. Upon advice from clinical colleagues it was decided to use a wider tube and it was noted that most other groups use a 25mm diameter tube. After initial trials such tubes gave cause for concern, having measured their impedance by connecting them as loads to the system. The main problem was that their impedance frequency response peaked sharply in the 2Hz to 40Hz range, the implication being that they would modify the flow spectrum at these frequencies. Therefore it was decided to use a purely resistive load made of a number of stainless steel tubes bound together. The tubes were short, 20mm, and offered a total resistance of less than $1hPal^{-1}s$, the volume of the new load further reduced the system deadspace. The resistor offers a constant load with frequency so does not alter the applied flow spectrum. More high frequency flow is lost as the impedance does not increase with frequency, however, this may be compensated for by increasing the overall flow level.

6.7 Summary

Few modifications have been made to the instrumentation. The main changes introduced included a new oscillatory airflow, which concentrated the power at integer frequencies at 1Hz intervals, with increased power at low frequencies. The development of a comb filter system enabled extraneous noise to be eliminated by only analysing pressure and flow signals at the applied frequencies. The combination

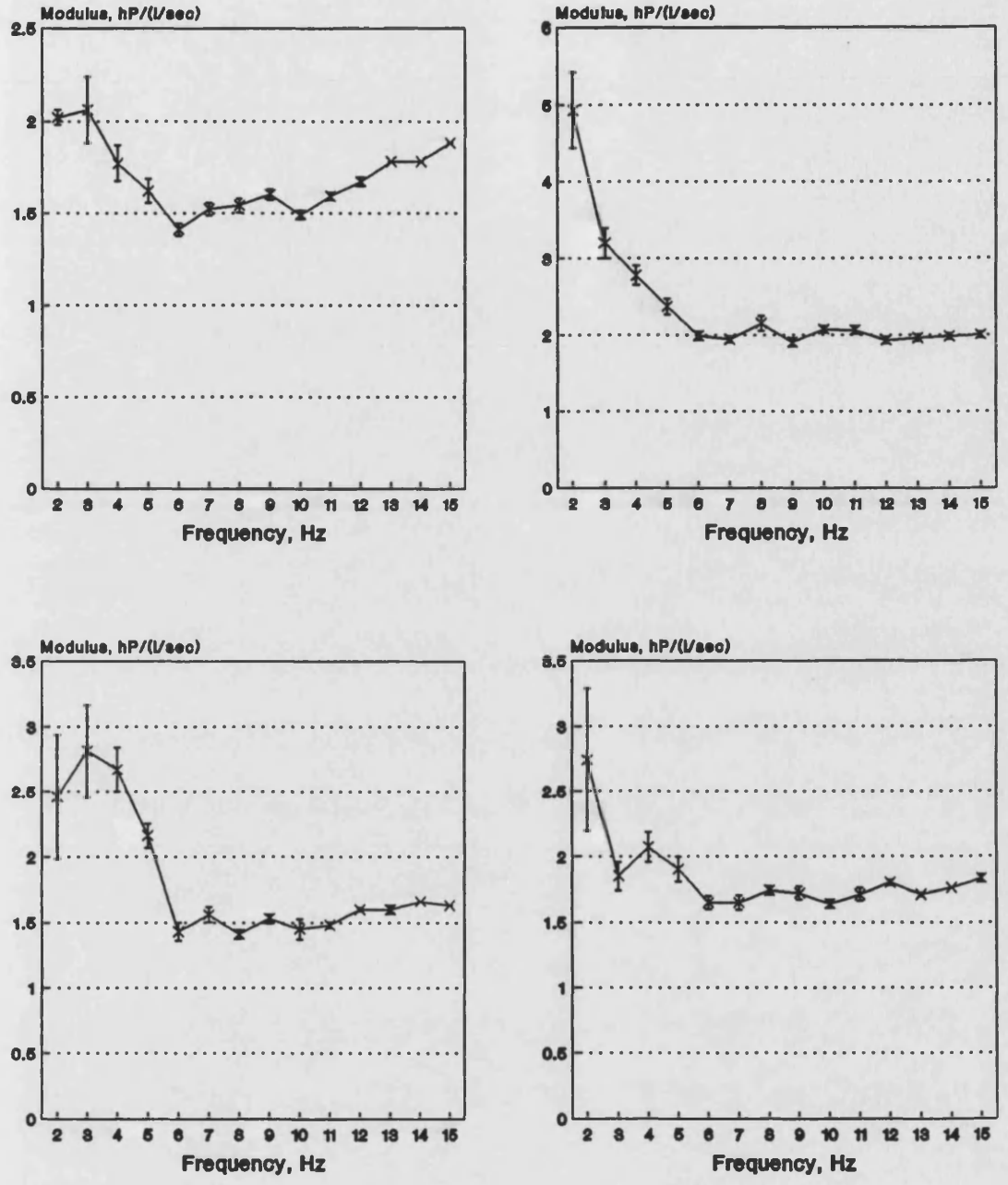

Figure 6.6 Impedance Modulus with 95% Confidence Limits - 4 Subjects

of these techniques resulted in dramatic improvements in coherence function values and therefore more reliable impedance data. The impedance data now exhibits smaller errors than those presented in the previous chapter, with data down to 4Hz having errors less than 4%. Figure 6.6 illustrates that data still has larger errors at 2Hz to 4Hz than higher frequencies.

Chapter 7 Improved Impedance Results

7.1 Introduction

Results are presented for a group of normal volunteers and a small patient group using the modified impedance instrumentation. As an improved oscillatory signal has been developed it was necessary to repeat the tests. This chapter takes the same format as the preliminary results chapter, however, the data set is presented in more detail as the increased coherence means there are less errors associated with the results. Three element resistive, capacitive, inertance models have been fitted to the normal data.

7.2 Impedance Results in Healthy Subjects

Figures 7.1 through 7.6 show typical impedance results for three female and three male subjects using the improved impedance equipment. Pressure and flow results were comb filtered prior to the frequency domain analysis. The results, which may be compared with the data from the prototype, illustrate the variation of impedance with frequency, again with three numeric indices being quoted in the information box at the bottom of the display. The figures give the average resistance between 5Hz and 8Hz, as well as the average over 27Hz to 30Hz and the resonant frequency. The resistance values have units of $hPal^{-1}s$. In these plots the data is not displayed if the coherence values fall below 0.6, with the dotted line in the coherence/resistance window being set at 0.95 which was the proposed threshold level. There is clear improvement in the data at low frequencies, with data down to 2Hz often being available. The impedance results follow the general second order form described in the literature. At low frequencies there is a

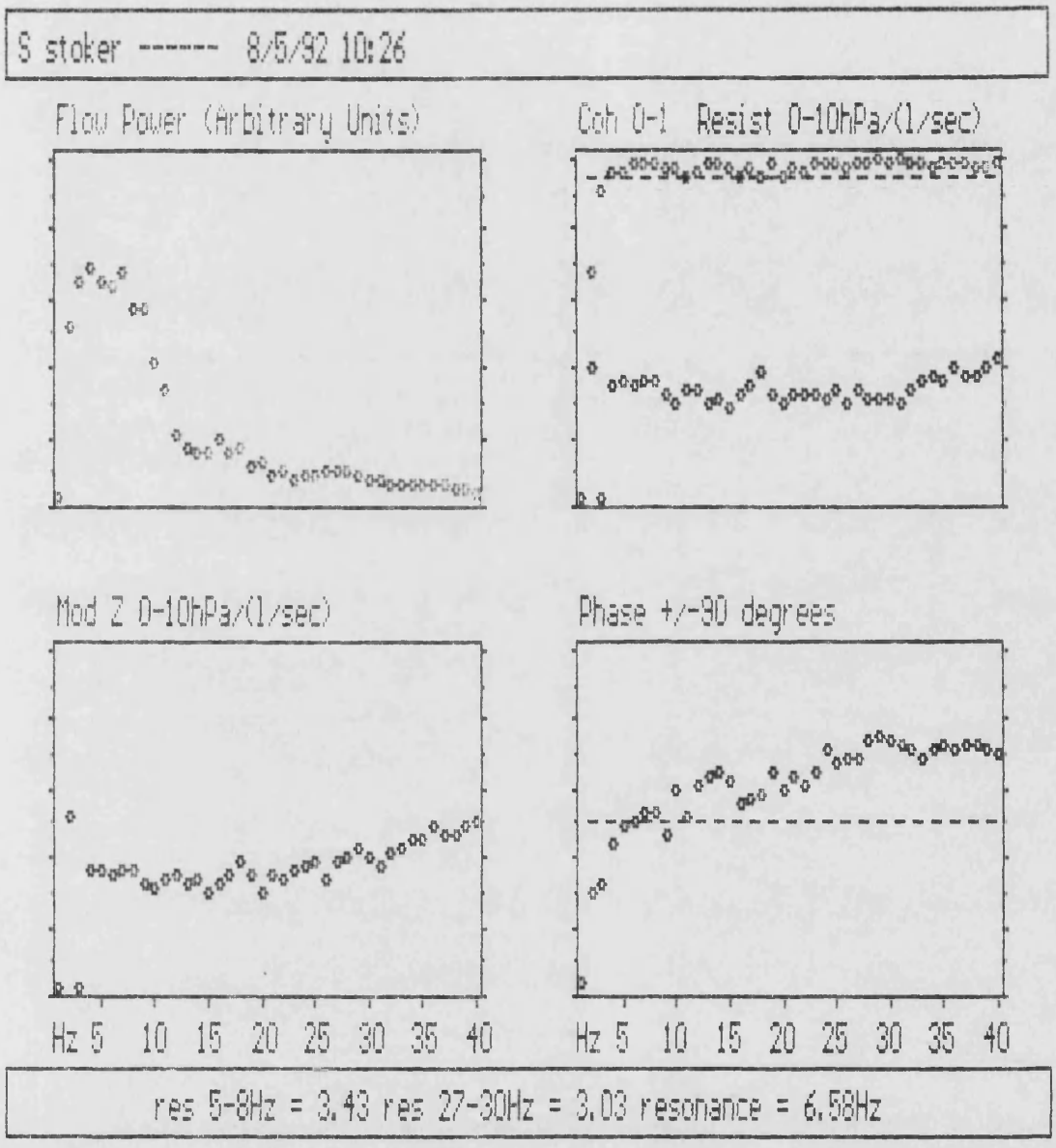

Figure 7.1 Impedance Results - Female Volunteer 1

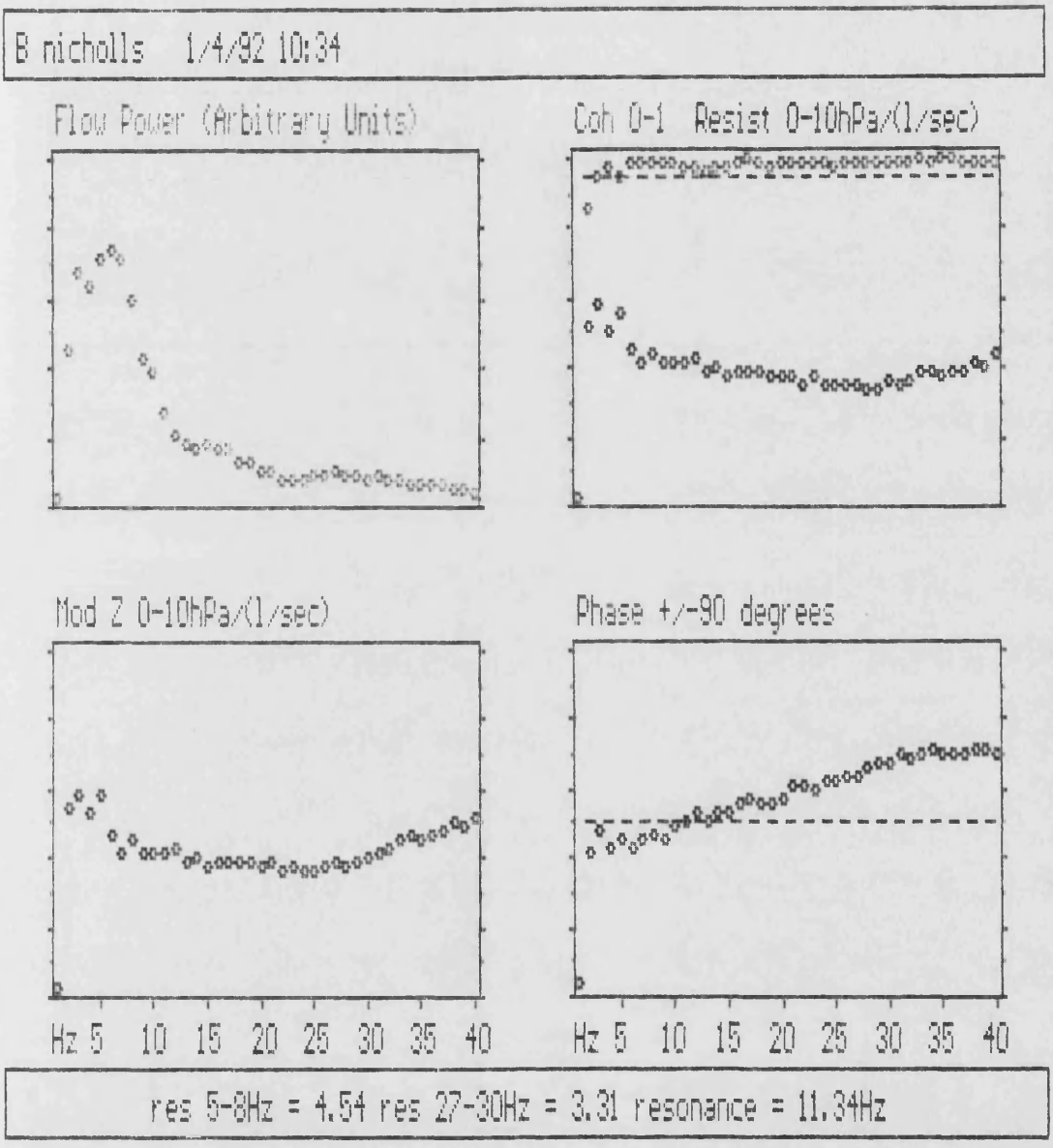

Figure 7.2 Impedance Results - Female Volunteer 2

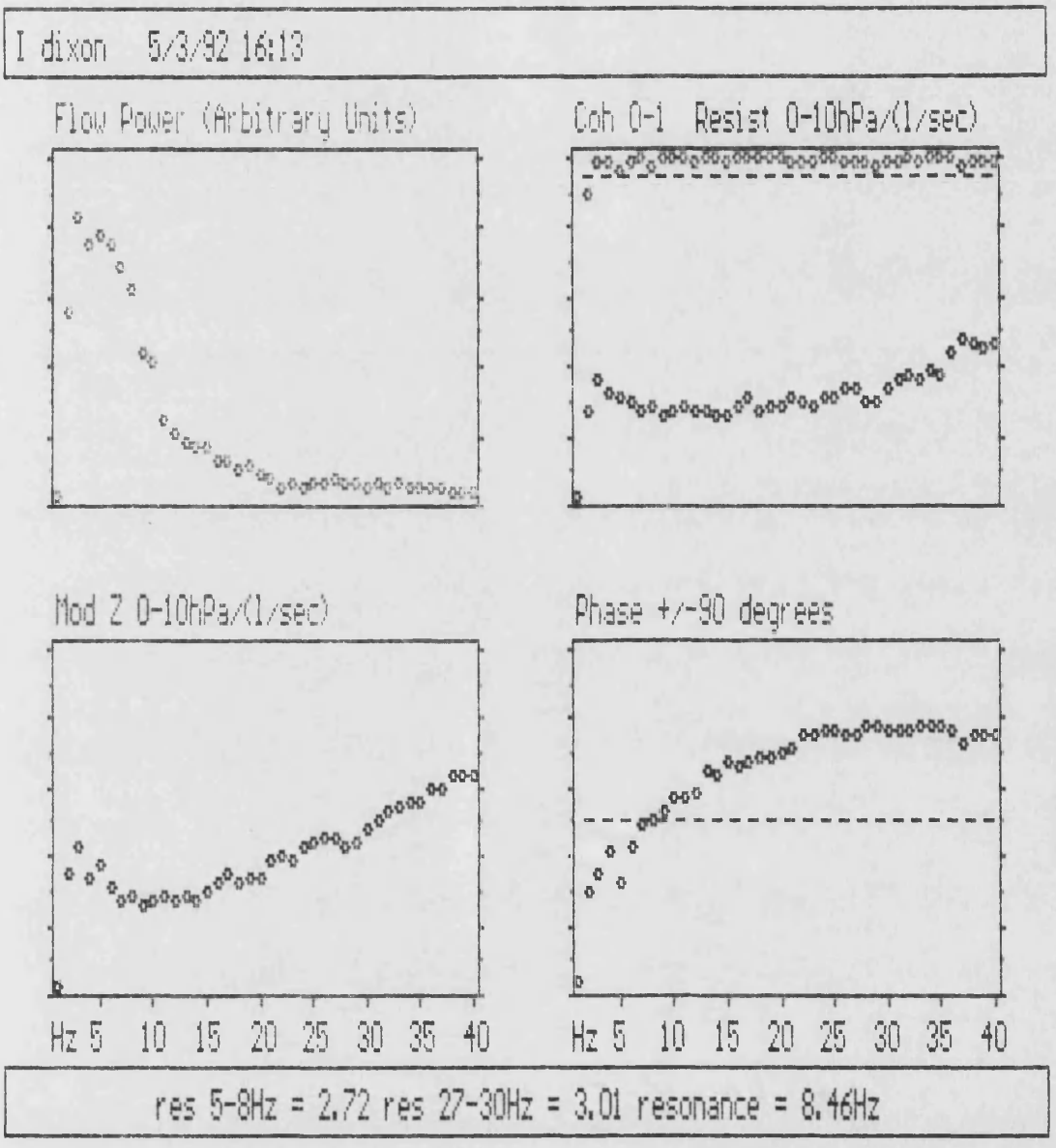

Figure 7.3 Impedance Results - Female Volunteer 3

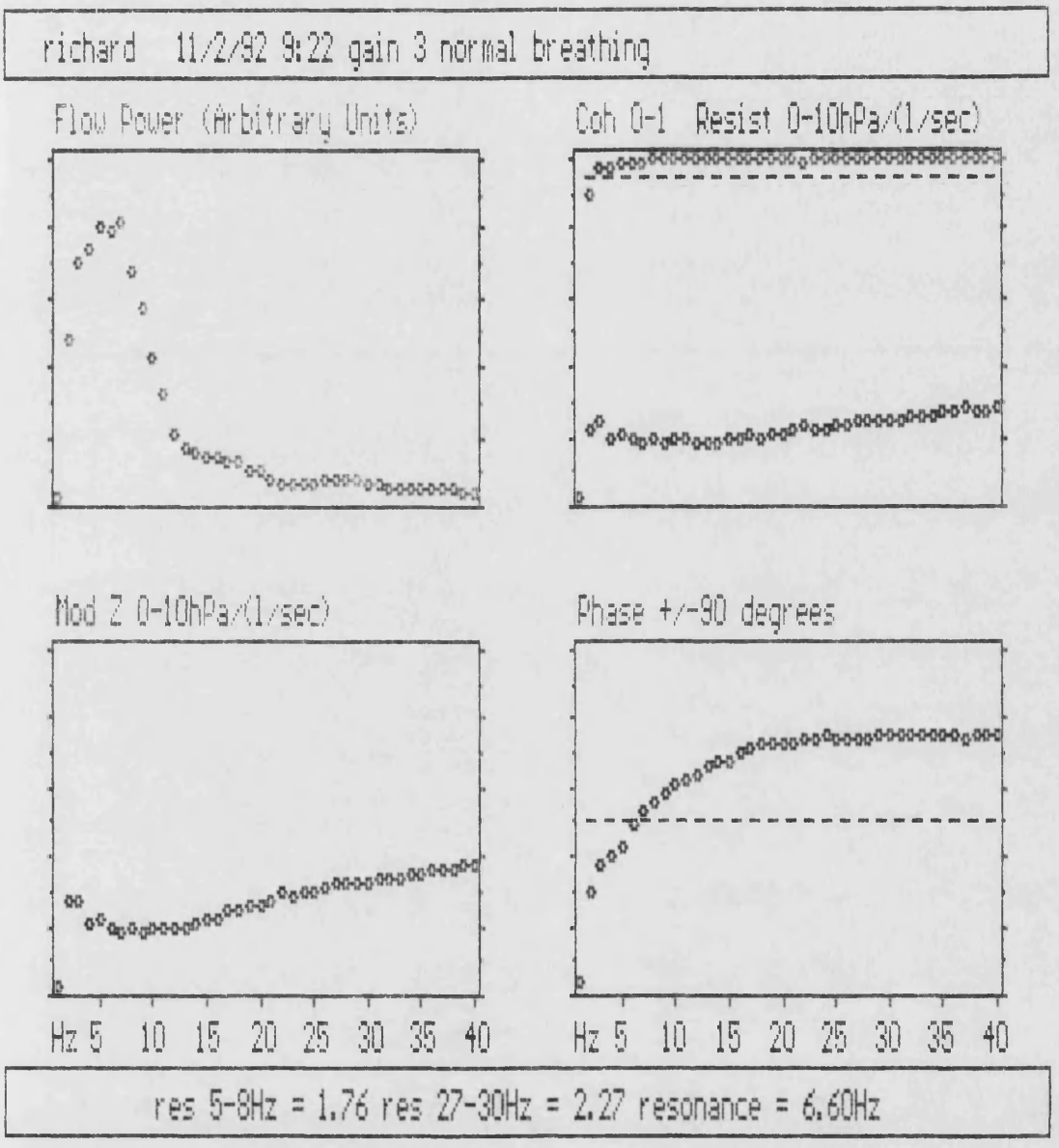

Figure 7.4 Impedance Results - Male Volunteer 1

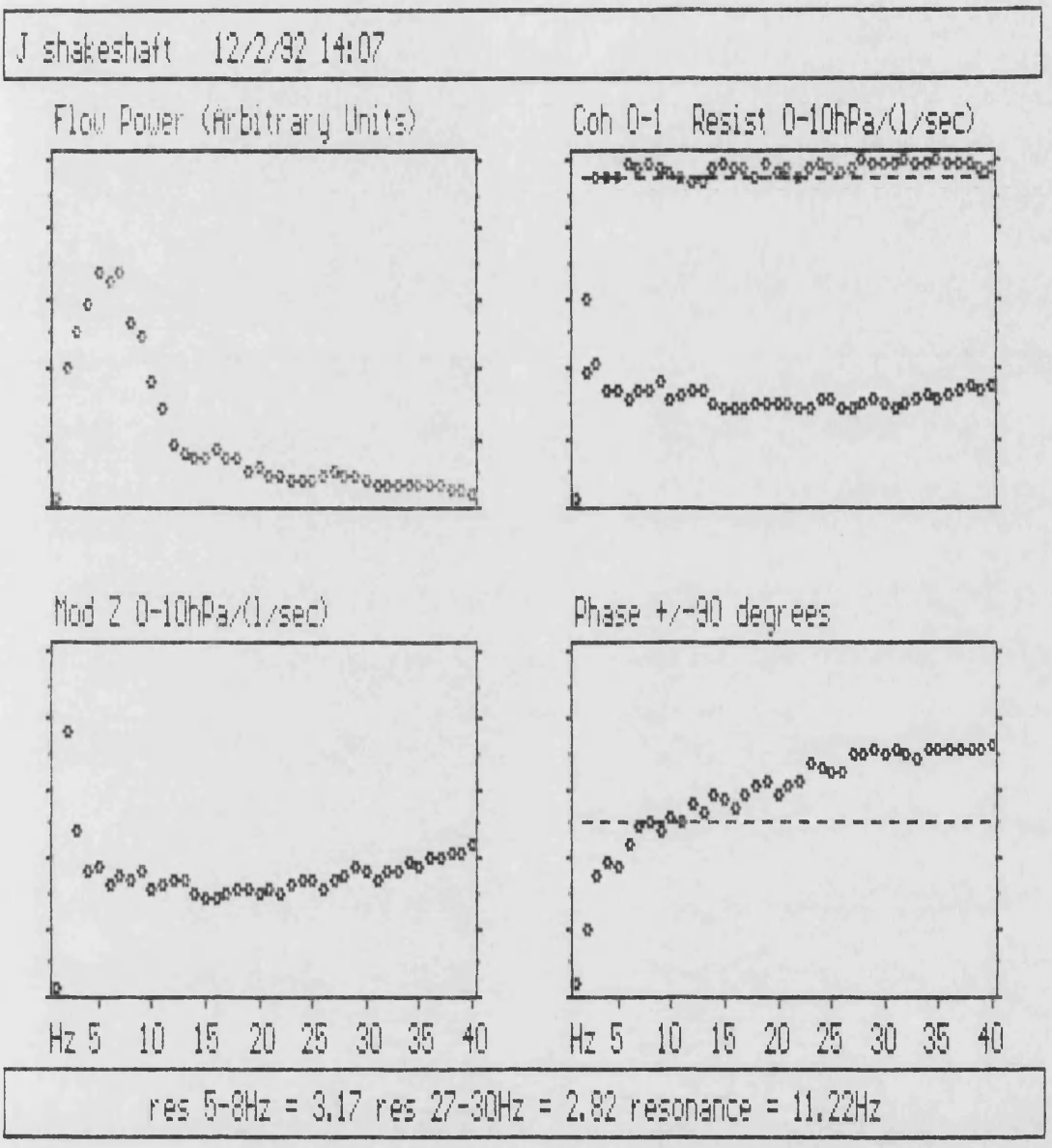

Figure 7.5 Impedance Results - Male Volunteer 2

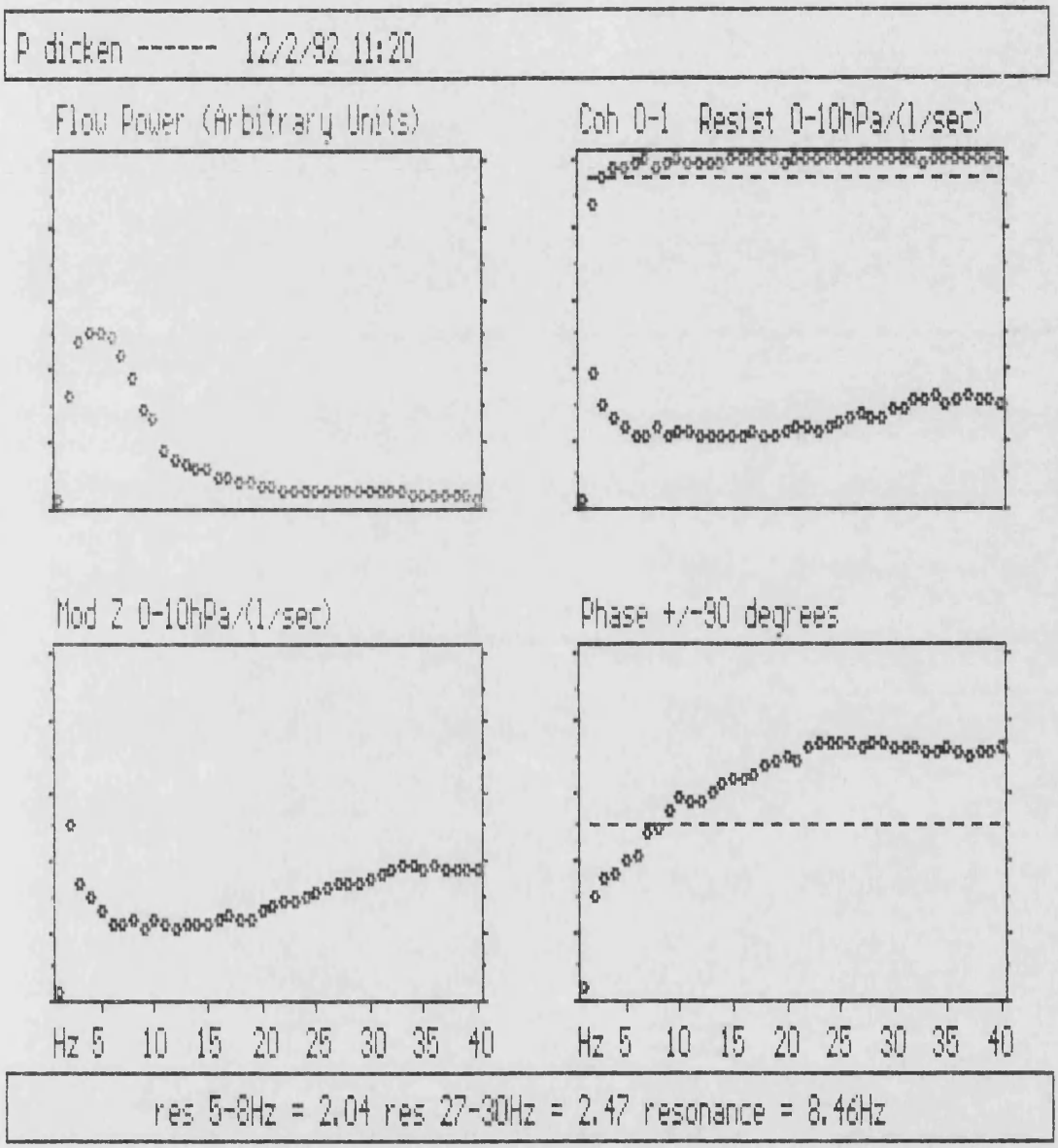

Figure 7.6 Impedance Results - Male Volunteer 3

negative phase shift and rise in modulus due to the contribution of compliance effects. As frequency increases resonance is observed between 8Hz to 10Hz, from which point the modulus and phase angle increase as the inertial effects become more dominant. The resistance estimate appears, on average, to increase with frequency, which is consistent with comparable published data. All subjects undertook forced expiratory tests following the impedance measurements and all results were within normal limits and unremarkable. Male and female numeric results are summarised in tables 7.1 and 7.2, with terms defined as follows:-

R - resistance computed from equation 2.1, $hPal^{-1}s$

L - inertance compute from equation 2.3, $hPal^{-1}s^2$

C - compliance computed from equation 2.2, $lhPa^{-1}$

f_{rmod} - resonance computed from LC model values, Hz

f_r - resonance measured from impedance data, Hz

R_6 - resistance at 6Hz, $hPal^{-1}s$

γ^2 - coherence function, 0-1

R_{5-8} - average resistance over 5Hz to 8Hz range, $hPal^{-1}s$

R_{27-30} - average resistance over the 27Hz to 30Hz range, $hPal^{-1}s$

Z_{40} - impedance modulus at 40Hz, $hPal^{-1}s$

θ_{40} - impedance argument at 40Hz, degrees

Subject	R	L	C	f_{rmod}	f_r	R_8	γ^2	$R_{5\text{-}8}$	$R_{27\text{-}30}$	Z_{40}	θ_{40}
1	1.94	0.012	0.067	5.6	6.0	1.47	2,3,2	1.45	2.27	3.66	44.0
2	2.70	0.012	0.031	8.1	7.4	2.17	4,4,2	2.25	2.91	4.39	29.9
3	1.86	0.011	0.044	7.2	6.6	1.68	3,3,4	1.77	1.88	3.56	54.5
4	2.19	0.013	0.025	8.9	8.2	1.93	4,3,3	1.68	2.34	4.04	49.8
5	2.77	0.009	0.022	11.7	10.47	2.84	3,2,4	2.92	2.52	3.60	37.5
6	2.06	0.011	0.030	8.9	7.5	2.05	3,4,3	2.21	2.00	3.51	47.7
7	2.48	0.012	0.116	4.3	6.4	2.02	2,2,2	1.97	2.91	4.07	37.2
8	2.68	0.011	0.051	6.6	7.6	2.38	3,4,3	2.51	2.71	4.08	36.8
9	2.56	0.013	0.029	8.2	9.2	2.84	3,4,4	2.72	2.46	4.34	47.0
10	1.64	0.012	0.030	8.6	8.4	1.53	4,4,5	1.48	1.85	3.26	52.7
11	2.70	0.009	0.025	10.4	9.6	3.04	4,4,3	2.82	2.69	3.66	38.5
12	1.89	0.010	0.032	8.8	8.8	1.94	4,4,5	1.99	1.95	3.25	49.2
13	2.51	0.012	0.030	8.6	9.0	2.69	4,3,5	2.61	2.57	3.47	46.1
14	2.27	0.011	0.044	7.1	6.7	2.09	4,3,4	2.12	2.46	3.66	41.9
15	3.03	0.009	0.025	10.9	8.9	2.98	4,2,2	3.02	3.05	3.82	32.3
16	2.49	0.010	0.037	9.5	7.1	2.57	4,4,4	2.58	2.50	3.65	42.9
Mean ± sd	2.36 ± 0.39	.011 ± 0.001	0.040 ± 0.023	8.3 ± 1.9	8.0 ± 1.3	2.14 ± .69	—	2.26 ± .51	2.44 ± .38	3.75 ± .34	43 ± 7.2
Coeff of Variation, %	17	12	59	23	16	32	—	22	15	9	17

Table 7.1 Normal Impedance Results Summary - Male Group.

Subject	R	L	C	f_{rmod}	f_r	R_8	γ^2	$R_{5\text{-}8}$	$R_{27\text{-}30}$	Z_{40}	θ_{40}
1	3.40	0.011	0.021	10.6	8.8	3.27	3,3,2	3.27	3.20	4.62	31.5
2	3.20	0.013	0.022	9.4	9.2	2.95	3,3,3	2.95	3.39	4.91	33.0
3	2.96	0.016	0.029	7.4	7.7	2.65	4,3,4	2.46	3.06	5.59	36.2
4	3.05	0.013	0.046	6.6	6.9	2.82	3,5,2	2.92	3.00	4.96	35.8
5	3.65	0.011	0.032	8.5	9.3	3.17	4,3,4	3.28	4.02	4.76	25.6
6	3.11	0.010	0.064	6.4	8.1	2.40	4,3,5	2.52	3.88	3.96	24.2
7	4.76	0.011	0.022	10.6	10.3	4.91	4,4,4	5.04	4.92	5.47	21.8
8	4.41	0.011	0.027	9.6	8.4	4.15	4,4,4	4.31	4.68	5.43	21.0
9	2.32	0.013	0.021	9.7	10.7	2.36	3,4,4	2.43	2.18	3.93	37.2
10	3.23	0.010	0.021	10.6	10.6	3.23	4,5,4	3.33	3.11	4.43	32.1
11	2.46	0.013	0.023	9.3	10.3	2.54	5,4,4	2.57	2.47	4.24	40.7
12	3.16	0.014	0.031	7.8	7.6	2.86	4,2,4	2.95	3.28	4.89	34.4
Mean ± sd	3.31 ± 0.70	.012 ± .002	0.03 ± 0.013	8.9 ± 1.5	9.0 ± 1.3	3.1 ± 0.75	—	3.17 ± .79	3.43 ± .82	4.76 ± .56	31.1 ± 6.5
Coefficient of Variation, %	21	15	43	17	14	24	—	25	24	12	21

Table 7.2 Normal Impedance Results Summary - Female Group.

Subject	R	L	C	f_{rmod}	f_r	R_θ	γ^2	$R_{5\text{-}8}$	$R_{27\text{-}30}$	Z_{40}	θ_{40}
1	2.06	0.011	0.056	6.3	6.5	1.76	3	1.77	2.28	3.60	44.0
2	1.90	0.011	0.074	5.5	6.6	1.37	3	1.46	2.22	3.51	43.3
3	1.91	0.012	0.063	5.8	6.3	1.43	2	1.45	2.22	3.67	44.7
4	1.93	0.012	0.052	6.2	6.5	1.64	3	1.59	2.15	3.72	44.5
5	1.82	0.012	0.071	5.4	6.1	1.41	2	1.39	2.10	3.56	43.5
6	1.94	0.012	0.077	5.2	6.2	1.45	3	1.48	2.22	3.68	43.5
7	1.96	0.012	0.072	5.4	6.4	1.51	2	1.49	2.30	3.61	44.0
8	1.95	0.012	0.058	6.0	6.3	1.57	3	1.48	2.26	3.63	43.5
9	1.90	0.013	0.072	5.3	5.4	1.33	2	1.37	2.26	3.73	43.8
Mean ± sd	1.93 ± 0.06	0.012 ± .0006	0.066 ± .009	5.68 ± .41	6.3 ± .36	1.50 ± .14	—	1.50 ± .12	2.22 ± .06	3.63 ± .07	43.9 ± .5
Coefficient of Variation %	3	5	14	7	6	9	—	8	3	2	1

Table 7.3 Impedance Results Summary - Variation Within a Male Subject.

7.3 Asthmatic and Healthy Smoker Results

Figures 7.8, 7.9 and 7.10 show the ability of the system to follow changes in lung mechanics before and after medication in one asthmatic volunteer. The subject deliberately suspended his medication and became severely wheezy in order to show a gross change from the normal group. Following medication the impedance of the system falls, with the resonant frequency and resistance reducing towards normal levels. It is also apparent that the shape of the impedance versus frequency curves are different to the normal examples of figures 7.4 through 7.6. The three graphs enable the time course of the response to treatment to be assessed.

Additionally table 7.4 shows the results for 4 females and the asthmatic male discussed above. The first three results are for volunteers who had respiratory symptoms, although their spirometric indices were normal. The fourth set of results in the table were for an asthmatic patient, who showed no improvement to her nebulised therapy as assessed by peak flow measurements. The impedance data showed a small yet quantifiable reduction in resistance post medication. None of the subjects in this group exhibit the slight increase in resistance with frequency. In fact the reverse is true, with the low frequency resistance indices exceeding the higher ones.

Table 7.5 shows a small group of young asymptomatic male smokers, who volunteered as part of the non patient group. None of them were particularly heavy smokers yet the frequency dependence of resistance seems to be absent, although the other parameters are not significantly different from the normal male group.

Sex	f_r	R_6	γ^2	R_{5-8}	R_{27-30}	Z_{40}	θ_{40}	Comment
female	11.6	4.27	5,3,5	4.2	3.11	4.48	32.4	Asthma
female	15.5	4.15	4,4,4	4.0	3.12	4.20	35.8	Exercise
female	21.8	3.96	7,4,-	3.96	2.95	2.95	35.4	Exercise
female	27.2	9.27	6	9.64	4.16	4.60	18.1	Asthma
	29.1	8.83	5	8.48	3.90	4.18	12.7	pre-med
	28.3	9.57	4	8.88	4.48	4.53	14.6	
	28.6	10.01	5	8.39	4.04	4.23	15.3	
	24.5	7.80	6	6.95	4.19	4.64	23.4	Post med
	23.0	7.22	5	6.95	4.50	4.99	23.1	
	21.6	7.15	6	6.74	4.2	4.79	24.5	
male	32.5	8.76	5	8.62	4.73	4.65	4.1	Asthma
	29.6	8.38	4	7.98	4.38	4.04	6.2	pre-med
	35.2	8.00	5	8.27	4.41	4.70	3.2	
	16.8	4.85	2	4.95	3.71	4.30	22.9	vent+5
	15.8	4.71	3	4.68	3.43	4.35	30.5	vent+10
	13.7	3.88	2	3.89	3.13	4.21	32.9	vent+20
	9.7	3.58	2	3.55	2.94	4.24	36.8	vent+30

Table 7.4 Asthmatic Volunteers - Including Examples Post Medication.

f_r	R_6	γ^2	R_{5-8}	R_{27-30}	Z_{40}	θ_{40}
8.7	2.04	5,2,4	1.98	1.95	3.38	49.8
9.0	3.30	5,4,4	3.13	2.76	4.6	42.8
9.3	1.89	2,4,3	1.81	1.81	3.89	49.1
10.5	2.63	5,4,4	2.57	1.98	3.14	44.6

Table 7.5 Impedance Results Summary - 4 Male Smokers.

7.4 Other Published Impedance Results.

It is of interest to compare the results obtained in our laboratory with other published data. The mean RLC values obtained in healthy males and females, reproduced from tables 7.1 and 7.2, are included in table 7.6 together with the values from Peslin's 1986 review, which were presented in the literature review as table 1.5. Recent normal data was also available from the 1990 workshop held for the European Commission, (Rotger *et al*, 1991 and Peslin *et al*,1991).

Additionally from the data of Rotger *et al*, 1991, the average resistance between 4Hz and 8Hz was given as 2.57±0.46hPal^{-1}s, between 28Hz and 32Hz the average was 2.55±0.38hPal^{-1}s and their estimate of resonant frequency was 6.8±0.4Hz. The reactance, averaged between 28Hz and 32Hz, was 3.68±0.45hPal^{-1}s. This parameter has not been quoted for our data, however using the resistive and reactive components the phase angle may be estimated as approximately 55°, which exceeds even our 40Hz values.

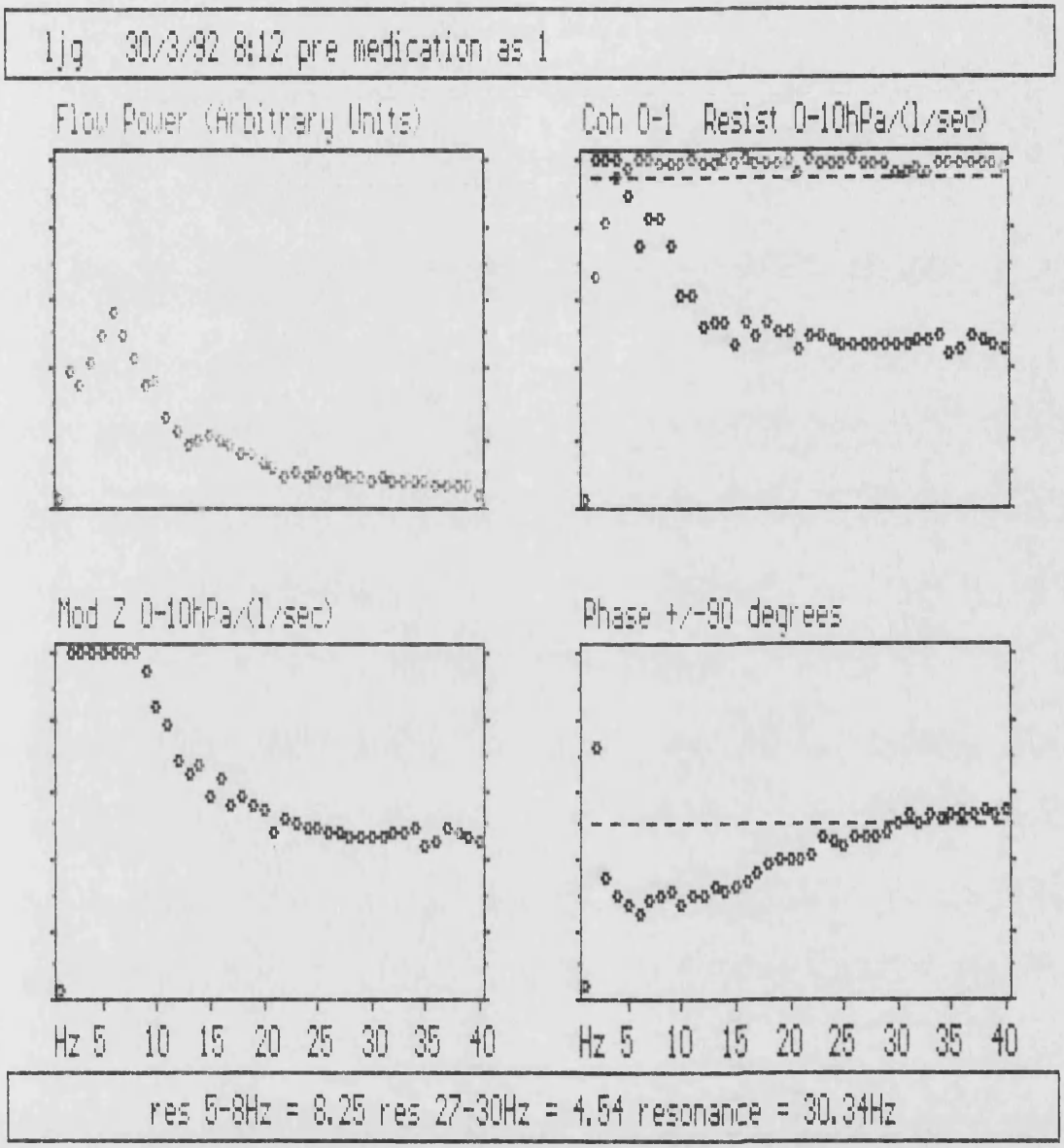

Figure 7.8 Impedance Results - Male Asthmatic Pre-medication

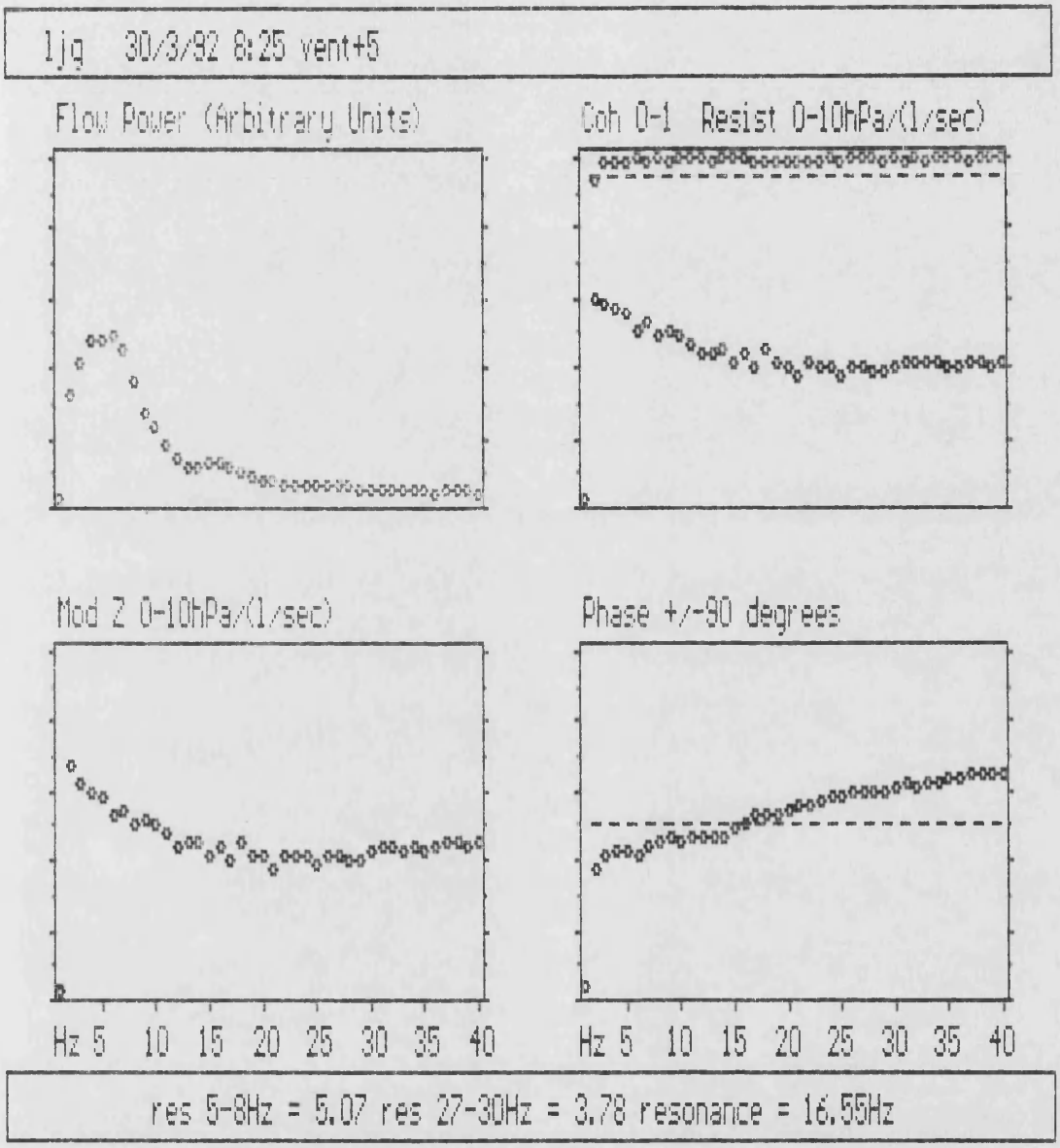

Figure 7.9 Impedance Results - Male Asthmatic Post Medication

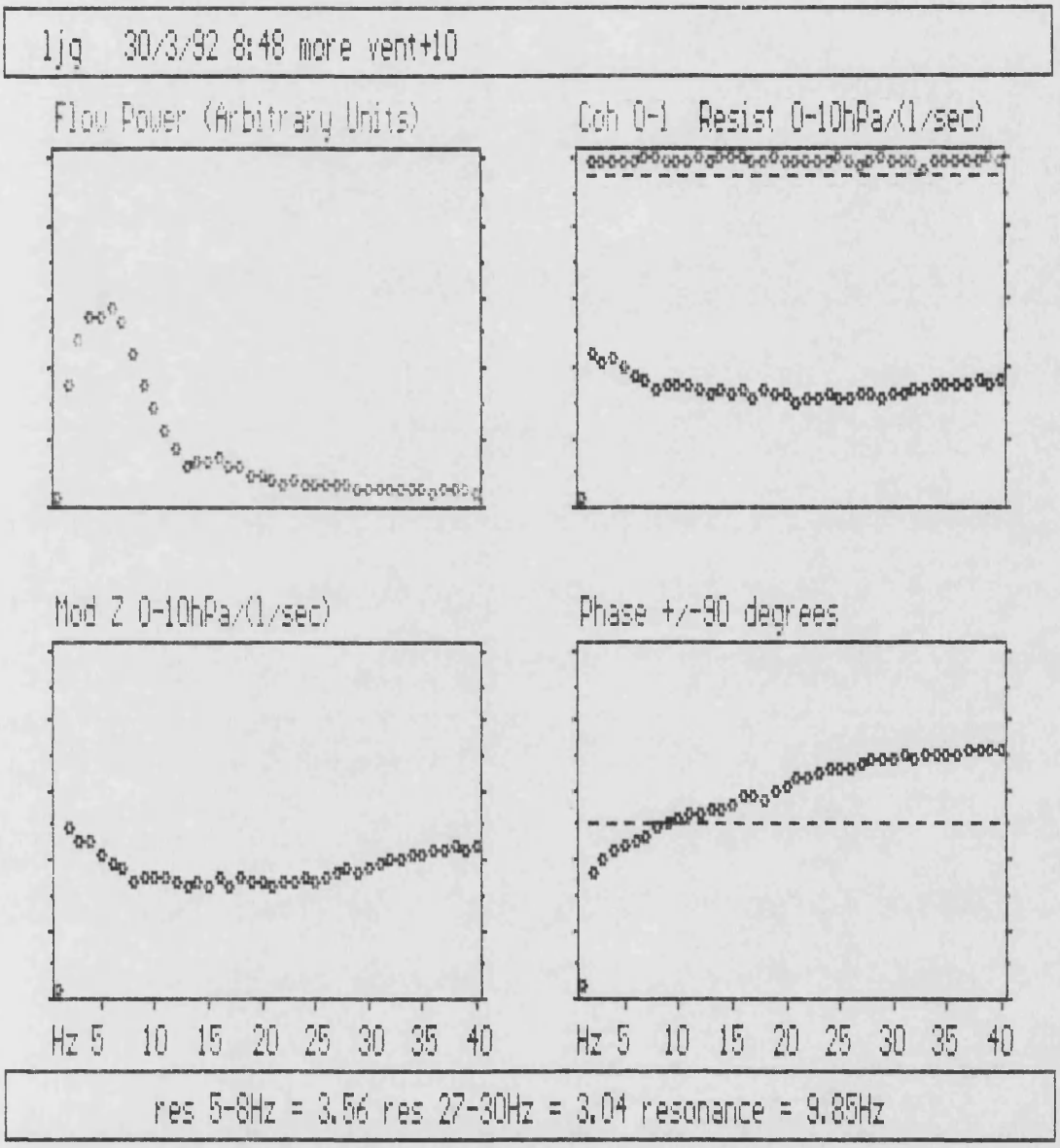

Figure 7.10 Impedance Results - Male Asthmatic Post Medication

Group	No	Sex	R $hPal^{-1}s$	L $Pal^{-1}s^2$	C $lhPa^{-1}$
Michaelson	10	male	2.08±0.41	1.46±1.07	.029±0.17
Hayes	12	mixed	2.09±0.44	0.74±0.24	.053±0.31
Nagels	15	mixed	2.47±0.19	1.00±0.10	.054±0.17
Peslin	28	male	2.36±0.83	1.01±0.27	.030±0.08
Peslin	19	female	3.24±0.79	1.19±0.37	.021±0.05
Eyles	5	mixed	2.66±0.65	0.68±0.26	.057±0.14
RUH, Bath	16	male	2.36±0.39	1.10±0.10	.040±0.23
RUH, Bath	12	female	3.31±0.70	1.20±0.20	.030±0.13
Rotger	7	mixed	2.39±0.42	2.01±0.25	.027±.04
Peslin	60	mixed	2.59±.64	1.02±0.33	.031±.003

Table 7.6 Survey of RLC Parameter Estimates, with local impedance data added, (labelled RUH, Bath)

7.5 Summary

The measurements reported in this chapter represent a considerable improvement over those obtained with the initial prototype. Coherence values of 0.95 have been used as a data rejection limit, which equates to an error on the impedance modulus of around 3% for our processing regime. As can be seen from tables 7.1, 7.2 and 7.3

impedance data is always available from 5Hz, virtually always from 4Hz and in many subjects even 2Hz. Having more confidence in the data means that a more complete impedance data set has been presented for the normal group, showing the range of data indices available. The resistance at 6Hz is commonly quoted in clinical papers so has been included. Averaging the resistance in the 5Hz to 8Hz range gives a similar value which may be compared with the 27Hz to 30Hz resistance to assess the frequency dependence of impedance. In both the normal male and female group there is a slight increase in resistance with frequency. The impedance data has been used to obtain model values, R, L, C, for the three element model described earlier. Measurements in one subject show the physiological variation of the parameters. The normal data shows good agreement with other published work, both in terms of absolute values and the statistical spread. The main cause for concern is the large coefficients of variation in capacitive estimates. In the case of our data this may be due to the fact that the model did not use any data below 4Hz which was identified as the lowest reliable frequency in all subjects. Certain other groups appear to have more tightly grouped compliance estimates.

In terms of asthmatic results in table 7.4 it is clear that the test is able to follow changes in resistance. No attempt was made to fit the RLC model to the data due to the marked frequency dependence of the resistance data.

The system was now made available for clinical service at the Royal United Hospital. The main use initially was to study the response following broncho dilators. In the majority of hospitalised patients data below 10Hz is often of little interest as gross changes

from normal have occurred. In terms of the normal data, however, the remainder of this thesis is devoted to studying the low frequency, (<5Hz), impedance data to see if it can be improved.

Chapter 8 Low Frequency Data Quality & Sources of Interference

8.1 Review

The results presented in the previous chapter show that in normal volunteers, reliable impedance data is available from 4Hz and above, with reliability being defined by coherence values reaching 0.95. Two asthmatic subject results illustrated the ability of the technique to follow changes in lung mechanics following medication. The instrumentation had proved acceptable to all subjects studied and it was felt that the device was in a form that could be used on a routine clinical basis. Initially the main application that was envisaged was monitoring the response of broncho dilators in asthmatics. In acute asthmatics the resonant frequency would be considerably above the normal range and the resistance rise with decreasing frequency is apparent by 6Hz. Therefore data in the 2Hz to 4Hz range is unlikely to provide much additional information. The impedance measurement will be less distressing for the patient and the results will enable changes in elastic recoil and respiratory resistance to be distinguished between.

To exploit the full potential of the test, however, does require the use of low frequency data. The results in asthmatic subjects represent gross changes in lung function, yet the early stages of lung disease would not result in such a gross change. Therefore the changes in impedance would be smaller and the results closer to the normal range. The rise in resistance with decreasing frequency might be below 5Hz. In terms of modelling it is also important that the parameter estimates are accurate for normal models before more complex models characterising disease are developed. The remainder of the thesis is

devoted to consideration of factors affecting the quality of the low frequency data.

The question which arose from the results presented in the previous chapter was why, even within the same subject, did the frequency at which the coherence achieved and then remained above 0.95 vary. Tables 7.1 and 7.2 from the previous chapter included the frequency from which coherence was acceptable, in each of the three runs per subject. The number of runs which were acceptable from 2Hz, 3Hz, 4Hz and 5Hz are summarised in table 8.1. The table shows that only 12 out of the 84 runs, (16 males and 12 females, 3 runs each), were acceptable from 2Hz. The number of results acceptable from 4Hz by contrast is 77, which includes the results which satisfied the 2Hz and 3Hz criteria. Seven of the results were only acceptable from 5Hz, however, it was discovered that this could be overcome by undertaking more runs in each subject. It was subsequently discovered that if six consecutive impedance measurements were undertaken then at least three had acceptable data from 4Hz upwards and the majority from lower frequencies. With each measurement taking only 16 seconds this is easily achievable.

2Hz	3Hz	4Hz	5Hz
12	24	41	7

Table 8.1 Lowest Acceptable Frequency Point - Number of Runs

Comb filtering has proven to be a powerful tool for use in improving the quality of data by eliminating extraneous noise at frequencies where no signal is applied. The filters effectively

synchronise the analysis with the applied oscillatory signal frequencies. The filter, however, cannot eliminate noise at frequencies which are within the filter bandpass region. One explanation for the fall in coherence at low frequencies could be that either pressure or flow, or both are affected by interference. The fact that the coherence does not reach the 0.95 threshold even after filtering may mean that some frequency components of the interference have been passed by the filters. As coherence improves with increasing frequency this suggests that the interference diminishes as frequency rises. The problem is compounded at low frequencies as the impedance rises due to the compliance of the system. Considering, by way of example, the compliance estimate for the normal male group of 0.04hPal^{-1}s, (table 7.1). At 2Hz the impedance due to this compliance is 2hPal^{-1}s, which by 5Hz would have fallen to 0.8hPal^{-1}s and the flow would have increased accordingly. It was for this reason that low frequency driving signals to the generator were increased in amplitude, however, there were limits to this approach. Firstly there is a physical limit of the generator travel and the output range of the analogue output card used to drive the device. Second and more importantly, if the applied signal becomes too large it may promote non linear behaviour of the respiratory system, (Daróczy *et al*, 1991, Rotger *et al*, 1991). Additionally the larger the signal amplitude the greater the sensation for the subject. The signal that was used in this study was designed such that the 2Hz, 3Hz and 4Hz components had the greatest amplitudes, as a rough guide they were approximately double the amplitude of all other frequency amplitudes, after the response of the generator had been corrected for.

It has been suggested by a number of authors, (Franken *et al*, 1983 Landser *et al*, 1976), that one source of interference is spontaneous respiration, which clearly affects both pressure and flow signals. Following on from this observation other workers , (Daróczy and Hantos, 1982, and Navajas *et al* 1989), have suggested alternative, so called unbiased, impedance estimators. Both works use the fact that the breathing components in the pressure and flow signals are related by the impedance of the measuring equipment, which is a linear system. Navajas *et al* measure the impedance of the airflow generator and this in the impedance calculation to eliminate the effect of breathing. Daróczy *et al* use the driving signal to the airflow generator to form cross spectra rather than the pressure and flow signals themselves. This eliminates the contribution of any uncorrelated noise sources, and it is assumed that the breathing signal and applied oscillations are uncorrelated.

Although at first sight this approach seemed appealing, it became apparent from the literature, (Cauberghs and van de Woestijne, 1991), that there were questions as to whether the results showed any improvement on the standard impedance estimator. In particular there was little evidence illustrating the application of the new estimators below 4Hz, which is the frequency range of interest to our group. It was also observed in our laboratory that results did not improve when measurements were made in apnoeic subjects. Although such measurements would be difficult to undertake in patients, it was possible to achieve this in a small number of trained subjects. Studying this further lead to the conclusion that pressure and flow signals were also contaminated by cardiac related interference. This subject has received no detailed

attention in the literature and was therefore investigated in more detail to see if the cardiac activity was playing a part in corrupting the low frequency impedance data. In terms of the frequency range of cardiac activity, the fundamental frequency is around 1.2Hz in normals and therefore the first few harmonics, directly overlap the low frequency impedance measurement range. By contrast the spontaneous respiration at around 0.2Hz to 0.4Hz is considerably further away in frequency terms.

8.2 Coherence Values - 1Hz to 14Hz

Figure 8.1 shows graphically the variation of coherence values with frequency in the range 1 to 14Hz for one data run in each of eight subjects studied. These measurements were made while the subjects continued to breathe. Although no oscillatory signal is applied at one hertz, mainly due to inadequacies in the output of the generator, it is informative to see the coherence value. The data has not been comb filtered and above 14Hz the coherence values all remain close to unity.

There is a general trend in all eight graphs and a number of interesting observations may be made regarding the variations in coherence with frequency. There appear to be three distinct phases, which roughly equate to the frequency regions 1-2Hz, 2-5Hz and above 5Hz respectively. Above 5Hz the coherence is gradually improving and the comb filtering regime appears to be capable of eliminating any extraneous noise which may be responsible for reducing the coherence values. The general trend over 2-5Hz phase is a gradual increase in coherence with frequency, suggesting that there is more noise contaminating the data at the lower frequencies in this band and that

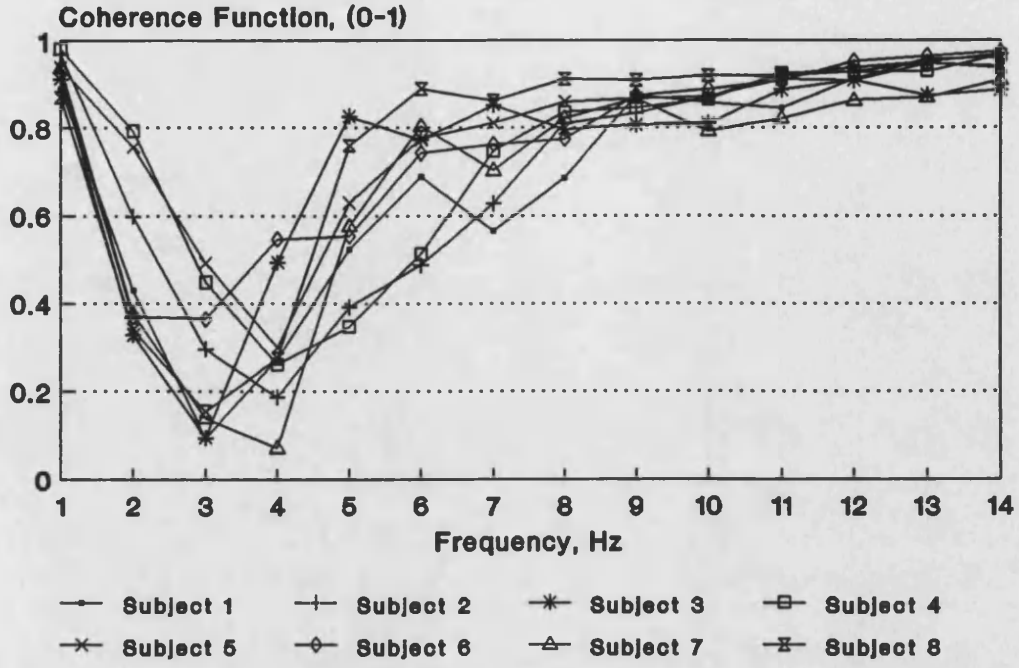

Figure 8.1 Variation of Coherence Function versus Frequency.

it may be having a greater effect due to lower signal levels. Poor signal to noise ratio will reduce coherence values so it might be thought that the applied oscillation lacked power at these frequencies. If this was the case then all data would be poor at these frequencies, whereas table 8.1 shows it varies between intra subject measurements. Below 2Hz the rise in coherence, almost to unity, indicates a strong linear dependence between the pressure and flow signals around 1Hz. At first sight this is curious as there is no applied signal at this point and if it was the result of leakage of power from the adjacent 2Hz frequency element then the coherence at 2Hz should be greater. It strongly suggests that there is related interference present in both the pressure and flow signals.

Figure 8.2 includes results, obtained by asking three volunteers to hold their breath at functional residual capacity, FRC. For

reference purposes, for each subject, a set of comb filtered coherence values from measurements made while respiration continued are also shown. A number of practice runs were undertaken to ensure that apnoeic measurements were made with a relaxed, open glottis. The pressure and flow data were scrutinised prior to analysis to ensure that they did not exhibit artefacts due to swallowing or respiratory efforts. These data sets were comb filtered prior to analysis, as with no respiration the expectation was that the coherence values should all have improved.

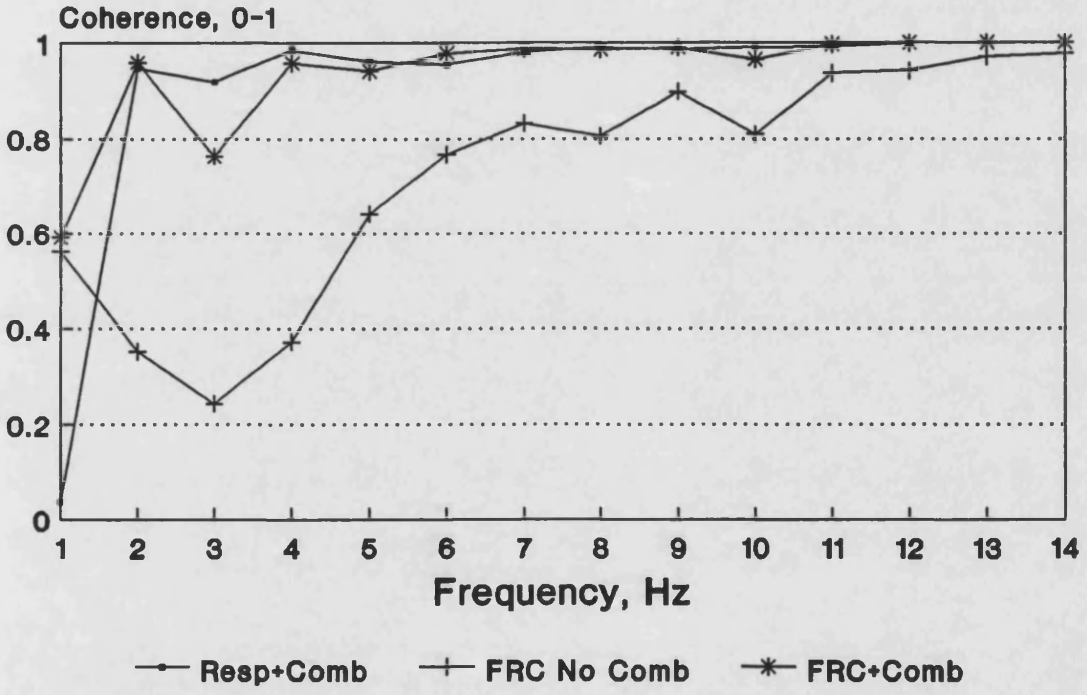

Figure 8.2 Coherence Values Apnoeic/Respiration Comparison: Subject 2

The results from this investigation were fascinating. The fact that coherence results did not dramatically improve in the apnoeic measurements tends to suggest that breathing is not the primary source of contamination. In fact in some results the coherence values are appreciably worse in the apnoeic results.

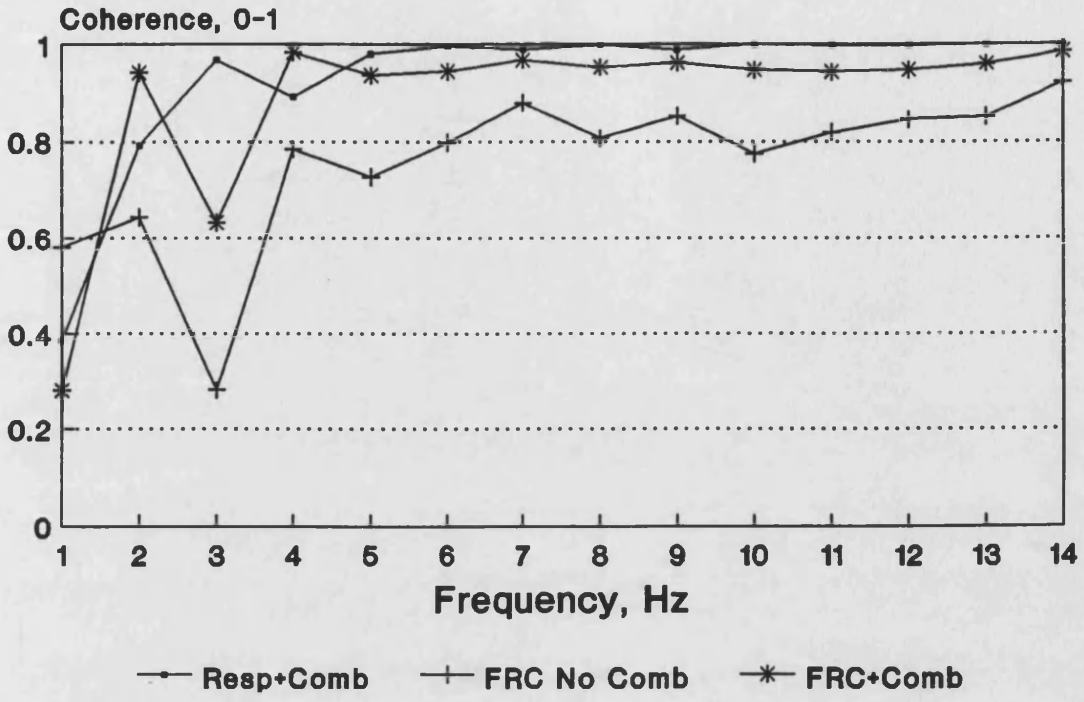

Figure 8.3 Coherence Values Apnoeic/Respiration Comparison: Subject 2

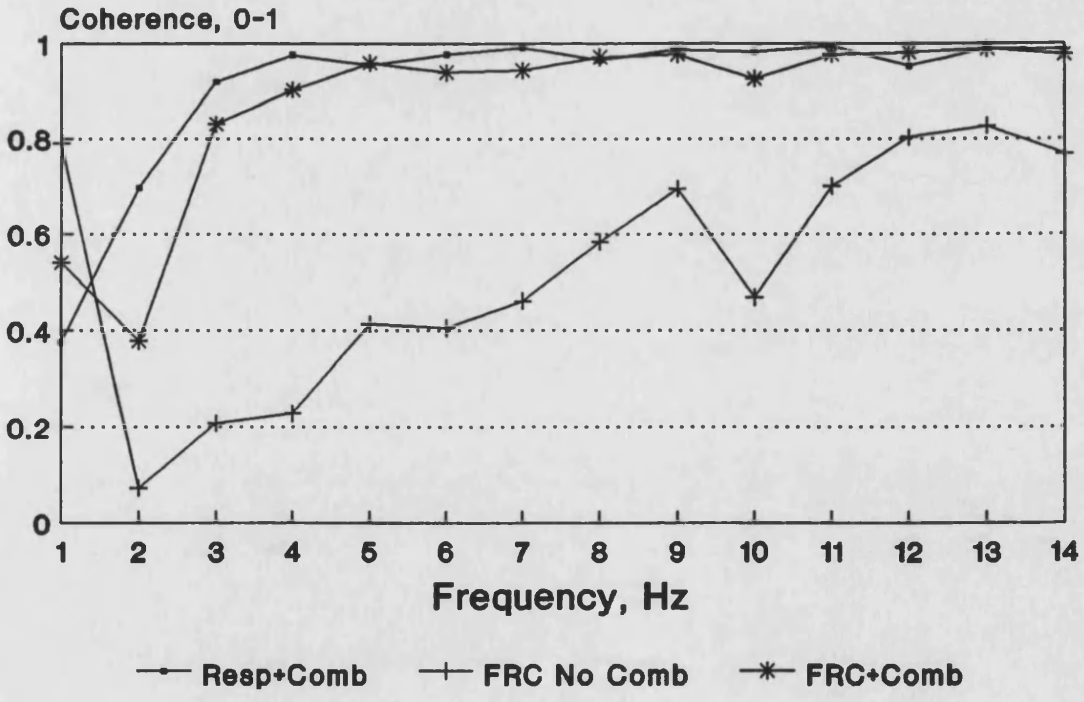

Figure 8.4 Coherence Values Apnoeic/Respiration Comparison: Subject 3

8.3 Cardiac Signal Identification in Pressure and Flow Waveforms

Having seen no improvement during the cessation of breathing, it was decided to assess the level of cardiac signal in both pressure and flow signals. The respiratory impedance system was modified to collect a cardiac related signal while pressure and flow were measured. The sampling rate for all signals was 128Hz, with a finger pulse waveform taken from a Simonsen and Weel, (8000 series module), optical pulse monitor. The additional cardiac signal was stored to disk, with the pressure and flow signals, allowing the retrospective analysis of the data.

Initially pressure and flow data were collected, while no oscillations were applied to the lungs. The standard sixteen second data set was displayed and visually inspected, two examples from two subjects are shown in figures 8.5 through 8.8, with the cardiac signal included for reference. It is immediately apparent in this data that there is activity on both the pressure and flow channels of regular activity which correlates with the cardiac waveform. The delays introduced by the Simonsen and Weel system, which will be different to the transducers and filter assembly, were not characterised. From a physiological viewpoint a delay between the pressure and flow traces compared to the cardiac waveform is to be expected, as the finger pulse will involve the pulse travelling down the arm, however, this cannot be determined from the graphs. The important point is that there is clear evidence of cardiac activity in the pressure and flow signals.

The time varying data was not as revealing in all subjects studied, as it is difficult to maintain a relaxed glottis without training. An alternative means of illustrating the relationship is to

calculate the cross power spectrum between the cardiac component and either the pressure or flow signal. This reflects components common to both in the frequency domain. The modulus of the cross power spectra, between cardiac and flow, for three subjects is shown in figures 8.9 to 8.11. The spectral resolution having been increased to 0.25Hz as integer steps will be unable to fully resolve the cardiac spectral peaks. The basic impedance analysis program was configured to analyse the 2048 data points in blocks of 512, data is displayed in the 0.5Hz to 4Hz range, with three examples shown for each subject. In each subject the spectra exhibit a peak at the cardiac fundamental frequency as well as power at subsequent harmonics. The variability of the heart rate accounts for the difference in spectra within and between subjects. Additionally this probably accounts for the variable values of comb filtered coherence values, depending on whether the cardiac spectrum is coincident with an applied oscillatory frequency.

Evidence of the relationship between the pressure and flow signal cardiac components is apparent when the coherence function is determined during breath holding while no oscillatory signal is applied. The impedance analysis was performed with the signals as described and figure 8.12 shows the coherence results.

8.4 Summary

Attention has been focused on the quality of low frequency impedance data. Using the coherence function to discriminate, it became apparent that even after the comb filtering had been applied data was not always acceptable below 5Hz.

The filter was minimising the impact of noise which is

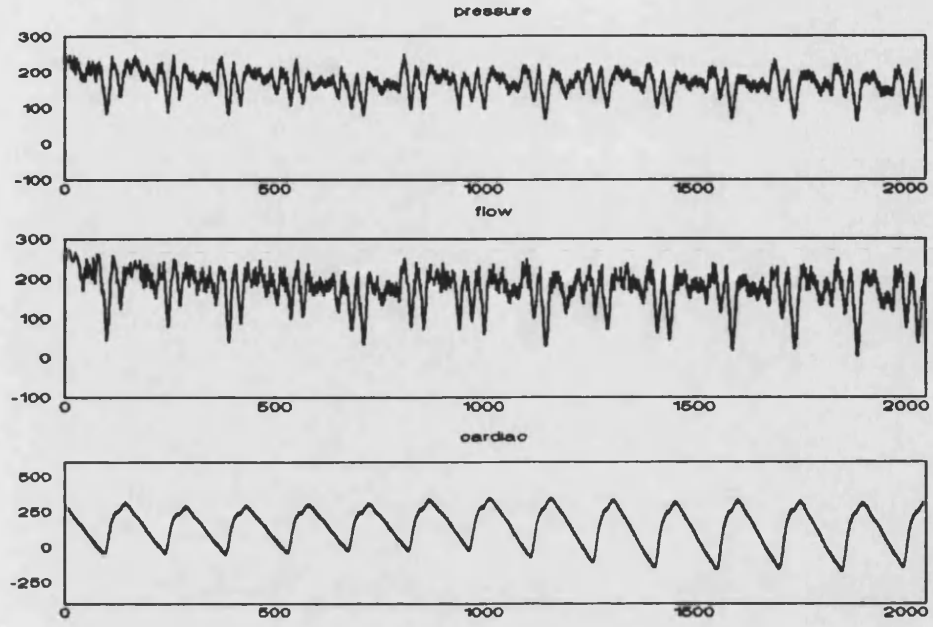

Figure 8.5 Pressure, Flow and Cardiac Signals - Subject 1

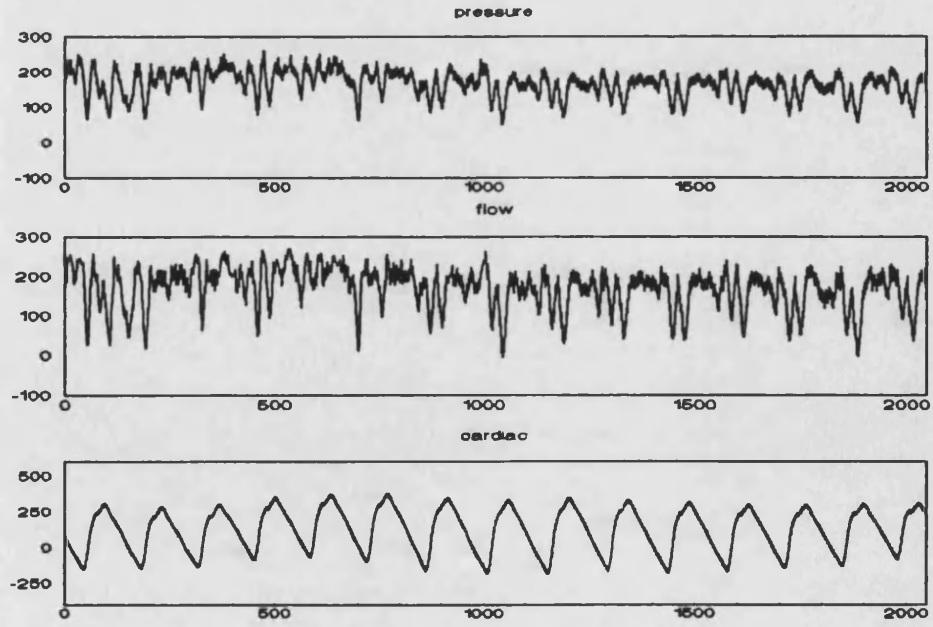

Figure 8.6 Pressure, Flow and Cardiac Signals - Subject 1

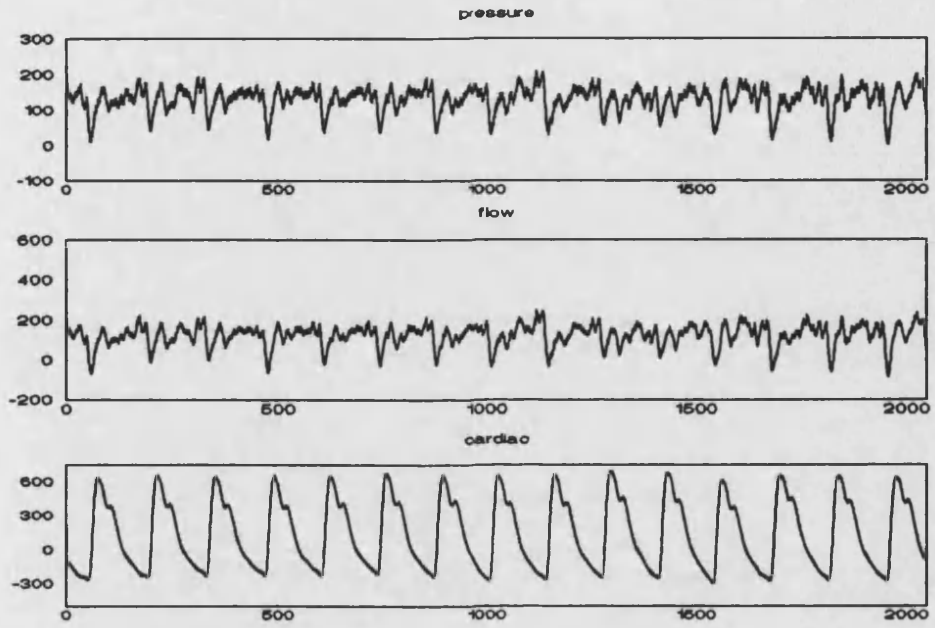

Figure 8.7 Pressure, Flow and Cardiac Signals - Subject 2

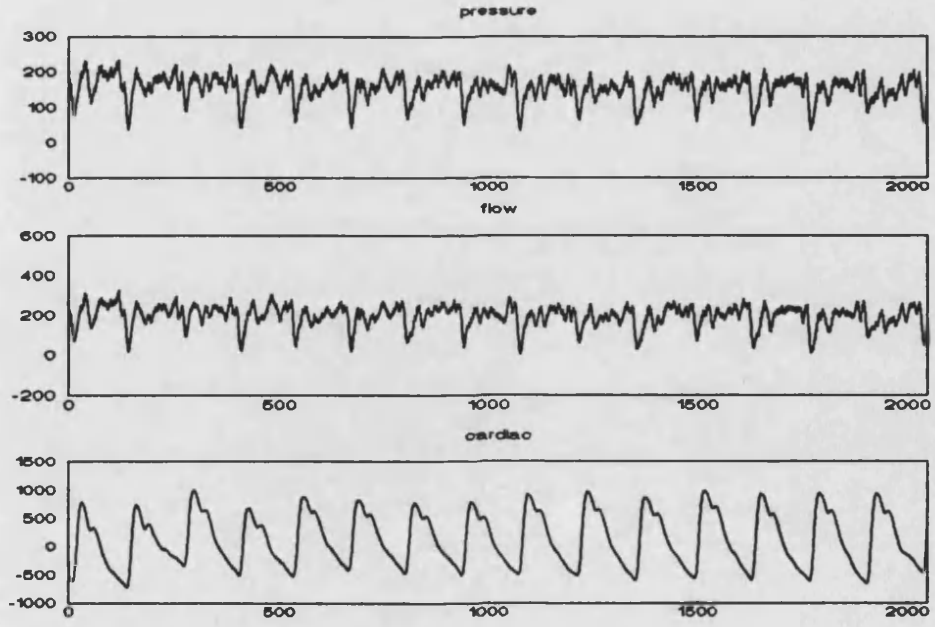

Figure 8.8 Pressure and Flow Signals - Subject 2

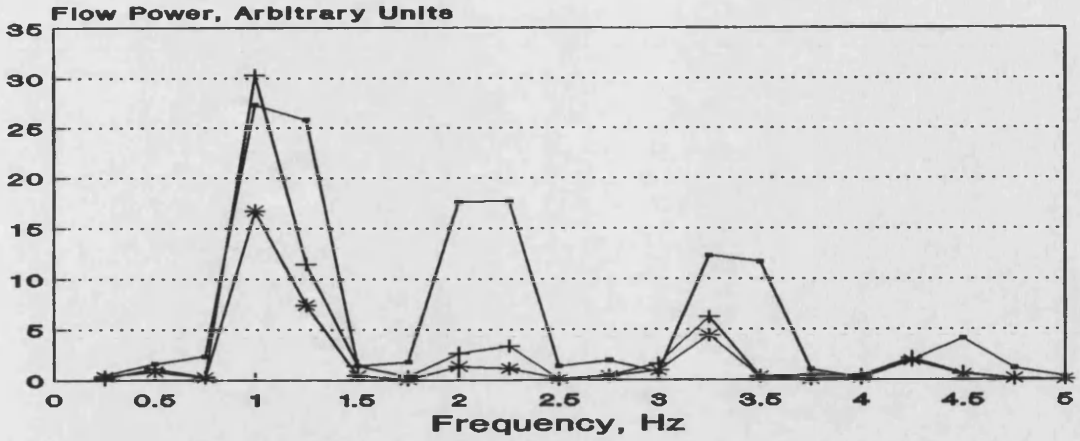

Figure 8.9 Cardiac-Flow Cross Power Spectrum Modulus - Subject 1

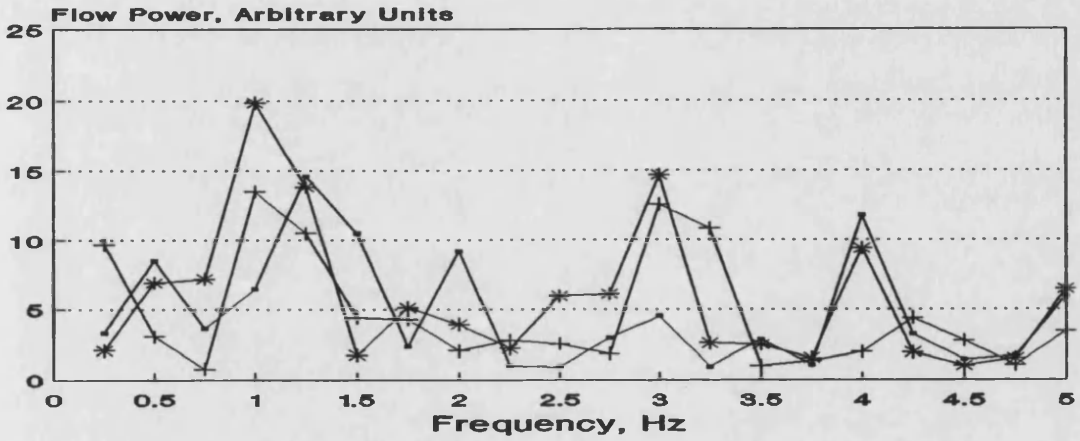

Figure 8.10 Cardiac-Flow Cross Power Spectrum Modulus - Subject 2

contributing to the degradation of data, it cannot however eliminate noise at the signal frequencies. The source of noise has been considered, initially it was thought that respiration was interfering with both pressure and flow data. Results obtained while subjects remained apnoeic, however, showed no improvements in coherence values. Cardiac activity is an alternative source of physiological interference and results have been presented showing evidence of cardiogenic interference on both pressure and flow signals. In some subjects it has been noted that coherence values in the 2Hz to 5Hz band were worse

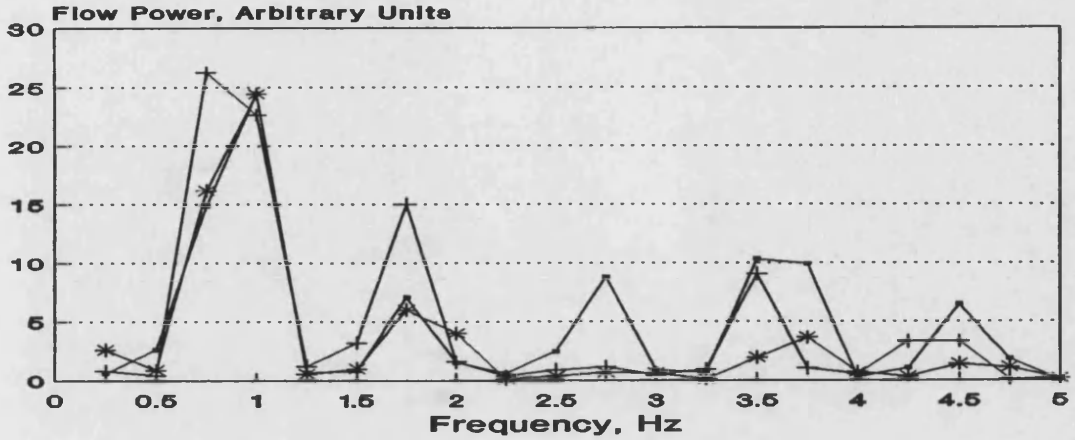

Figure 8.11 Cardiac-Flow Cross Power Spectrum Modulus - Subject 3

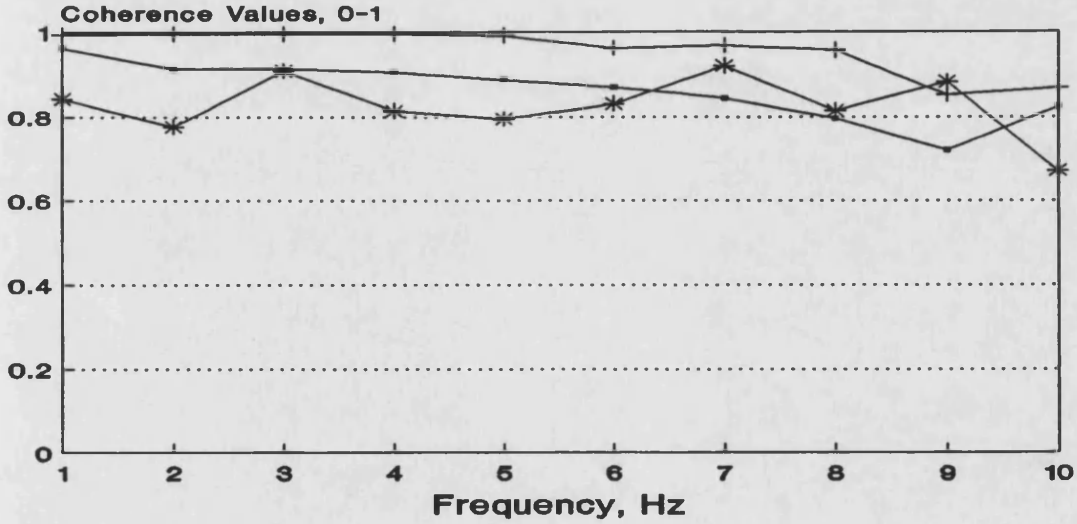

Figure 8.12 Coherence Values, 3 Apnoeic Subjects, No Applied Signal

during breath holding measurements and it seems likely that this could be explained by cardiac activity.

The coherence function exhibited three distinct phases, both during respiration and breath holding, which may possibly be explained as follows. At 1Hz, coherence values are high as no signal is present and the relationship this signifies between pressure and flow is due to the cardiac component, or respiratory they both carry. Above 5Hz,

cardiac and respiratory harmonics become insignificant and the applied oscillatory power dominates, so coherence improves. The 2Hz to 5Hz range is most interesting as the cardiac components are strong, oscillatory signals are present so there are effectively two signals in competition.

One factor which will account for a reduction in coherence, from a systems viewpoint, is that the output, in this case flow, is arising from more than one input. It may therefore be possible to reformulate the impedance analysis, which has always been treated as a single input, single output problem, in terms of multiple input, single output systems theory. The cardiac signal being considered, conceptually, as an additional input. Building on this premise, subsequent chapters develop these ideas with the ultimate aim being to try to eliminate any cardiac components in the pressure and flow signals in an attempt to improve the quality of low frequency impedance data.

Chapter 9 Impedance Signal Simulation

9.1 Introduction

Cardiac components have been identified in both the pressure and flow signals used to compute respiratory impedance. The previous chapter illustrated that the interference occupied the 1Hz to 5Hz frequency and varied according to the heart rate. The question which arose was could such small signals influence the impedance estimate and to investigate this further a simulation was undertaken.

9.2 Simulation System

A 3 element series RLC model was used, the impedance of which was computed using circuit theory. For a given pressure signal the flow signal was calculated using the system impedance and pressure. The calculation was achieved in the frequency domain and the flow signal then transformed to the time domain. The signals could then be scaled to match typical pressure and flow signals encountered in the respiratory impedance system. The pressure signal used was the actual signal used to drive the vibration generator, but with the correction for the generator and bellows eliminated. Values of resistance, capacitance and inductance were set to be similar to values encountered in normal subjects, ($R=2.36 hPa l^{-1} s$ $L=0.011 hPa^{-1} s^2$ and $C=0.04 l hPa^{-1}$). The signals were then corrupted and analysed using the impedance program to assess the impact, particularly on the coherence function, of the interference. The results are presented in figures 9.1 through 9.5 and tabulated in table 9.1. The first row in the table shows impedance data, (modulus, argument and resistance), and the coherence

values at 5Hz. From figure 9.1 it is apparent that subjecting the simulated pressure and flow signals to the impedance analysis results in an acceptable estimate of the model parameters. Interference is added first to the flow waveform at 4.5Hz and 5Hz and then at 5Hz to both pressure and flow, in order to quantify the effect.

	Raw Pressure and Flow				Comb Filtered			
Noise	Z	θ	R	γ^2	Z	θ	R	γ^2
None	2.40	-11.7	2.36	.998	2.41	-10.9	2.36	.998
±10, 4.5Hz Flow	2.44	-11.4	2.39	.807	2.42	-10.6	2.37	.998
±20, 4.5Hz Flow	2.48	-11.4	2.43	.506	2.43	-9.8	2.39	.997
±10, 5Hz Flow	-1.53	-5.3	-1.53	.983	1.53	-4.8	1.52	.995
±10, 5Hz* Flow	3.40	23.7	3.11	.943	3.43	23.9	3.13	.944
±10, 5Hz Press-Flow	1.90	-6.3	1.88	1.00	1.90	-5.8	1.89	1.00
±10, 5Hz* Press-Flow	3.03	13.54	2.95	.967	3.05	13.7	2.96	.967

Table 9.1 Impedance Z, Phase θ, Resistance R, and Coherence Values, γ^2 at 5Hz, with interference. (* = $3\pi/2$ phase shift)

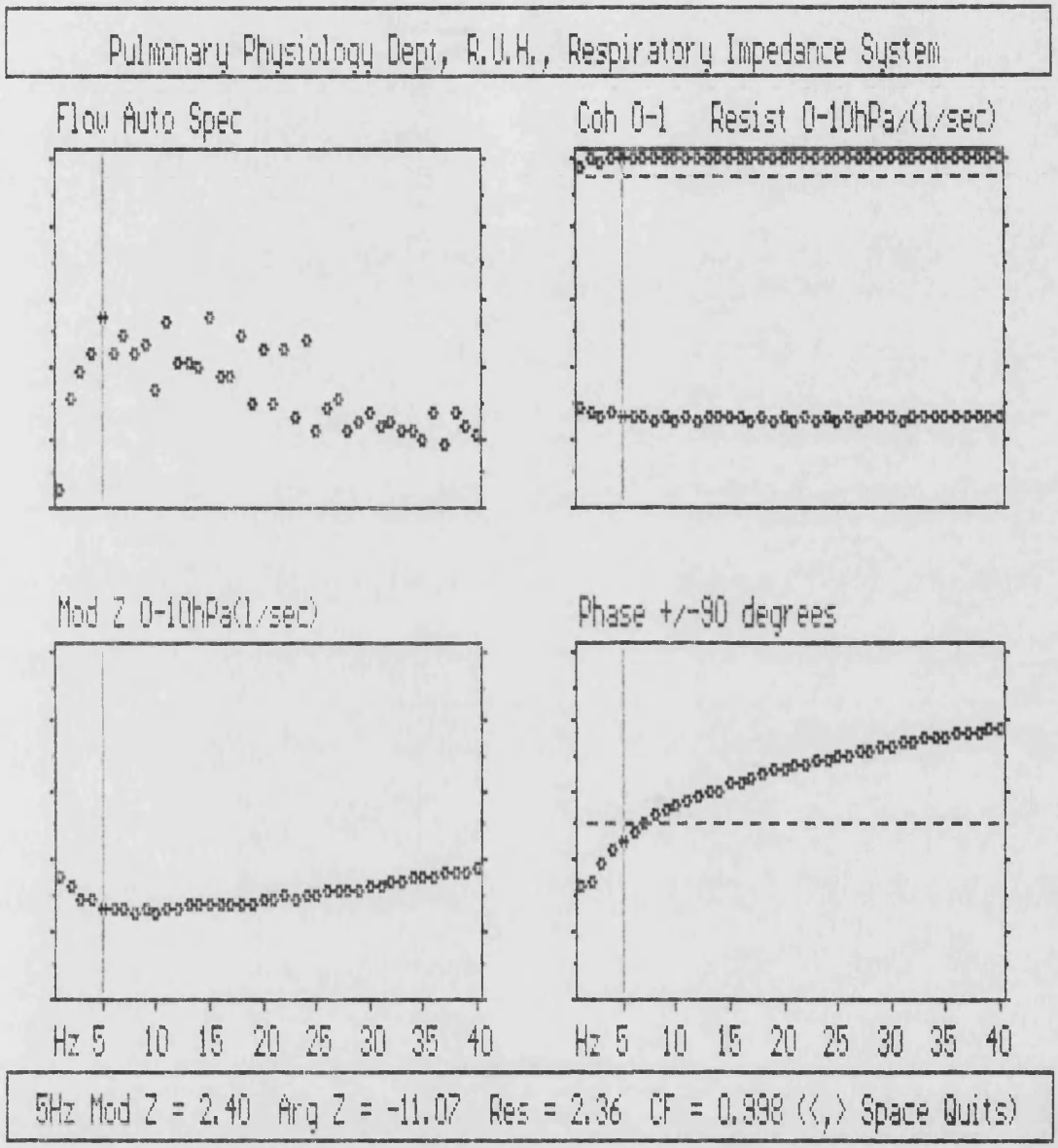

Figure 9.1 Pressure and Flow Simulation, RLC Model

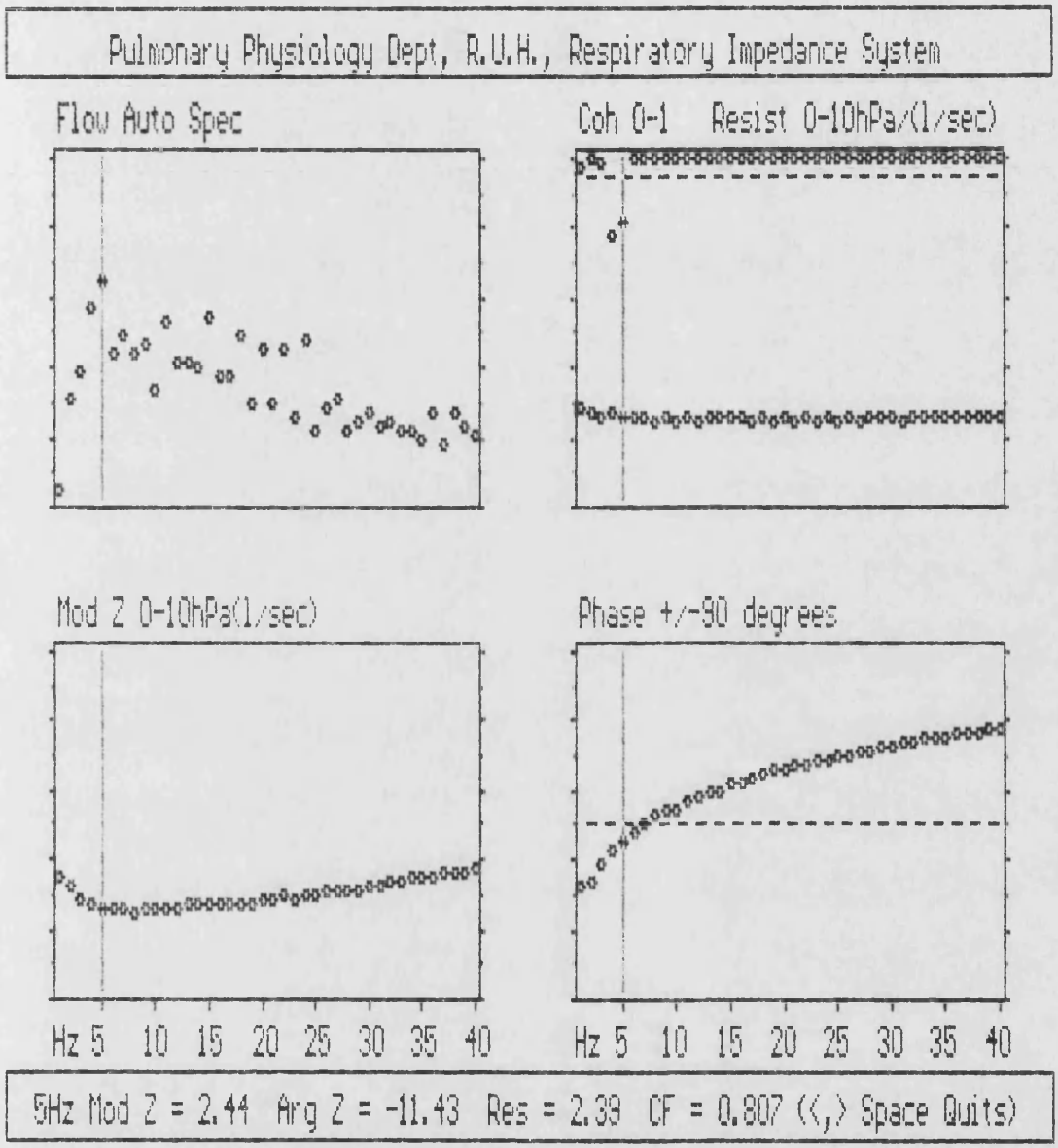

Figure 9.2 RLC Simulation, 4.5Hz Sinewave Added to Flow

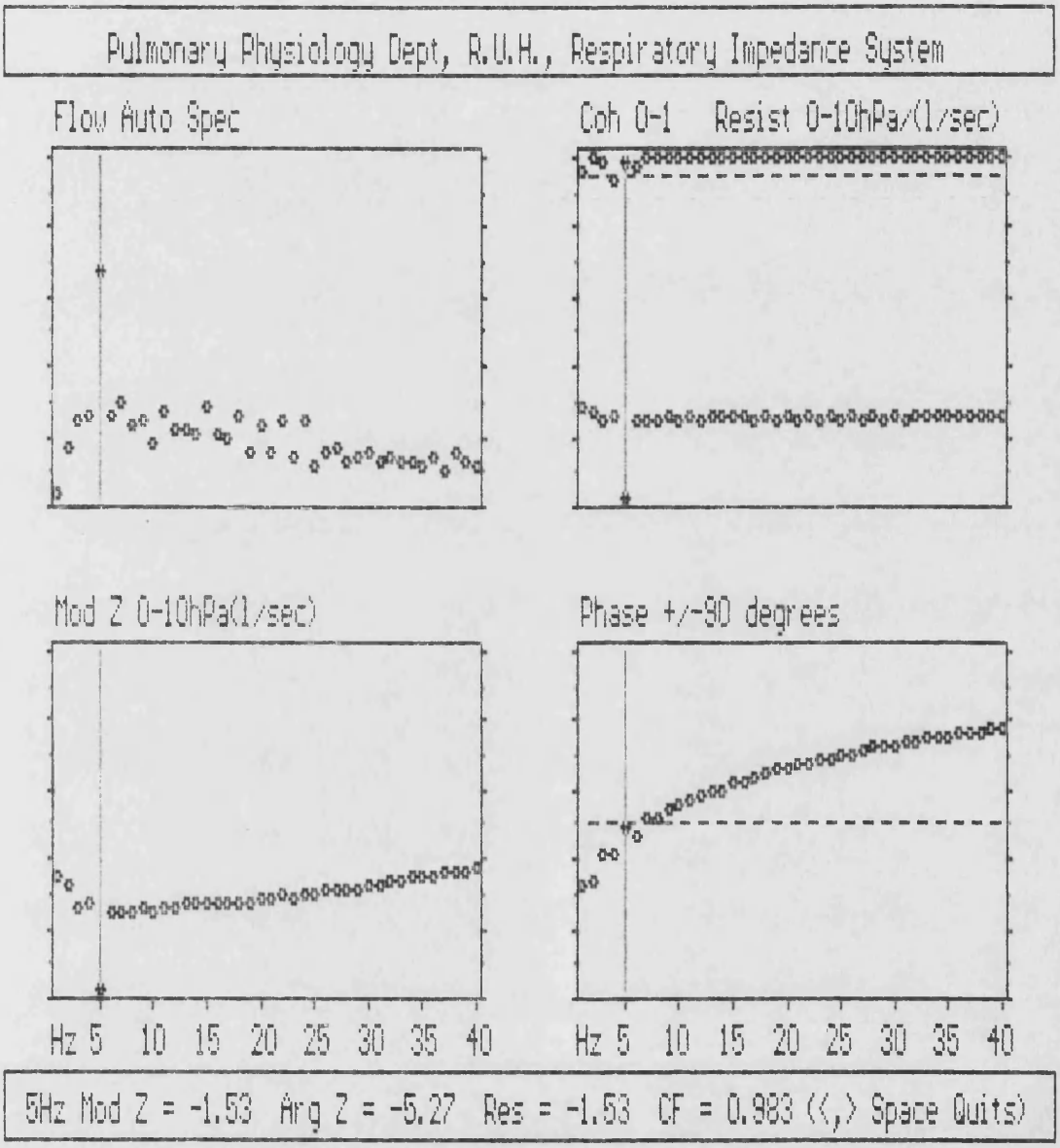

Figure 9.3 RLC Simulation, 5Hz Signal Added to Flow

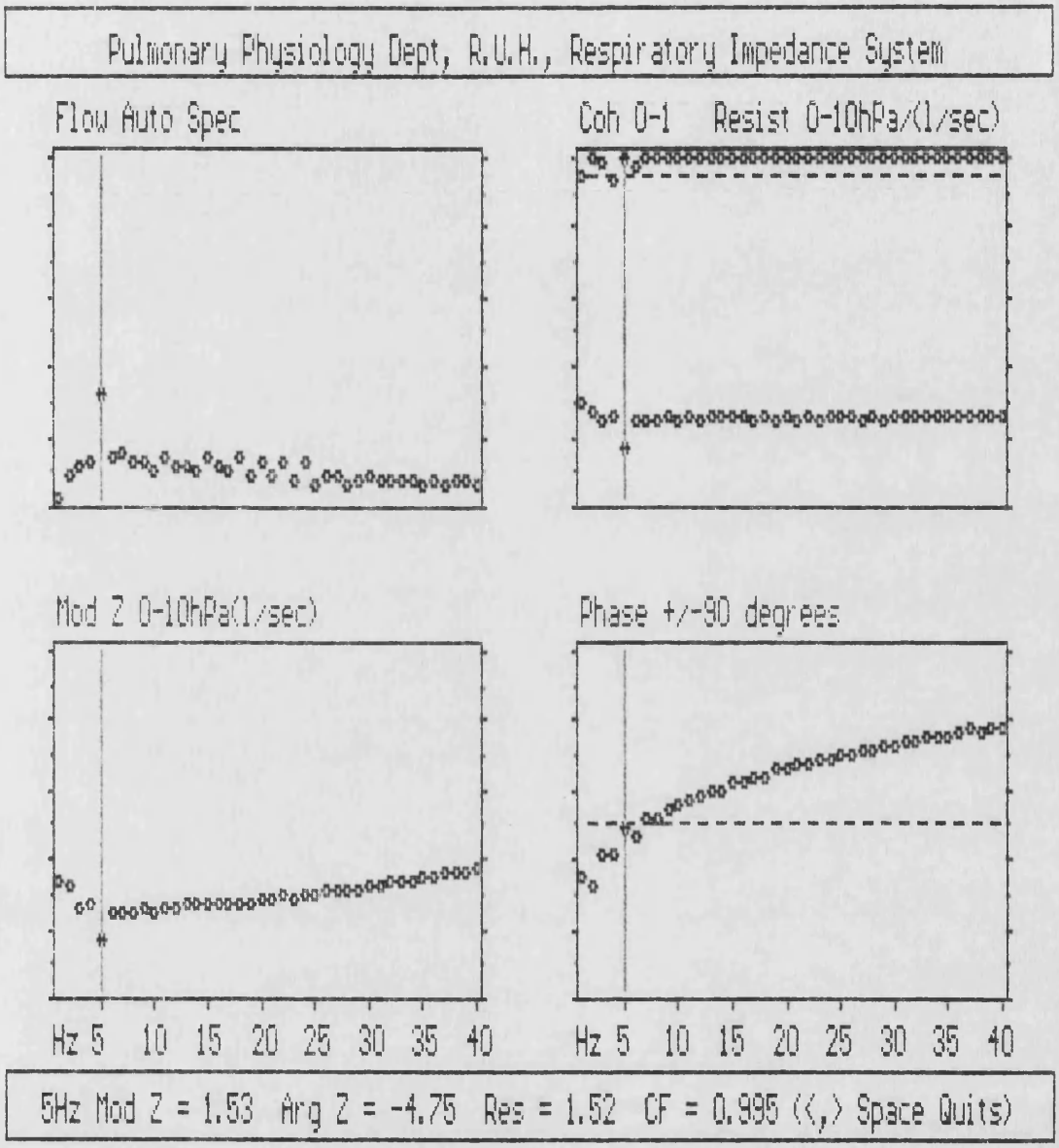

Figure 9.4 Results from 9.3 Comb Filtered

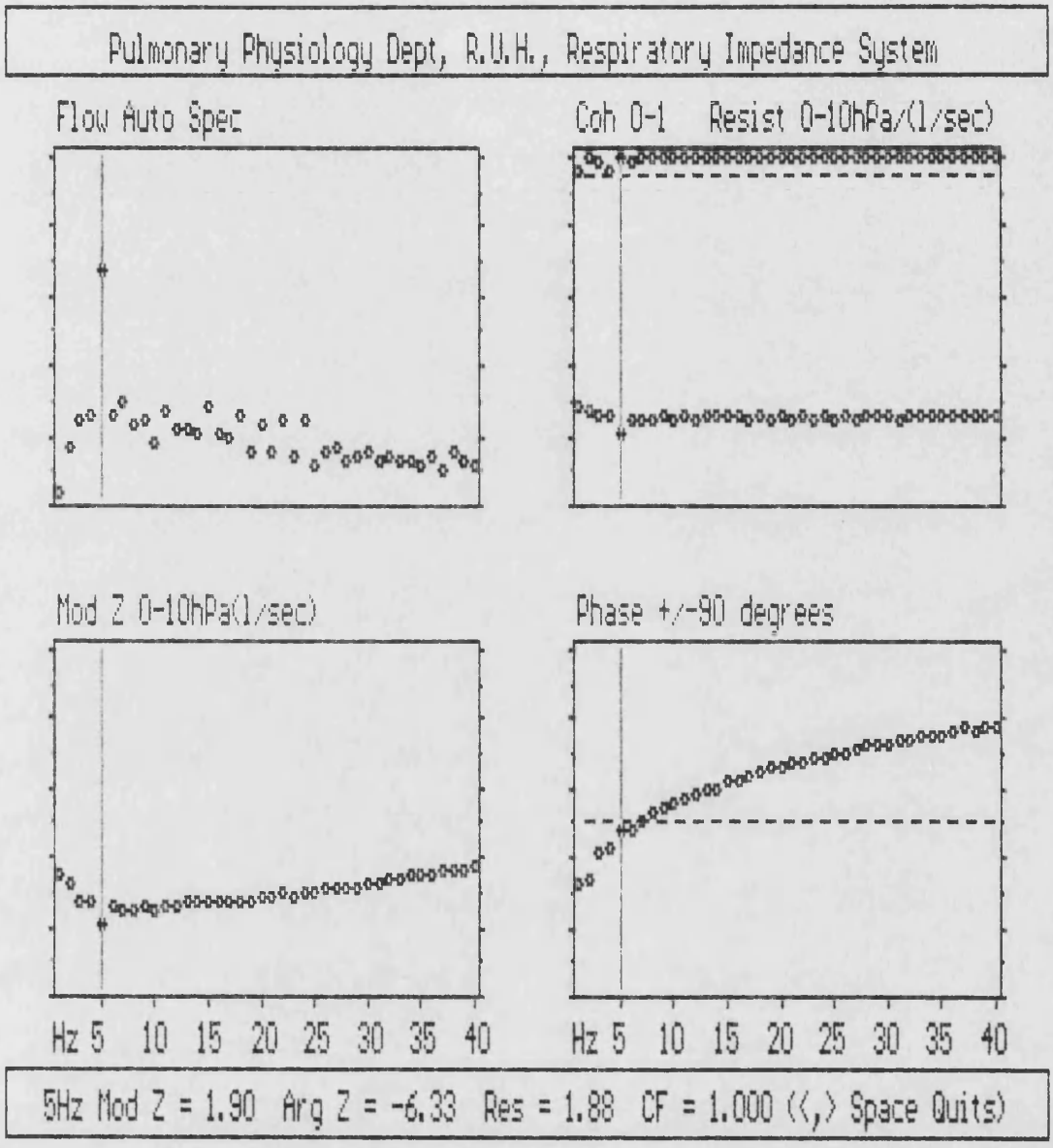

Figure 9.5 RLC Simulation, 5Hz Added to Pressure and Flow

9.3 Discussion of Simulation Results.

With no interference added the model value of resistance is correctly estimated. Adding in a 4.5Hz sinewave of amplitude ±10 machine units, (2048 units = $0.84ls^{-1}$), to the flow signal is detected by the reduced coherence with the impedance estimates deviating from the true values. Application of the comb filter improves the coherence and reduces the estimation errors. Doubling the sinewave amplitude further decreases the coherence and again the comb filter improves the data. If, however, a 5Hz sinewave is added the coherence is not so markedly reduced, yet the data is nonsensical. By changing the phase of the interference the effect on the estimates is dramatically different. As the 5Hz sinewave is coincident with the centre frequency of one filter element the pre and post filtered results are similar. The final pair of results show a 5Hz sine wave added to both pressure and flow which, as expected, will not reduce the coherence as there is a relationship between pressure and flow due to the interference. The levels of ±10 units was to ensure the amplitude of the interference was comparable to the cardiac interference, (figures 8.5 to 8.8).

In summary the following points may be made:

1. Interference coincident in frequency with an applied oscillation will affect the data more, and coherence less, than noise at a non integer frequency. The phase relationship between the noise and signal has a bearing.
2. Interference on both pressure and flow signals will not be reflected by a reduced coherence value.
3. The comb filter cannot eliminate noise within the

filter element bandpass region.

4. To use the coherence functions with confidence it is necessary to know the frequency distribution of the noise source.

9.4 Adaptive Filtering of Cardiac Noise

During the simulation work attempts were also made to eliminate the cardiac interference using adaptive filters. Unlike conventional fixed frequency filters an adaptive noise cancellation system will dynamically adjust its response to minimise the noise, which can overlap the signal frequency range. The subject is well reviewed by Widrow *et al* (1975). An adaptive noise canceller was developed using the cardiac signal as a reference input to the adaptive filter element. The pressure and flow signals were adaptively filtered and although a reduction in cardiac interference was observed at the fundamental cardiac frequency, higher frequency interference remained. This work was presented at the EEC Concerted Action Group's final workshop, (the paper presented is included as appendix B).

Chapter 10 The Impedance Calculation Reconsidered

10.1 Introduction

The previous chapter illustrated that coherence functions must be interpreted with care. Coherence values will not be reduced if there is correlated noise on both pressure and flow channels, however, the data will be corrupted. Furthermore, the comb filter will not eliminate noise at the filter bandpass, although the coherence values may be increased post filtering. Cardiogenic activity appears on both pressure and flow waveforms and will therefore act as a correlated noise source. It is also responsible for creating high coherence values at 1Hz, where no signal is applied.

To have confidence in the filtered results it is necessary to gain additional information regarding the frequency distribution of the noise. Such information may then be used to discriminate between otherwise plausible coherence functions. One approach to this problem is to reconsider the impedance analysis as a multiple input, single output problem. The theory underlying such an analysis enables statements to be made regarding the contribution of each input to the output and in certain circumstances to eliminate the effects of a range of outputs. Additional coherence functions are also available giving information regarding the relationship between inputs.

In the first instance the analysis centred around a two input single output model, where the cardiac activity and applied oscillatory pressure are inputs and the flow signal is the output. It should be emphasised this is purely a conceptual model in that the cardiac signal is arising from the heart within the thorax, while the pressure is

applied externally at the mouth. Therefore, in the following analysis some equations may have no direct physical meaning, rather they are mathematical descriptors which enable the interference to be considered. It should also be stressed that this approach is only of relevance in the 2Hz to 5Hz range where multiple input behaviour is observed. Measurements made in this chapter are all during breath holding, although ultimately respiration could be considered as a third input to the model.

10.2 Multiple Input Single Output System Theory

For the single input, single output system shown in figure 10.1 the frequency response function, H and coherence between input and output, γ_{xy}^2, are restated as equations 10.1 and 10.2.

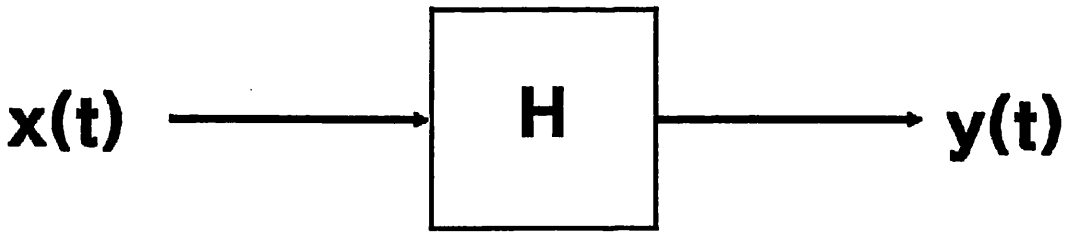

Figure 10.1 Single Input System

$$H_{xy} = \frac{G_{xy}}{G_{xx}} \qquad 10.1$$

$$\gamma_{xy}^2 = \frac{|G_{xy}|^2}{G_{xx}G_{yy}} \qquad 10.2$$

To extend this basic model, consider the two input, single output system represented by the block diagram of figure 10.2. The inputs

$x_1(t)$, $x_2(t)$ and output $y(t)$, may be Fourier transformed yielding, X_1, X_2 and Y, each of which are functions of frequency. The output of the system is given by equation 10.3, where H_1 and H_2 are the two system frequency response functions. Considering the practical application of these ideas, let $x_1(t)$ represent the cardiac signal, $x_2(t)$ the applied pressure oscillations and $y(t)$ be the resulting flow. In terms of the system responses, H_1 is of no physical relevance, whereas the reciprocal of H_2 is the respiratory impedance.

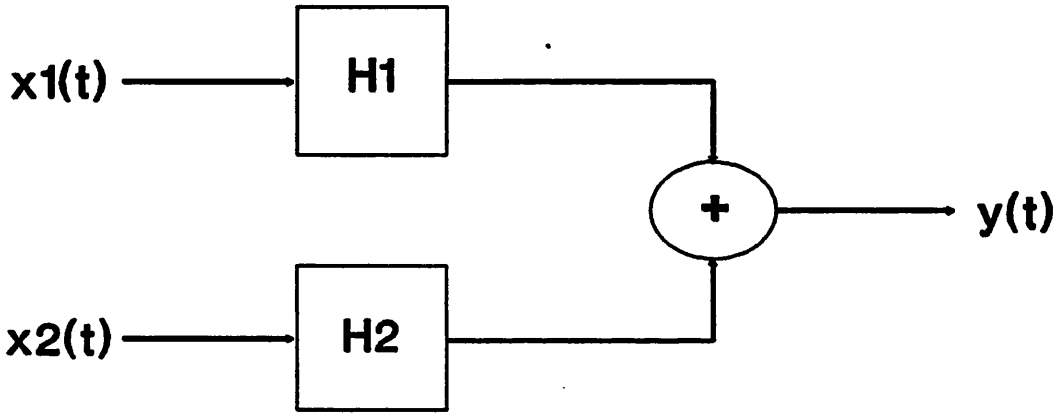

Figure 10.2 Two Input System

From the work of Bendat and Piersol a general expression for the cross spectra between any input, in a multiple input system, and the output is given by equation 10.4. Applying this formula to the two input system described, results in two cross power spectra given in equations 10.5 and 10.6.

$$Y = X_1H_1 + X_2H_2 \qquad 10.3$$

$$S_{iy} = \sum_{j=1}^{q} H_j S_{ij} \qquad j=1,2....q \qquad 10.4$$

$$G_{1y} = H_1 G_{11} + H_2 G_{12} \qquad 10.5$$

$$G_{2y} = H_1 G_{21} + H_2 G_{22} \qquad 10.6$$

By algebraic manipulation it is possible to rewrite equations 10.5 and 10.6 in terms of H_1 and H_2, as equations 10.7 and 10.8

$$H_1 = \frac{G_{22}G_{1y} - G_{12}G_{2y}}{G_{11}G_{22} - |G_{12}|^2} \qquad 10.7$$

$$H_2 = \frac{G_{11}G_{2y} - G_{21}G_{1y}}{G_{11}G_{22} - |G_{12}|^2} \qquad 10.8$$

There are now three coherence functions that may be estimated, namely γ_{12}^2, γ_{1y}^2, and γ_{2y}^2 as defined in equations 10.9, 10.10 and 10.11.

$$\gamma_{12}^2 = \frac{|G_{12}|^2}{G_{11}G_{22}} \qquad 10.9$$

$$\gamma_{1y}^2 = \frac{|G_{1y}|^2}{G_{11}G_{yy}} \qquad 10.10$$

$$\gamma_{2y}^2 = \frac{|G_{2y}|^2}{G_{22}G_{yy}} \qquad 10.11$$

The coherence function in equation 10.11 is the standard coherence function determined throughout the thesis, giving information regarding the relationship between pressure and flow. The other two coherence functions will provide additional information illustrating the effect of cardiac data on both the flow and the pressure signals. In the case of a single input output system coherence values of unity

indicate that the output is wholly accounted for by the input. In the two input model discussed the coherence functions are interpreted a little differently. It is assumed that there is a correlation between the inputs such that γ_{12}^2 is above zero but less than unity. If zero, this means there is no correlation between the inputs and the problem effectively reduces to two single input single output systems. The cross spectral terms between the inputs would also vanish and the system frequency response functions, equations 10.7 and 10.8, would therefore also reduce to the familiar cross spectra to input auto spectra ratio discussed in Chapter 3. Alternatively if the coherence between inputs is unity then there exists a complete linear dependence between them and therefore a third response function, called H_{12} for example, exists and the model must be reconstructed. The earlier results illustrated that there is a relationship between pressure and cardiac signals, however, later in this chapter the coherence functions defined above will be computed to confirm the exact values in the 2Hz to 5Hz region of interest. In the multiple input model the coherence function γ_{1y}^2, for example, may be used to compute the coherent output spectrum relating the cardiac input, $x_1(t)$ to output, $y(t)$. The interpretation of this spectrum is that it represents the spectral output at $y(t)$ due to $x_1(t)$ passing through both H_1 and H_2.

10.3 Multiple Coherence Functions

Data from a number of apnoeic subjects was recorded while the oscillatory signal was applied and the cardiac signal was also recorded. Table 10.1 shows the three coherence functions defined above, quoted at 1Hz, 2Hz and 3Hz, with three sets of data presented

for each subject. The analysis produces a vast amount of data which needs to be condensed to focus on particular issues, the choice of the three integer frequencies was to enable statements to be made which apply to the first two impedance measurement frequencies, 2Hz and 3Hz, as well as 1Hz where no signal is applied.

	γ_{2y}^2			γ_{1y}^2			γ_{12}^2		
	1Hz	2Hz	3Hz	1Hz	2Hz	3Hz	1Hz	2Hz	3Hz
1	.99	.78	.75	.36	.74	.54	.28	.77	.69
	.98	.94	.82	.42	.53	.42	.30	.34	.49
	.96	.99	.95	.66	.27	.61	.76	.28	.30
2	.51	.55	.51	.51	.58	.38	.51	.58	.38
	.97	.72	.85	.78	.11	.30	.71	.34	.29
	.95	.51	.78	.57	.17	.50	.58	.21	.54
3	.74	.54	.62	.32	.40	.43	.48	.10	.32
	.98	.45	.39	.55	.14	.66	.51	.40	.32
	.87	.18	.27	.86	.49	.22	.73	.03	.31

Table 10.1 Coherence values for 3 volunteers, showing coherence relationships, (for definitions see text).

It is not meaningful to average coherence values between data sets, so the three sets of measurements for each subject serve to show

the variability of data. The variation in coherence values is due to the natural variation of the heart rate as well as noise introduced during the measurements associated with respiratory efforts and activity of the glottis. A number of points emerge from the table, to start with the fact that coherence values relating the cardiac signal to the other two signals are non zero and less than unity means the two input model discussed may well be applicable over this frequency range. The high γ_{2y}^2 values at 1Hz are thought to be due the presence of cardiac components in both pressure and flow, as no signal is applied at this frequency. An immediate question which arises is why similar levels of 1Hz coherence are not apparent between the cardiac and flow signals. One explanation may be that the cardiac signal recorded has travelled down the arm so there will be a delay between the signals which might introduce bias due to propagation time delays. There appears to be similar coherence values for the cardiac to pressure and cardiac to flow signals at each of the three frequencies.

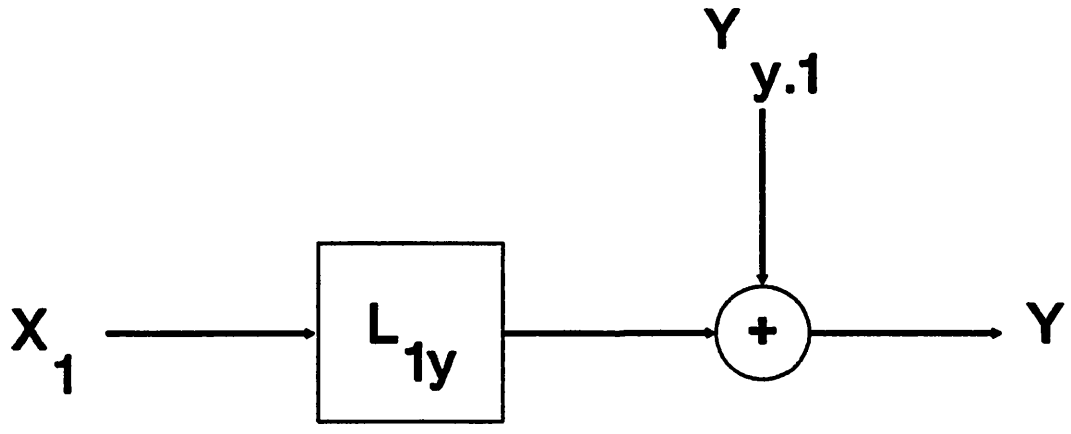

Figure 10.3 Conditioned Analysis - Output Term

10.4 Conditioned Spectral Analysis

When considering a multiple input, single output system it is possible to eliminate the effects of unwanted inputs using conditioned spectral analysis techniques. The mathematical basis for such an analysis relies on developing new models which characterise the relationship between unwanted inputs and both the required input, as well as the output. For a two input system the analysis is reasonably straightforward. Assume that the effects of the first input $x_1(t)$ are to be removed from the analysis. First the models of figure 10.3 and figure 10.4 are defined showing the relationship between $x_1(t)$ and the other input and output.

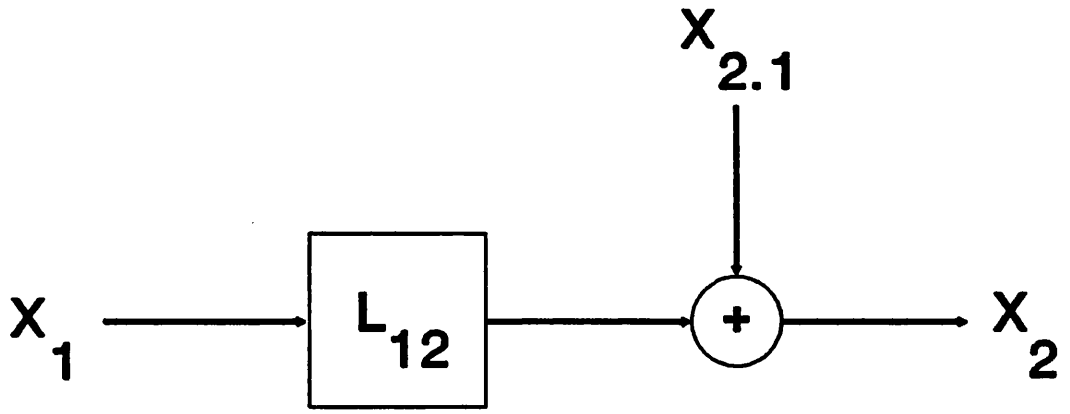

Figure 10.4 Conditioned Analysis - Second Input Term

The use of capital letters for inputs and output represent the Fourier transformed time varying signals and the analysis which follows is in the frequency domain. The use of a period in the spectral subscript signifies a conditioned spectra, which is not directly measurable. The conditioned spectra have the effects of the variable on the right of the period eliminated. In physical terms such an

analysis is the equivalent of turning off the unwanted input. Obviously this is impossible in the case of the cardiac signal, therefore the analysis allows this to be achieved mathematically. From figures 10.3 and 10.4, equations defining $X_{2.1}$ and $Y_{y.1}$ may be written, as equations 10.12 and 10.13. System response functions, L_{12} and L_{1y}, defined using cross and auto spectra as equations 10.14 and 10.15, represent the optimum linear systems to predict $x_2(t)$ and $y(t)$ from $x_1(t)$.

$$Y_{y.1} = Y - L_{1y}X_1 \qquad 10.12$$

$$X_{2.1} = X_2 - L_{12}X_1 \qquad 10.13$$

$$L_{12} = \frac{G_{12}}{G_{11}} \qquad 10.14$$

$$L_{1y} = \frac{G_{1y}}{G_{11}} \qquad 10.15$$

Applying this approach to the impedance calculation problem,

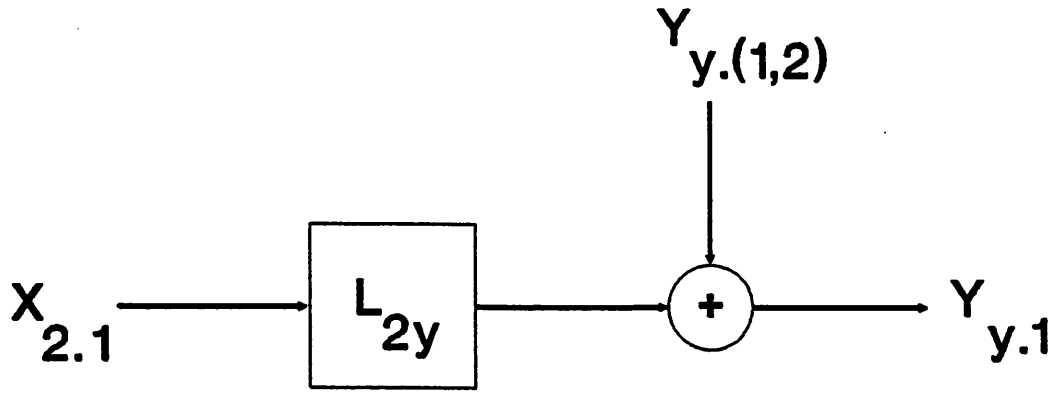

Figure 10.5 Conditioned Analysis - Complete Model

where the cardiac signal is viewed as the first input, means that the two systems defined in figure 10.2 account for the presence of cardiac components in both pressure and flow signals. The next step is to use the conditioned spectra to develop a single input, single output model, shown in figure 10.3, which enables L_{2y} to be estimated. This is the frequency response function from which an impedance estimate is obtained with the effects of the cardiac components eliminated. It is important to remember that many of the intermediate steps in this process yield results of no physical significance, however, L_{2y} is the same as H_{2y}. This holds for any value of γ_{12}^2 as $X_{2.1}$ may only pass through H_{2y} to produce $Y_{y.1}$ as the path through H_{1y} has been removed by the analysis. It is worth noting that the order of subscript parameters associated with the response functions are of importance as they must reflect physically realisable systems, hence inputs must precede outputs. In the case of cardiac interference the cardiac signal must occur before it can be seen on either pressure or flow so L_{1y} and L_{12} are acceptable model parameters. The conditioned input and output auto spectra and the cross power spectrum between the second input and the output are given in equations 10.16, 10,17 and 10.18 respectively.

$$G_{22.1} = X_{2.1}^* X_{2.1} \qquad 10.16$$

$$G_{yy.1} = Y_{y.1}^* Y_{y.1} \qquad 10.17$$

$$G_{2y.1} = X_{2.1}^* Y_{y.1} \qquad 10.18$$

These spectra are referred to as residual spectra by Bendat and Piersol, on whose work the following analysis was based. By

substituting equations 10.12 and 10.14 into 10.17, $G_{yy.1}$ may be determined, giving equation 10.19, which reduces to equation 10.20.

$$G_{yy.1} = \left[Y^* - \frac{G_{1y}}{G_{11}} X_1^*\right]\left[Y - \frac{G_{1y}}{G_{11}} X\right] \qquad 10.19$$

$$G_{yy.1} = G_{yy}(1-\gamma_{12}^2) \qquad 10.20$$

Equation 10.21 gives $G_{22.1}$, derived as equation 10.20 was, which is of a similar form to the result for $G_{yy.1}$.

$$G_{22.1} = G_{22}(1-\gamma_{12}^2) \qquad 10.21$$

Using the definition of $G_{2y.1}$ from equation 10.18 and substituting using equations 10.12 and 10.13, gives equation 10.22, which in turn reduces to equation 10.23.

$$G_{2y.1} = \left[X_2^* - \frac{G_{21}}{G_{11}} X_1^*\right]\left[Y - \frac{G_{1y}}{G_{11}} X_1\right] \qquad 10.22$$

$$G_{2y.1} = G_{2y} - \left[\frac{G_{1y}}{G_{11}}\right] G_{21} \qquad 10.23$$

Now that terms are available for $G_{2y.1}$ and $G_{22.1}$ it is possible to determine L_{2y}, equation 10.24

$$L_{2y} = \frac{G_{2y}\left[1 - \frac{G_{21}G_{1y}}{G_{11}G_{2y}}\right]}{G_{22}(1-\gamma_{12}^2)} \qquad 10.24$$

Using the residual spectra a partial coherence function may be calculated from equation 10.25.

It is important to note that the residual spectra and resulting frequency response function and partial coherence are all computed

$$\gamma^2_{2y.1} = \frac{|G_{2y.1}|^2}{G_{22.1}G_{yy.1}} \qquad 10.25$$

using the ordinary spectral quantities. This holds for the special case of two inputs, more inputs would necessitate an iterative computation strategy using the conditioned Fourier transforms. A number of observations may be made about the above formulae. As the coherence functions γ_{1y}^2 and γ_{12}^2 increase, the spectra G_{yy} and G_{22} are increased due to interference effects of the first input. Conversely, as power of the interference diminishes, eventually resulting in G_{12} becoming zero, the estimate L_{2y} reduces to the ratio of the cross power spectra, G_{2y}, over G_{22}, as for a single input, single output system. The role of the partial coherence function, $\gamma_{2y.1}^2$, is to indicate the proportion of the output spectrum which is accounted for by the second input, with the effects of the first input eliminated. Thus giving an insight into the true linear dependence between the second input and the output.

From the three measured signals the following conditioned variables were determined, γ_{2y}^2, γ_{1y}^2, γ_{12}^2, $G_{yy.1}$, $G_{22.1}$ and $G_{2y.1}$, remembering that signal one represents the cardiac signal which is to be conditioned out of the analysis. When the above spectra are available it is then possible to compute $\gamma_{2y.1}^2$, the partial coherence function between pressure and flow. The calculations were achieved by extending the normal respiratory impedance analysis program which computes, for two input signals, the auto spectra, cross spectrum and coherence function. In the interests of readability the frequency dependence of the above variables has not been written, however, values

of all the above spectra are available for each frequency point. The frequency spectral resolution being dictated by the sampling rate and number of points in the Fourier transform.

Results are presented showing the ordinary pressure to flow coherence function and the partial coherence function for frequencies in the 2Hz to 10Hz range. It was decided to leave the spectral resolution at 1Hz, which is representative of the resolution of the final clinical system. Additionally the pressure, flow and cardiac data were all comb filtered prior to the conditional analysis. The comb filter had bandpass elements of 0.05Hz bandwidth, at integer frequency intervals, the data was sampled for 16 seconds at a rate of 128Hz with results being transformed in 128 point blocks and averaged with 50% block overlap. The rationale being that even after the filtering, data is still poor at low frequencies so again the findings would be directly applicable to the clinical system where the filter is routinely applied. Although it has been observed that data above 5Hz is of good quality it was felt that applying the conditioned analysis over this extended range may allow differences to be identified between a good data region as opposed to a poor one.

Figures 10.6, 10.7 and 10.8 show graphically the three basic coherence functions as well as the partial coherence function for three apnoeic subjects.

10.5 Partial Coherent Output Spectra Analysis

It is of interest to use the conditioned spectral analysis techniques, outlined above, to produce partial coherent output spectra in the 2Hz to 5hz range. These spectra are a means by which it is

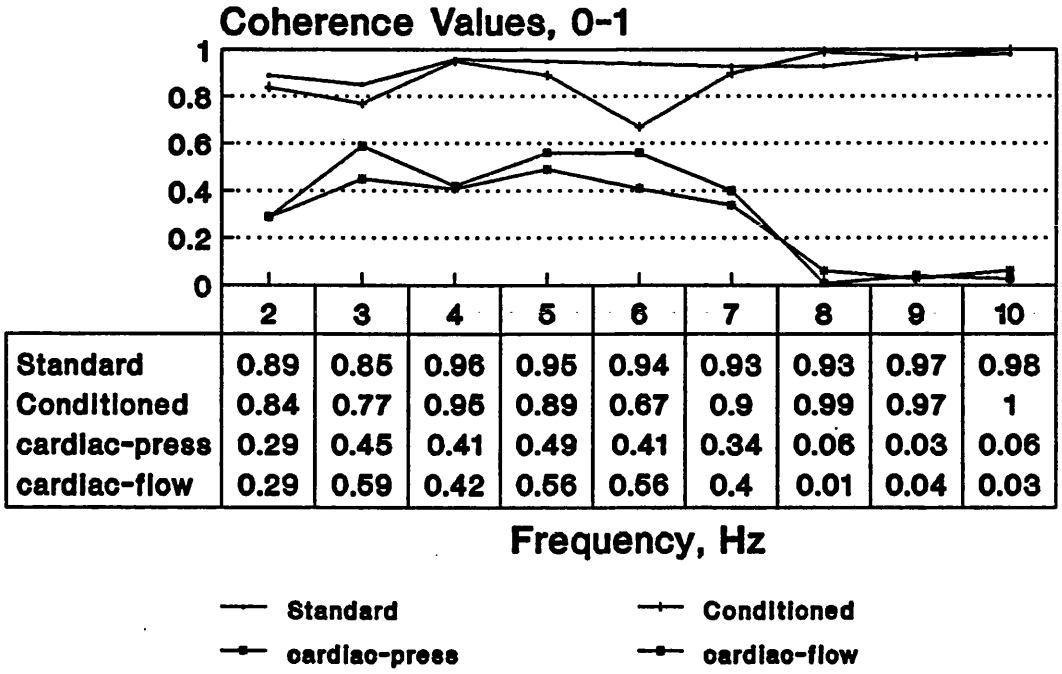

Figure 10.6 Partial and Single Coherence Functions - Subject 1

possible to identify the relative contribution of the two inputs to the output. The basic coherent output power spectrum is formed by multiplying the coherence function with the output power spectrum, the result indicates the amount of the output due to the input, with the remainder being attributed to noise. In the case of a multiple input system it is possible to define partial coherent output spectra by multiplying the conditioned output spectrum by the partial coherence function. Equation 10.26 gives $G_{y:1}$, the content of the power spectra attributable to input one, the cardiac input. With equation 10.27 giving $G_{y:2.1}$, the content of the output power spectrum due to the second input, the applied pressure signal, having conditioned out the effects of the cardiac signal. In the absence of any noise sources then the output due to both inputs is then the sum of $G_{y:1}$ and $G_{y:2.1}$.

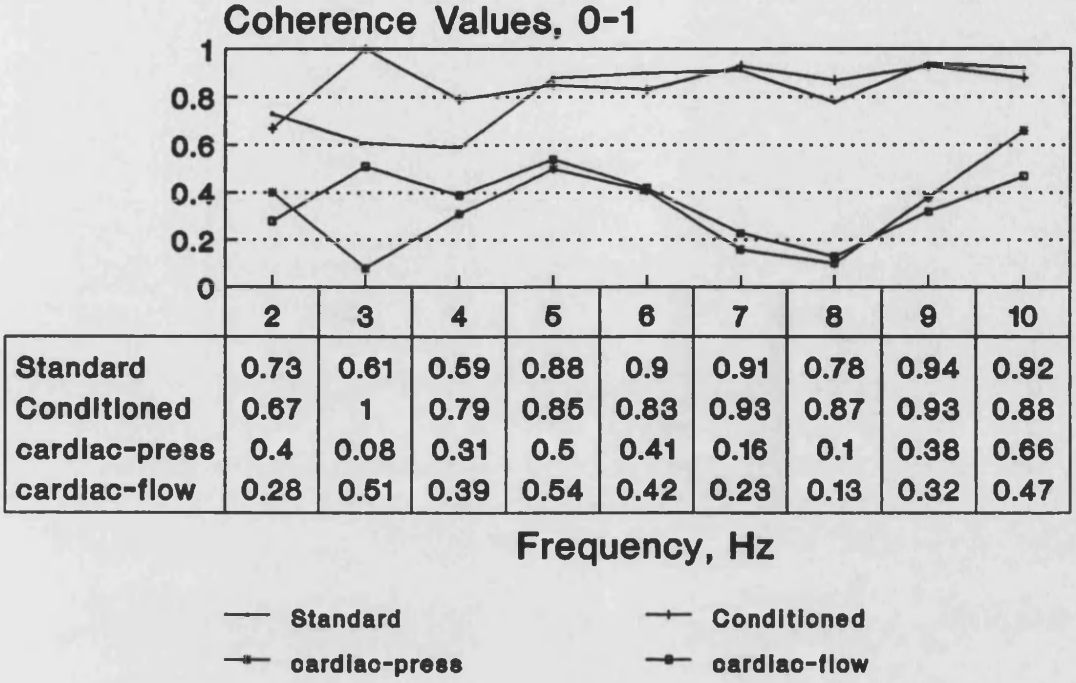

	2	3	4	5	6	7	8	9	10
Standard	0.73	0.61	0.59	0.88	0.9	0.91	0.78	0.94	0.92
Conditioned	0.67	1	0.79	0.85	0.83	0.93	0.87	0.93	0.88
cardiac-press	0.4	0.08	0.31	0.5	0.41	0.16	0.1	0.38	0.66
cardiac-flow	0.28	0.51	0.39	0.54	0.42	0.23	0.13	0.32	0.47

Figure 10.7 Partial and Single Coherence Functions - Subject 2

$$G_{y:1} = \gamma_{1y}^2 G_{yy} \qquad 10.26$$

$$G_{y:2.1} = \gamma_{2y.1}^2 G_{yy.1} \qquad 10.27$$

The two coherent output spectra defined above give an idea of the relative contributions of the two inputs to the output. The following results show the percentage of the measured output spectrum due to each input. As the percentages are all that are of interest, γ_{1y}^2 and the product of $\gamma_{2y.1}^2$ and $(1-\gamma_{1y}^2)$ is all that need be quoted. The actual magnitude of the output spectrum is of less importance than its makeup. Results are given for 5 runs in three subjects first while breathholding at total lung capacity, then at functional residual capacity. The cardiac signal was again recorded from the finger of the subjects. These results have not been comb filtered.

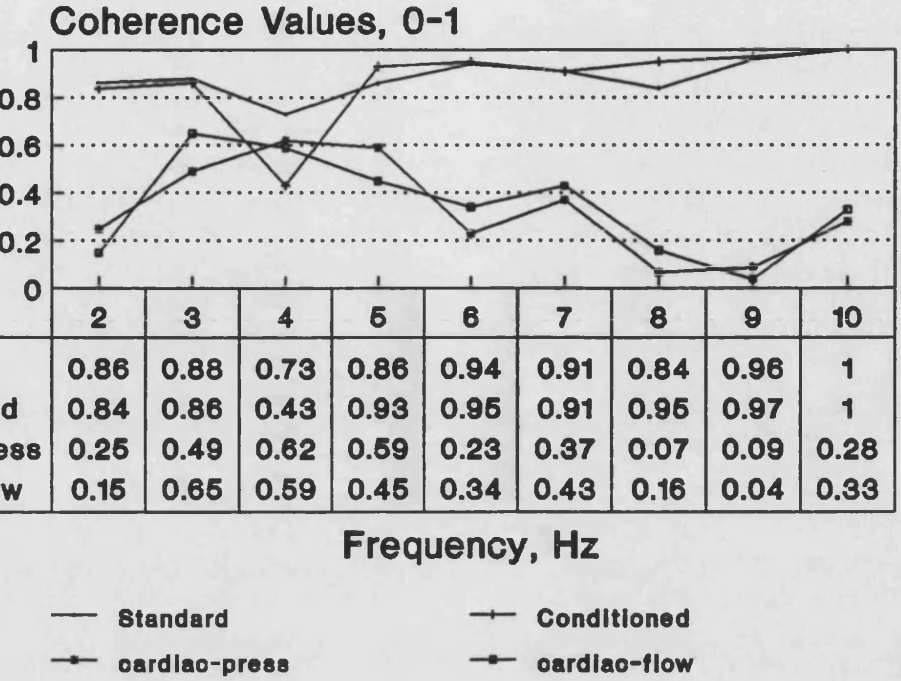

	2	3	4	5	6	7	8	9	10
Standard	0.86	0.88	0.73	0.86	0.94	0.91	0.84	0.96	1
Conditioned	0.84	0.86	0.43	0.93	0.95	0.91	0.95	0.97	1
cardiac-press	0.25	0.49	0.62	0.59	0.23	0.37	0.07	0.09	0.28
cardiac-flow	0.15	0.65	0.59	0.45	0.34	0.43	0.16	0.04	0.33

Figure 10.8 Partial and Single Coherence Function - Subject 3

10.6 Discussion of Results

By computing additional coherence functions it is possible to assess the relationship between the cardiac signal and the pressure and flow waveforms. Thus giving an insight into the frequency distribution of the cardiac noise on both pressure and flow. By using the conditioned spectral analysis it is possible to determine the partial coherence function relating pressure and flow signals. It is clear from the figures that the cardiac related signals are populating the 2Hz to 5Hz frequency range in the subjects shown and that the conditioned coherence values differ from the standard coherence values at certain frequencies. There is little else that can be said at this stage regarding the applicability of the partial coherence function as it has only been applied in a small test group. Thinking through the practical use of these additional coherence functions several points

arose. Firstly to more accurately see, in terms of frequency, whether the coherence values were coincident with applied signal strength it may well be necessary to increase the spectral resolution to achieve this. Secondly the finger pulse waveform does not include much information regarding the higher frequency components seen on the pressure and flow traces showing cardiac interference. It is likely therefore that an alternative cardiac reference signal with a greater frequency content may yield a clearer picture and make these ideas more applicable. It would be possible, for instance, to record the cardiac signal from the ear, which is anatomically closer to the mouth. For these reasons no attempt was made to compute impedance using the conditioned spectra as it was felt that the ideas were insufficiently advanced.

The proportioning of the measured flow spectrum between cardiac components and applied sinusoidal excitation was useful, as it gives an idea of the relative amplitude distribution of the two sources. It is apparent from tables 10.2 to 10.7 that there is a difference between intra subject runs in the proportion of the output attributable to cardiac activity. It was envisaged that such information could be used to discriminate between good and bad sets of data, thereby leading to more reliable impedance estimates. Such discrimination would complement the coherence function approach. The question is how to use the information available. As would be expected the cardiac component in the flow spectrum, $G_{y:1}$, decreases with increasing frequency, with the converse being true for the flow attributable to the applied pressure wave, $G_{y:2.1}$. Theoretically one would expect, in a noise free environment for the sum of the two components to equal 100%. It is

interesting to note that in subject 1 (table 10.2), at 1Hz where no signal is applied the terms do add up to virtually 100%, with the subject's heart rate being exactly 1Hz. A further interesting observation is that in run 3 in subject 2 (table 10.3), the $G_{y:2.1}$ term is close to 100%. During this measurement the subject had his glottis closed, therefore no cardiac components were observed and the impedance estimate was of the mouth. This gives confidence in the analysis as the cardiac component dramatically reduced, even at 1Hz.

Comparing tables 10.2, 10.3 and 10.4, with 10.5, 10.6 and 10.7 is informative, with the latter three tables showing results while breath holding with the lungs at end expiration (frc), *i.e.* at a lower volume than total lung capacity. It is observed in subject's 1 and 2 that the cardiac component percentages are reduced at frc and on average the proportion attributable to the applied pressure has increased. Indeed this is apparent from the basic impedance data and standard coherence functions, giving further credit to the use of $G_{y:1}$ and $G_{y:2.1}$ as data discriminators. The third subject experienced more difficulty in breath holding so the results are the pressure and flow waveforms tended to be noisier. Ultimately these ideas would have to be used in breathing subjects for them to be clinically applicable.

The ideas presented offer additional information on the sources of noise affecting pressure and flow signals during the impedance measurement. The computation of the additional conditioned spectra is not difficult having collected the cardiac waveform. More data, increased frequency resolution, and perhaps a wider bandwidth cardiac signal are necessary to practically use the extra information.

	Run 1		Run 2		Run 3		Run 4		Run 5	
Frq Hz	$G_{y:1}$ %	$G_{y:2.1}$ %	$G_{y:1}$ %	$G_{y:2.1}$ %	$G_{y:1}$ %	$G_{y:2.1}$ %	$G_{y:1}$ %	$G_{y:2.1}$ %	$G_{y:1}$ %	$G_{y:2.1}$ %
1	21	57	5	72	43	47	16	65	32	56
2	26	14	8	11	8	13	1	29	16	22
3	32	23	7	46	13	25	17	31	34	27
4	34	28	15	7	3	47	7	26	19	28
5	12	29	20	25	18	19	6	34	18	26
6	1	57	8	47	16	26	7	37	6	39
7	2	50	19	30	9	49	7	46	0	49
8	10	33	0	29	2	37	8	40	4	28
9	8	74	4	61	7	51	4	68	4	52
10	2	56	23	41	7	30	4	43	1	26

Table 10.2 Coherent Output Spectra Percentages - Subject 1 TLC. (Solid line at 1Hz indicates no signal applied at this frequency). Subject's Resting Heart Rate = 60beats/minute.

	Run 1		Run 2		Run 3		Run 4		Run 5	
Frq Hz	$G_{y:1}$ %	$G_{y:2.1}$ %	$G_{y:1}$ %	$G_{y:2.1}$ %	$G_{y:1}$ %	$G_{y:2.1}$ %	$G_{y:1}$ %	$G_{y:2.1}$ %	$G_{y:1}$ %	$G_{y:2.1}$ %
1	8	40	5	43	8	8	12	12	21	33
2	16	42	13	61	4	82	14	26	5	62
3	24	32	4	27	9	82	5	22	22	33
4	12	42	10	50	0	92	7	70	15	42
5	17	37	4	34	3	89	3	50	7	44
6	1	64	3	60	0	95	6	69	0	64
7	1	68	3	65	0	98	23	53	2	61
8	1	61	0	54	3	96	9	56	5	57
9	4	63	8	5	6	93	3	82	11	51
10	3	60	4	56	1	91	2	74	9	63

Table 10.3 Coherent Output Spectra Percentages - Subject 2 TLC. (Solid line at 1Hz indicates no signal applied at this frequency). Subject's Resting Heart Rate < 50beats/minute.

	Run 1		Run 2		Run 3		Run 4		Run 5	
Frq Hz	$G_{y:1}$ %	$G_{y:2.1}$ %	$G_{y:1}$ %	$G_{y:2.1}$ %	$G_{y:1}$ %	$G_{y:2.1}$ %	$G_{y:1}$ %	$G_{y:2.1}$ %	$G_{y:1}$ %	$G_{y:2.1}$ %
1	9	70	4	37	9	5	18	7	17	66
2	5	13	1	20	5	59	3	28	5	8
3	11	18	5	25	2	67	16	35	8	25
4	14	45	4	33	4	83	3	72	2	22
5	6	54	3	28	7	87	4	79	2	40
6	5	49	8	31	7	91	1	85	7	38
7	1	64	6	41	1	96	1	90	7	42
8	9	60	3	39	17	80	12	78	1	59
9	11	66	10	38	13	86	2	92	3	69
10	3	55	2	38	5	92	3	84	10	38

Table 10.4 Coherent Output Spectra Percentages - Subject 3 TLC. (Solid line at 1Hz indicates no signal applied at this frequency). Subject's Resting Heart Rate > 60beats/minute.

	Run 1		Run 2		Run 3		Run 4		Run 5	
Frq Hz	$G_{y:1}$ %	$G_{y:2.1}$ %	$G_{y:1}$ %	$G_{y:2.1}$ %	$G_{y:1}$ %	$G_{y:2.1}$ %	$G_{y:1}$ %	$G_{y:2.1}$ %	$G_{y:1}$ %	$G_{y:2.1}$ %
1	4	62	4	44	11	58	9	58	45	34
2	3	35	1	34	3	22	2	24	1	27
3	5	22	18	21	13	19	14	15	2	31
4	5	36	5	43	0	36	1	39	1	42
5	0	64	1	73	1	71	5	67	0	63
6	4	74	1	86	0	85	1	77	4	74
7	9	77	4	75	7	76	11	70	6	72
8	2	81	2	73	3	78	2	75	0	89
9	11	80	2	80	5	78	1	81	2	92
10	11	71	4	74	7	62	3	64	8	82

Table 10.5 Coherent Output Spectra Percentages - Subject 1 FRC. (Solid line at 1Hz indicates no signal applied at this frequency). Subject's Resting Heart Rate = 60beats/minute.

	Run 1		Run 2		Run 3		Run 4		Run 5	
Frq Hz	$G_{y:1}$ %	$G_{y:2.1}$ %	$G_{y:1}$ %	$G_{y:2.1}$ %	$G_{y:1}$ %	$G_{y:2.1}$ %	$G_{y:1}$ %	$G_{y:2.1}$ %	$G_{y:1}$ %	$G_{y:2.1}$ %
1	2	14	25	23	49	23	21	36	11	60
2	3	45	2	71	24	41	7	67	7	70
3	4	41	0	61	44	13	4	59	14	46
4	10	52	1	78	16	70	12	70	3	74
5	0	64	1	77	2	78	3	91	6	73
6	5	69	2	77	9	77	5	93	3	89
7	4	68	2	80	3	85	6	91	3	85
8	8	69	4	89	21	63	0	96	2	85
9	0	85	3	85	42	46	4	93	6	85
10	11	60	4	80	3	82	3	89	3	78

Table 10.6 Coherent Output Spectra Percentages - Subject 2 FRC. (Solid line at 1Hz indicates no signal applied at this frequency). Subject's Resting Heart Rate < 50beats/minute.

	Run 1		Run 2		Run 3		Run 4		Run 5	
Frq Hz	$G_{y:1}$ %	$G_{y:2.1}$ %	$G_{y:1}$ %	$G_{y:2.1}$ %	$G_{y:1}$ %	$G_{y:2.1}$ %	$G_{y:1}$ %	$G_{y:2.1}$ %	$G_{y:1}$ %	$G_{y:2.1}$ %
1	27	32	37	16	0	23	5	42	4	2
2	3	7	9	11	1	8	16	3	10	43
3	3	19	4	12	8	15	2	11	0	59
4	10	13	1	9	2	9	4	9	11	60
5	11	22	19	16	7	41	2	19	4	63
6	14	19	0	22	12	26	2	19	28	37
7	1	22	4	24	11	40	7	14	5	73
8	2	35	6	45	3	65	0	19	12	68
9	3	31	3	38	3	62	8	29	1	79
10	0	21	7	39	0	43	1	14	17	56

Table 10.7 Coherent Output Spectra Percentages - Subject 3 FRC. (Solid line at 1Hz indicates no signal applied at this frequency). Subject's Resting Heart Rate > 60beats/minute.

Chapter 11 Concluding Remarks

11.1 Summary of the Work

The work presented effectively splits into two distinct sections. Firstly, one of the aims of the project was to provide the hospital with an impedance measurement system, which has been achieved. The main use of the system to date has been in bronchial challenge testing. The instrumentation is easy to use and may be moved between the bedside and laboratory. A clear advantage to patients is that measurements are made without having to undertake a forced expiration, which can be distressing for severely ill patients. Additionally more measurements may be made following drug administration as the patient will not tire. The impedance results enable changes in resistance and compliance to be differentiated between, which spirometric indices will not do. As patients with advanced lung disease have higher resistances and resonant frequencies, low frequency data is often of little importance.

The major focus of this work, however, has been the consideration of factors affecting low frequency impedance data. It is not until this has been fully addressed that subtle changes in respiratory mechanics can be identified with confidence. This has been investigated by considering measurements in normal individuals and examining the reliability and the spread of impedance data and derived indices. Inadequacies in the early instrumentation were overcome through choice of airflow and enhancements to the signal processing. The comb filter approach dramatically improves coherence values and data quality. Post filtered low frequency impedance data still exhibited variability and sources of physiological interference were

explored to assess their effect. Many groups have considered respiration as the main source of physiological interference, however, our group focused on cardiogenic interference which has not been assessed by other workers in the field. Evidence of cardiac activity was shown on both pressure and flow signals.

The final chapters concentrated on the integrity of the coherence function, and methods by which to characterise the cardiac interference and its impact on the impedance data. The limitations of the coherence function were studied and attempts were made to further quantify the noise distribution using additional coherence functions and conditioned spectral analysis techniques. The latter techniques showed in gross terms the impact of the noise, however, more data was necessary to explore the full potential of the multiple input, single output approach introduced.

In conclusion this work has furthered the understanding of the coherence function as applied to respiratory impedance measurements, has identified an additional source of interference to impedance data and proposed a new impedance estimator, which remains to be tested.

11.2 Future Work

It is interesting to reflect on the direction the reported work would take if it was commenced again today. A similar generator would have been developed as the deficiencies with loudspeakers are becoming apparent to other groups, as they try to make measurements in ventilated subjects. The literature still contains no information on the effects of cardiac interference so this also would have still been undertaken. The early prototype, however, would have taken a different

form, as there is considerably more information available, largely from the Concerted Action Group, on the design and relative merits of oscillatory airflow and choice and validation of transducers. Many groups now are using precision Fleisch flowheads, which although their frequency response is worse than screen type this can be corrected for in the computer. Attempts would also have been made to make measurements at much lower frequencies, which was precluded by our generator. Such measurements below 1Hz appear useful as they equate more closely to respiration frequencies. A fascinating study would have been to look at the spread of data at these frequencies, which are below the cardiac frequency and therefore free of cardiogenic interference. The use of unbiased estimators to determine impedance would also have been worth exploring in more detail.

In terms of our own research, the most interesting point to pursue is probably the cardiac interference question. The work failed to either eliminate cardiac interference by adaptive filtering or discriminate its presence using the conditioned analysis. It became apparent that the cardiac signal lacked frequency content and was too dissimilar to the related interference on the pressure and flow signals. The acquisition of an alternative cardiac signal would be interesting to assess. Our understanding of the conditioned spectral analysis techniques developed during the latter stages of the work and with hindsight it would perhaps have been better to develop the partial coherent output spectra with increased frequency resolution. This may have enabled a more accurate statement of the noise distribution. It would also be interesting to change the applied oscillations for each subject so that they were not coincident with the cardiac spectrum.

Bibliography

Bendat, J. S. and Piersol, A. G. (1971). *Random Data: Analysis and Measurement Procedures*. New York: Wiley-Interscience.

Bendat, J. S. and Piersol, A. G. (1980). *Engineering Applications of Correlation and Spectral Analysis*. New York: John Wiley & Sons.

Bergland G. D. (1969). A guided tour of the fast Fourier transform. *IEEE Spectrum*. **6**, 41-52.

Cauberghs M. and van de Woestijne K. P. (1983). Mechanical properties of the upper airway. *J. Appl. Physiol.* **55**, 335-342.

Cauberghs M. and van de Woestijne K. P. (1991). Errors in the estimation of respiratory impedance: use of an unbiased estimator. *Eur. Respir. Rev.* **1**, Review 3, 206-9.

Cooley J. W. and Tukey J. W. (1965). An algorithm for the machine calculation of complex Fourier series. *Math. Comput.* **19**, 297-301.

Cotes, J. E. (1979). *Lung Function Assessment and Application in Medicine*. Oxford: Blackwell Scientific.

Daróczy B. and Hantos Z. (1982). An improved forced oscillatory estimation of respiratory impedance. *Int. J. Biomed. Comput.* **13**, 221-235.

Darőczy B. and Hantos Z. (1990). Generation of optimum pseudorandom signals for respiratory impedance measurements. *Int. J. Biomed. Comput.* **25**, 21-31.

Darőczy B., Fabula A. and Hantos Z. (1991). Use of noninteger-multiple pseudorandom excitation to minimise nonlinear effects on impedance estimation. *Eur. Respir. Rev.* **1, Review 3**, 183-7.

Delavault E., Saumon G. and Georges R. (1980). Identification of transducer defect in respiratory impedance measurements by forced random noise. *Resp. Physiol.* **40**, 107-117.

DuBois A. B., Brody A. W., Lewis D. H. and Burgess Jr. B. F. (1956). Oscillation Mechanics of Lungs and Chest in Man. *J. Appl. Physiol.* **19**, 653-8.

Eyles J. G. and Pimmel R. L. (1981). Estimating respiratory mechanical parameters in parallel compartment models. *IEEE Trans. Biomed. Eng.* **BME-28**, 313-7.

Farrē R., Peslin R., Navajas D., Gallina C. and Suki B. (1989). Analysis of the dynamic characteristics of pressure transducers for studying respiratory mechanics at high frequencies. *Med. Biol. Eng. Comput.* **27**, 531-7.

Farrē R., Rotger M. and Navajas D. (1990). Time domain filter to improve signal-to-noise ratio in respiratory impedance measurements.

Med. Biol. Eng. Comput. **29**, 18-24.

Fisher A. B., DuBois, A. B. and Hyde, R. W. (1968). Evaluation of the forced oscillation technique for the determination of resistance to breathing. *J. Clin. Invest.* **47**, 2045-2057.

Franken H., Clément J., and van de Woestijne K. P. (1983). Systematic and random errors in the determination of respiratory impedance by means of the forced oscillation technique: a theoretical study. *IEEE Trans. Biomed. Eng.* **BME-30**, 642-651.

Goldman M. L., Knudson R. J., Mead J., Peterson N., Schwaber J. R. and Wohl M. E. (1970). A simplified measurement of respiratory resistance by forced oscillation. *J. Appl. Physiol.* **28**, 113-6.

Grimby G., Takishima T., Graham W, Macklem P and Mead J. (1968). Frequency dependence of flow resistance in patients with obstructive lung disease. *J. Clin. Invest.* **47**, 1455-1465.

Hirano K., Nishimura S. and Mitra S. K. (1974). Design of digital notch filters. *IEEE Trans. Comm.* **COM-22**, 964-971.

Hogg J. C., Macklem P. T. and Thurlbeck W. M. (1968). Site and nature of airway obstruction in chronic obstructive lung disease. *N. Engl. J. Med.* **278**, 1355.

Hyatt R. E., Zimmerman I. R., Peters G. M. and Sullivan W. J. (1970).

Direct writeout of total respiratory resistance. *J. Appl. Physiol.* **28**, 675-8.

International Commission on Radiological Protection. (1975). *Report of the Task Group on Reference Man.* Oxford: Pergamon Press. ICRP Report 23.

Kjeldgaard J. M., Hyde R. W., Speers D. M. and Reichert W. W. (1976). Frequency dependence of total respiratory resistance in early airway disease. *Am. Rev. Resp. Dis.* **114**, 501-7.

Lándsér F. J., Nagels J., Demedts M., Billiet L. and van de Woestijne K. P. (1976). A new method to determine the frequency characteristics of the respiratory system. *J. Appl. Physiol.* **41**, 101-6.

Lándsér F. J., Nagels J., Clément J. and van de Woestijne K. P. (1976). Errors in the measurement of total respiratory resistance and reactance by forced oscillations. *Resp. Physiol.* **28**, 289-301.

Macklem P. T. and Mead J. (1967). Resistance of central and peripheral airways measured by a retrograde catheter. *J. Appl. Physiol.* **22**, 395.

Macklem P. T. (1972). Obstruction in small airways: a challenge to medicine. *Am. J. Med.* **52**, 721.

McFadden Jr. E. R., Kiker R., Holmes B. and deGroot W. J. (1974). Small airway disease. *Am. J. Med.* **57**, 171-182.

Mead J, Turner J. M., Macklem P. T. and Little J. B. (1967). Significance of the relationship between lung recoil and maximum expiratory flow. *J. Appl. Physiol.* **22**, 95.

Mead J. (1969). contribution of compliance of airways to frequency-dependent behaviour of lungs. *J. Appl. Physiol.* **26**, 670-3.

Michaelson E. D., Grassman E. D. and Peters W. R. (1975). Pulmonary mechanics by spectral analysis of forced random noise. *J. Clin. Invest.* **56**, 1210-1230.

Navajas D., Farré R., Rotger M. and Peslin R. (1988). A new estimator to minimise the error due to breathing in the measurement of respiratory impedance. *IEEE Trans. Biomed. Eng.* **BME-35**, 1001-1005.

Oppenheim, A. V. and Schafer, R. W. (1975). *Digital Signal Processing.* Englewood Cliffs, N.J.: Prentice Hall.

Pelle G., Lorino H., Perez J., Lorino A. and Harf A. (1984). Modelling of the transfer function of the flow transducer used in ventilatory impedance measurements. *IEEE Trans. Biomed. Eng.* **BME-31**, 356-361.

Peslin R. (1984). In-phase rejection requirements for measuring respiratory input impedance. *J. Appl. Physiol.* **56**, 804-9.

Peslin R., Duvivier C., Didelon J. and Gallina C. (1985). Respiratory impedance measured with head generator to minimise upper airway shunt.

J. Appl. Physiol. **59**, 1790-5.

Peslin R. (1986). Méthodes de mesure de l'impédance respiratoire totale par oscillations forcées. *Bull. Eur. Physiopathol. Respir.* **17**, 93-105.

Pimmel R. L., Tsai M. J., Winter D. C. and Bromberg P. A. (1978). Estimating central and peripheral respiratory resistance. *J. appl. Physiol.* **45**, 375-380.

Pimmel R. L., Winter D. C. and Bromberg P. A. (1980). Forced oscillatory parameters of the canine respiratory system with altered vagal tone. *IEEE Trans. Biomed. Eng.* **BME-27**, 146-9.

Pimmel R. L., Fullton J. M., Ginsberg J. F., Hazucha M. J., Haak E. D., McDonnell W. F. and Bromberg P. A. (1981). Correlation of airway resistance with forced random noise resistance parameters. *J. Appl. Physiol.* **51**, 33-9.

Rotger M., Peslin R., Farré R. and Duvivier C. (1991). Influence of amplitude, phases and frequency content of pseudorandom pressure input on impedance data and their variability. *Eur. Respir. Rev.* **1, Review 3**, 178-182.

Slutsky A. S. and Drazen, J. M. (1978). Estimating central and peripheral respiratory resistance: an alternative analysis. *J. appl. Physiol.* **45**, 375-380.

Sobol B. J. (1968). Tests of ventilatory function not requiring maximal subject effort. *Am. Rev. Res. Dis.* **97**, 869-879.

Tsai M. J. and Pimmel, R. L. (1979). Computation of respiratory resistance, compliance and inertance from forced oscillatory impedance data. *IEEE Trans. Biomed. Eng.* **BME-26**, 492-3.

West, J. B. (1985). *Respiratory Physiology - the essentials.* Baltimore: Williams and Wilkins.

Widrow B., Glover Jr. J. R., McCool J. M., Kaunitz J., Williams C. S., Hearn R. H., Zeidler J. R., Dong Jr. E. J. and Goodlin R. C. (1975). Adaptive noise cancellation: principles and applications. *Proc. IEEE.* **63**, 1692-1716.

Williams S. P., Fullton J. M., Tsai M. J., Pimmel, R. L. and Collier, A. M. (1979). Respiratory impedance and derived parameters in young children by forced random noise. *J. Appl. Physiol.* **47**, 169-174.

Appendix A - Respiratory Impedance Instruction Manual

Respiratory Impedance System

Instruction Manual

Pulmonary Physiology Department
Royal United Hospital
Bath

Draft Version

January 1992

Respiratory Impedance System

Switch On Sequence

1. Plug in the extension lead, turn on the mains supply, then depress the grey reset switch on top of the plug. Check that a red indicator is displayed in the transparent window.

2. Turn on the black PA 100E amplifier by rotating the 'master gain' knob clockwise. Ensure the knob is then left at the zero level (i.e. rotated as fully anti-clockwise as possible without turning the amplifier off). Check that the green 'power on' and red 'signal clamp' indicators both illuminate.

3. Finally, switch on the computer by raising the red switch on the computer. The monitor obtains power directly from the computer. The respiratory impedance program will automatically run, and the screen display should appear.

Switch Off Sequence

1. Rotate the 'master gain' control anti-clockwise to the zero setting, (without actually turning the device off).

2. Quit the program by returning to the main menu and selecting function key F10. Having quit, the computer will automatically park the heads on the hard disk, and the computer may now be turned off.

3. Switch the amplifier off by clicking the 'master gain' knob further anti-clockwise.

4. Disconnect the extension lead from the mains socket, thus ensuring power is totally removed from the trolley.

Note: The printer may be left switched on all the time.
The transducers and associated circuits are powered whenever the extension lead is connected to the mains supply.

Respiratory Impedance System Documentation

1 Introduction.

A system has been developed to enable the rapid determination of respiratory impedance (RZ) via the oscillatory airflow technique. The following documentation describes the use of the prototype developed by the Pulmonary Physiology and Medical Physics Departments of the Royal United Hospital, Bath.

The technique enables measurements to be made with minimal subject cooperation, therefore it may be applied in adults, children, neonates and mechanically ventilated patients. Currently, data is being obtained in adults, breathing normally, (whilst wearing a nose-clip), in the seated position. Respiratory impedance, defined as the ratio of pressure to flow, is a complex, frequency dependent indicator of respiratory mechanics. By analysing variations of impedance with frequency, it is thought that information regarding the regional distribution of mechanical parameters may be obtained. If so, then it may be possible to identify increases in peripheral airways resistance, whilst subjects remain asymptomatic. Impedance data is available in the range 2-40Hz, and being a mathematically complex variable may be represented in two equivalent ways. Data may be presented as the magnitude of the impedance and a phase angle, or alternatively split into resistive and reactive (i.e. inertial and compliant) components. During the developmental stages data will be available in both forms, thus enabling an evaluation of the optimum form in which to ultimately present results.

The following sections comprise a description of the system components, and an introduction to the application software.

2 Hardware Summary

An outline of the main components within the system is shown in block diagram form in Figure 1. To calculate impedance it is necessary to generate an oscillatory airflow containing frequencies in the range 2-40Hz in 1Hz steps. This is achieved by generating a signal within the computer which is then fed to a power amplifier driving an electro-dynamic vibration generator. This in turn excites a set of bellows producing the oscillatory airflow. Pressure and flow are measured close to the mouth using validyne pressure gauges. These signals are filtered, digitised, and processed to obtain impedance information at each frequency present in the airflow. The breathing port shown on the block diagram is a resistance to atmosphere through which the subject breathes.

3 System Software

3.1 Overview

The RZ application software has been written using Borland Turbo Pascal v5.5, and utilising a fast spectral analysis library (Cambridge Electronic Design). The menu driven software has two main modes of operation:

On-line data collection

Retrieval of stored data

The information box at the base of the screen is designed to keep the user informed about program status by displaying menu options, prompts and progress messages. function key numbers following headings, illustrate which menu option needs to be selected. The 'setup' option shown on the main menu is currently not accessible.

3.2 Data Collection [F1]

Having selected the data acquisition menu, the following steps are involved.

3.2.1 Patient Identification [F1]

This option allows patient details to be entered via the keyboard. Upon selection the user is prompted to enter, in turn: surname, forenames and hospital number. Errors may be corrected using the backspace key when typing it in, however the data cannot be altered once it has been accepted. The data upon entry is displayed in the information box at the top of the screen. This data only needs to be typed in once per patient.

3.2.2 Amplifier Control

Ensure the 'master gain' control is set to zero. Now press the reset button on the amplifier. The 'master gain' control may now be set to 2.

3.2.3 Executing a Run [F2]

Upon selection, the user will be prompted for a comment to describe the forthcoming run. Having typed the comment, but prior to accepting it by pressing <enter>, it is now that the patient is asked to go onto the mouthpiece. The subject should wear a nose-clip, breathe normally whilst gently supporting the cheeks with the palms of the hands. Next the enter key is pressed, the comment accepted and the oscillatory airflow will begin. The system is now in the data preview stage. Impedance data will appear on the screen, updated at 1 second intervals. The subject should

be given a few seconds to accommodate to the manoeuvre, and the data should be superficially examined to check that it appears valid. If it does, then the space bar should be depressed and the 16 second data acquisition period will commence; otherwise the preview may be terminated by hitting any other key. Once the main 16 second acquisition phase has started it cannot be aborted.

3.2.4 Data Storage

Upon completion of the run the raw pressure and flow data are automatically saved. The subject's surname is used as a disk filename. Each file comprises an entry recording patient details, followed by run data (i.e. raw data plus comment). Subsequent runs are added to the end of the disk-file.

The program checks filenames before writing to disk to ensure that the user is aware of any potential conflict with duplicate filenames. If the name has not been used before, then a new file is created and no user response is required. If the name exists, then the user is asked if it is the correct file and if so the data appended to it. Otherwise, the user is prompted to enter an alternative name, perhaps the simplest strategy to suggest is to add the first letter of the forename to the surname to create a unique, yet recognisable filename. Only the first 8 letters of the surname will be used for the filename.

3.3 Data Re-Analysis [F2]

3.3.1 Recalling Data [F1]

All raw data is stored in one directory, and the user has no opportunity to select an alternative. Therefore data retrieval is a simple task of selecting one of the named files displayed on the screen. As the number of subjects increases, the list of available files will eventually exceed one page. When this occurs the user will be prompted to press a key to see subsequent pages, currently all pages would have to be viewed before a filename is prompted for. When a file is chosen, the available runs are displayed together with the date, time and associated comment. Similar to the filenames, if the number of runs exceeds the display space available on one page they will be listed on subsequent pages. Again a key press will advance from one page to the next. When all available runs have been displayed, the user is prompted to enter the required run number.

Alternatively pressing <enter> automatically selects the first run, which is recalled, analysed and displayed. Subsequent runs may then be superimposed on the first by repeatedly pressing the <enter> key. Whilst more runs are available this process will continue. The display may be cleared at any point by pressing the space bar, with any other key terminates the process, clears the screen and displays the current run.

3.3.2 Editing Data [F2]

Currently this option is not available. On selection, it will do no more than display the raw data in 16 by 1 second blocks. This in itself is useful to see if either pressure or flow channel saturated the transducer amplifiers during measurements.

3.3.3 Pre-processing Data [F3]

By applying a number of narrow band-pass filters to the raw pressure and flow signals, it is possible to improve the data, particularly at low frequencies. Currently, however, this filtering regime takes about 60 seconds to achieve. Thus when this option is selected a message appears informing the user the filter is in progress. Ultimately these filters will be speeded up.

3.4 Data Summary

All data is displayed graphically to enable a rapid visual assessment of the quality and rough values. To quantify the data and to examine subtleties within the data it is necessary to display the numerical values at each frequency. The program has a number of numerical display modes. Additionally, colour graphical printouts are available.

3.4.1 Cursor Data

A facility exists to scroll through the data using a cursor, with the data displayed at the cursor frequency in the information box. This enables a combination of graphical and numeric data simultaneously, though only at one frequency point. This option is automatically entered following data analysis, and is quit when the user presses the space bar. On occasions it may be necessary to re-enter the cursor data option, this is achieved by pressing the <alt> key and the letter 'C' together. The display format is illustrated in the Figure 2, showing an example of a typical normal.

3.4.2 Tabular Data

This option shows all available impedance data for the current run, from 2-40Hz in 2Hz steps, thus it all appears on one page. The numeric data option is offered to the user when the cursor data program has finished. To enter this display mode at other times is possible by pressing <alt> and 'D' simultaneously.

3.4.3 Data Printout

A hard copy, colour printout of the current display is activated, from most points of the program by pressing <alt> and 'P'. It is currently necessary to ensure the printer is on-line prior to attempting a print operation.

3.5 Quit Options

At each menu level a quit option exists, accessed by function key F10. This moves control to the higher menu levels. When at the main menu the quit option exits the program. There is a delay on quitting the program, thus if F10 is pressed accidentally by hitting any key within the 2-3 second delay the command to quit is cancelled. Having quit the computer automatically parks the hard disks, with no further processing possible. If it is necessary to re-enter the program the simplest route is by simultaneously holding down the <Ctrl>,<Alt> and <Del> keys thus causing the computer to re-boot.

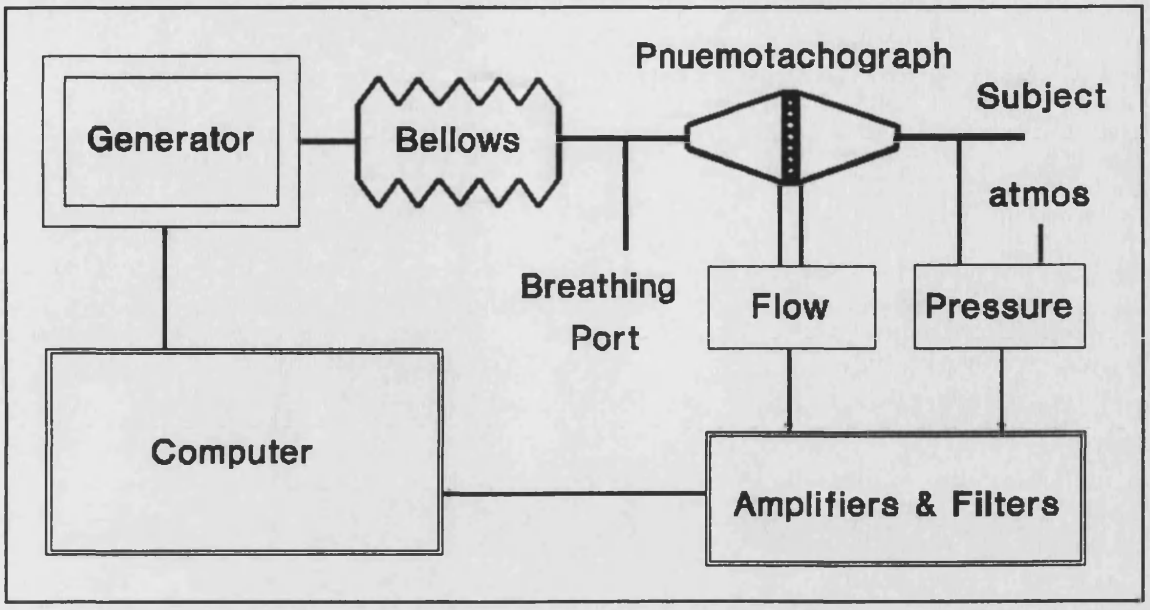

Figure 1 : Respiratory Impedance Instrumentation

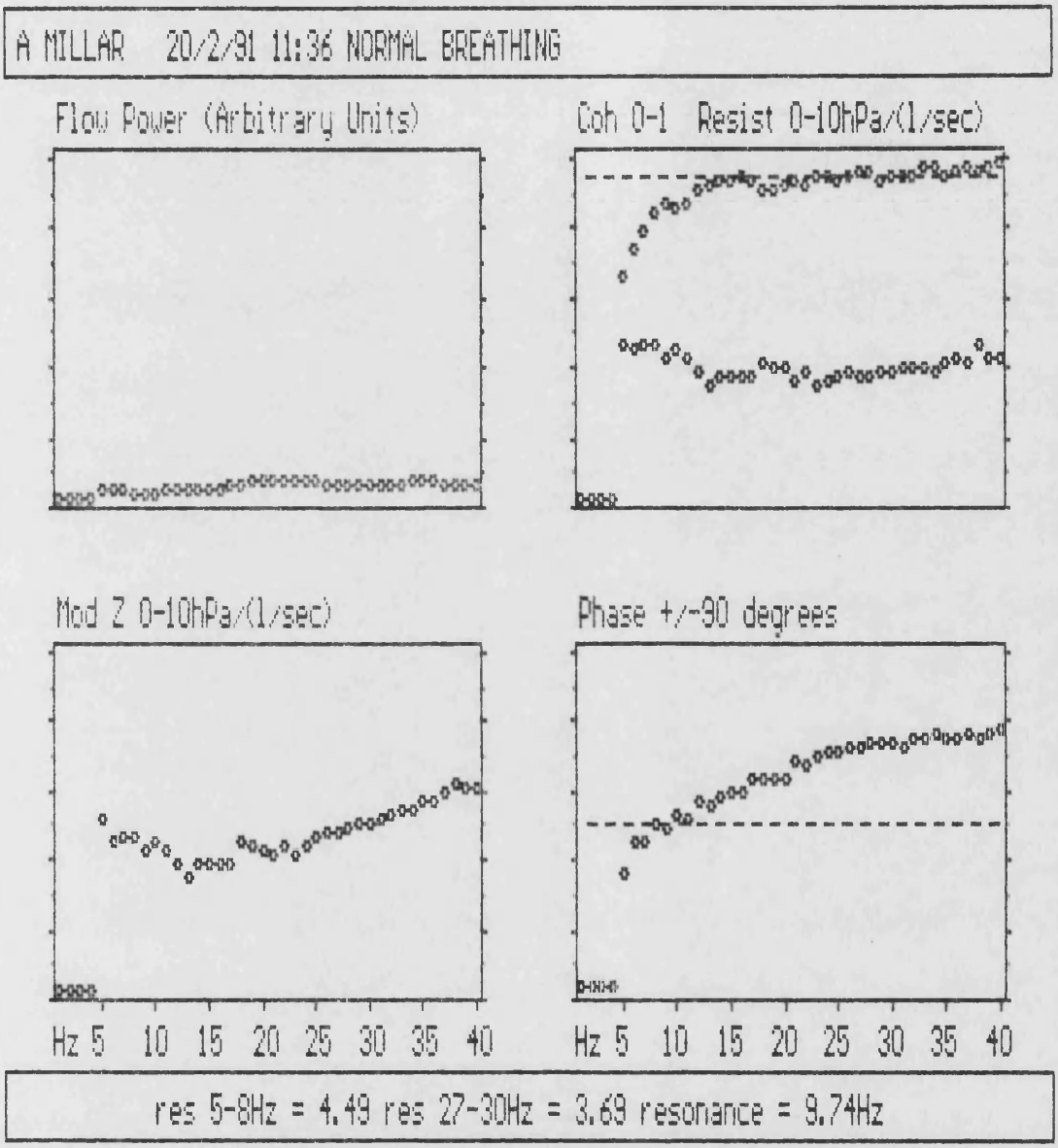

Figure 2 : Normal Data Example

Appendix B

Paper presented to the European Economic Community, Respiratory Impedance Concerted Action Group, Zeist, Holland, 8-9th March 1993.

A special issue of the European Respiratory Review is to be published including this work.

Appendix B.1

The Assessment of Cardiogenic Interference on Respiratory Input Impedance Measurements and Attempts to Minimise Effects Using Adaptive Filtering

Scott, R. S. & Grant, L. J.

Regional Medical Physics Service
Royal United Hospital
Combe Park, Bath
ENGLAND, BA1 3NG

Telephone 0225 824082
Fax 0225 447535

Running Head: Cardiac Interference in Respiratory Impedance

Keywords: respiratory input impedance, cardiogenic interference, adaptive filtering

Appendix B.2

Abstract

Low frequency, (1-5Hz), respiratory impedance measurements have exhibited greater variability then results at higher frequencies. Respiration has been cited as one source of interference responsible for degrading data quality. We have suggested that cardiac activity also has a bearing on these low frequency measurements. This is supported by illustrating that there are cardiac components present in both pressure and flow signals used for impedance measurements. Having identified their presence an adaptive noise cancelling technique has been developed to minimise them.

Introduction

Impedance, defined as the ratio of pressure over flow, is a mathematically complex, frequency dependent parameter used to characterise system mechanics. By applying a composite oscillatory airflow to the lung and analysing the resulting pressure and flow signals respiratory impedance may be determined at each frequency present in the applied airflow, (1,2). The technique requires minimal subject cooperation and is therefore applicable in all age groups, as well as mechanically ventilated subjects. The results enable the respiratory system to be modelled using electrical circuit analogues, (3). As impedance comprises resistive and reactive components this means changes in elastic properties of the lung may be separated from changes in airway resistance.

A system has been developed to determine respiratory impedance over the frequency range 2 to 40Hz. During the validation of our instrumentation it became apparent that results below 10Hz exhibited greater variability, as assessed by the coherence function which is an indicator of data reliability. This problem continued even when measurements were made in apnoeic subjects, therefore breathing, which has been cited as a source of interference (4), could not be held wholly responsible. It was postulated that cardiac related interference may also have a bearing on data quality and this was investigated by estimating frequency spectra with no applied signal while subjects held their breath. Having confirmed the presence of cardiac components in the pressure and flow signals used to compute impedance, an adaptive filter was developed to minimise these artifacts. A fixed frequency filter is inapplicable as the cardiac signal overlaps the applied oscillatory airflow at low frequencies.

Methods

An electro dynamic vibration generator coupled to a set of phosphor bronze bellows was used to generate the oscillatory airflow, containing sinusoidal frequencies in the range 2 to 40Hz in integer multiples. The power amplifier driving the generator received its input from a digital to analogue converter resident in a micro computer. The Opus Turbo V computer was used to generate the oscillatory signal as well as running the main impedance application program, written in Borland Turbo Pascal. The program samples pressure, flow and an optional cardiac signal at 128Hz, then calculates impedance via the cross power spectrum method as described by Michaelson *et al*, (1). A commercial integer signal processing package was imbedded in the program enabling rapid computation of Fourier transforms and spectral manipulation. The program allows 2048 data points to be stored, representing 16 seconds of data, with flexibility in the Fourier transform length depending on the required spectral resolution. Increasing the transform length increases the spectral resolution but means fewer blocks are available to average in the frequency domain. The averaging process is essential to ensure smooth impedance estimates. Pressure and flow are measured close to the mouth using Validyne pressure gauges and a screen pneumotachograph, as mouth pressure is determined with respect to atmosphere the impedance measurements include chest wall and lung tissue components.

Ultimately it is envisaged that the system will be routinely used in the general hospital environment, with impedance data being presented at 1Hz intervals. The purpose of this study, however, was to focus on the low frequency data where components due to cardiac activity may be present. Therefore the spectral resolution was

increased to 0.25Hz otherwise cardiac harmonics, which are unlikely to be at integer frequencies may be missed. The work effectively divided into two parts, initially attempts were made to identify cardiac components in the recorded pressure and flow signals. A cardiac signal was recorded using a finger pulse monitor, (Simonsen & Weel 8000 series module), simultaneously with the pressure and flow signals while no oscillatory signal was applied to the lung. The time varying pressure and flow data were scrutinised for evidence of cardiac activity, and the frequency domain cross power spectrum between flow and cardiac signals were compared. The second element of the investigation involved the development and evaluation of an adaptive filter in an attempt to minimise the effect of cardiac components on the pressure and flow data. Such filters may be configured to act as noise cancelling systems, see Figure 1. The signal plus noise is delayed and applied to the summing junction shown. A reference signal which is correlated with the noise, but not the signal, is applied to the adaptive filter block, the filter output is subtracted from the delayed input signal. The output of the system is used to control the impulse response of the filter block. As the system settles the filter response adjusts such that the output signal is similar to the noise in the input, with the two cancelling at the output of the summing junction leaving only the required signal. The question which arises is how to implement the filter and control algorithm. The simplest way to do this is to use a digital filter where difference equations characterise the frequency response, so by altering the coefficients in the equation the response is modified. Finite impulse response filters, (FIR), are most commonly used for adaptive techniques as they are unconditionally stable. The difference equation for a tapped delay

line implementation of an FIR filter is given in equation 1 and forms the basis of our adaptive filter system. The algorithm used to adjust the filter coefficients, (see equation 2), appears deceptively simple, however must be treated with care. The rate at which the system converges is determined by the factor mu, larger values mean more rapid adaption at the expense of a greater ultimate error. It is necessary to ensure that mu remains less than
2 divided by the total power present in the reference signal. Initially all filter coefficients are set to zero, with mu typically set to a tenth of the upper limit, defined above, determined for each signal. A 128 coefficient filter was implemented, with the error signal being computed with each new filter output. The error signal is then used to compute a new set of filter coefficients, thus adapting the filter response.

$$y(n) = w_1x(n) + w_2x(n-1) + w_3x(n-2) + \ldots\ldots + w_Lx(n-(L-1)) \quad (1)$$

$$\begin{aligned} e(n) &= 2\mu(x(n-L/2) - y(n)) \\ w_k(n+1) &= w_k(n) + e(n)x(k-1) \qquad k=0..(L-1) \end{aligned} \quad (2)$$

For a full derivation and discussion of these adaptive techniques, refer to Widrow et al (5). The approach taken was to consider the finger pulse cardiac signal as a reference input to the adaptive filter, using the filter as shown in figure 1 as an element in the noise canceller. The system could then be applied to either pressure or flow signals prior to spectral analysis to eliminate cardiac related components. The cardiac finger pulse is in no way correlated with the applied oscillatory signal. The noise canceller was tested by detecting a sinusoidal signal buried in random noise.

Results

Pressure, flow and cardiac signals were recorded in a small group of volunteers who remained apnoeic during the manoeuvre. Lung volumes were not measured, however, subjects were asked to remain as close as possible to total lung capacity for the duration of the measurements. Figures 2 and 3 show two eight second periods of time varying data taken from two subjects for illustration. Figure 4 shows the cardiac-flow cross power spectrum in the 1 to 4Hz range, each graph contains the three 16 second measurements. Each measurement block split into 512 lengths for analysis and averaging. These initial measurements are with no applied oscillatory signal.

Respiratory impedance measurements , with the additional cardiac signal collected simultaneously, were made while the subjects remained apnoeic. The adaptive noise canceller was applied to three sets of the data for each of the three subjects. The reduction in flow spectra at 1,2 and 3Hz are shown in table 1. The figures were obtained by dividing the initial flow spectrum values by the post adaptive filtered data.

Discussion

The purpose of this work was to assess cardiac related interference in pressure and flow signals used in respiratory impedance measurements. It is difficult to quantify how such interference would affect impedance results, however, the cardiac frequency spectrum directly overlaps the 1 to 3Hz range. Evidence of poor coherence values at these frequencies, in the absence of breathing, tends to suggest cardiac activity as the likely cause.

Figures 2 and 3 show particularly clear examples of activity related to the finger pulse records. Although the signal levels are small there is clear evidence of a cardiac influence on the pressure and flow channels. It is difficult to make noise free measurements, ensuring the glottis is open, so not all sections of data show such obvious a correlation in the time domain. By considering the cardiac-flow cross spectra of figure 4, the relationship is again apparent in the frequency domain. The cardiac fundamental is common to both cardiac and flow signals, with the first few harmonics containing enough power to be identified. Further evidence of the low frequency relationship is provided by the coherence function. The standard pressure to flow coherence is close to unity around the cardiac components, even with no oscillations applied, as there is a cardiac relationship present in both pressure and flow.

Having identified cardiac components, an attempt was made to minimise them. The adaptive filter based noise canceller was seen to reduce the power in the flow signal. This was most obvious, from Table 1, at 1Hz, the reduction at 2 and 3Hz being less obvious. Though at 2 and 3Hz an oscillatory signal was being applied so perhaps the reduction has eliminated cardiac components. More work needs to be

done on optimising the adaptive filter techniques as the performance appears to be somewhat variable, also our experiments have been in apnoeic subjects and it will be necessary to consider how breathing may affect filter performance. The aim would be to filter pressure and flow prior to impedance determination, thereby eliminating the cardiac interference and increasing the possibility of more reliable data in the 1 to 3Hz range.

Acknowledgements

Equipment was purchased with funds provided by the Wessex Regional Health Authority, Research Committee.

Subject	1Hz	2Hz	3Hz
1	16.4	4.5	3.3
	24.7	6.0	2.4
	13.9	1.3	1.9
2	8.1	2.6	1.5
	5.0	1.0	1.0
	3.7	1.5	1.1
3	4.6	1.4	1.8
	4.8	1.5	3.4
	1.4	1.0	1.6

Table 1 Factors by which flow power spectra values are reduced following noise cancellation.

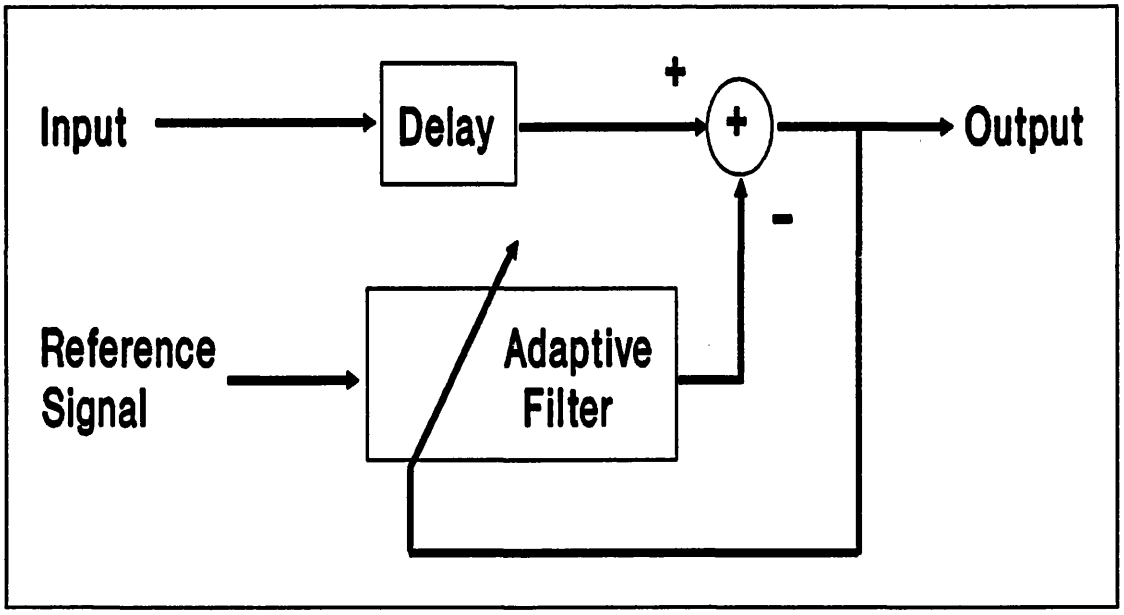

Figure 1 Adaptive Noise Canceller Block Diagram

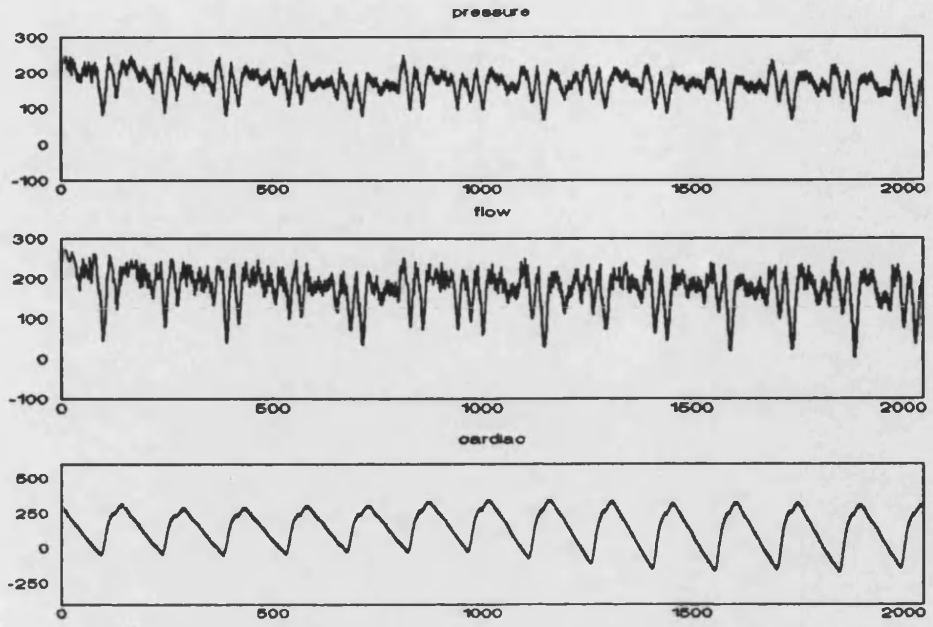

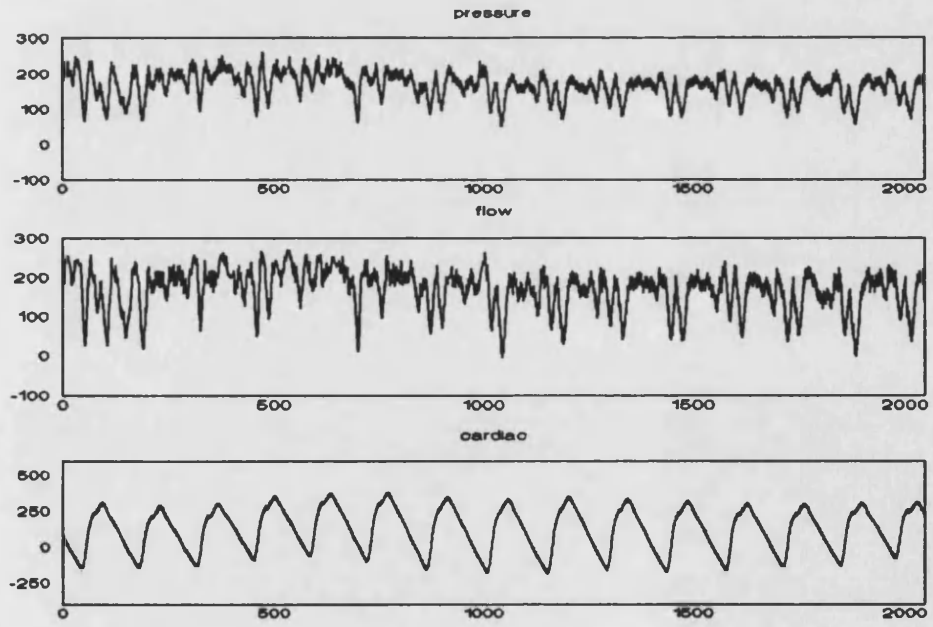

Figure 2 Pressure, Flow and Cardiac Signals - 8 seconds, 1024 points, y axis, digitised parameter values.

Appendix B.13

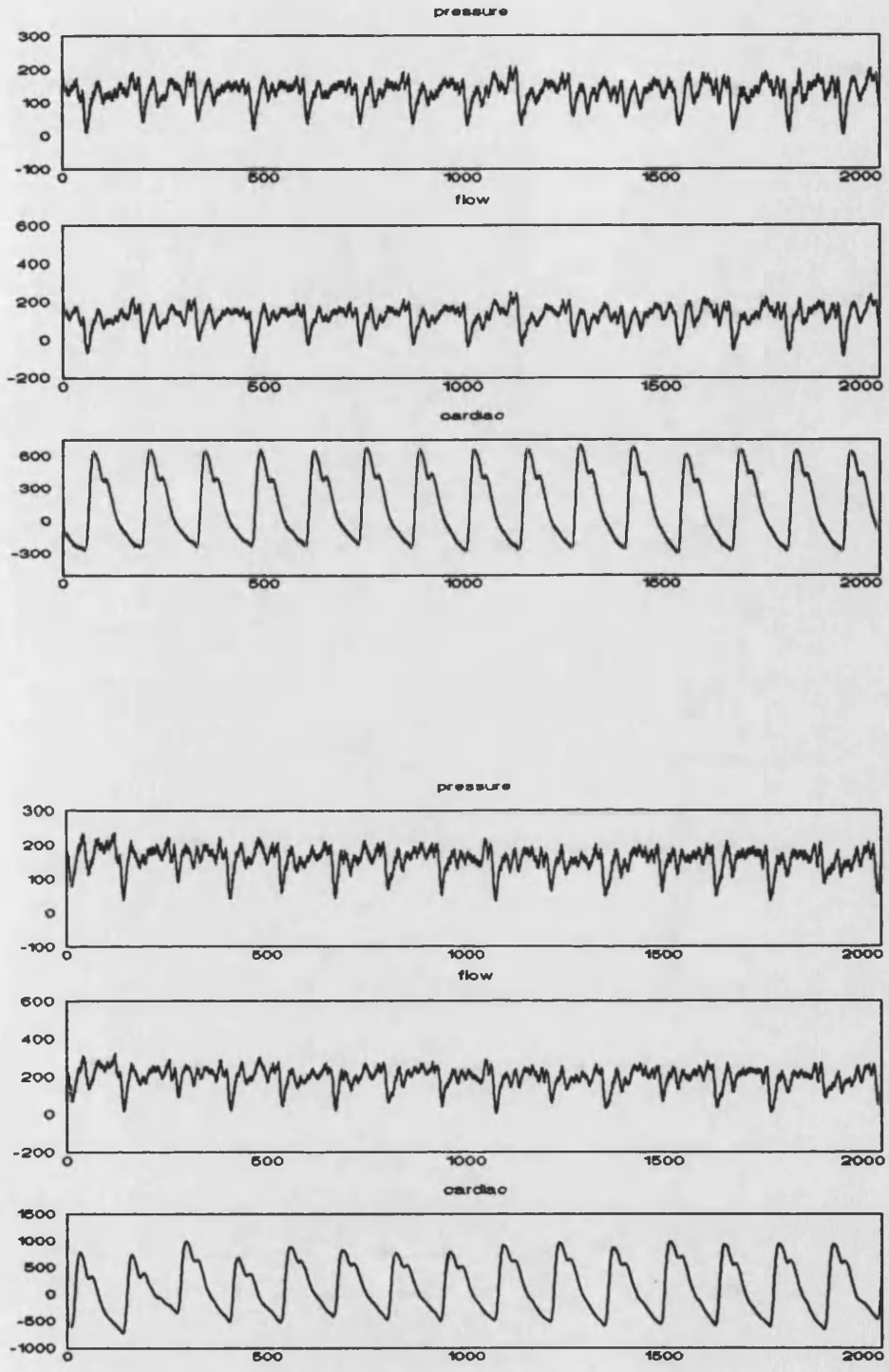

Figure 2 Pressure, Flow and Cardiac Signals - 8 seconds, 1024 points, y axis, digitised parameter values.

Appendix B.14

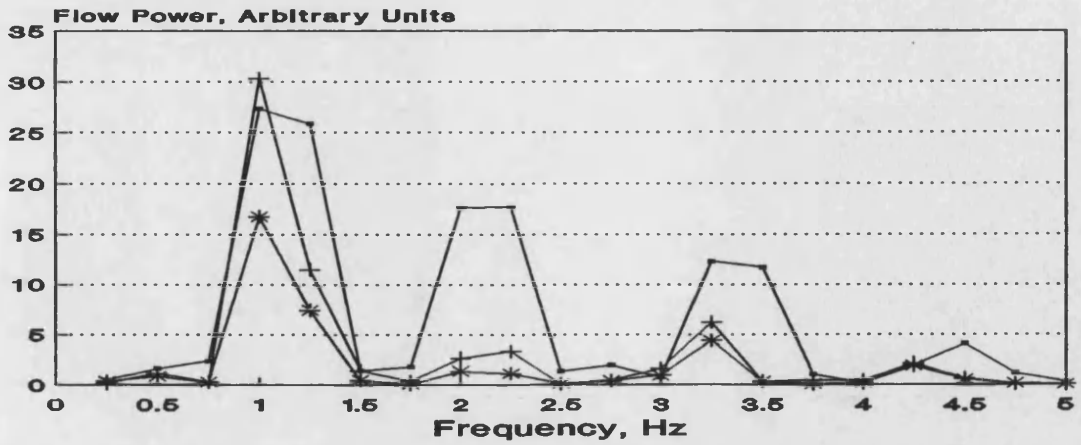

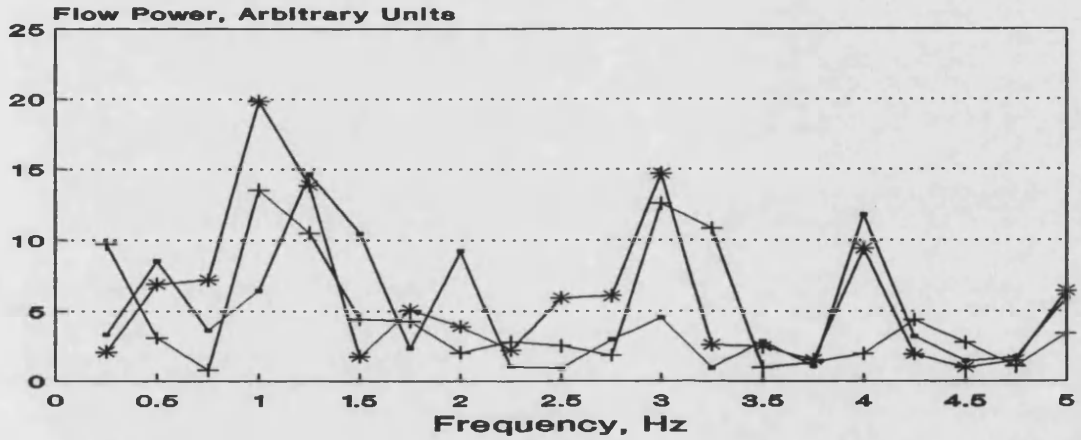

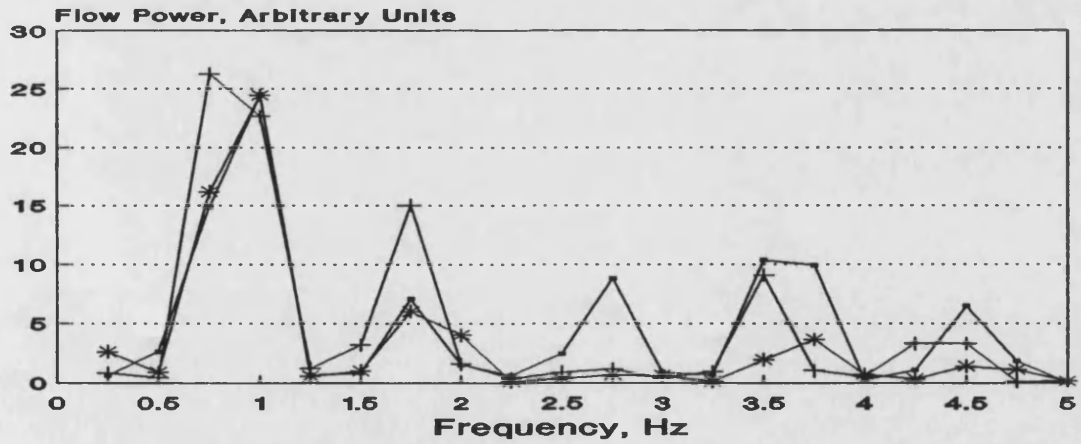

Figure 4 Cardiac-Flow Cross Spectra, 3 Volunteers.

References

1. Michaelson ED, Grassman ED, Peters WR. - Pulmonary mechanics by spectral analysis of forced random noise. *J Clin Invest*, 1975, **56** 1210-1230.

2. Lándsér FJ, Nagels J, Demedts M, Billiet L, van de Woestijne KP. - A new method to determine the frequency characteristics of the respiratory system. *J Appl Physiol*, 1976, **41**, 101-6.

3. Peslin R, Papon J, Duvivier C, Richalet J. - Frequency response of the chest: modelling and parameter estimation. *J Appl Physiol*, 1975, 38, 523-534.

4. Franken H, Clément J, van de Woestijne. - Systematic and random errors in the determination of respiratory impedance by means of the forced oscillation technique: A theoretical study. *IEEE Trans Biomed Eng*, 1983, **BME-30**, 642-651.

5. Widrow B, Glover Jr JR, McCool JM, Kaunitz J, Williams CS, Hearn RH, Zeidler JR, Dong Jr E, Goodlin RC. - Adaptive noise cancelling: principles and application. *Proc IEEE*, 1975, **63**, 1693-1719.